CO_2 Disposal Into Alberta Basin Aquifers - Phase III:

Hydrogeological and Numerical Analysis of CO_2 - Disposal in Deep Siliciclastic and Carbonate Aquifers in the Lake Wabamun Area

CO_2 DISPOSAL INTO ALBERTA BASIN AQUIFERS - PHASE III:

Hydrogeological and Numerical Analysis of $C0_2$-Disposal in Deep Siliciclastic and Carbonate Aquifers in the Lake Wabamun Area

-by-

D.H.-S. Law
Stefan Bachu
W.D. Gunter

-at the-

Alberta Research Council
PO Box 8330
Edmonton, Alberta
Canada, T6H 5X2

C-1995-2

July, 1995

Alberta Geological Survey Open File Report 1995-6
Available from the Alberta Department of Energy
Alberta Geological Survey
Information Sales
Phone 403 422-3767

-funded by-

Environment Canada
Natural Resources Canada
&
TransAlta Utilities Corporation

ACKNOWLEDGEMENTS AND DISCLAIMER

The funding for this project from Natural Resources Canada, Environment Canada, Alberta Research Council and TransAlta Utilities Corporation is acknowledged with thanks. Environment Canada's contribution was derived from PERD (The Federal Interdepartmental Program of Energy Research and Development). The foregoing clauses are also applicable to those agencies and companies.

Reference herein to any specific commercial product, process, or service by trade name, trademark, manufacturer, or otherwise, does not necessarily constitute or imply its endorsement, recommendation, or favoring by the ARC. The views and opinions of the authors expressed herein do not necessarily state or reflect those of ARC.

EXECUTIVE SUMMARY

Because of the climate-warming effect of CO_2 released to the atmosphere, measures should be taken to reduce, utilize or dispose of industrial CO_2 emissions. For landlocked large sources of CO_2, such as thermal power plants located in the interior of continents, one solution for reducing CO_2 emissions into the atmosphere is its utilization in enhanced oil recovery processes (EOR), and disposal into deep sedimentary aquifers or depleted oil and gas reservoirs. Previous laboratory work by Gunter et al. (1993) has shown that it is possible to trap CO_2 in sedimentary formations through geochemical reactions. Conceptual work by Bachu et al. (1994) has shown that CO_2 can be hydrodynamically trapped in deep open aquifer systems for extremely long periods of time (up to millions of years) because of the slow velocity and long path of CO_2 movement in the subsurface. This creates an alternative to using depleted oil or gas reservoirs which have limited capacity, or utilizing CO_2 in EOR operations which only delay the release of CO_2 into the atmosphere.

A number of coal-based thermal power plants with a total capacity of more than 4,000 MW are located near Lake Wabamun in central Alberta, Canada. A hydrogeological study of the sedimentary succession at this site in the Alberta Sedimentary Basin was undertaken in order to identify aquifers which meet various requirements for CO_2 disposal, particularly with regard to depth and confinement. Two aquifers, the relatively thick carbonate Nisku aquifer (60 m thick) and the thin siliciclastic Glauconitic Sandstone aquifer (13 m thick), were selected (based on their properties and groundwater flow characteristics) for further investigation. Numerical modelling was used to study the capacity of these aquifers to accept large quantities of CO_2 injected in the supercritical state and to retain this CO_2 for long periods of time. The multi-phase, multi-component numerical model STARS, developed by the Computer Modelling Group (CMG) of Calgary, Alberta, Canada, was used to simulate the isothermal flow of injected CO_2 and aquifer water in rocks of variable properties. The capacity of the system to receive and retain CO_2 was examined for a whole series of parameters including aquifer depth and thickness, properties of host rock and

water (i.e. porosity, permeability, salinity and temperature), and injection characteristics (e.g. injection pressure).

Even generally low-permeability (6 md) aquifers, which are common in the Alberta Basin, can accept and retain large quantities of injected CO_2 for long periods of time, provided that near-well zones of high permeability (100-400 md) (termed "sweet" zones) are found, in order to attain high injection rates without reaching pressure limits imposed by rock-fracturing thresholds. The numerical simulations indicated that disposal of 2,000 t/d/well and 12,000 t/d/well of CO_2 was possible for the thin siliciclastic Glauconitic Sandstone aquifer and the thick carbonate Nisku aquifer, respectively, under optimum conditions. The overall results show that injection of CO_2 in the supercritical state into deep aquifers in sedimentary basins is viable and offers a short-to-medium term solution for reducing the emission of CO_2 into the atmosphere.

Based on these simulations and a steady state, radial outflow well model, a correlation was developed for predicting CO_2 injectivity into homogenous aquifers taking into account aquifer thickness, depth, permeability anisotropy and the physical properties of CO_2. A chart was also prepared for prediction of CO_2 injection rates into deep aquifers in locally high permeability "sweet" zones. The effect of a high permeability near-well zone or "sweet" zone is to increase the injectivity of CO_2 up to three times, depending on the regional permeability and on the size and permeability of the sweet zone. Both these tools can be used to target aquifers for detailed evaluation for CO_2 disposal and long term storage in other parts of the Alberta Sedimentary Basin or in other sedimentary basins of the world.

RÉSUMÉ EXÉCUTIF

À cause de l'effet de réchauffement du climat par le CO_2 relâché dans l'atmosphère, des mesures devraient être prises afin de réduire, utiliser ou disposer des émissions industrielles de CO_2. Une solution pour la réduction des émissions de CO_2 dans l'atmosphère des sources importantes de CO_2, entourées de terre, telles que les centrales thermiques situées à l'intérieur des continents, serait leur utilisation dans les procédés de recouvrement amélioré de l'huile (*enhanced oil recovery: EOR)*, ou encore la disposition dans les aquifères sédimentaires profondes ou dans les réservoirs épuisés d'huile ou de gaz. Le travail de laboratoire antérieur de Gunter et al. (1993) a montré qu'il est possible de piéger le CO_2 dans les formations sédimentaires par l'intermédiaire de réactions géochimiques. Le travail conceptuel de Bachu et al. (1994) a montré que le CO_2 peut être piégé hydrodynamiquement dans les systèmes profonds d'aquifère ouverte pour des périodes extrêmement longues (jusqu'à des millions d'années) grâce à la faible vélocité et au long cheminement du mouvement du CO_2 sous la surface. Ceci constitue une alternative à l'utilisation des réservoirs épuisés d'huile ou de gaz qui ont une capacité limitée, ou à l'utilisation du CO_2 dans les opérations de EOR qui ne font que retarder le relâchement du CO_2 dans l'atmosphère.

Un nombre de centrales thermiques à base de charbon, avec une capacité totale de plus de 4,000 MW, sont situées près du lac Wabamun dans le centre de l'Alberta, au Canada. On a entrepris une étude hydrogéologique de la succession sédimentaire à ce site du bassin sédimentaire albertain afin d'identifier les aquifères qui satisfont aux exigences variées de disposition du CO_2, particulièrement en ce qui a trait à la profondeur et au confinement. Deux aquifères, l'aquifère carbonatée relativement épaisse (60 m d'épaisseur) de Nisku et l'aquifère siliciclastique mince (13 m d'épaisseur) de grès glauconitique, ont été choisies (sur la base de leurs propriétés et des caractéristiques de l'écoulement des eaux souterraines) pour une investigation future. La modélisation numérique a été utilisée dans l'étude de la capacité de ces aquifères à accepter de grandes quantités de CO_2 injecté à l'état supercritique et à retenir ce CO_2 pour de longues périodes de temps. Le modèle numérique polyphasique et à plusieurs constituants, STARS, développé par le "Computer Modelling Group" (CMG) de Calgary, en Alberta, au Canada, a été utilisé pour simuler l'écoulement isothermique du CO_2 injecté et de l'eau de l'aquifère dans des roches à propriétés variées. La capacité du système à recevoir et à retenir le CO_2 a été examinée pour toute une série de paramètres incluant la profondeur et l'épaisseur de l'aquifère, les propriétés des roches

hôtes et de l'eau (i.e. la porosité, la perméabilité, la salinité et la température) et les caractéristiques de l'injection (e.g. la pressure d'injection).

Même les aquifères à perméabilité généralement basse (6 md), qui sont communes dans le bassin albertain, peuvent accepter et retenir de grandes quantités de CO_2 injecté sur de longues périodes de temps, à condition qu'il existe près du puits des zones à haute perméabilité (100-400 md) (appelées zones "sweet"), afin d'obtenir de hauts taux d'injection sans atteindre les limites de pression imposées par les seuils de fracturation des roches. Les simulations numériques ont indiqué que la disposition de 2,000 t/j/puits de CO_2 et 12,000 t/j/puits de CO_2 était possible pour l'aquifère mince siliciclastique de grès glauconitique et l'aquifère épaisse carbonatée de Nisku, respectivement, sous des conditions optimums. Les résultats globaux montrent que l'injection de CO_2 à l'état supercritique dans les aquifères profondes des bassins sédimentaires est viable et offre une solution à court ou moyen terme à la réduction de l'émission de CO_2 dans l'atmosphère.

Basé sur ces simulations et sur un modèle de puits à état stable et à écoulement radial, une corrélation a été développée pour la prédiction de l'injectivité du CO_2 en aquifères homogènes en tenant compte de l'épaisseur de l'aquifère, de sa profondeur, de l'anisotropie de sa perméabilité et des propriétés physiques du CO_2. Une charte a aussi été préparée pour la prédiction des taux d'injection de CO_2 dans les aquifères profondes dans les zones "sweet" à haute perméabilité locale. L'effet d'une zone à haute perméabilité près du puits, ou zone "sweet", est d'augmenter l'injectivité du CO_2 jusqu'à trois fois, dépendant de la perméabilité régionale et de la taille et de la perméabilité de la zone "sweet". Ces deux outils peuvent être utilisés pour choisir les aquifères pour une évaluation détaillée de disposition du CO_2 et emmagasinement à long terme dans d'autres parties du bassin sédimentaire albertain ou dans d'autres bassins sédimentaires du monde.

ACKNOWLEDGEMENTS

Tom McCann, T.J. McCann and Associates Ltd., kindly provided engineering advice as required. The authors wish also to express their gratitude to the funding agencies and representatives on the management committee which made possible this research work: Alberta Department of Energy (J.K. Kleta, D.E. Macdonald), Natural Resources Canada (F.M. Mourits) , Environment Canada (V.R. Marwaha) and TransAlta Utilities Corporation (D. Drysdale).

TABLE OF CONTENTS

LIST OF APPENDICES

LIST OF TABLES

LIST OF FIGURES

1. INTRODUCTION

Carbon dioxide is a greenhouse gas which contributes to global climate warming. Long-term effective CO_2 disposal is essential for reducing greenhouse effects in the short and medium terms until new technologies for limiting CO_2 generation and for its utilization are being developed and implemented. For landlocked large sources of CO_2 like thermal power plants in western Canada, the best approaches for reducing CO_2 emissions into the atmosphere are its use for enhanced oil recovery (Bailey and MacDonald, 1993) and disposal into deep sedimentary aquifers (Bachu et al., 1994). In a previous study, Alberta Oil Sands Technology and Research Authority (AOSTRA) has examined the feasibility of removing 50,000 tonnes/day of CO_2 from atmospheric emissions in Alberta and Saskatchewan by utilizing CO_2 in enhanced oil recovery (EOR) operations (Bailey and McDonald, 1993; Todd and Grand, 1993). Throughout the study it became apparent that EOR operations will not necessarily be capable of utilizing all the CO_2 envisaged to be removed from atmospheric emissions, particularly after the CO_2 injected in oil fields begins to be recovered at extraction wells. In this case, CO_2 will have to be disposed of by other means, of which injection into depleted gas reservoirs or deep aquifers is the most suitable for Alberta (Bachu et al., 1994). Carbon dioxide can be injected into deep aquifers either directly at source or at the EOR site, whereas pipeline transport of the CO_2 may be necessary to depleted gas reservoirs (depending on their location). One target previously identified (Gunter et al., 1994) is the thin Glauconitic Sandstone aquifer in the Lake Wabamun area in the vicinity of the Sundance and Genesee power plants. The hydrogeology of the Glauconitic Sandstone aquifer is reviewed in Chapter II. For the purpose of selecting another injection aquifer in Alberta, the geology of the sedimentary succession is analyzed at the main CO_2 sources and proposed EOR sites identified by AOSTRA. For CO_2 injection purposes, the host aquifer must be at depths greater than 800 m (van der Meer, 1992). The selection of a second site is made in Chapter III. The hydrogeology of the second site, the Nisku Carbonate aquifer, is given in Chapter IV.

The setup and properties defined for numerical simulation runs to study the injectivity and capacity of the two selected aquifers to accept large quantities of CO_2 injected in the supercritical state and to retain this CO_2 for long periods of time are given in Chapter V. The numerical results for the Glauconitic Sandstone and the Nisku Carbonate aquifers are given in Chapters VI and VII, respectively. The generalizations of these numerical results are given in Chapter VIII and the conclusions are drawn in Chapter IX.

2. GLAUCONITIC SANDSTONE AQUIFER HYDROGEOLOGY

In Phase II (Gunter et al., 1994), based on geological, geochemical and economic considerations, it was decided to study, in detail, the hydrogeology of the Mannville Group strata in the Lake Wabamun area, the site of two-thirds of Alberta's coal-fired power generating capacity. Information from more than 300 wells drilled in the area was used in defining and characterizing the geology, lithology, mineralogy, porosity and permeability of the rocks in the Mannville stratigraphic interval (which occurs at depths greater than 1300 meters). Bottom hole temperature measurements, formation water analyses and drillstem tests were used to characterize the hydrogeological regime of formation waters. A summary of the Phase II study findings follows.

The Mannville Group strata in the area of interest consist of the Ellerslie Member, Ostracod Beds, Glauconitic Sandstone and Grand Rapids Formation. The strata generally dip to the southwest with a slope of 7 m/km. The mainly siltstone and sandstone Ellerslie Member was deposited on the sub-Cretaceous unconformity, which explains its variable thickness from less than 10 m to more than 60 m. The predominantly mudstone Ostracod Beds conformably overlies the Ellerslie Member, averaging 18 m in thickness. The Glauconitic Sandstone is formed of sandstones approximately 13 m thick. It is overlain by a continuous basal shale zone of the Grand Rapids Formation which averages 10 m in thickness. The rest of the Grand Rapids Formation, comprised of interbedded sands and shales, averages approximately 120 m in thickness.

There is neither a vertical nor an areal trend in porosity and permeability distributions in the Mannville Group strata in the area of interest, although there are regions of locally high and low values. Only two wells contain core analyses for the Grand Rapids Formation and the Glauconitic Sandstone, while for the Ostracod Beds and the Ellerslie Member there are enough data for a more meaningful analysis. The porosity of the Glauconitic Sandstone and the Ellerslie Member is high on average (12%). The

permeability of Mannville strata is generally low, of the order of 5 to 10 md on average. However, local permeabilities as high as 100 to 200 md have been measured both in core and drillstem tests.

Hydrostratigraphically, the Ellerslie Member and the lower portion of the Ostracod Beds form an aquifer, overlain by the aquitard comprised of the remainder of the Ostracod Beds. The overlying Glauconitic Sandstone and Grand Rapids aquifers are separated by the intervening aquitard formed by the basal shale layer of Grand Rapids Formation. The composition of formation water in the Mannville Group in the study area varies as much within units as it does from unit to unit and place to place. Salinities range from approximately 25,000 to 50,000 mg/l. The flow of formation water in the Ellerslie aquifer is generally from south-southeast toward the north, driven by a drop in hydraulic head from approximately 1000 to 600 m. The flow in the Glauconitic Sandstone aquifer is different, with hydraulic heads varying in the 550 to 590 m range and flow direction generally to the northeast. Hydraulic heads in the Grand Rapids aquifer are in the same range as in the Glauconitic Sandstone aquifer. Geothermal gradients in the area are around 30°C/km. Temperatures in the Glauconitic Sandstone aquifer vary in the 50 to 60°C range because of the southwestward dip of the strata.

The CO_2-trapping capability of the Glauconitic Sandstone aquifer was assessed based on detailed mineralogical analysis of drill core, autoclave experiments and geochemical modelling. Basic aluminosilicate minerals identified in the Glauconitic Sandstone aquifer, which could contribute to the trapping capacity of the aquifer, were feldspars and glauconite. Experiments on potential CO_2-trapping reactions in the Glauconitic Sandstone were carried out at 105°C and 90 bars CO_2 pressure for one month, but very little reaction was seen on this time scale. These experiments and field time scales were evaluated by geochemical modelling using rate data from the literature for the minerals making up the Glauconitic Sandstone. The geochemical model PATHARC predicted times from 6 to 40 years for the experiments to come to

equilibrium. Extending the modelling to the field, CO_2-trapping reactions take a minimum of 100 years to complete after the formation water has equilibrated at the temperature of the Glauconitic Sandstone aquifer (i.e. 54°C) and at the proposed injection pressure of the CO_2 (260 bars). Every square kilometre of the Glauconitic Sandstone aquifer could sequester approximately 0.5 megatons of CO_2 by these mineral-trapping reactions, once the CO_2-charged formation water has swept through.

From this analysis of rock properties and hydrogeology of formation water in the Mannville Group strata in the study area (Tp. 50-52, R. 3-5W5M) the preferred aquifer for CO_2 disposal is the Glauconitic Sandstone for the following reasons:

(i) It is the most homogeneous of all Mannville Group units in the succession;

(ii) Hydrostratigraphically it is confined by the shaley Ostracod Beds and Basal Grand Rapids aquitards;

(iii) It has generally good porosity (12% on average);

(iv) It has low regional-scale permeability (10 md on average), which is needed for hydrodynamic entrapment, slow dispersion and high sweep ratio;

(v) It has high permeability in places (100 md), which is needed for avoiding high pressure build up in the near-well region at sites of CO_2 injection;

(vi) It has a siliciclastic based mineralogy with clays present, which will contribute to the mineral trapping of CO_2 through geochemical reactions;

(vii) There is no hydrocarbon production from this unit, unlike the Ellerslie Member, thus, avoiding unwarranted contamination of energy resources.

3. AQUIFER DISPOSAL SITE SELECTION: SITE NO. 2

The amount of CO_2 produced by the thermal power plants in the Lake Wabamun area (with more than 4000 MW capacity) is by far the largest in Alberta. Thus, it is expected that only a small amount of the CO_2 produced in this area could be disposed of by injection into the thin Glauconitic Sandstone aquifer. The remainder of CO_2 will have to be either used for EOR operations at far away sites or disposed of by injecting it into a deeper aquifer in the Lake Wabamun area.

Major sources of CO_2 emissions, such as power and petrochemical plants, oil sands plants and heavy oil upgraders, refineries and pulp and paper mills, were identified in the AOSTRA study (Bailey and MacDonald, 1993) and ranked based on quantity and quality of CO_2, location and ability of facility retrofitting for CO_2 removal. The following facilities in Alberta were selected for case studies (Figure 1): Sundance power plant (Lake Wabamun area), Novacor plant at Joffre, and the Hanlan-Robb gas plant. The bi-provincial heavy oil upgrader at Lloydminster, another selected major CO_2 source, is located on the Alberta-Saskatchewan border. AOSTRA's study envisaged the CO_2 transportation by pipeline to the following oil fields in Alberta: Carson Creek, Pembina and Redwater, for EOR use. The stratigraphy of the AOSTRA sites are examined below for the potential of aquifer disposal of CO_2.

At Hanlan Robb (Tp. 46, R16 W5 Mer) gas is produced from Middle Devonian strata below the Ireton Formation (Figure 2). The first aquifers confined by thick, shaley, regional-scale aquitards are found in the Colorado Group at depths greater than 2,600 m. The most shallow potential injection aquifers could be the Cardium and Viking sandstone, found at 2,600 m and 3,200 m depth, respectively (Figure 2). However, Cardium is generally a producing horizon (e.g. the giant Pembina field some 60 km east of Hanlan Robb).

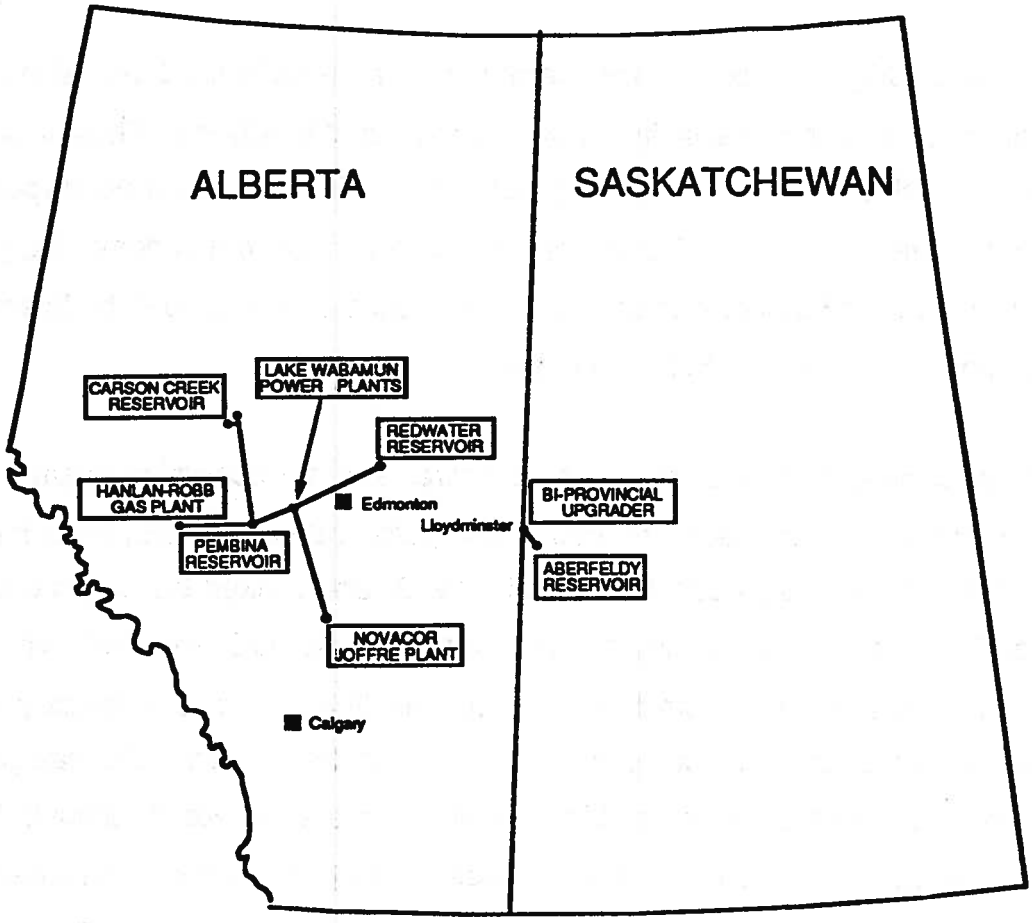

Figure 1. Location of major CO_2 sources in Alberta and of oil fields with potential for CO_2 utilization in EOR operations (after Bailey and McDonald, 1993).

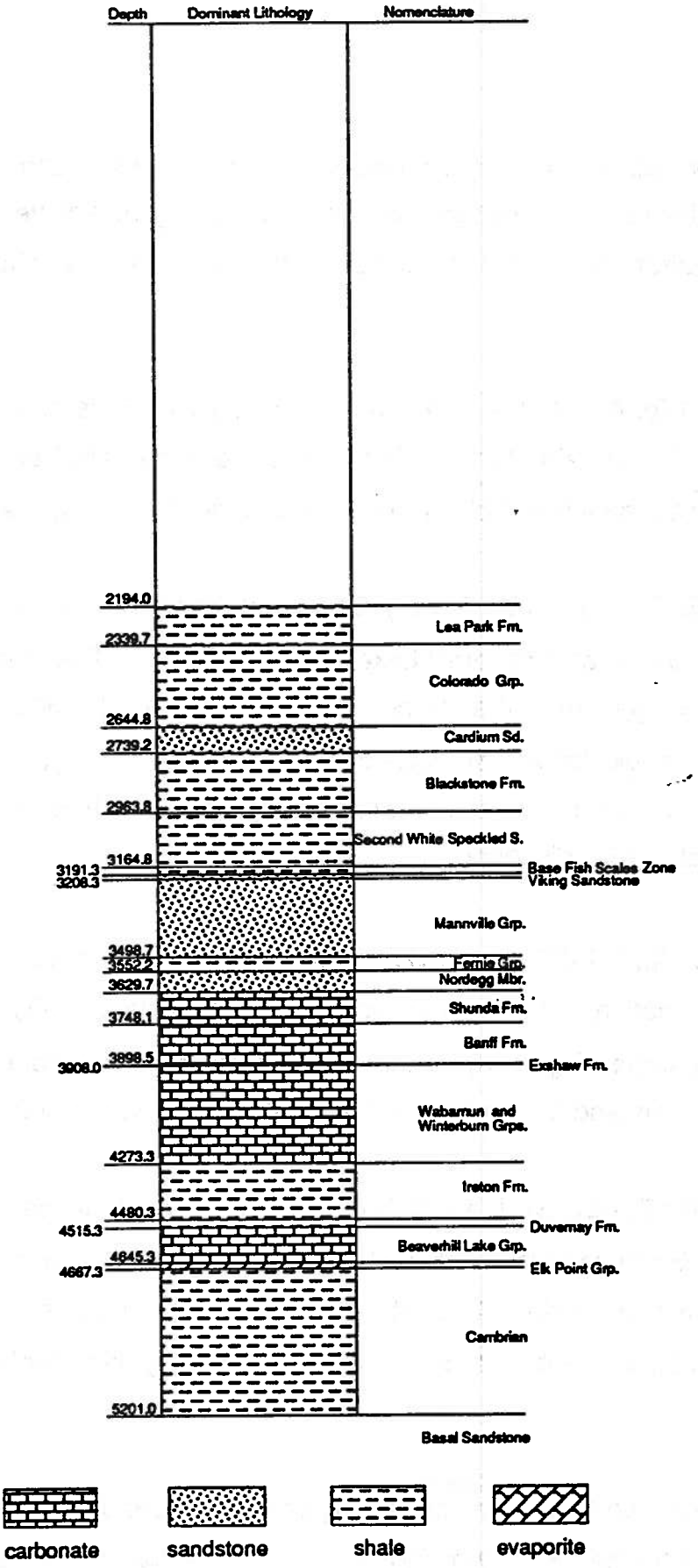

Figure 2: Representative well, Hanlan Robb (46-5-16-10-06).

At Joffre (Tp. 39, R26 W4 Mer), the Viking Sandstone aquifer, found at 1,536 m depth, is the most shallow aquifer confined by thick, shaley regional-scale aquitards (Figure 3). Deeper aquifers are the siliciclastic Blairmore (Mannville) overlying the Banff carbonates.

At Lloydminster (Tp. 49, R1 W4 Mer), the sedimentary basin is much shallower, such that the only aquifer suitable for CO_2 injection is the carbonate Red River Formation, overlain and confined by the thick evaporitic Prairie aquiclude (Figure 4).

At Carson Creek (Tp. 63, R12 W5 Mer), CO_2 could be used for enhanced oil recovery from the Middle Devonian Beaverhill Lake Group (Figure 5). The most shallow aquifer suitable for CO_2 injection is the Viking Sandstone, found at 1,503 m depth. Other, deeper aquifers could be the siliciclastic Blairmore (Mannville), and the carbonate Shunda, Banff, Wabamun and Winterburn (Figure 5), although their depth may increase the cost of CO_2 disposal.

At Pembina (Tp. 49, R8 W5 Mer), CO_2 could be used for enhanced oil recovery from the Cardium Formation. The most shallow aquifer suitable for CO_2 injection is again the Viking Sandstone (Figure 6), found at 1,754 m depth. Deeper aquifers are the siliciclastic Mannville and the carbonate Banff, Wabamun, Winterburn, etc.

At Redwater (TP 57, R22 W4 Mer), CO_2 could be used for enhanced oil recovery from the Leduc Fm. Because of the sedimentary basin being shallower and of hydrocarbon resources in Devonian carbonate strata, the only aquifer suitable for CO_2 disposal is the Basal Sandstone, found at 2,151 m depth, confined by thick shales and evaporites (Figure 7).

From a lithological point of view, the Viking and Basal sandstones are generally the cleaner. The siliciclastic Mannville (Blairmore) and predominantly carbonate Shunda,

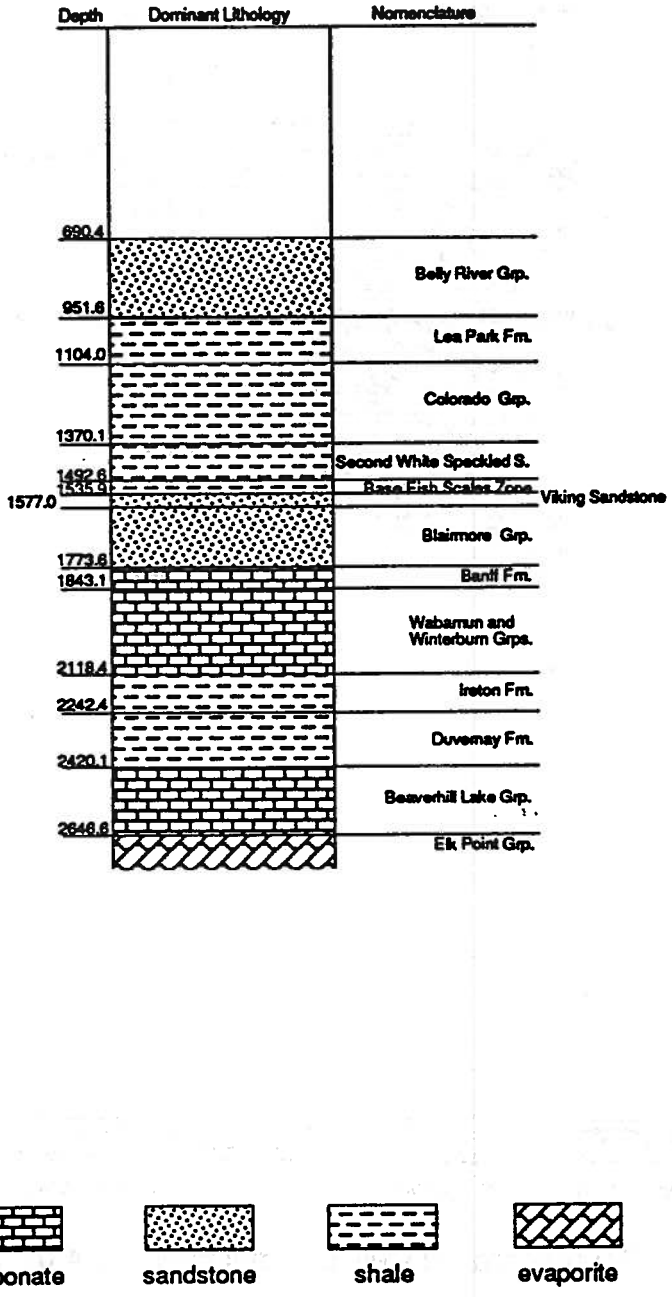

Figure 3: Representative well, Joffre (39-4-26-08-09).

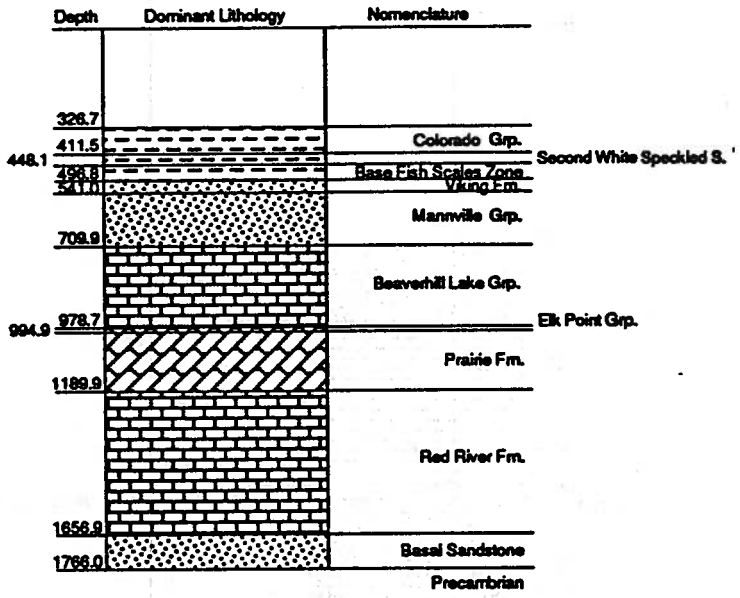

Figure 4: Representative well, Lloydminster (49-4-01-15-10).

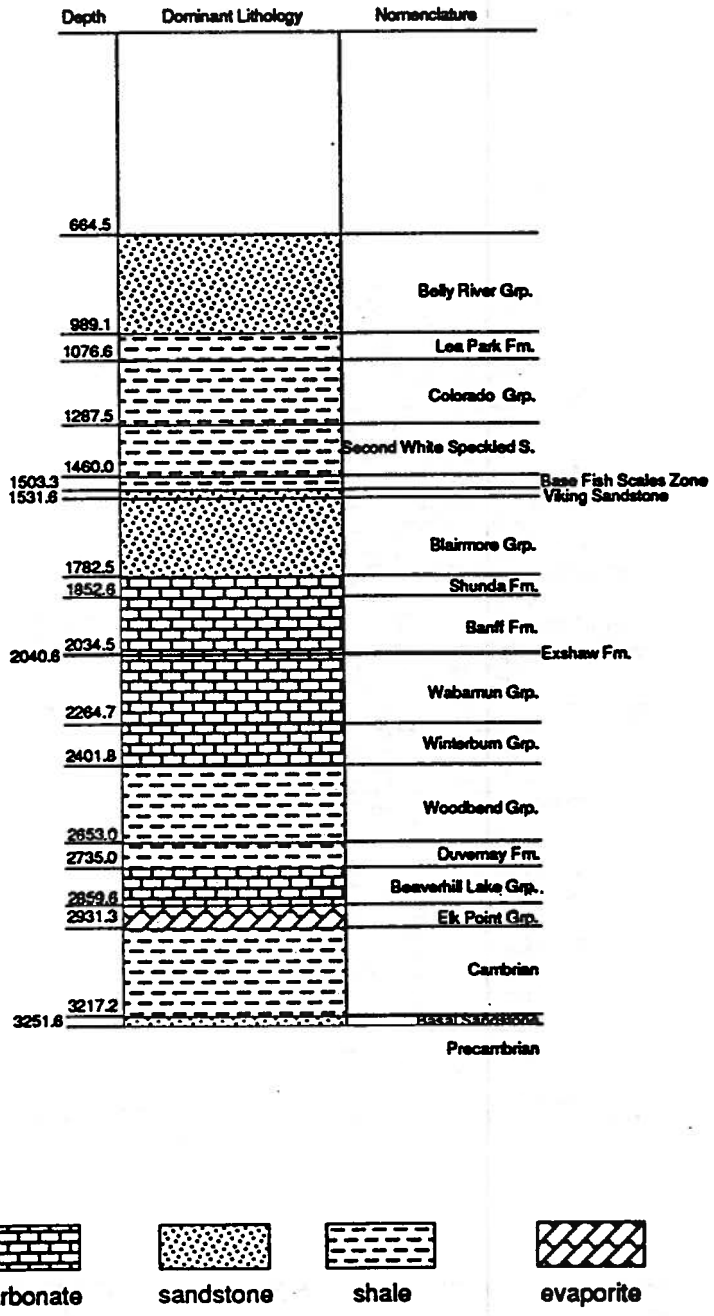

Figure 5: Representative well, Carson Creek (63-5-12-36-06).

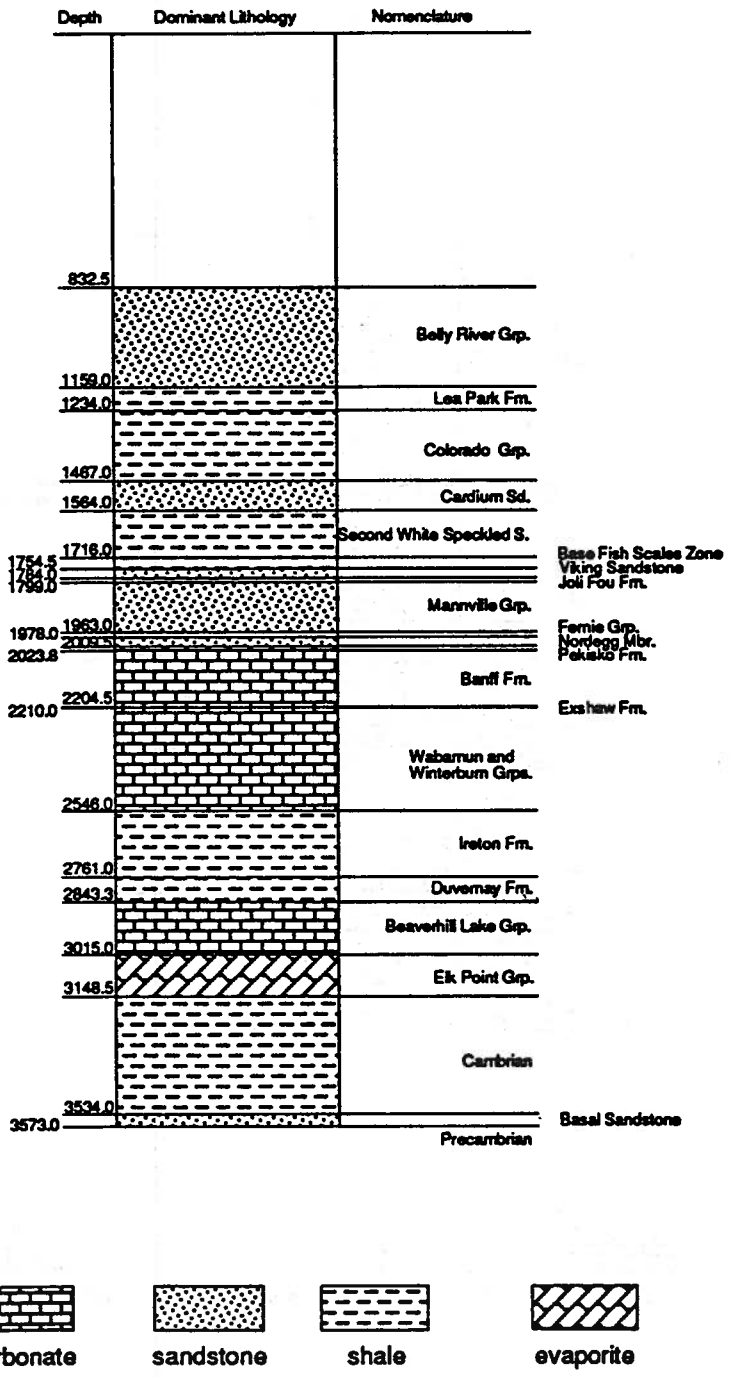

Figure 6: Representative well, Pembina (49-5-08-27-11).

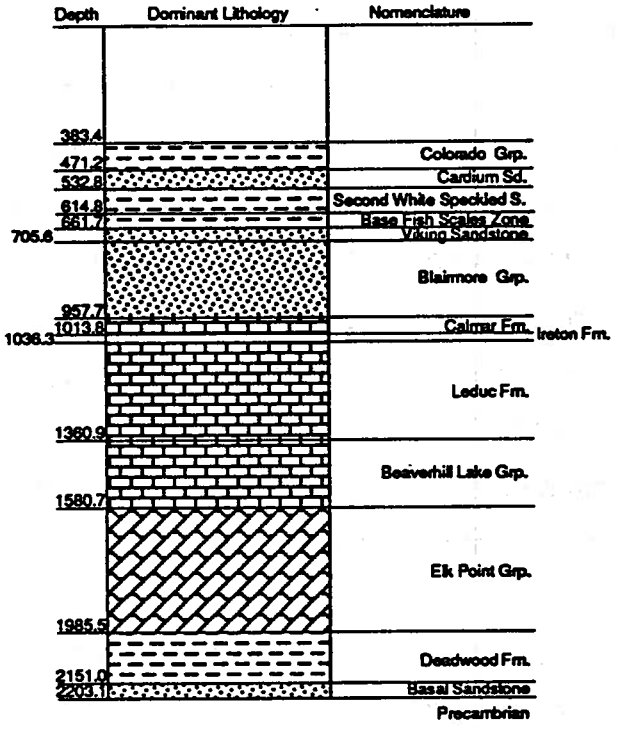

Figure 7: Representative well, Redwater (57-4-22-34-01).

Banff, Wabamun and Winterburn are of a mixed lithology, with shaley discontinuous layers present throughout, which affect the porosity and permeability of these units. In terms of data availability, it is expected that there are insufficient data to properly characterize the Red River and Basal Sandstone aquifers at the Lloydminster and Redwater sites, respectively, because of their relative depth in the sedimentary succession and lack of hydrocarbon resources leading to drilling in these units. Thus, it seems that the Viking Sandstone aquifer would be a good candidate for hydrogeological characterization and numerical simulation of CO_2 injection because it is confined both above and below by shaley aquitards. However, the Viking aquifer is thin, similarly to the Glauconitic Sandstone aquifer in the Lake Wabamun area, with probably a limited capacity for CO_2 disposal. Besides, except for central Alberta, the Viking aquifer at these sites is found at great depth, comparable to the depth of much thicker carbonate aquifers in central Alberta.

In the Lake Wabamun area, below the Glauconitic Sandstone Aquifer, are thick carbonate aquifers, confined by regional aquitards (Figure 8). The negative effects of injecting CO_2 into deep carbonate aquifers in the Lake Wabamun area will be the higher cost per injection well due to greater depth, and lack of geochemical trapping of CO_2 (Gunter et al., 1993a). However, these effects will probably be more than offset by possibly higher rates of injection and greater aquifer capacity for receiving and storing CO_2, not withstanding the savings in not having to transport CO_2 by pipeline to great distances. Thus, selecting a second aquifer for CO_2 injection in Lake Wabamun area is recommended because it will probably allow the potential disposal of all the CO_2 produced by the largest source points in Alberta.

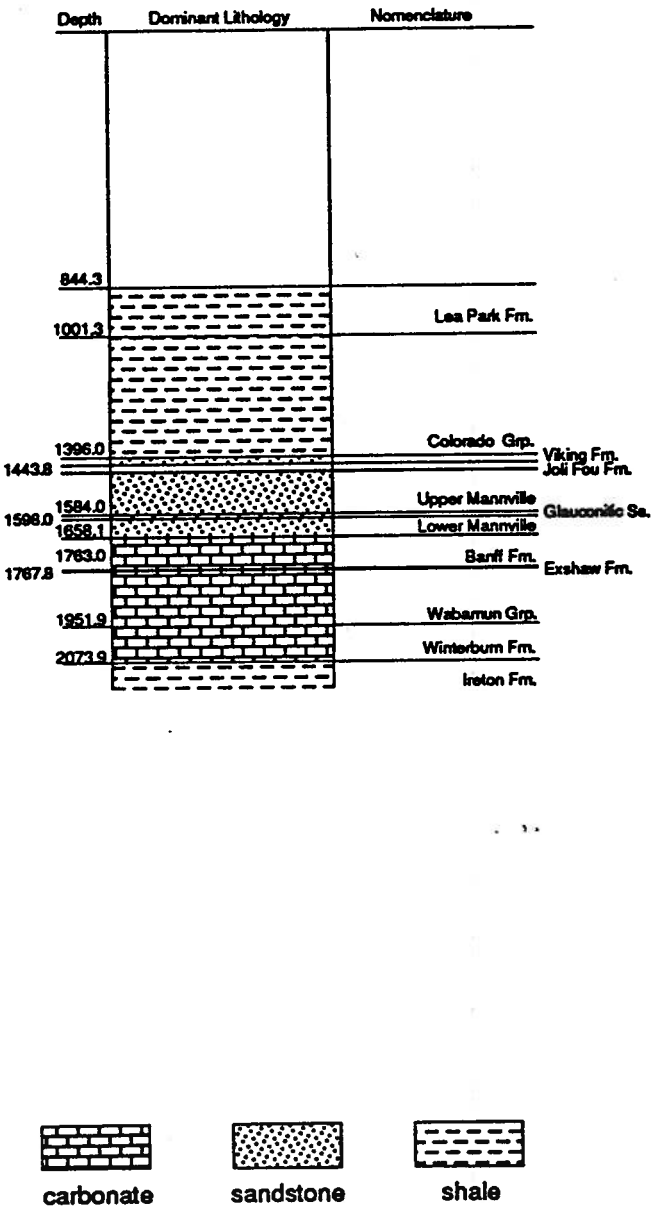

Figure 8: Representative well, Lake Wabamun (52-5-5-1-5).

4. NISKU CARBONATE AQUIFER HYDROGEOLOGY

The stratigraphy of the sedimentary succession in the Lake Wabamun study area (Figure 9) is comprised of siliciclastic (mostly shales) Cambrian strata at the base, overlain by a thick succession of carbonate-dominated Devonian and Mississippian rocks, which, in turn, are unconformably overlain by a thick succession of shale-dominated Cretaceous and Tertiary strata (Figure 8). Erosion after the Laramide orogeny has removed most of the Tertiary rocks in the area. A thin veneer of glacial Pleistocene deposits cover the top of the bedrock. The ground surface (Figure 10) varies in elevation between 660 m and 860 m. The Upper Devonian carbonate strata of the Winterburn and Wabamun groups represent probably the most suitable injection aquifers below the Cretaceous Mannville Group. Although more than 300 wells were drilled in the study area, most of them end at the sub-Cretaceous unconformity immediately below the Mannville Group. Less than 20 wells penetrate the deeper Wabamun and Winterburn groups. Thus, the following hydrogeological characterization of these strata is based on a sparse, limited data distribution, and should be considered accordingly.

4.1 Geology and Hydrostratigraphy

As a result of significant pre-Jurassic and pre-Cretaceous erosion, most of the Mississippian strata and the entire Pennsylvanian-to-Triassic succession are absent in the study area. The siliciclastic Cretaceous Mannville Group strata and remnants in places of the Jurassic Nordegg Member overlie the eroded Mississippian Banff Formation comprised of shaly carbonates (Table 1). The Banff Formation is underlain by the thin shales of the Exshaw Formation which constitute a regionally significant aquitard (Bachu, 1995). Thus, although shale units are present within both the Banff Formation and the overlying Mannville Group, on a basin scale they form a single aquifer system (Bachu, 1995). The Exshaw Formation overlies the limestone-dominated Devonian Wabamun Group, whose structure top varies in elevation

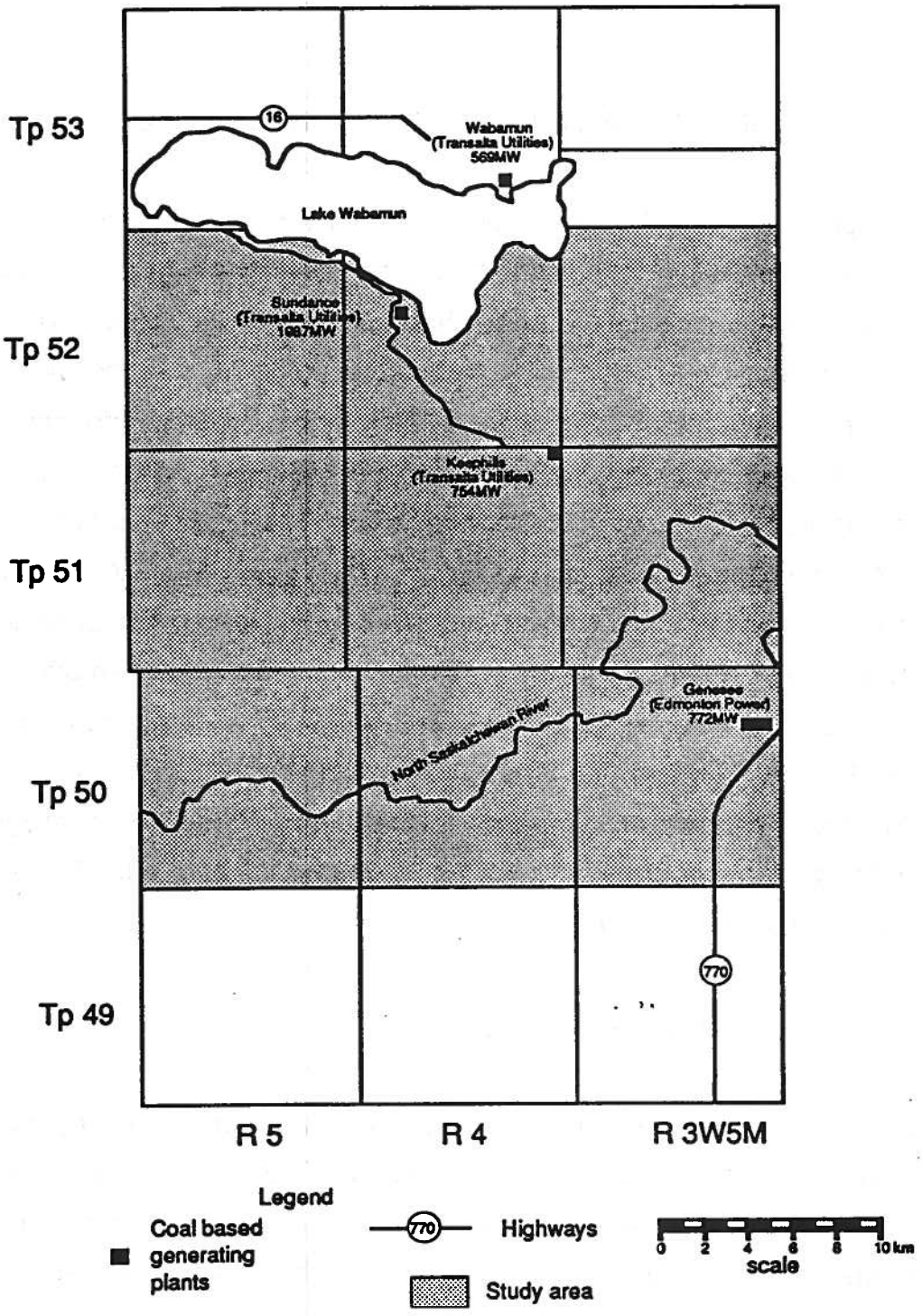

Figure 9. Location of major power plants in the Lake Wabamun region in relation to the study area.

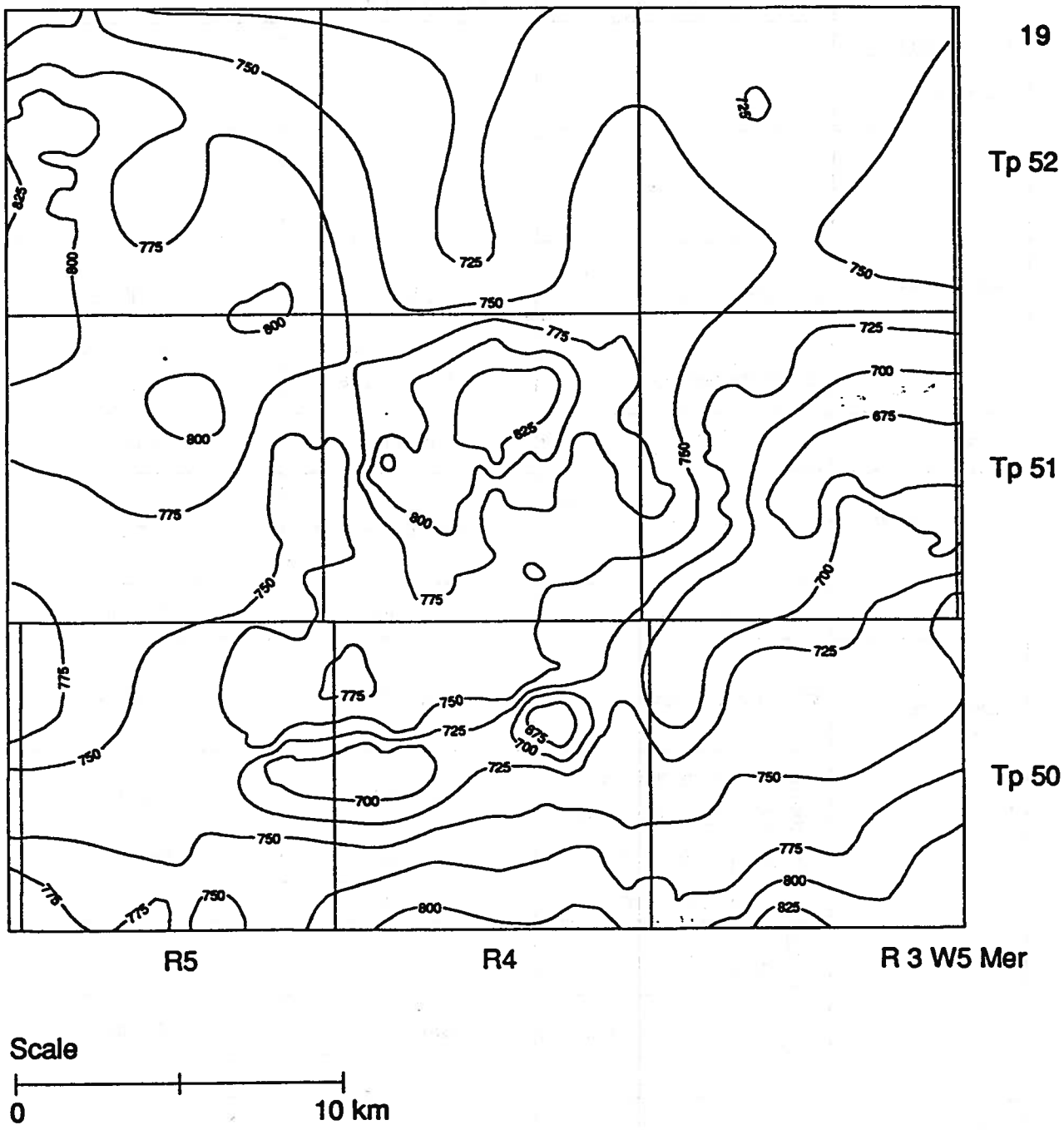

Figure 10. Ground surface topography in the Lake Wabamun area.

PERIOD	STRATIGRAPHY		DOMINANT LITHOLOGY	HYDROSTRATIGRAPHY
Quaternary / Tertiary				
Cretaceous				
	Colorado Group		Shale	Aquitard
	Mannville Group		Sandstone (Shale)	Aquifer
Jurassic	Nordegg Member		Carbonate	Aquifer
Mississippian	Banff Fm.		Carbonate (Shale)	Aquifer
	Exshaw Fm.		Shale	Aquitard
Devonian	Wabamun Group		Limestone	Aquifer
	Winterburn Group	Graminia Fm. / Blue Ridge Fm.	Dolomite	Aquifer
		Calmar Fm.	Shale	Aquitard
		Nisku Fm.	Dolomite	Aquifer
	Woodbend Group	Ireton Fm.	Shale	Aquitard
		Cooking Lake Fm.	Carbonate	Aquifer
Cambrian				
Precambrian				

Table 1. Stratigraphy, dominant lithology and hydrostratigraphy of the Woodbend-Colorado sedimentary succession in Lake Wabamun study area.

between -1130 m and -760 m in the study area (Figure 11). The top of the aquifer dips to the southwest with a slope of 8.7 m/km (Figure 11). The dolomite-dominated Winterburn Group underlies the Wabamun Group. A thin shaly layer (Calmar Formation) forms an aquitard hydrogeologically separating the Winterburn Group strata into two parts. The upper part (Graminia and Blue Ridge formations), which are in direct hydraulic contact with the overlying Wabamun Group, form together with the latter a single aquifer, the Wabamun-Winterburn (Table 1). This aquifer varies in thickness between 157 m and 240 m, with the thicker parts in the central and northern regions of the study area (Figure 12). The thin Calmar aquitard (10 m on average, Figure 13), separates the Wabamun-Winterburn aquifer from the underlying Nisku aquifer (Table 1), the lowermost formation of the Winterburn Group. The structure top of the Nisku aquifer varies in elevation from -1310 m in the southwest to -990 m in the northeast, with an average slope of 8.9 m/km (Figure 14). The Nisku aquifer is thinner than the Wabamun-Winterburn aquifer, varying in thickness between 25 m and 103 m (Figure 15). The aquifer itself is thinner in the central and northern regions of the study area, thickening westward and to the southeast (Figure 15). The Nisku aquifer (Winterburn Group) is underlain by the thick shales of the Ireton Formation (Woodbend Group), which forms a regionally significant aquitard (Bachu, 1995).

4.2 Aquifer Properties

From the point of view of CO_2 injection into deep sedimentary strata, the relevant aquifer properties are rock permeability and porosity, and formation water chemistry, pressure and temperature. Unfortunately, because so few wells penetrate the Wabamun-Winterburn stratigraphic interval in the study area, very few data are available for characterizing the Wabamun-Winterburn and Nisku aquifers. The distributions of wells with relevant data for the two aquifers are shown in Figures 16 and 17, respectively.

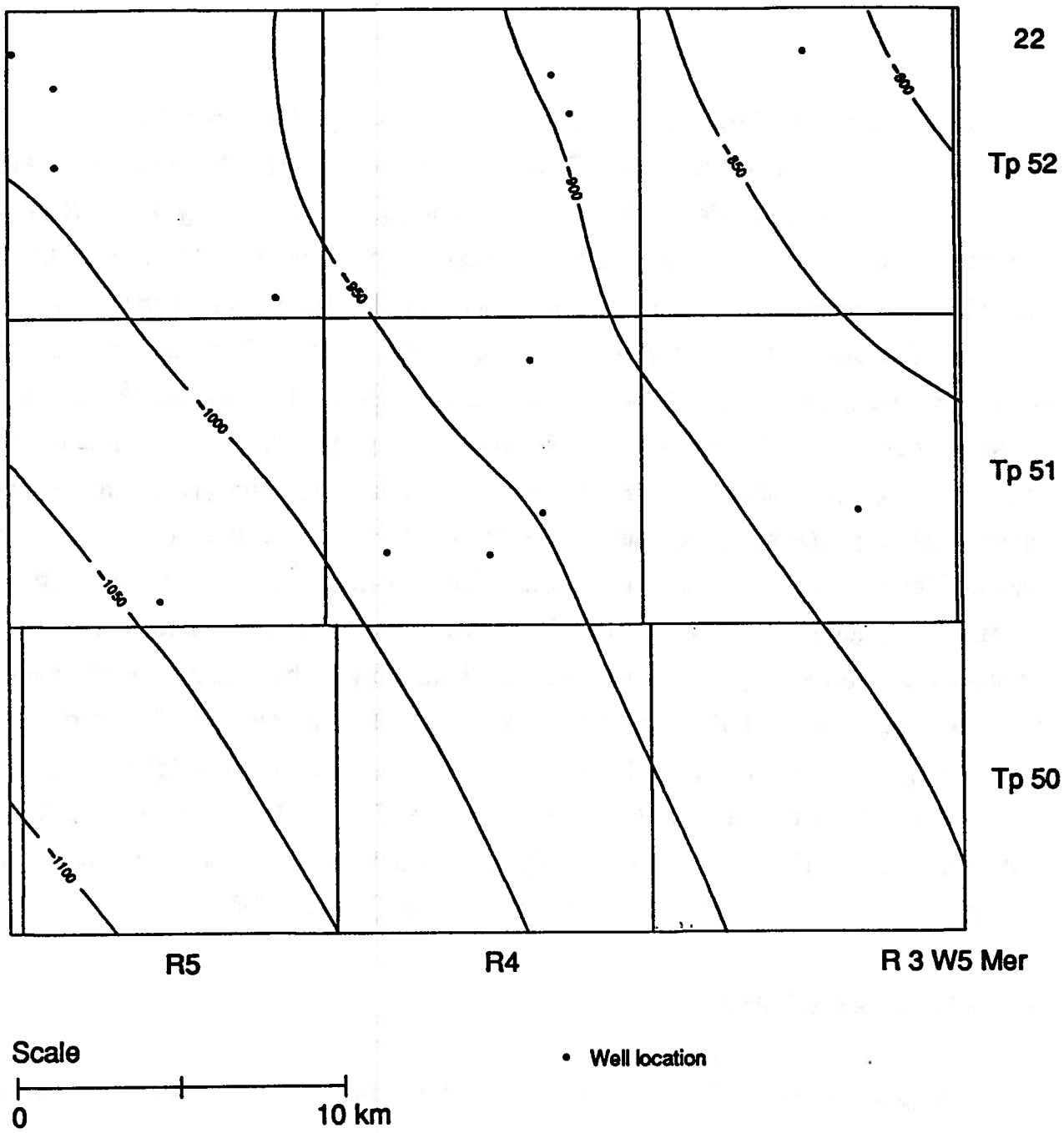

Figure 11. Structure top elevation (m) of the Wabamun Group.

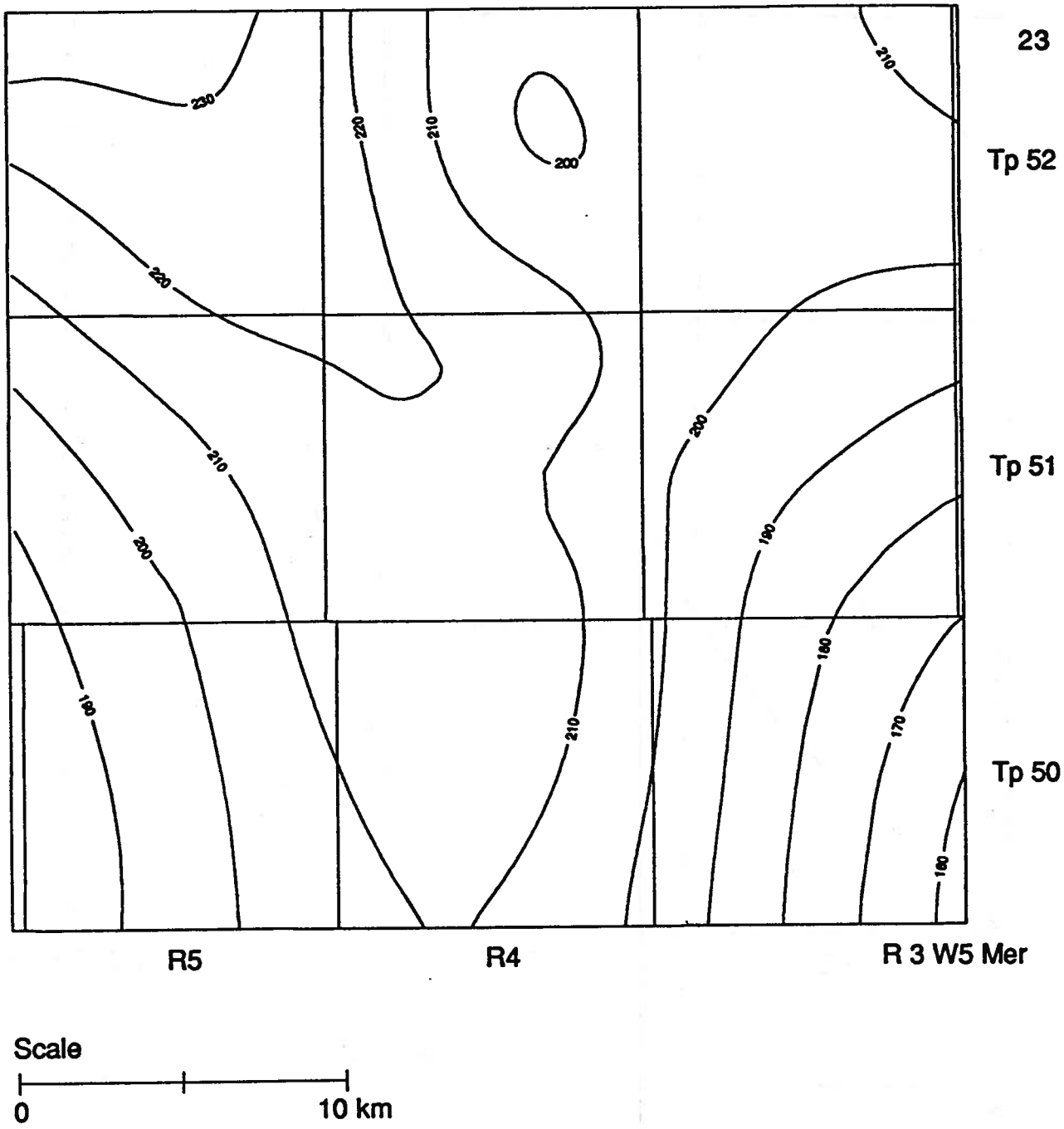

Figure 12. Isopach (m) of the Wabamun-Winterburn aquifer.

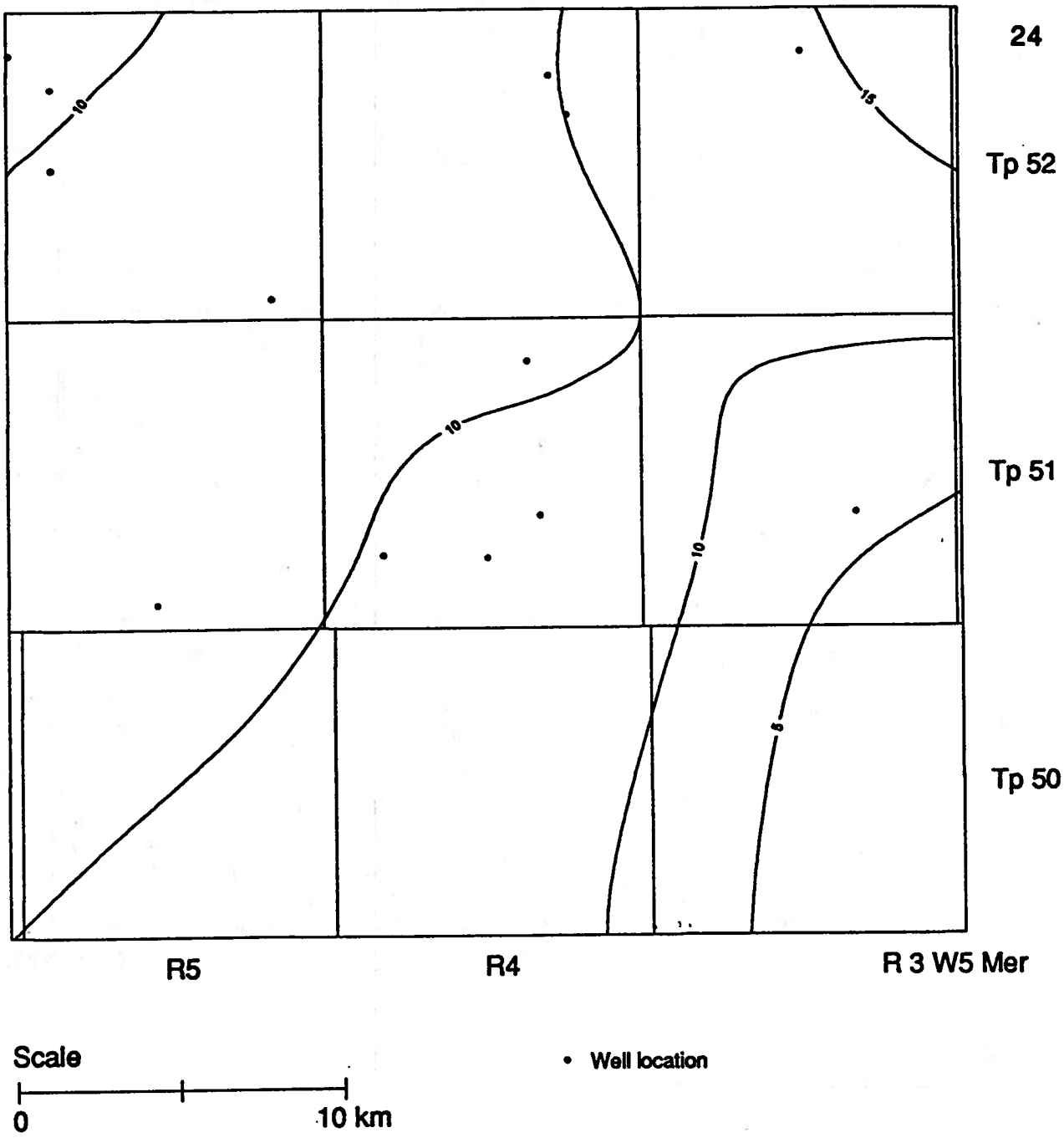

Figure 13. Isopach (m) of the Calmar aquitard.

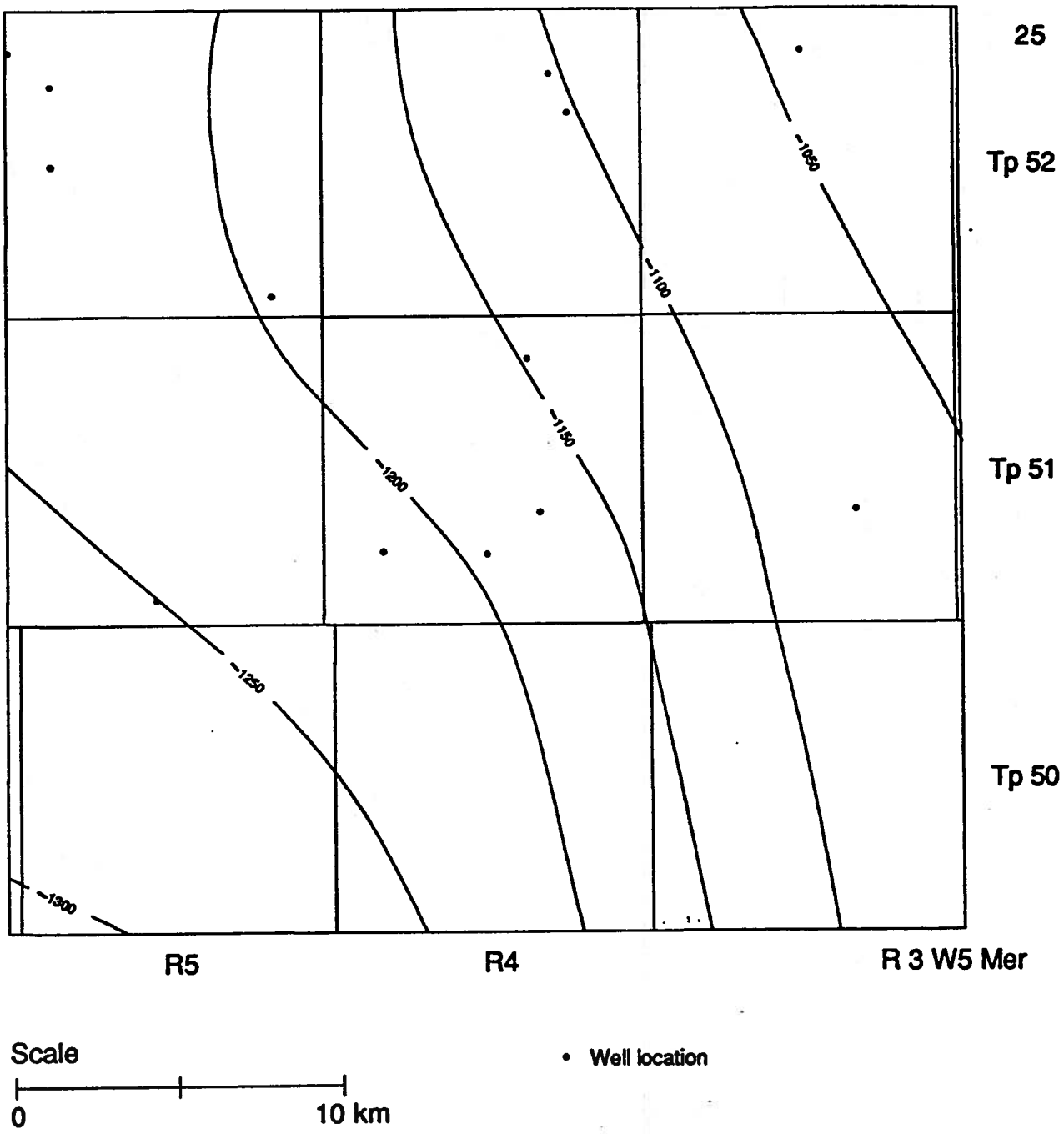

Figure 14. Structure top elevation (m) of the Nisku Formation.

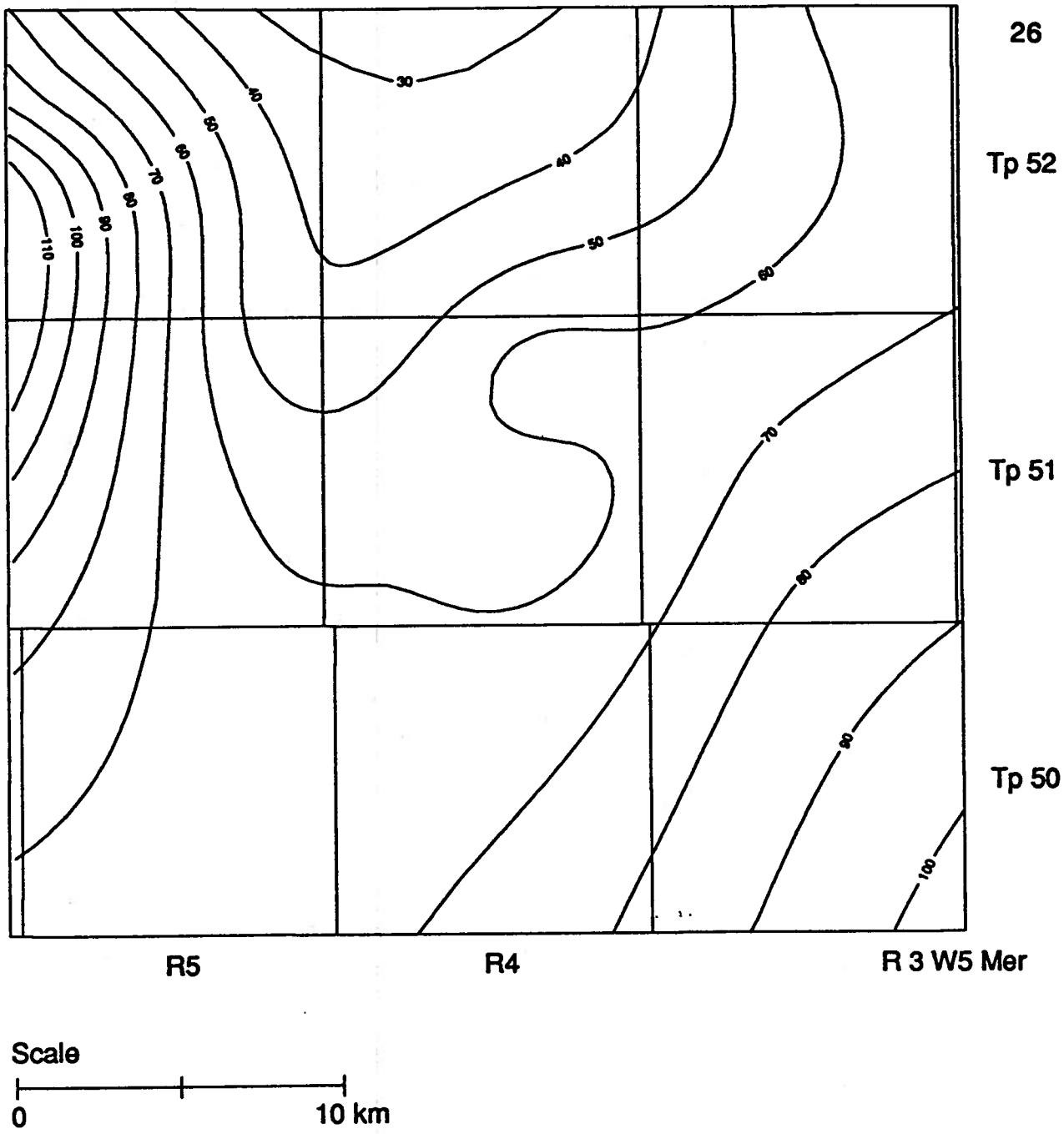

Figure 15. Isopach (m) of the Nisku aquifer.

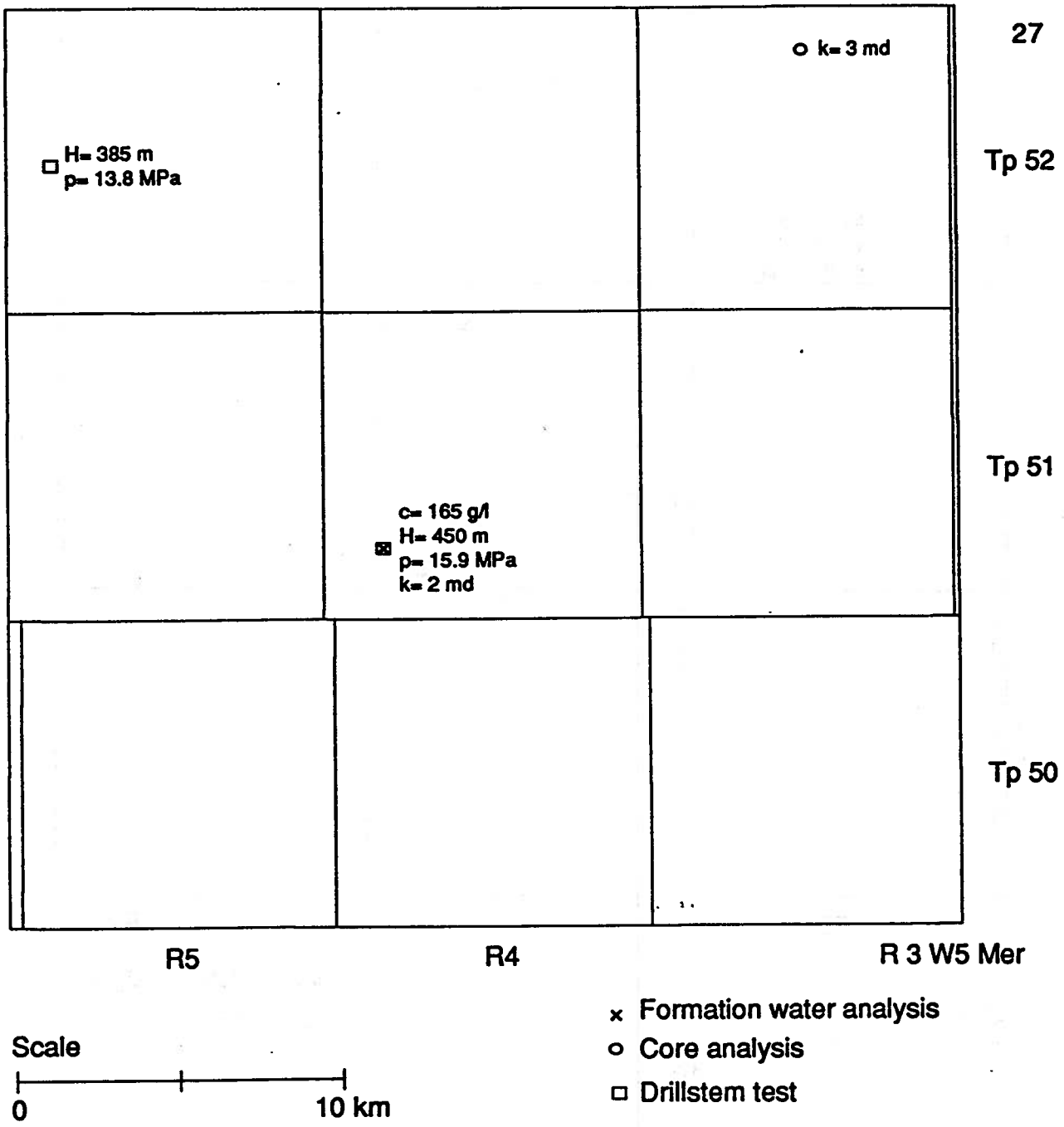

Figure 16. Distribution of wells with core, drillstem test and formation analysis data in the Wabamun aquifer.

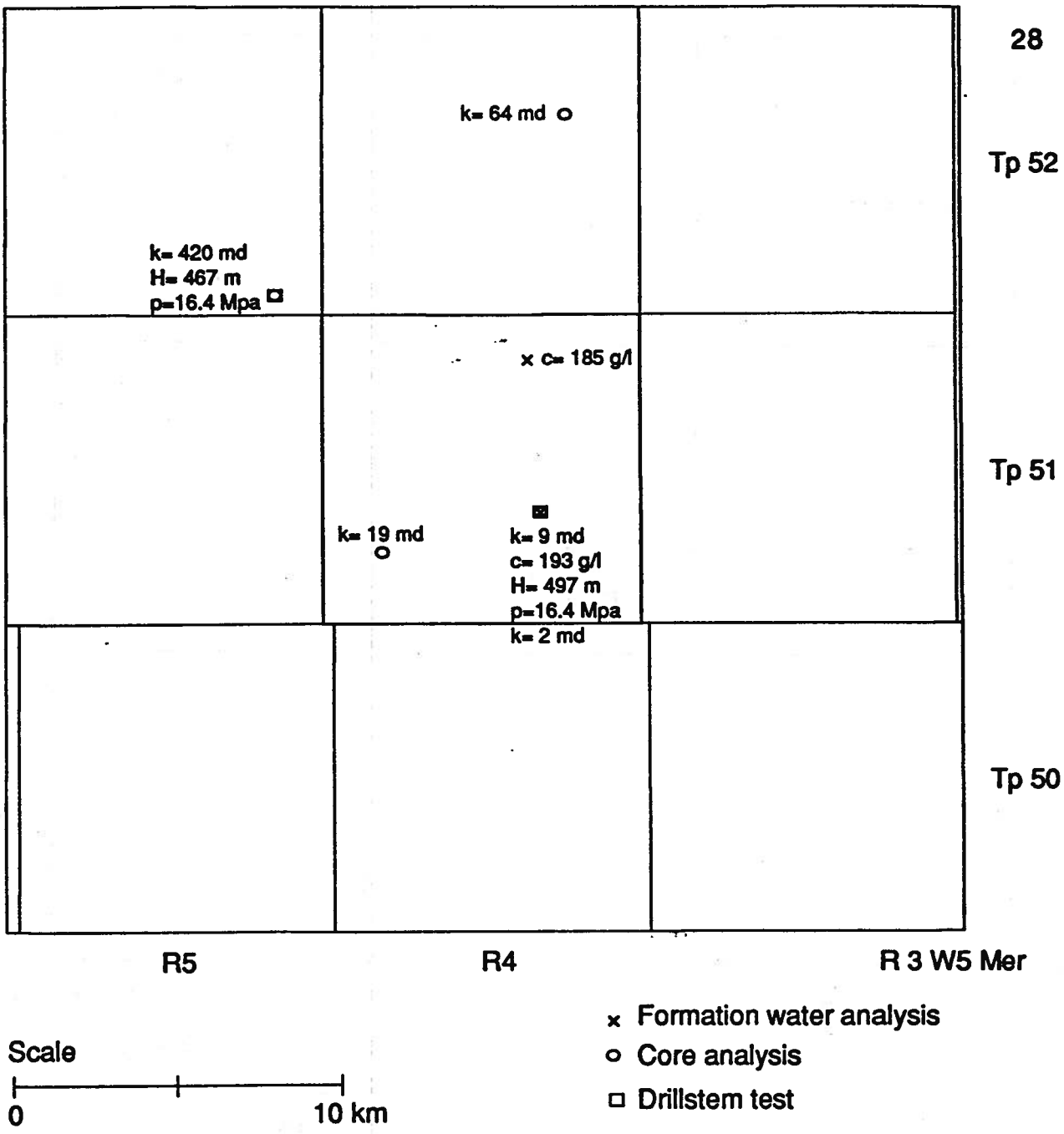

Figure 17. Distribution of wells with core, drillstem test and formation analysis data in the Nisku aquifer.

4.2.1 Permeability and Porosity

Rock permeability was measured in both core and drillstem tests. The two types of measurement represent different scales. Core analysis data represent volume-averaged values corresponding to the plug scale (cm), while drillstem test data correspond to the well scale (m). Only one drillstem test each in the Wabamun-Winterburn and Nisku aquifers contain data which allow permeability calculations. The corresponding values are 10^{-15} m^2 (1 md) for the Wabamun-Winterburn aquifer, and 2 x 10^{-15} m^2 (2 md) for the Nisku aquifer. Permeability was measured for 9 plugs from a single well in the Wabamun-Winterburn aquifer, and for 153 plugs from core taken in 4 wells penetrating the Nisku aquifer. The plug-scale permeability data exhibit a very high variability, spanning several orders of magnitude. Measured values vary from less than 10^{-15} m^2 (1 md) to 4 x 10^{-11} m^2 (40,000 md), indicating high vertical and lateral variability. Effective well-scale permeability values are obtained from plug-scale measurements using a generalized weighted mean (power average) (Bachu, 1991; Desbarats and Bachu, 1994). The well-scale permeability value for the Wabamun-Winterburn well with core data is 3 x 10^{-15} m^2 (3 md). The well-scale permeability values for the four Nisku wells with core data vary between 9 x 10^{-15} m^2 and 4.2 x 10^{-13} m^2 (9 and 420 md, respectively), with an average of 4.7 x 10^{-14} m^2 (47 md). The vertical anisotropy (k_v/k_h) of the Nisku aquifer is 0.27, calculated on the basis of 83 plug analyses containing measurements of both horizontal and vertical permeability. No similar information is available in the study area for the Wabamun-Winterburn aquifer. The data, although scarce, show that the permeability of these carbonate aquifers is generally low, of the same order of magnitude as for the siliciclastic Glauconitic Sandstone aquifer studied previously, but that zones of very high permeability exist. Thus, it seems that favourable conditions exist for CO_2 injection and hydrodynamic entrapment, namely high near-well permeability and low far-field permeability (Bachu et al., 1994).

Rock porosity is measured only on core plugs. Again data scarcity and measurement

scale preclude a proper aquifer characterization, particularly when fracture and vuggy porosity is not measured and taken into account. The average plug-scale porosity for both Wabamun-Winterburn and Nisku aquifers is 6-8%.

4.2.2 Formation Water

As mentioned previously, very few formation water analyses and drillstem tests are available for the Wabamun-Winterburn interval in the study area. After applying various automatic and manual culling procedures for standard formation water analyses (Hitchon and Brulotte, 1994), only one analysis was retained for the Wabamun-Winterburn aquifer (Figure 16) and two for the Nisku aquifer (Figure 17 and Appendix I). The salinity of Wabamun formation water is high (165,000 mg/l total dissolved solids). The salinity for the deeper Nisku aquifer is higher, in the 190,000 mg/l range, consistent with the general pattern for the Alberta basin (Bachu, 1995).

The very few pressure measurements from drillstem tests available for both aquifers do not allow construction of potentiometric surfaces and determination of flow directions. Measured pressures in the Wabamun-Winterburn aquifer vary between 13.8 and 15.9 MPa, while in the Nisku aquifer they are of the order of 16.4 MPa. Since pressure normally varies with depth, these values are not indicative as such if these aquifers are under hydrostatic conditions or not. The freshwater hydraulic heads corresponding to these measured pressures are 385 m to 459 m for the Wabamun-Winterburn aquifer, and 467 m to 497 m for the Nisku aquifer. Compared with ground surface elevations in the 700-800 m range, these hydraulic head values show that both aquifers are under pressured with respect to hydrostatic conditions, a situation which is favorable for CO_2 injection. The differences in hydraulic head values between the two aquifers, although not conclusive because of data scarcity, indicate that the intervening thin Calmar aquitard is strong enough to separate the flow systems in these two aquifers. On a regional scale, the flow direction in the Wabamun-Winterburn and Nisku aquifers is north-northeastward (Bachu, 1995).

The temperature of formation waters increases with depth, such that no single value can be used to characterize the aquifers in the study area. However, temperature can be estimated based on depth, geothermal gradient and multi-annual average ground temperature. In the study area, the last two have values of 5.6°C and 30°C/km (Bachu and Burwash, 1991). For depths varying between 1520 m and 2190 m, the corresponding temperature variation in the two aquifers is in the range of 51-71°C, depending on location.

For the estimated or measured ranges of temperature, pressure and salinity variations characteristic of the Wabamun-Winterburn and Nisku aquifers, the variations in formation water properties are: 1140-1150 kg/m^3 for density, 750-900 μPa.s for dynamic viscosity, and 0.65 - 0.80 μm^2/s for kinematic viscosity. Given the low range of salinity variation, the last two depend more on temperature variations, hence on depth, than on the concentration of dissolved solids.

Based on the available information, it seems that the Nisku aquifer, although deeper and thinner than the overlying Wabamum-Winterburn aquifer, is more suitable for CO_2 injection because of generally higher average permeability and because of the potential of finding areas of extremely high permeability favourable to maintaining low injection pressures or achieving high injection rates.

5. SETUP AND PROPERTIES DEFINED FOR NUMERICAL SIMULATIONS

The objective of this numerical study is to investigate the injectivity and capacity of two selected aquifers in the Lake Wabamun area in central Alberta, Canada, to accept large quantities of CO_2 injected in the supercritical state and to retain them for long periods of time. Two aquifers, the thin siliciclastic Glauconitic Sandstone aquifer (13 m thick on average) and the relatively thick carbonate Nisku aquifer (60 m thick on average), were selected based on their confinement, properties and groundwater flow characteristics obtained from hydrogeological analysis.

A 2-D (= two dimensional) radial pattern numerical simulation around a single vertical injector was used which allowed CO_2 to be injected into either the Glauconitic Sandstone aquifer or the Nisku aquifer. The location of this injector was chosen near the southeast corner of Tp. 52, R4 W5 Mer (Figure 18) based on existing well data. The hydrogeological analysis of the Glauconitic Sandstone aquifer (Figure 28, Gunter et al., 1994), this injector was anticipated to be located in a "sweet" zone, that is a **zone of locally high permeability** of approximately 100 md surrounded by a low permeability region of 2 to 25 md.

5.1 Aquifer Properties Used in Simulations

5.1.1 Aquifer Characteristics

Based on the hydrogeological analysis of the Glauconitic Sandstone (Gunter et al., 1994; summarized in Chapter II of this report) and the Nisku (Chapter IV of this report) aquifers, the aquifer characteristics near the selected injector location are given in Table 2. The average aquifer temperature was estimated based on a ground surface average temperature of 6°C and a geothermal gradient in the area of approximately 30°C/km (Bachu and Burwash, 1991).

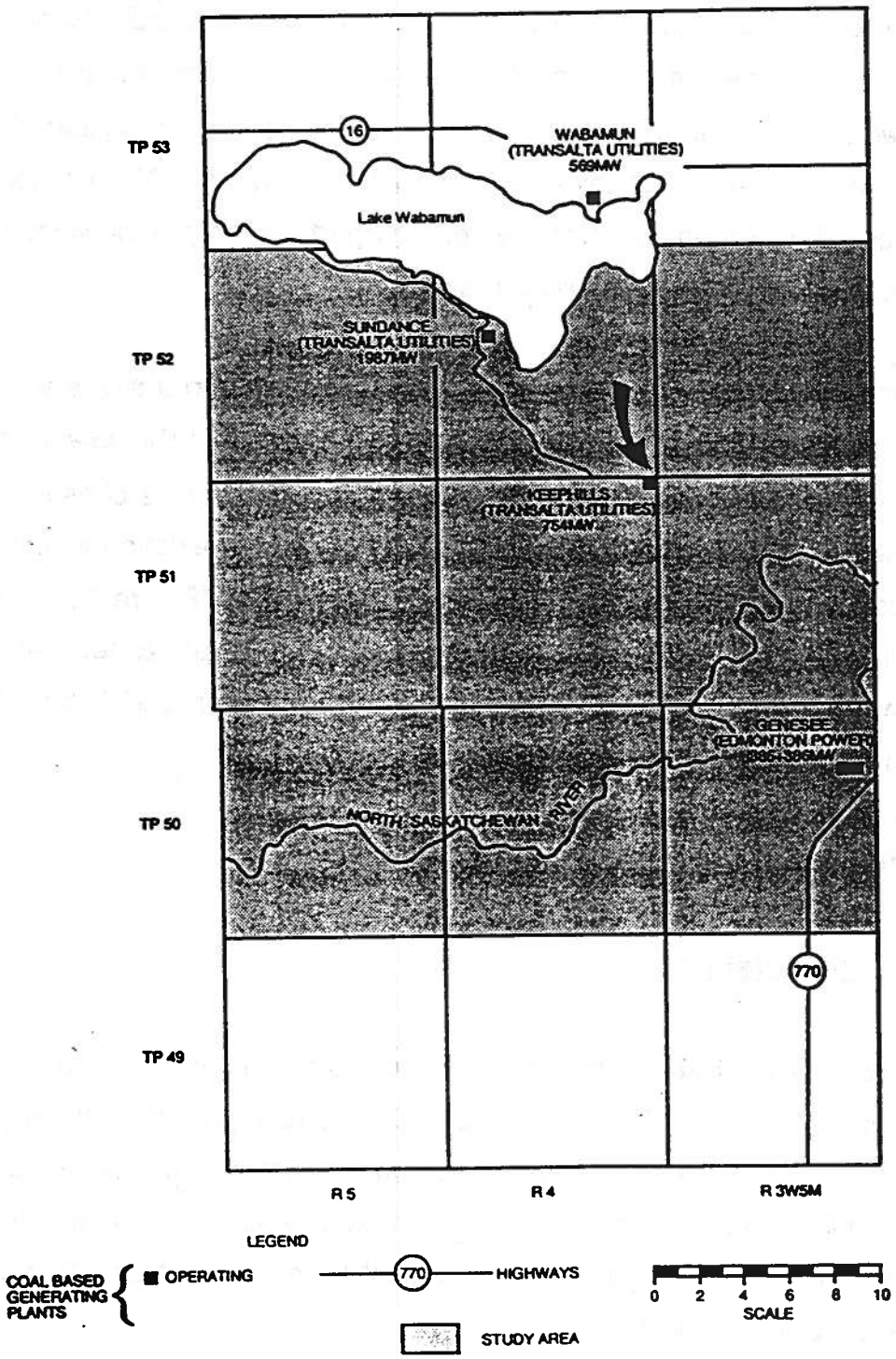

Figure 18: Selection of CO_2 disposal site in Lake Wabamun area

	Glauconitic Sandstone	Nisku
Depth at the Injection Site:	1480 m	1860 m
Average Thickness at Inj. Site:	13 m	60 m
Aquifer Slope (dip to southwest):	5 m/km	8.9 m/km
Porosity:	6 - 12%	6 - 12%
Absolute Permeability:		
Horizontal:	6.2 - 100 md	6.2 - 400 md
Vertical Anisotropy:	0.3	0.27
Average Temperature:	50°C	60°C
Pressure at Top of Aquifer:	12.4 MPa	16.0 MPa
Fracture Pressure:	33.5 MPa	42.1 MPa

Table 2: Aquifer characteristics used in numerical simulation

A compressibility of 4.5 x 10^{-7} /kPa was used for both the sandstone and the carbonate in the numerical simulation. The fracture pressure at the top of the aquifer was estimated based on a gradient of 22.61 MPa/km (i.e. 1 psi/ft) that related the minimum principal stress to the weight of the overburden.

In the numerical simulation, the following assumptions were made:

- The aquifers are homogeneous except for the cases where a "sweet" zone existed.
- The thickness of the aquifers were uniform.
- The small dip of the aquifers to the southwest is negligible for the purpose of this study and, therefore, was ignored.
- The CO_2 in the aquifer was in the supercritical state and was treated as a single phase fluid which had properties between a gas and a liquid.
- The relative permeability curves for the CO_2-water system shown in Figure 19 were not measured but are considered typical curves for the water-oil system in Alberta oil reservoirs with a zero residual CO_2 saturation.
- The capillary pressure effect may not be significant, as the pressure changes (in the order of 1 - 10 MPa) during CO_2 injection were believed to be few orders of magnitude higher than the estimated, and therefore, was neglected capillary pressure.

5.1.2 Fluid Properties

The properties of the aqueous and the supercritical CO_2 phases in the Glauconitic Sandstone and the Nisku aquifers are given in Table 3. The density and viscosity of the formation water are taken from Rowe and Chou (1970) and Kestin et al. (1981), respectively. For the Glauconitic Sandstone aquifer, the density of CO_2 at 50°C varies from 696 kg/m^3 at 12.4 MPa to 888 kg/m^3 at 30 MPa over the range of pressures

End Point for CO_2 Relative Permeability Curve = 0.8

End Point for Water Relative Permeability Curve = 1.0

Residual CO_2 Saturation = 0

Irreducible Water Saturation = 0.11

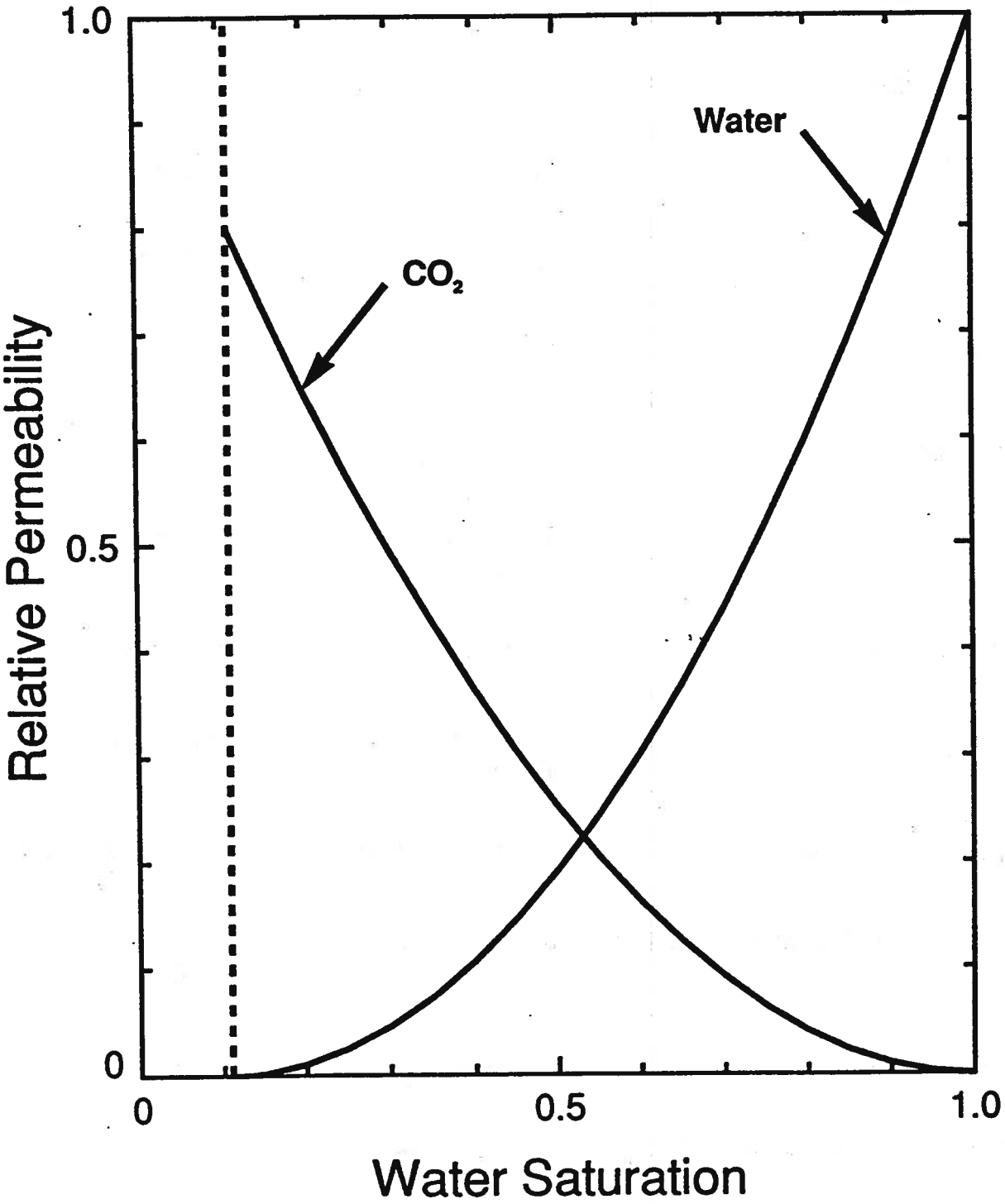

Figure 19: Relative permeability curves for CO_2-water system

	Glauconitic Sandstone	Nisku
Temperature at the Inj. Site:	50°C	60°C
Aqueous Phase		
Salinity:	40,000 mg/l	190,000 mg/l
Density:	1030 kg/m^3	1155.5 kg/m^3
Viscosity:	0.617 mPa-s	0.840 mPa-s
CO_2 Phase		
Density:	696 kg/m^3 @ 12.446 MPa	713 kg/m^3 @ 16 MPa
Compressibility:	1.22 x 10^{-5} /kPa	8.92 x 10^{-6} /kPa
Viscosity:	0.068 mPa-s @ 20 MPa	0.081 mPa-s @ 30 MPa
Dispersion Coefficient in Water:	3.074 x 10^{-4} m^2/d	3.707 x 10^{-4} m^2/d
CO_2-Water Equilibrium Constant:	0.0603 @ 20 MPa	0.0760 @ 30 MPa

Table 3: Fluid properties used in numerical simulation

encountered during CO_2 injection. For the Nisku aquifer, the density of CO_2 at 60°C varies from 713 kg/m^3 at 16 MPa to 887 kg/m^3 at 38 MPa. These CO_2 density values were estimated using a linear regression based on the published data (Clark, 1966) of CO_2 specific volumes (i.e. reciprocal of densities) versus pressure at different temperatures, as shown in Figure 20.

For the Glauconitic Sandstone aquifer, the viscosities of CO_2 at 50°C varied from approximately 0.050 mPa-s at 12.4 MPa to 0.088 mPa-s at 30 MPa (McHugh and Krukonis,1986). A constant intermediate value of 0.068 mPa-s chosen at 20 MPa was used in the numerical simulation. On the other hand, for the Nisku aquifer, the viscosities of CO_2 at 60°C varied from approximately 0.050 mPa-s at 16 MPa to 0.091 mPa-s at 40 MPa. A constant intermediate value of 0.081 mPa-s chosen at 30 MPa was used in the numerical simulation. The effect of pressure on the CO_2 viscosity over the 12 to 40 MPa pressure range during CO_2 injection was minor and was neglected in this numerical study.

In the numerical simulation, CO_2 was allowed to dissolve in the aqueous phase due to the high solubility of CO_2 in water. However, the solubility of water in CO_2 is relatively small and was neglected in the numerical simulation. It is noted that the CO_2 dissolved into the aqueous phase was assumed not to change the water density at the pressures and temperatures of modelling. The equilibrium K-values for CO_2 in water (i.e. the mole fraction of CO_2 in the aqueous phase divided by the mole fraction of CO_2 in the CO_2 phase) as functions of pressure and temperature were estimated using the linear correlations given in Figure 21. In these correlations, the effect of the salinity of the water on CO_2 solubility was not considered. For the Glauconitic Sandstone aquifer, the K-values for CO_2 in water at 50°C varied from 0.0375 at 12.4 MPa to 0.0902 at 30 MPa. For the Nisku aquifer, the K-values for CO_2 in water at 60°C vary from 0.0404 at 16 MPa to 0.0960 at 38 MPa.

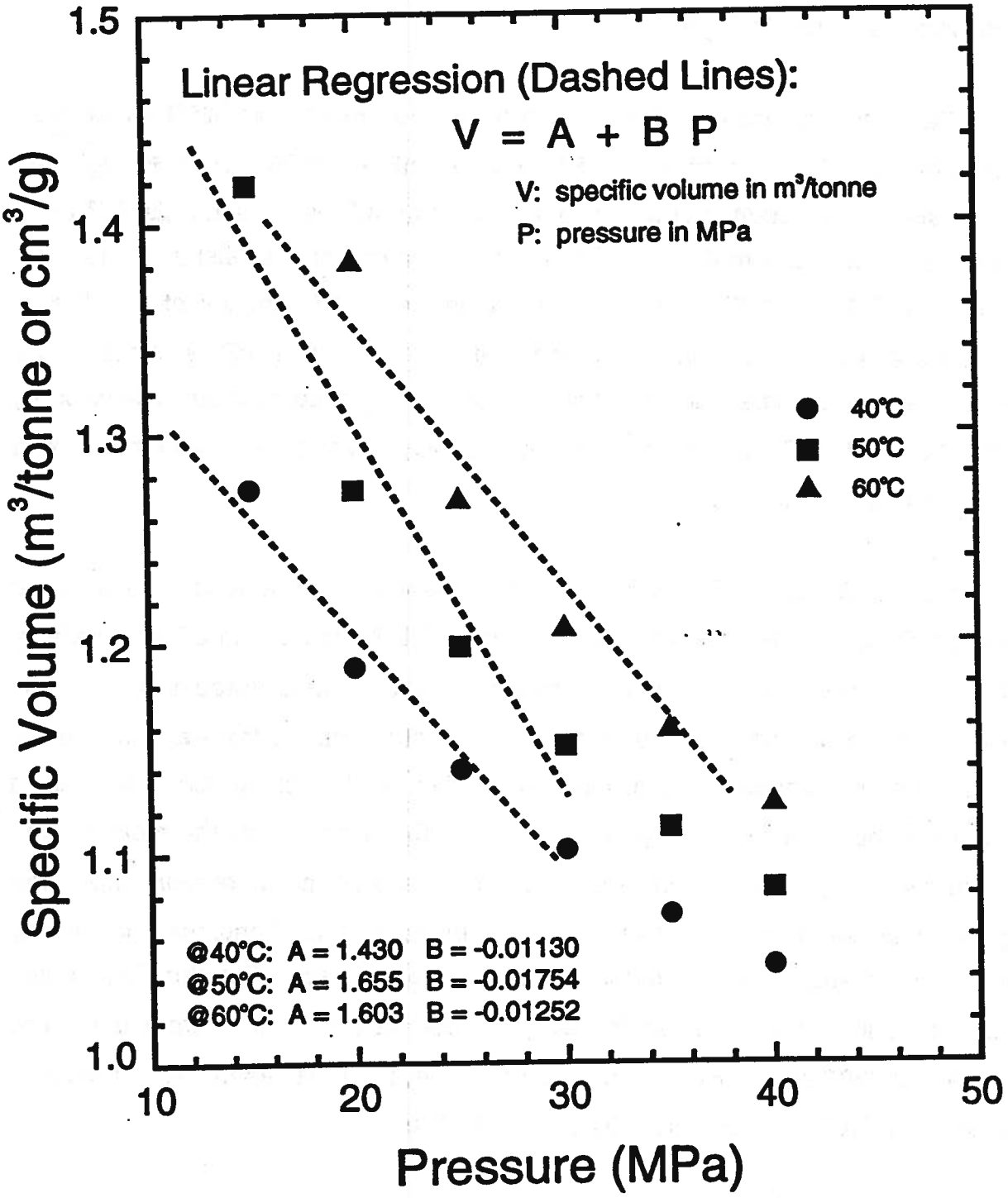

Figure 20: Specific volume of supercritical CO_2

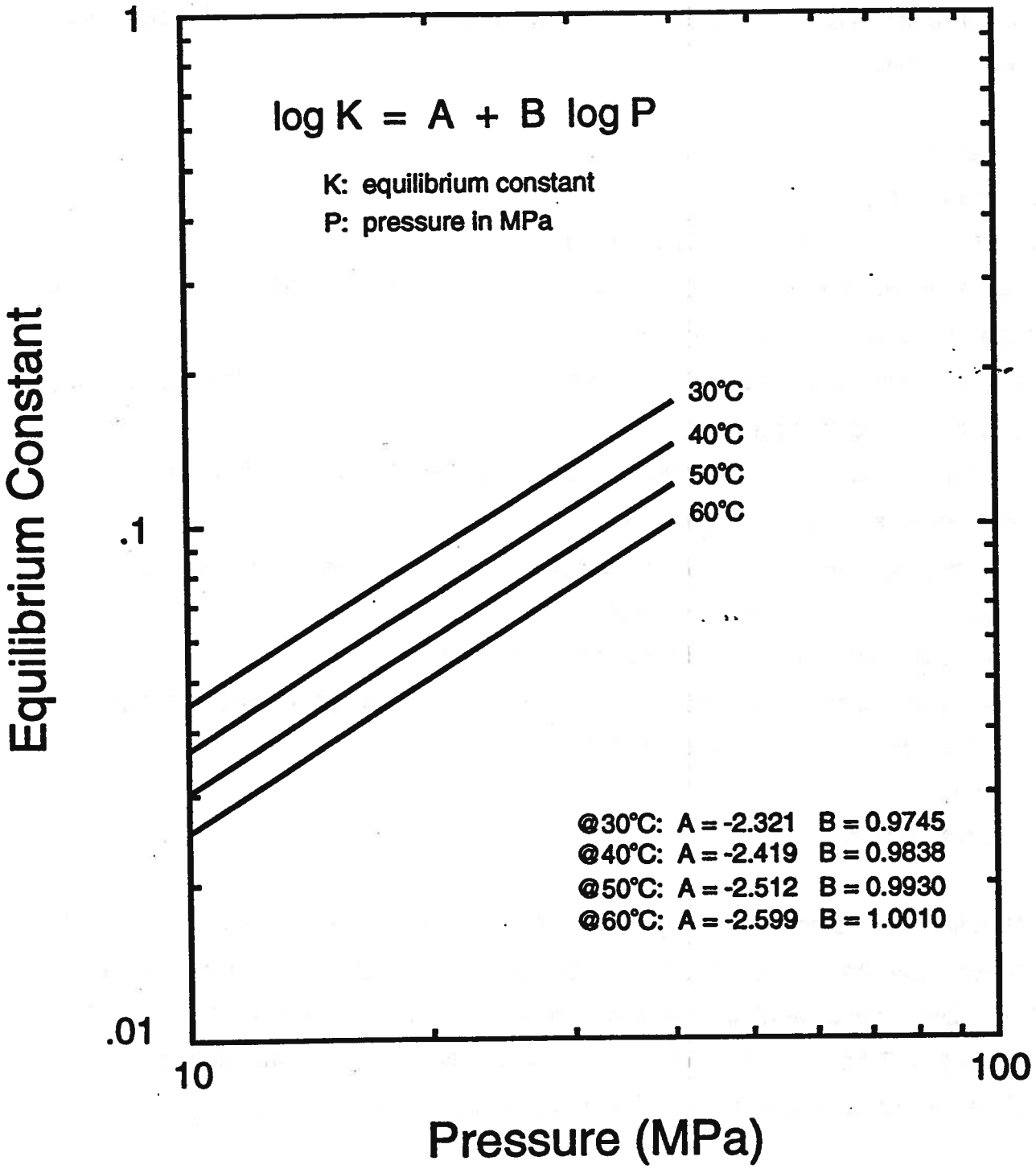

Figure 21: Equilibrium constant for CO_2-water system

5.2 Numerical Simulator

The multi-phase, multi-component numerical simulator STARS (1990), developed by the Computer Modelling Group (CMG) in Calgary, Alberta, Canada, was used in this numerical study. Some of the features of the STARS model used in the numerical simulation include:

- isothermal;
- 2-D radial grid system;
- 2 phases (i.e. CO_2 and aqueous phase);
- 2 components (i.e. formation water, and CO_2 both as a separate phase in the supercritical state and dissolved in water);
- pressure and temperature dependent equilibrium K-values describing CO_2 solubility in aqueous phase;
- flows of injected CO_2 and aquifer water governed by Darcy's law (i.e. relative permeabilities for CO_2-water system);
- semi-analytical aquifer model for calculating water flow at the outflow boundary (Appendix 11.4.1, Gunter et al., 1993b);
- total mobility weighted, multi-block vertical injector; and
- radial flow well model fully coupled to the aquifer through an analytical solution at the boundaries of the numerical model.

5.3 Grid Pattern

A 2-D radial grid system with 132 gridblocks (i = 66, j = 1, k = 2) and 330 (i = 66, j = 1, k = 5) was used to partition into blocks, a 7 km region around a vertical wellbore in both the Glauconitic Sandstone and the Nisku aquifers (Figure 22). At the outflow boundary (i.e. 7 km from the injector), a semi-analytical aquifer model was used to calculate the outward water flow from this region into an infinite aquifer.

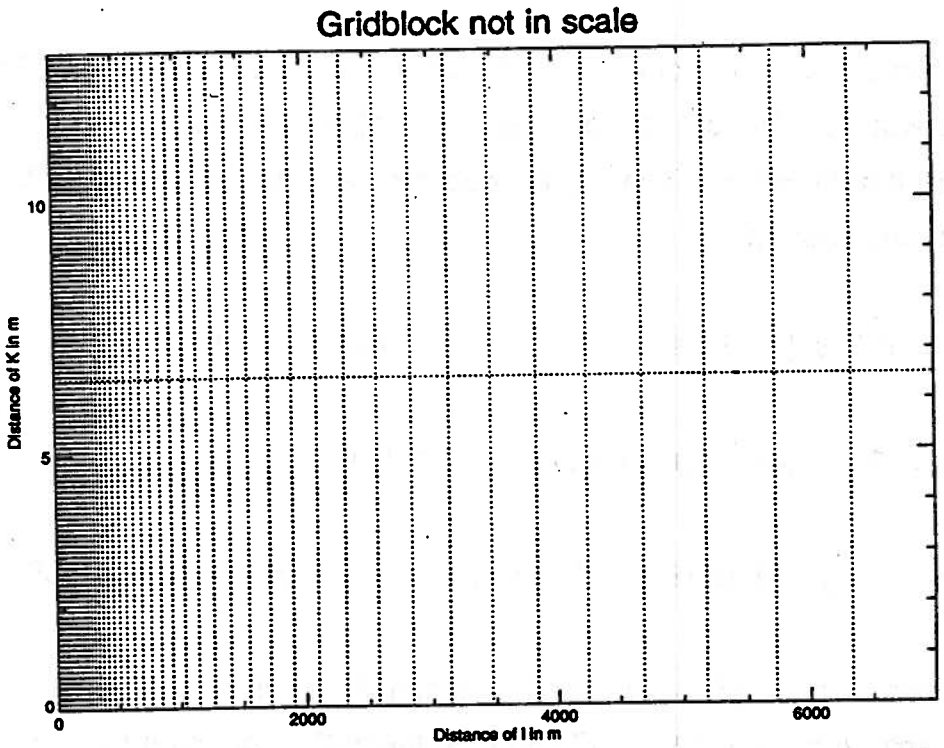

(a) Glauconitic Sandstone aquifer (66 × 1 × 2)

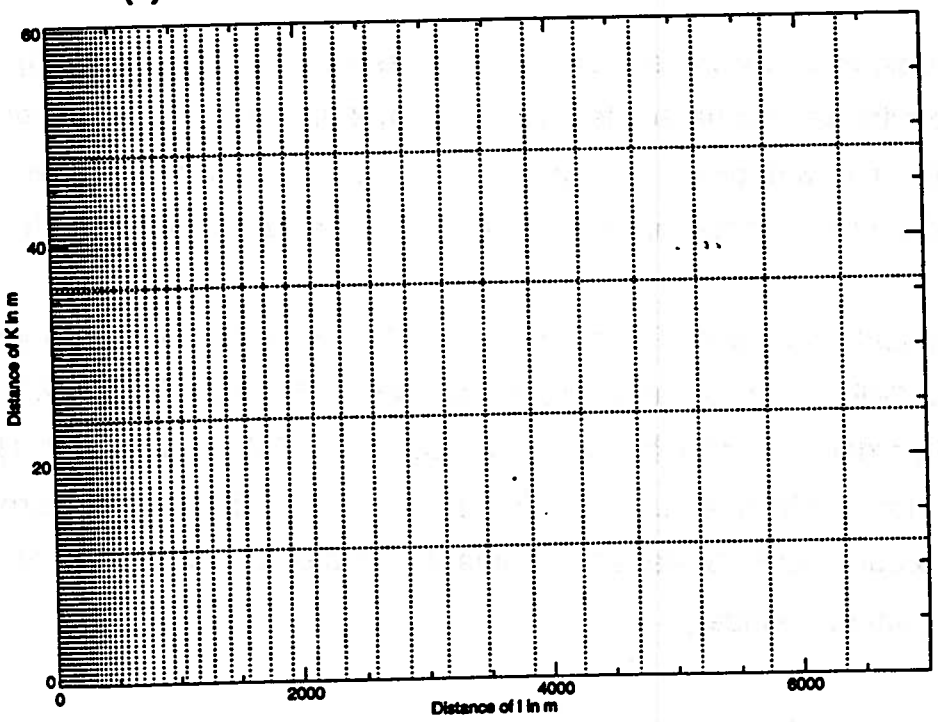

(b) Nisku Carbonate aquifer (66 × 1 × 5)

Figure 22: 2-D radial grid system

The 66 gridblocks in the radial direction (i-direction) cover a distance of 7 km. The gridblock sizes were set based on an exponential stretch which allowed increasing resolution near the injector. The radial coordinate was transformed to a new coordinate (r) by the relation:

$$r_i = 9.503\ (e^{0.10005\,(i-1)} - 1) \quad \text{for } i = 1, 2, \ldots\ldots, 67 \qquad (1)$$

where: $r_1 = 0$ m, $r_2 = 1$ m, and $r_{67} = 6999.2$ m

and $$(r_{i+1} - r_i) = 1.105226^{(i-1)} \times (r_2 - r_1) \quad \text{for } i = 1, 2, \ldots\ldots, 66 \qquad (2)$$

It should be noted that the gridblock size in the radial direction (i-direction) vary from 1 m near the injector (i.e. $r_2 - r_1$) to 667.3 m near the outflow boundary (i.e. $r_{67} - r_{66}$).

A singular gridblock with a dimension of 360° was used in the angular (j) direction. For the Glauconitic Sandstone aquifer (13 m thick), 2 uniform gridblocks were used in the axial (k) direction with dimensions of 6.5 m each. For the Nisku aquifer, 5 uniform gridblocks in the axial (k) direction were used with dimensions of 12 m each.

In some numerical simulations for the Nisku aquifer with high permeability values of 100-400 md, a 2-dimensional radial grid system with 375 gridblocks (i = 75, j = 1, k = 5) was used in order to extend the outflow boundary to 17.2 km (Equation 1) from the injector. The increase in number of gridblocks from 66 to 75 in the radial direction was necessary in order to ensure that at any time during the simulated injection, CO_2 did not reach the outflow boundary.

5.4 Injection Strategies

In most numerical simulations, pure CO_2, at the average aquifer temperature, was

injected at a constant injection pressure which was set to 90% of the fracture pressure at the top of the aquifer. The injection pressures were 30.12 MPa and 37.86 MPa for the Glauconitic Sandstone and Nisku aquifers, respectively. In a few numerical simulations for the Glauconitic Sandstone aquifer, an injection pressure of 25.15 MPa (i.e. 2 times the initial hydrostatic pressure at the bottom of the aquifer) was used in order to investigate the effect of injection pressure on the injectivity of the CO_2.

The injector radius was set to 0.0762 m (or 3"). In all the numerical simulations except one, the vertical injector was completed at an interval covering the entire thickness of the aquifer (13 m for the Glauconitic Sandstone aquifer and 60 m for the Nisku aquifer). In the case of one numerical simulation for the Nisku aquifer, the injector was completed for an interval of 13 m at the bottom of the aquifer in order to investigate the effect of completion size on the injectivity of CO_2. It was noted in previous numerical simulations (Gunter et al., 1993b), the injector radius had very little effect on the injectivity of CO_2 in a hypothetical aquifer in the Lake Wabamun area. On the other hand, in the same study (Gunter et al., 1993a) has shown that the effect of completion length on the injectivity of CO_2 was quite significant as the injectivity increased with the size of the completion interval.

5.5 Numerical Simulations

Characteristics of numerical simulations for the Glauconitic Sandstone and the Nisku aquifers are given in Tables 4 and 5, respectively. All the numerical simulations which is considered a 30-year CO_2 injection period, were conducted to examine the CO_2 injectivity in deep aquifers in the Lake Wabamun area for a whole series of parameters including aquifer depth and thickness, properties of host rock and water (i.e. porosity, permeability, salinity and temperature), and injection characteristics (e.g. injection pressure and injector completion).

All numerical simulations were performed on a Sun Workstation, SPARC station 2.

Typical runs with 132 and 330 gridblocks took approximately 1 and 4 CPU hours, respectively.

Homogeneous Glauconitic Sandstone Aquifer

Radial Grid System: 66 x 1 x 2 (location of outflow boundary = 7 km)
Injector Radius = 0.0762 m Injector Completion = 13 m

Run No.	Porosity	Horizontal Permeability	Injection Pressure
CO2_60	0.12	6.2 md	25.15 MPa
CO2_61	0.12	30 md	25.15 MPa
CO2_62	0.12	100 md	25.15 MPa
CO2_71	0.12	6.2 md	30.12 MPa
CO2_72	0.12	30 md	30.12 MPa
CO2_73	0.12	100 md	30.12 MPa
CO2_74	0.06	6.2 md	30.12 MPa
CO2_75	0.06	30 md	30.12 MPa
CO2_76	0.06	100 md	30.12 MPa

Table 4: Characteristics of the numerical simulations for CO_2 injection in the Glauconitic Sandstone aquifer

Heterogeneous Glauconitic Sandstone Aquifer

Radial Grid System: 66 x 1 x 2 (location of outflow boundary = 7 km)
Injector Radius = 0.0762 m Injector Completion = 13 m

Horizontal Permeability = 100 / 6.2 md

Run No.	Porosity	Radius of 100 md Zone	Injection Pressure
CO2_80	0.12	0.51 km	30.12 MPa
CO2_81	0.12	1.04 km	30.12 MPa
CO2_82	0.12	2.10 km	30.12 MPa

Horizontal Permeability = 100 / 30 md

Run No.	Porosity	Radius of 100 md Zone	Injection Pressure
CO2_83	0.12	0.51 km	30.12 MPa
CO2_84	0.12	1.04 km	30.12 MPa
CO2_85	0.12	2.10 km	30.12 MPa

Table 4: Characteristics of the numerical simulations for CO_2 injection in the Glauconitic Sandstone aquifer (continued)

Homogeneous Nisku Aquifer

Radial Grid System: 66 x 1 x 5 (location of outflow boundary = 7 km)
Injector Radius = 0.0762 m Injector Completion = 60 m

Run No.	Porosity	Horizontal Permeability	Injection Pressure
CO2_109	0.12	6.2 md	37.86 MPa
CO2_108	0.12	30 md	37.86 MPa
CO2_107	0.12	100 md	37.86 MPa
CO2_106*	0.12	400 md	37.86 MPa
CO2_102	0.06	6.2 md	37.86 MPa
CO2_103	0.06	30 md	37.86 MPa
CO2_104*	0.06	100 md	37.86 MPa
CO2_105*	0.06	400 md	37.86 MPa
CO2_101**	0.06	6.2 md	37.86 MPa

* Radial Grid System: 75 x 1 x 5 (location of outflow boundary = 17.2 km)
** Injector Completion = 13 m (bottom of aquifer)

Table 5: Characteristics of the numerical simulations for CO_2 injection in the Nisku aquifer

Heterogeneous Nisku Aquifer

Radial Grid System: 66 × 1 × 5 (location of outflow boundary = 7 km)
Injector Radius = 0.0762 m Injector Completion = 60 m

Horizontal Permeability = 100 / 6.2 md

Run No.	Porosity	Radius of 100 md Zone	Injection Pressure
CO2_110	0.12	0.51 km	37.86 MPa
CO2_111	0.12	1.04 km	37.86 MPa
CO2_112	0.12	2.10 km	37.86 MPa

Horizontal Permeability = 100 / 30 md

Run No.	Porosity	Radius of 100 md Zone	Injection Pressure
CO2_113	0.12	0.51 km	37.86 MPa
CO2_114	0.12	1.04 km	37.86 MPa
CO2_115	0.12	2.10 km	37.86 MPa

Table 5: Characteristics of the numerical simulations for CO_2 injection in the Nisku aquifer (continued)

Heterogeneous Nisku Aquifer

Radial Grid System: 66 × 1 × 5 (location of outflow boundary = 7 km)
Injector Radius = 0.0762 m Injector Completion = 60 m

Horizontal Permeability = 400 / 6.2 md

Run No.	Porosity	Radius of 400 md Zone	Injection Pressure
CO2_116	0.12	0.51 km	37.86 MPa
CO2_117	0.12	1.04 km	37.86 MPa
CO2_118	0.12	2.10 km	37.86 MPa

Horizontal Permeability = 400 / 30 md

Run No.	Porosity	Radius of 400 md Zone	Injection Pressure
CO2_119	0.12	0.51 km	37.86 MPa
CO2_120	0.12	1.04 km	37.86 MPa
CO2_121	0.12	2.10 km	37.86 MPa

Table 5: Characteristics of the numerical simulations for CO_2 injection in the Nisku aquifer (continued)

6. NUMERICAL RESULTS FOR THE GLAUCONITIC SANDSTONE AQUIFER

Numerical predictions of cumulative CO_2 injection, CO_2 injection rate, CO_2 saturation contours and pressure distribution near the bottom of the aquifer as a function of time are given in Appendix II for all the numerical simulations of injecting CO_2 in the Glauconitic Sandstone aquifer.

For the thin siliciclastic Glauconitic Sandstone aquifer, realistically, disposal of 2.8×10^6 to 2.2×10^7 tonnes of CO_2 over a period of 30 years can be achieved which corresponded to average CO_2 injection rates ranging from 128 to 2,009 t/d/well. Approximately 17 to 22 wt% of the injected CO_2 dissolved in the aqueous phase at the average aquifer temperature of 50°C. Even for this thin aquifer (13 m thick), there is evidence of CO_2 override to the top part of the aquifer. In general, CO_2 propagated less than 5 km away from the injector after an injection period of 30 years, except for the case of the highest permeability (i.e. 100 md) and the lowest porosity (i.e. 0.06).

6.1 Effect of Injection Pressure

The effect of injection pressure on CO_2 injection could be studied by comparing the results from two series of simulations, CO2_60-CO2_62 and CO2_71-CO2_73. A typical comparison of cumulative CO_2 injection and CO_2 injection rate for the case of porosity of 0.12 and horizontal permeability of 6.2 md is given in Figure 23. It was found that the injection pressure had a significant effect on the amount of CO_2 injected. For the same aquifer characteristics, approximately 50% more CO_2 could be injected when the injection pressure was increased from 25.15 to 30.12 MPa.

Glauconitic Sandstone Aquifer

EFFECT OF INJECTION PRESSURE

Aquifer Porosity = 0.12 Aquifer Permeability = 6.2 md (horizontal)

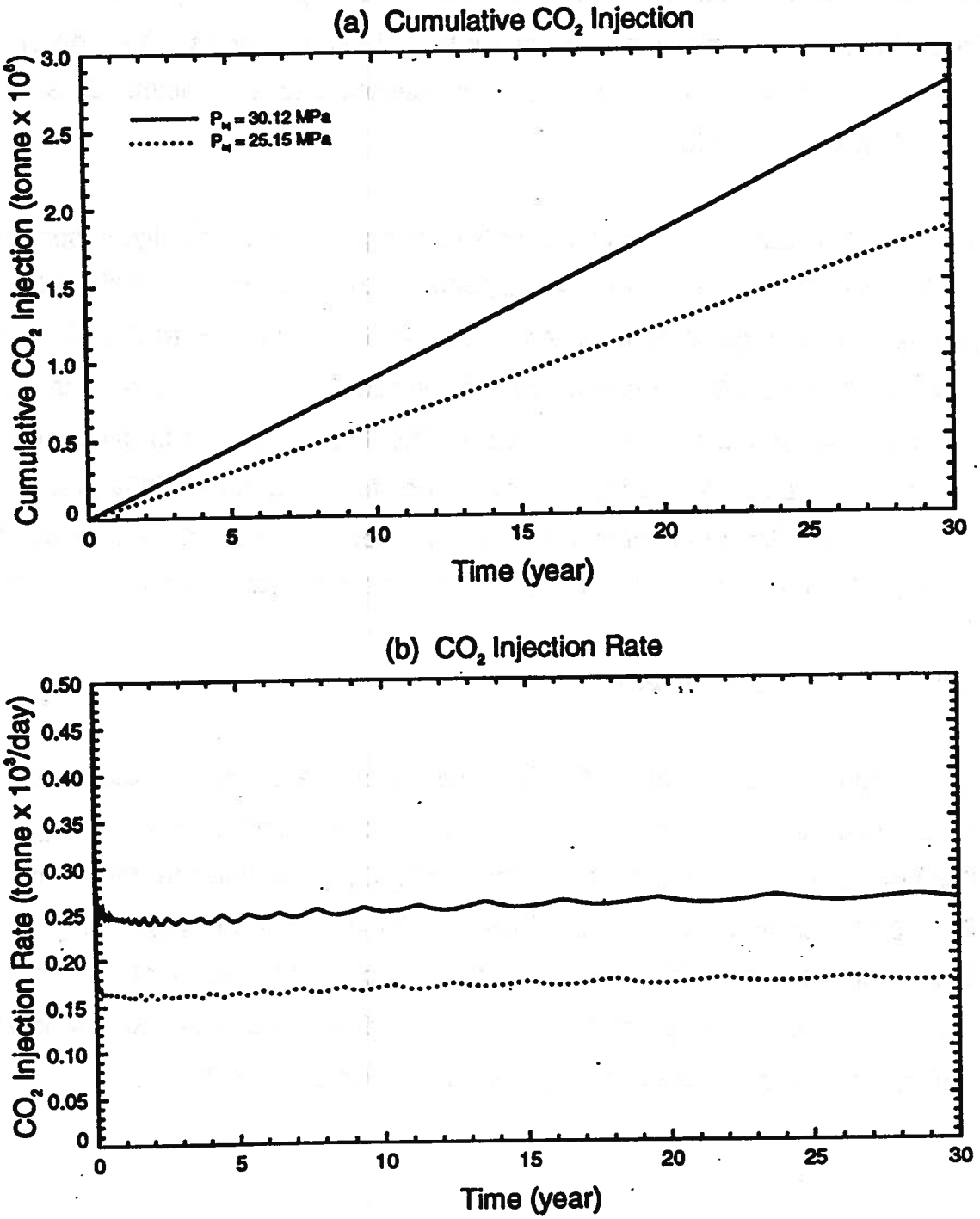

Figure 23: Effect of injection pressure on CO_2 injection for Glauconitic Sandstone aquifer

6.2 Effect of Porosity

The effect of porosity on CO_2 injection could be studied by comparing the results from two series of simulations, CO2_71-CO2_73 and CO2_74-CO2_76. A typical comparison of cumulative CO_2 injection and CO_2 injection rate for the case of horizontal permeability of 6.2 md and injection pressure of 30.12 MPa is given in Figure 24. It was found that the porosity had very little effect on the amount of CO_2 injected. For an aquifer having the same permeability, the amount of CO_2 injected was slightly higher and the aquifer pressurized slightly faster for the case of the lower porosity (i.e 0.06). But, as anticipated, CO_2 propagated farther away from the injector for the case of the lower porosity.

6.3 Effect of Permeability

The effect of permeability on CO_2 injection could be studied by comparing the results from the simulations CO2_71-CO2_73 for a porosity of 0.12 and simulations CO2_74-CO2_76 for a porosity of 0.06. Comparisons of cumulative CO_2 injection and CO_2 injection rate for porosities of 0.12 and 0.06 are shown in Figures 25 and Figure 26, respectively. It was found that the permeability had a very significant effect on the amount of CO_2 injected. For the same injection characteristics, a CO_2 volume more than 15 times higher could be injected when the permeability of the aquifer was increased from 6.2 to 100 md. Correspondingly, CO_2 propagation, away from the injector, increased from 1.2 km for a permeability of 6.2 md to 4.7 km for a permeability of 100 md for the case of 0.12 porosity. It was also found that the aquifer with a higher permeability pressurized faster than the aquifer with a lower permeability due to the higher injection rate.

The average water flow rates at the outflow boundary (7 km away from the injector), caused by CO_2 injection ranged from approximately 20 cm/yr for the aquifer with a

Glauconitic Sandstone Aquifer

EFFECT OF POROSITY

Aquifer Permeability = 6.2 md (horizontal)
Injection Pressure = 30.12 MPa

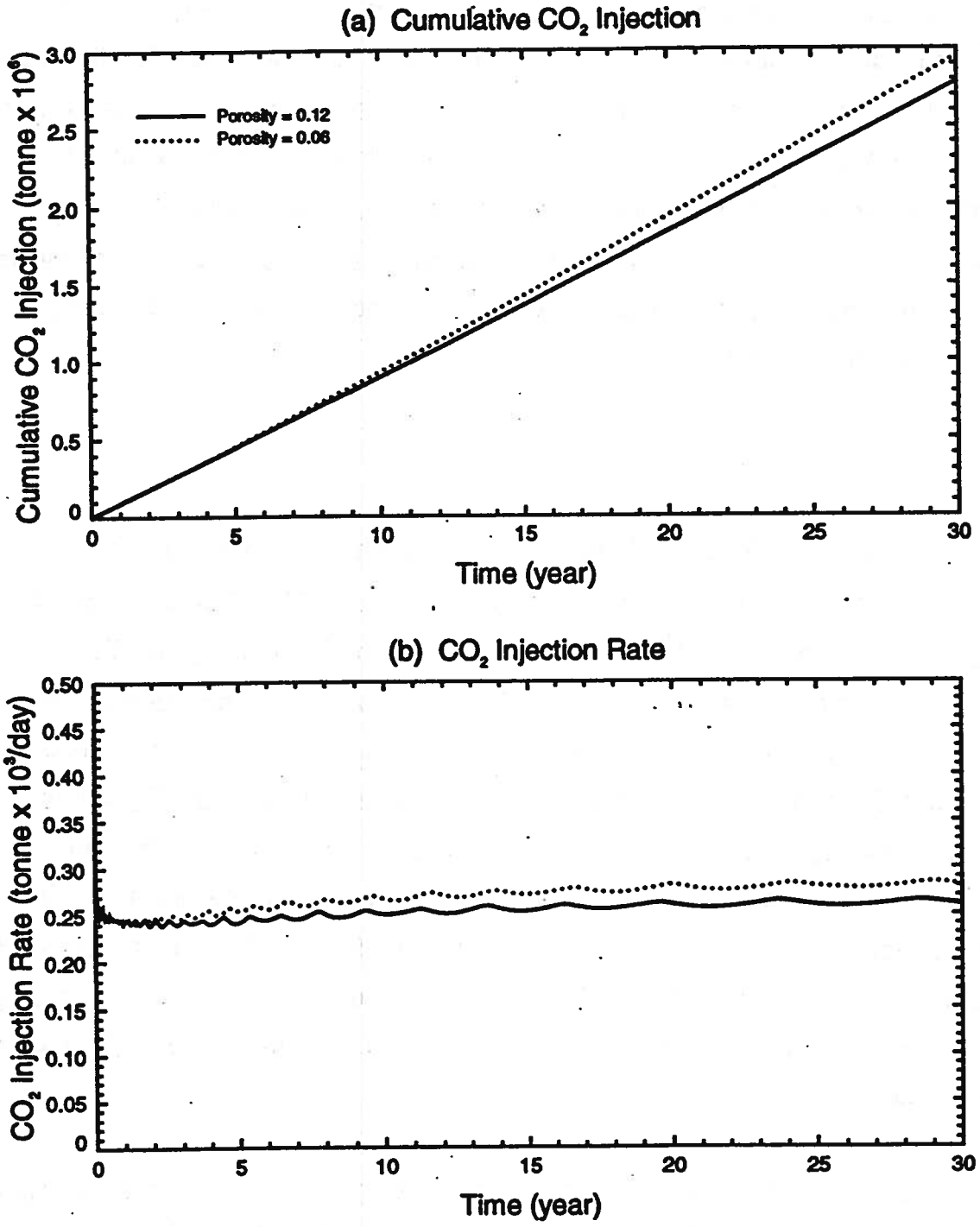

Figure 24: Effect of porosity on CO_2 injection for Glauconitic Sandstone aquifer

Glauconitic Sandstone Aquifer

EFFECT OF ABSOLUTE PERMEABILITY

Aquifer Porosity = 0.12
Injection Pressure = 30.12 MPa

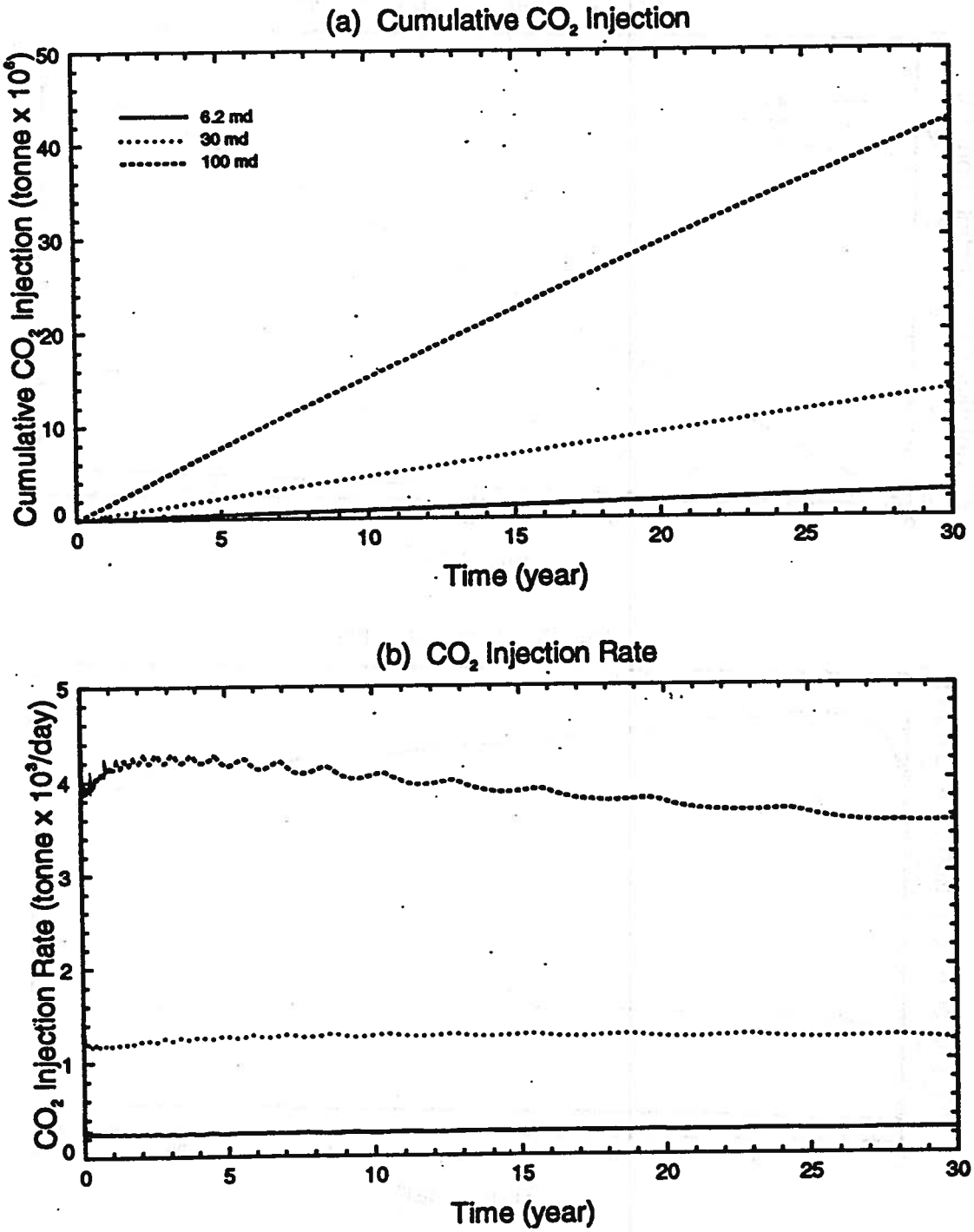

Figure 25: Effect of permeability on CO_2 injection for Glauconitic Sandstone aquifer with porosity of 0.12

Glauconitic Sandstone Aquifer

EFFECT OF ABSOLUTE PERMEABILITY

Aquifer Porosity = 0.06
Injection Pressure = 30.12 MPa

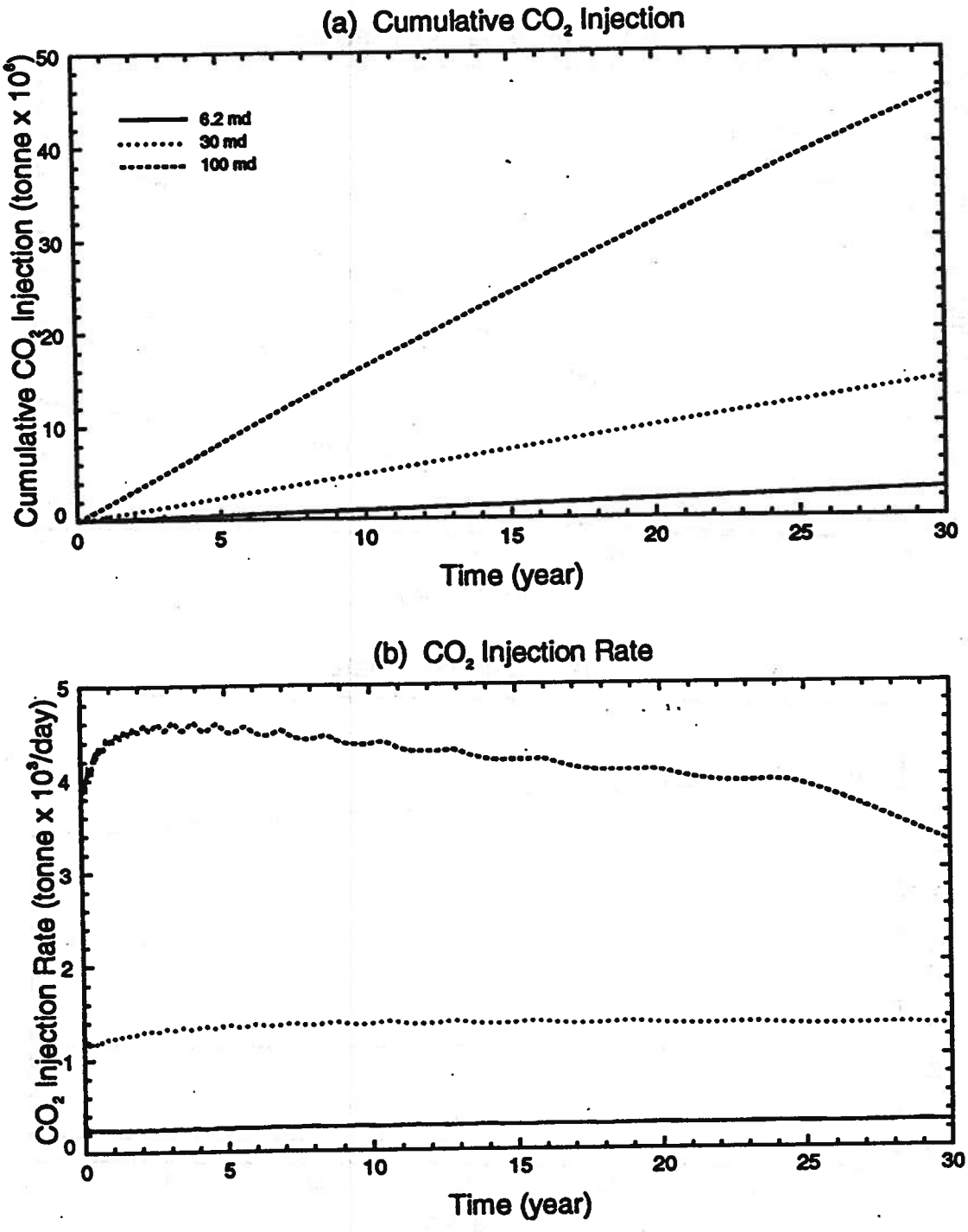

Figure 26: Effect of permeability on CO_2 injection for Glauconitic Sandstone aquifer with porosity of 0.06

permeability of 6.2 md to approximately 300 cm/yr for the aquifer with a permeability of 100 md, as shown in Figure 27. This indicates that CO_2 disposal in the Glauconitic Sandstone aquifer has an effect on the natural flow of the aquifer (approximately 1 cm/yr) far away from the injector.

6.4 Effect of Existence of a "Sweet" Zone

The effect of the existence of a locally high permeability zone or "sweet" zone on CO_2 injection could be studied by comparing the results from simulations CO2_80-CO2_82 to simulation CO2_71 for a "sweet" zone of locally high permeability of 100 md surrounded by a low permeability region of 6.2 md and simulations CO2_83-CO2_85 to simulation CO2_72 for a "sweet" zone of locally high permeability of 100 md surrounded by a low permeability region of 30 md. The radii of the "sweet" zones considered were 0.51, 1.04 and 2.10 km. Comparison of cumulative CO_2 injection and CO_2 injection rate for the aforementioned two cases are given in Figures 28 and 29, respectively. A summary of the cumulative CO_2 injection after 30 years for all the numerical simulations with the existence of a "sweet" zone is given in Figure 30. It was found that the amount of CO_2 injected increases with the size of the "sweet" zone radius. The existence of a "sweet" zone of locally high permeability of 100 md even with a radius of only 0.51 km, allowed the amount of CO_2 injected to increase by 1.8 and 1.4 times from the case of no "sweet" zone for an aquifer with permeabilities of 6.2 and 30 md, respectively. The existence of a "sweet" zone of locally high permeability of 100 md with a large radius of 2.10 km, allowed the amount of CO_2 injected to increase by 2.5 and 1.6 times from the case of no "sweet" zone for an aquifer with permeabilities of 6.2 and 30 md, respectively.

The average water flow rates at the outflow boundary 7 km away from the injector well for the cases with the existence of a "sweet" zone are given in Figure 31. Due to the existence of a "sweet" zone with radius as large as 2.10 km and permeability of 100

md, average water rates at 7 km away from the injector could increase 2 and 1.4 times after 30 years for the aquifer with permeabilities of 6.2 and 30 md, respectively.

Glauconitic Sandstone Aquifer

EFFECT OF PERMEABILITY AND POROSITY

Solid Lines: Porosity = 0.12

Dashed Lines: Porosity = 0.06

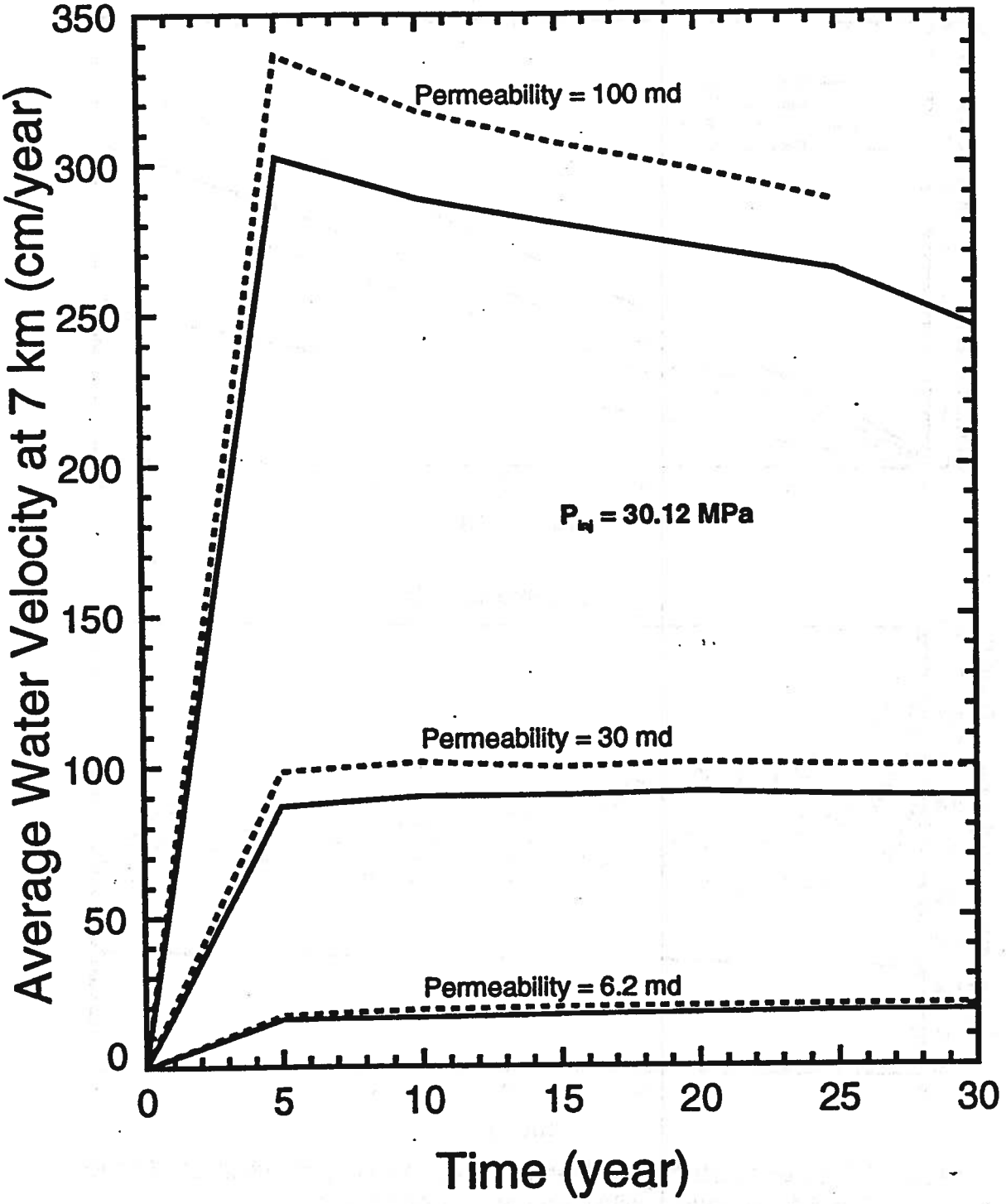

Figure 27: Average water velocity at 7 km away from injector for Glauconitic Sandstone aquifer with different permeabilities and porosities

Glauconitic Sandstone Aquifer

EFFECT OF 100 md ZONE RADIUS

Aquifer Porosity = 0.12 Aquifer Permeability = 6.2 md (horizontal)
Injection Pressure = 30.12 MPa

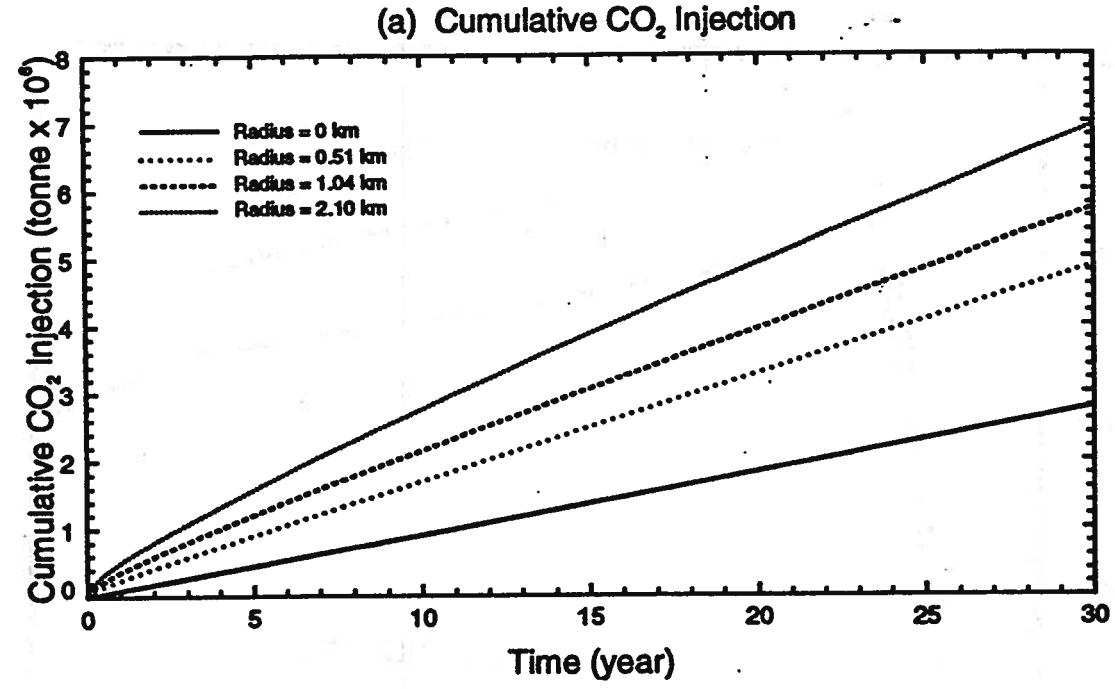

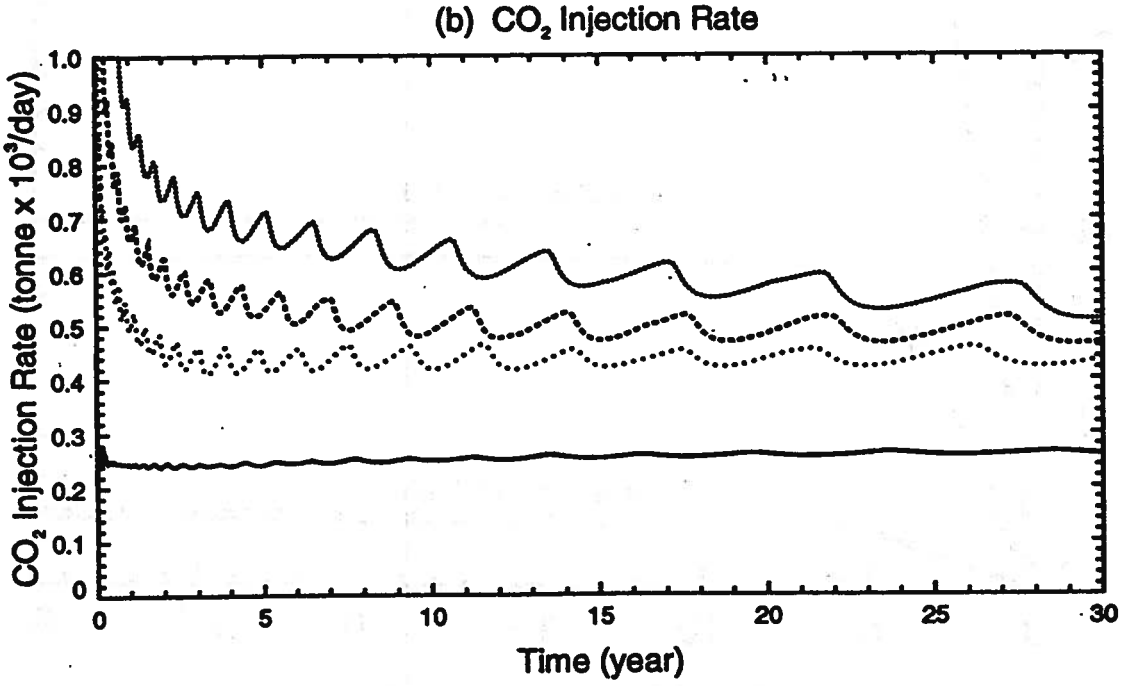

Figure 28: Effect of existence of "sweet" zone on CO_2 injection for Glauconitic Sandstone aquifer with permeability of 6.2 md

Glauconitic Sandstone Aquifer

EFFECT OF 100 md ZONE RADIUS

Aquifer Porosity = 0.12 Aquifer Permeability = 30 md (horizontal)
Injection Pressure = 30.12 MPa

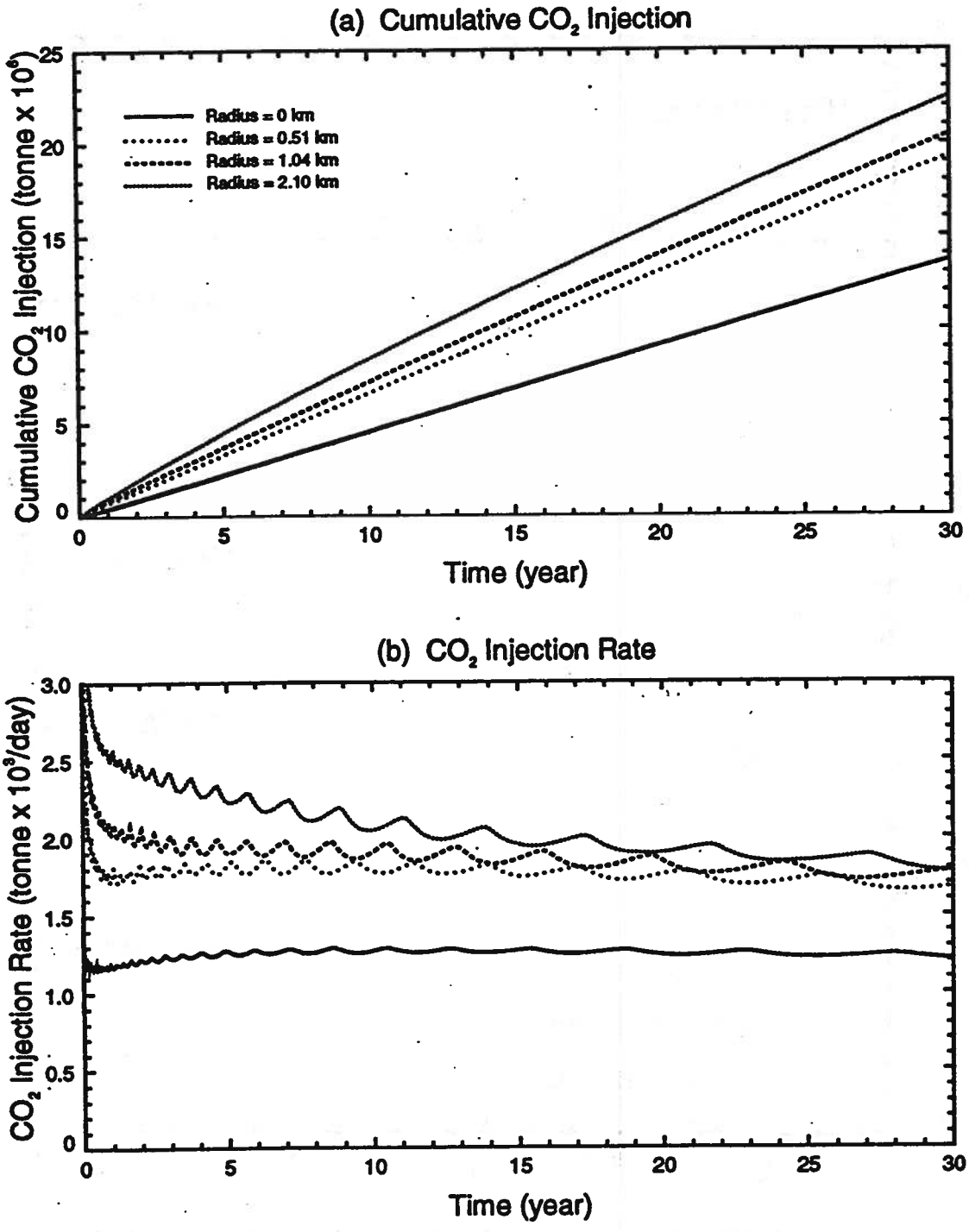

Figure 29: Effect of existence of "sweet" zone on CO_2 injection for Glauconitic Sandstone aquifer with permeability of 30 md

Glauconitic Sandstone Aquifer

EFFECT OF PERMEABILITY DISTRIBUTION

Closed Symbols: Permeability = 100/30 md (Circles)

Open Symbols: Permeability = 100/6.2 md (Circles)

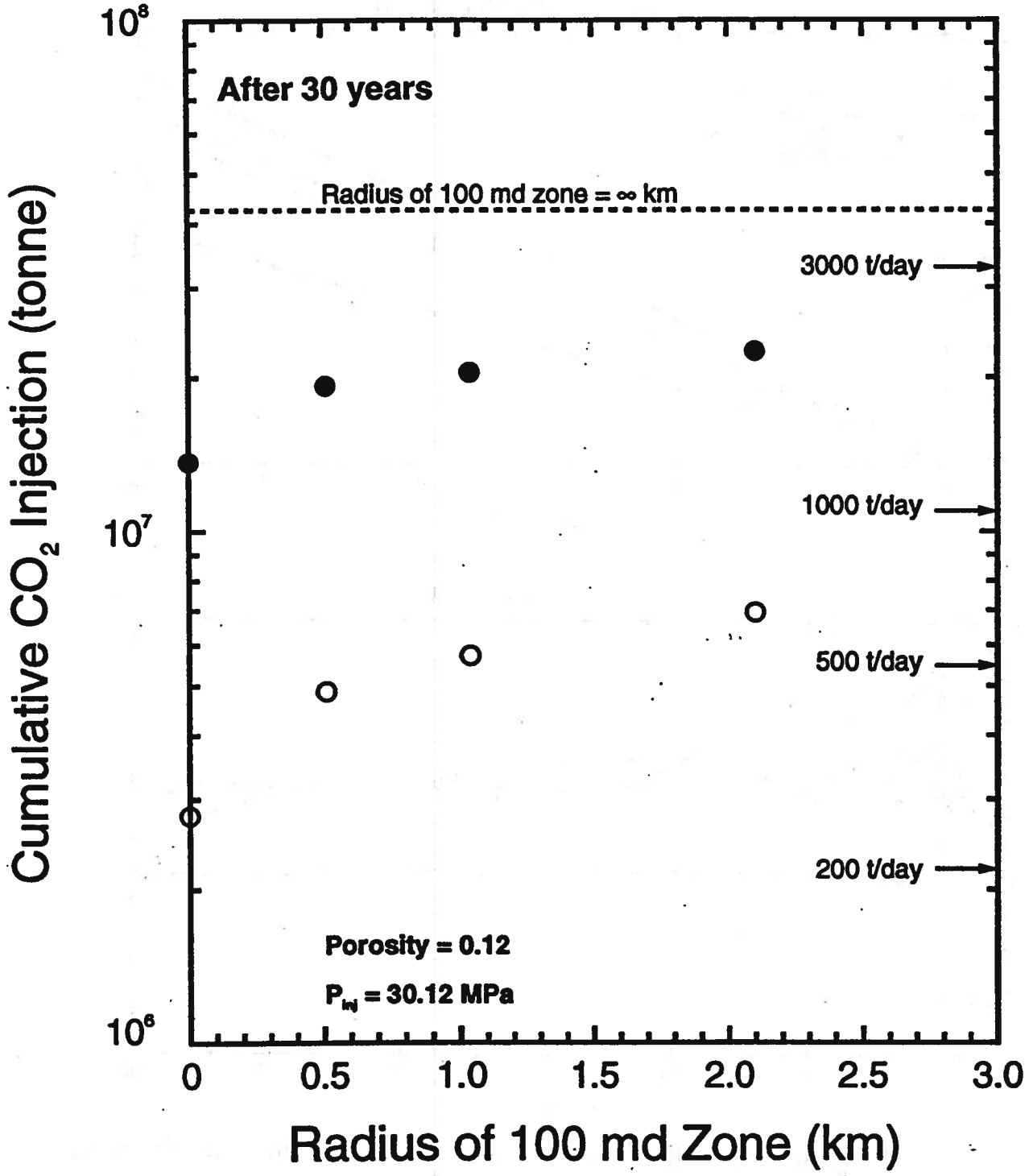

Figure 30: Cumulative CO_2 injection after 30 years for Glauconitic Sandstone aquifer with the existence of "sweet" zone

Glauconitic Sandstone Aquifer

EFFECT OF PERMEABILITY DISTRIBUTION

Solid Lines: homogeneous aquifer

Dashed and Dotted Lines: aquifer with 100 md zone

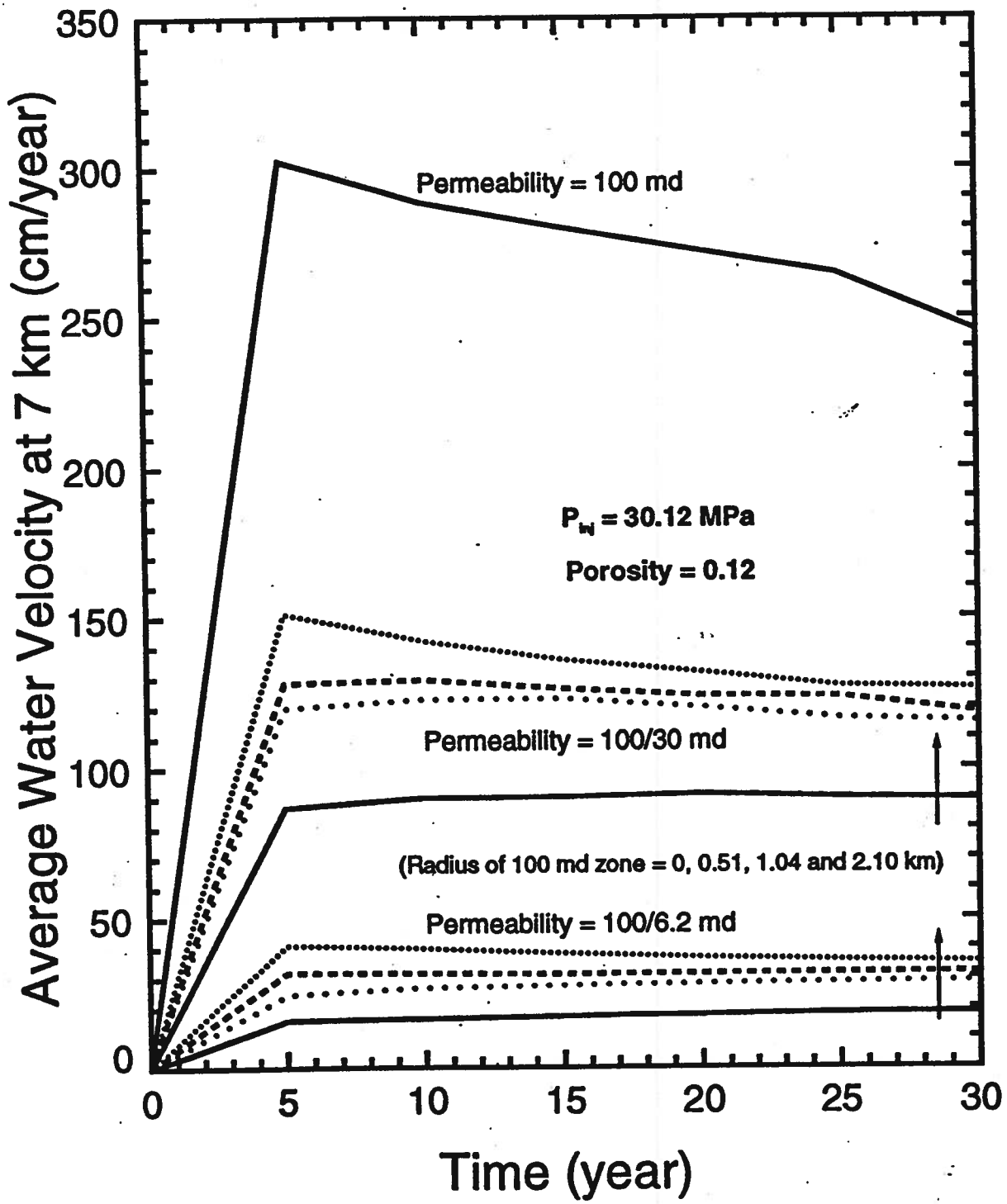

Figure 31: Average water velocity at 7 km away from injector for Glauconitic Sandstone aquifer with the existence of "sweet" zone

7. NUMERICAL RESULTS FOR THE NISKU AQUIFER

Numerical predictions of cumulative CO_2 injection, CO_2 injection rate, CO_2 saturation contours and pressure distribution near the bottom of the aquifer as a function of time are given in Appendix III for all the numerical simulations of injecting CO_2 in the NIsku aquifer.

For the relatively thick Nisku aquifer, realistically, disposal of 1.3×10^7 to 1.3×10^8 tonnes of CO_2 over a period of 30 years can be achieved which corresponds to average CO_2 injection rates ranging from 1,163 to 11,872 t/d/well. Approximately 16 to 25 wt% of the injected CO_2 dissolves in the aqueous phase at the average aquifer temperature of 60°C. Due to the thick aquifer (60 m thick), CO_2 override to the top part of the aquifer was very significant. In general, CO_2 propagates less than 5 km away from the injector after an injection period of 30 years, except for the cases of the higher permeabilities (i.e. 100 and 400 md).

7.1 Effect of Injector Completion

The effect of well completion on CO_2 injection could be studied by comparing the results from two simulations, CO2_101 and CO2_102. Comparison of cumulative CO_2 injection and CO_2 injection rate for the case of porosity of 0.06 and horizontal permeability of 6.2 md is given in Figure 32. It was found that the injector completion had a significant effect on the amount of CO_2 injected. For the same aquifer characteristics, approximately 96% more CO_2 could be injected when the injector completion interval was increased from 13 m at the bottom of the aquifer to the entire thickness of the aquifer of 60 m. The aquifer pressurizes faster when a large injector completion interval was chosen due to the higher CO_2 injection rate. In order to maximize the injectivity of CO_2 in the Nisku aquifer, an injector completion interval that covered the entire thickness of the aquifer was chosen.

Nisku Aquifer

EFFECT OF WELL COMPLETION

Aquifer Porosity = 0.06 Aquifer Permeability = 6.2 md (horizontal)
Injection Pressure = 37.86 MPa

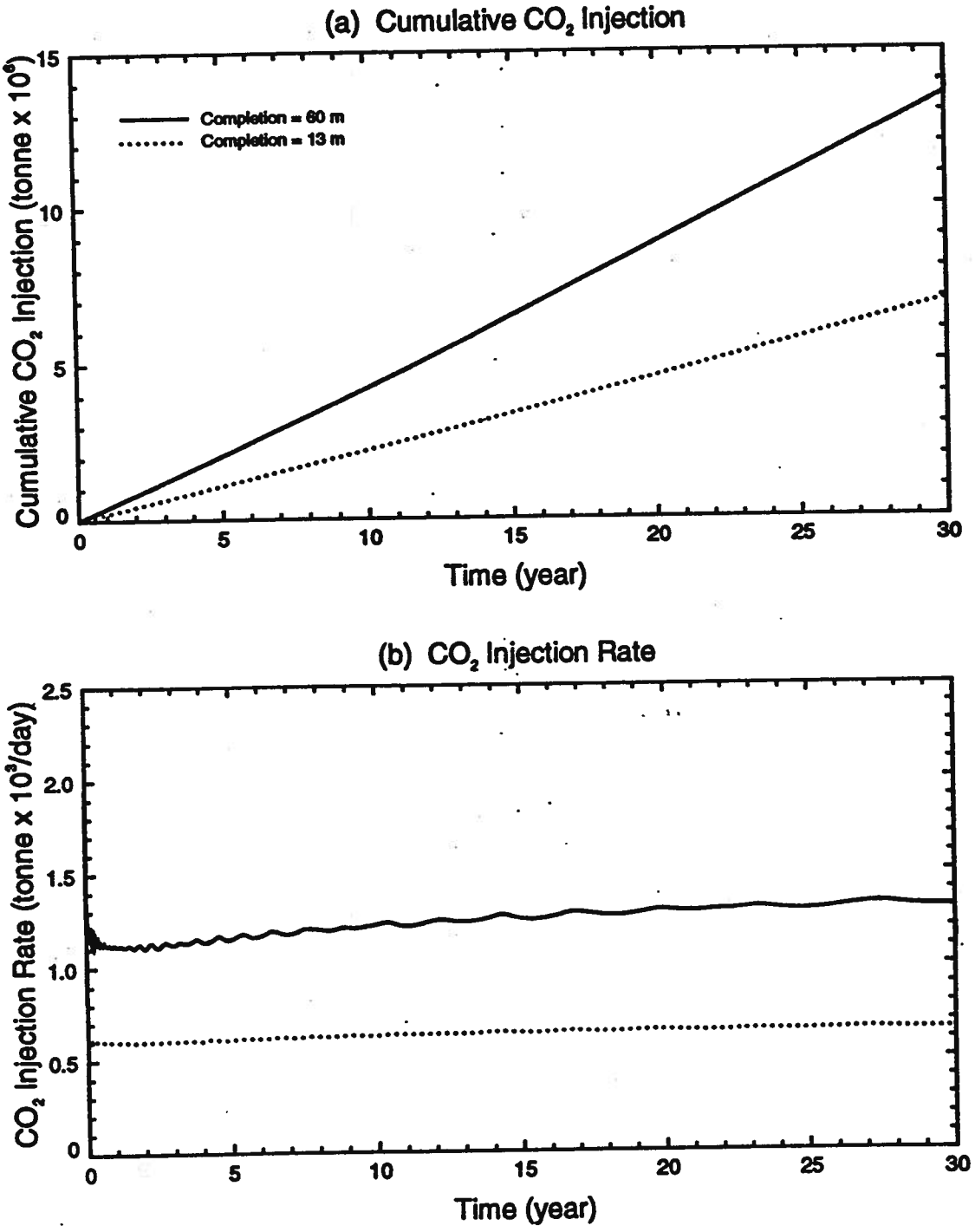

Figure 32: Effect of injector completion on CO_2 injection for Nisku aquifer

7.2 Effect of Porosity

The effect of porosity on CO_2 injection could be studied by comparing the results from two series of simulations, CO2_106-CO2_109 and CO2_102-CO2_105. A typical comparison of cumulative CO_2 injection and CO_2 injection rate for a horizontal permeability of 6.2 md and injection pressure of 37.86 MPa is shown in Figure 33. The porosity had very little effect on the amount of CO_2 injected, very similar to the predictions for CO_2 disposal in the Glauconitic Sandstone aquifer. For an aquifer having the same permeability, the amount of CO_2 injected under the same injection characteristics was slightly higher and the aquifer pressurized slightly faster for the case of the lower porosity (i.e 0.06). As anticipated, CO_2 propagates farther away from the injector for the case of the lower porosity.

7.3 Effect of Permeability

The effect of permeability on CO_2 injection could be studied by comparing the results from simulations CO2_106-CO2_109 for porosity of 0.12 and simulations CO2_102-CO2_105 for porosity of 0.06. Comparisons of cumulative CO_2 injection and CO_2 injection rate for porosities of 0.12 and 0.06 are given in Figures 34 and 35, respectively. It was found that the permeability had a very significant effect on the amount of CO_2 injected. For the same injection characteristics, more than 16 and 65 times of CO_2 could be injected when the permeability of the aquifer was increased from 6.2 to 100 and 400 md, respectively. Correspondingly, CO_2 propagation, away from the injector, increased from 1.2 km for a permeability of 6.2 md to 6 and 13 km for permeability values of 100 and 400 md, respectively for the case of a porosity of 0.12. It was also found that the aquifer with a higher permeability pressurized faster than the aquifer with a lower permeability due to the higher injection rate.

The average water flow rates, at the outflow boundary (7 km away from the injector),

Nisku Aquifer

EFFECT OF POROSITY

Aquifer Permeability = 6.2 md (horizontal)
Injection Pressure = 37.86 MPa

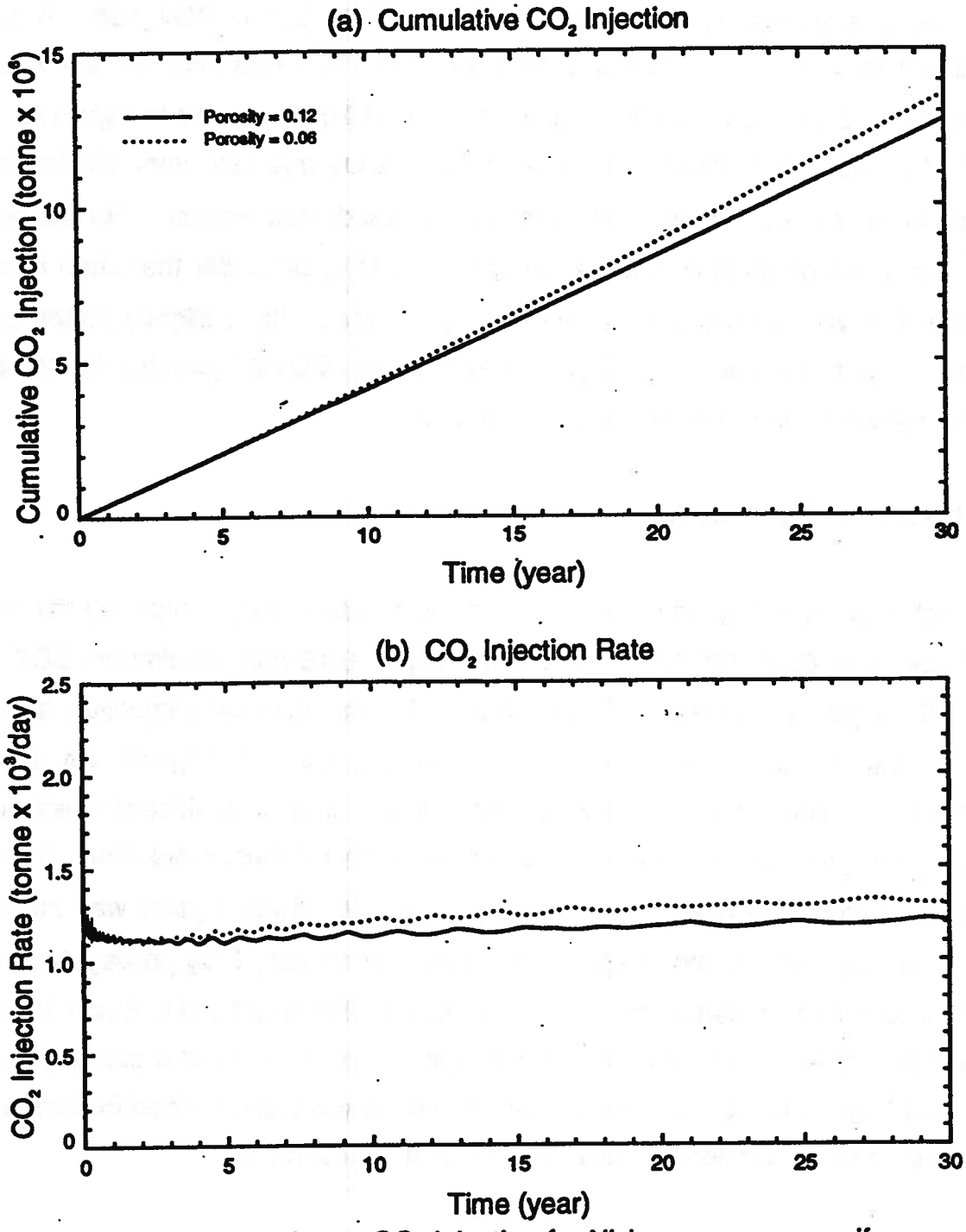

Figure 33: Effect of porosity on CO_2 injection for Nisku aquifer

EFFECT OF ABSOLUTE PERMEABILITY

Aquifer Porosity = 0.12
Injection Pressure = 37.86 MPa

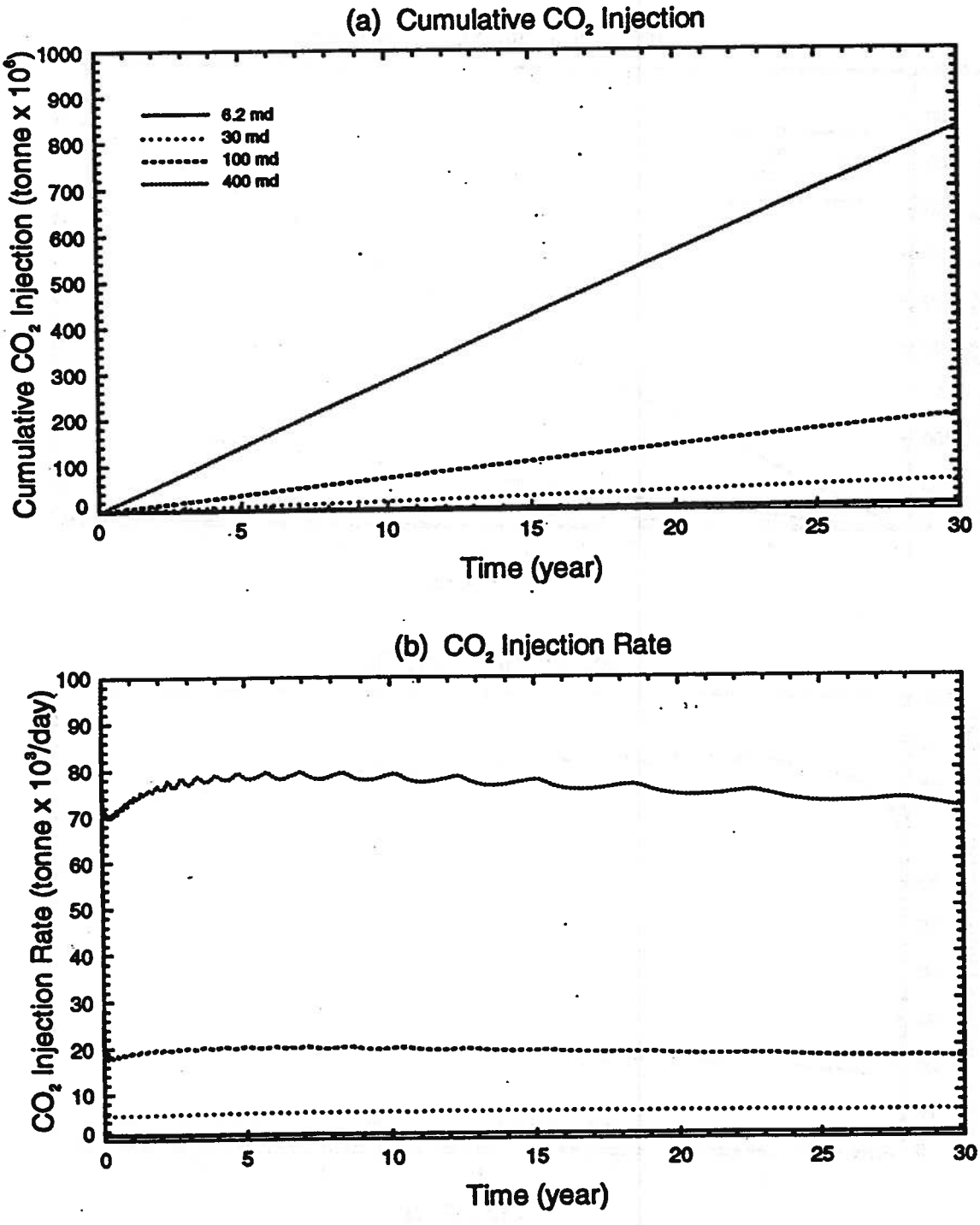

Figure 34: Effect of permeability on CO_2 injection for Nisku aquifer with porosity of 0.12

EFFECT OF ABSOLUTE PERMEABILITY

Aquifer Porosity = 0.06
Injection Pressure = 37.86 MPa

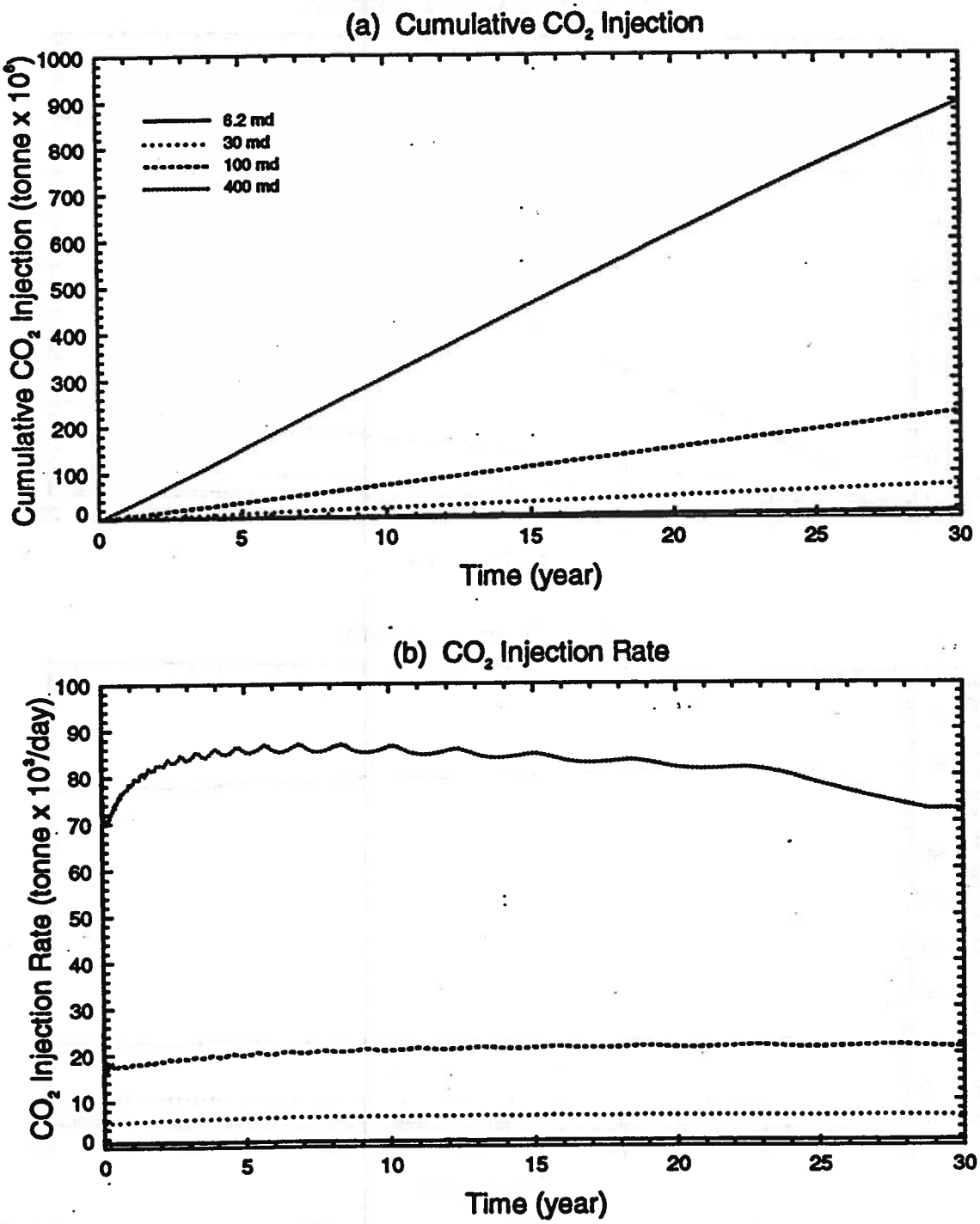

Figure 35: Effect of permeability on CO_2 injection for Nisku aquifer with porosity of 0.06

caused by the CO_2 injection, ranged from approximately 20 cm/yr for the aquifer with a permeability of 6.2 md to approximately 300 cm/yr for the aquifer with a permeability of 100 md, as shown in Figure 36. This indicated that the CO_2 disposal in the Nisku aquifer had an effect on the natural flow of the aquifer (approximately 1 cm/yr) far away from the injector. It was noted that for the aquifer with a permeability of 400 md, average water rates due to CO_2 injection at 7 km away from the injector were not calculated mainly because CO_2 flow occurred at this outflow boundary.

7.4 Effect of Existence of a "Sweet" Zone

The effect of the existence of a locally high permeability zone, termed a "sweet" zone, on CO_2 injection could be studied by comparing the results from two series of simulations CO2_110-CO2_112 and CO2_116-CO2_118 to simulation CO2_109 for "sweet" zones of locally high permeabilities of 100 and 400 md, respectively, surrounded by a low permeability region of 6.2 md and another two series of simulations CO2_113-CO2_115 and CO2_119-CO2_121 to simulation CO2_108 for "sweet" zone of locally high permeabilities of 100 and 400 md, respectively surrounded by a low permeability region of 30 md. The radii of the "sweet" zones considered were 0.51, 1.04 and 2.10 km. Comparison of cumulative CO_2 injection and CO_2 injection rate for the aforementioned four cases are given in Figures 37-40, respectively. A summary of the cumulative CO_2 injection after 30 years for all the numerical simulations with the existence of a "sweet" zone is given in Figure 41. It was found that the amount of CO_2 injected increased with the "sweet" zone radius. The existence of a "sweet" zone of locally high permeability of 100 md, even with a radius of only 0.51 km, allowed the amount of CO_2 injected to increase by 1.7 and 1.4 times from the case of no "sweet" zone for an aquifer with permeabilities of 6.2 and 30 md, respectively. The existence of a "sweet" zone of locally high permeability of 100 md with a large radius of 2.10 km, allowed the amount of CO_2 injected to increase by 2.8 and 1.7 times from the case of no "sweet" zone for an aquifer with permeabilities of 6.2

EFFECT OF PERMEABILITY AND POROSITY

Solid Lines: Porosity = 0.12

Dashed Lines: Porosity = 0.06

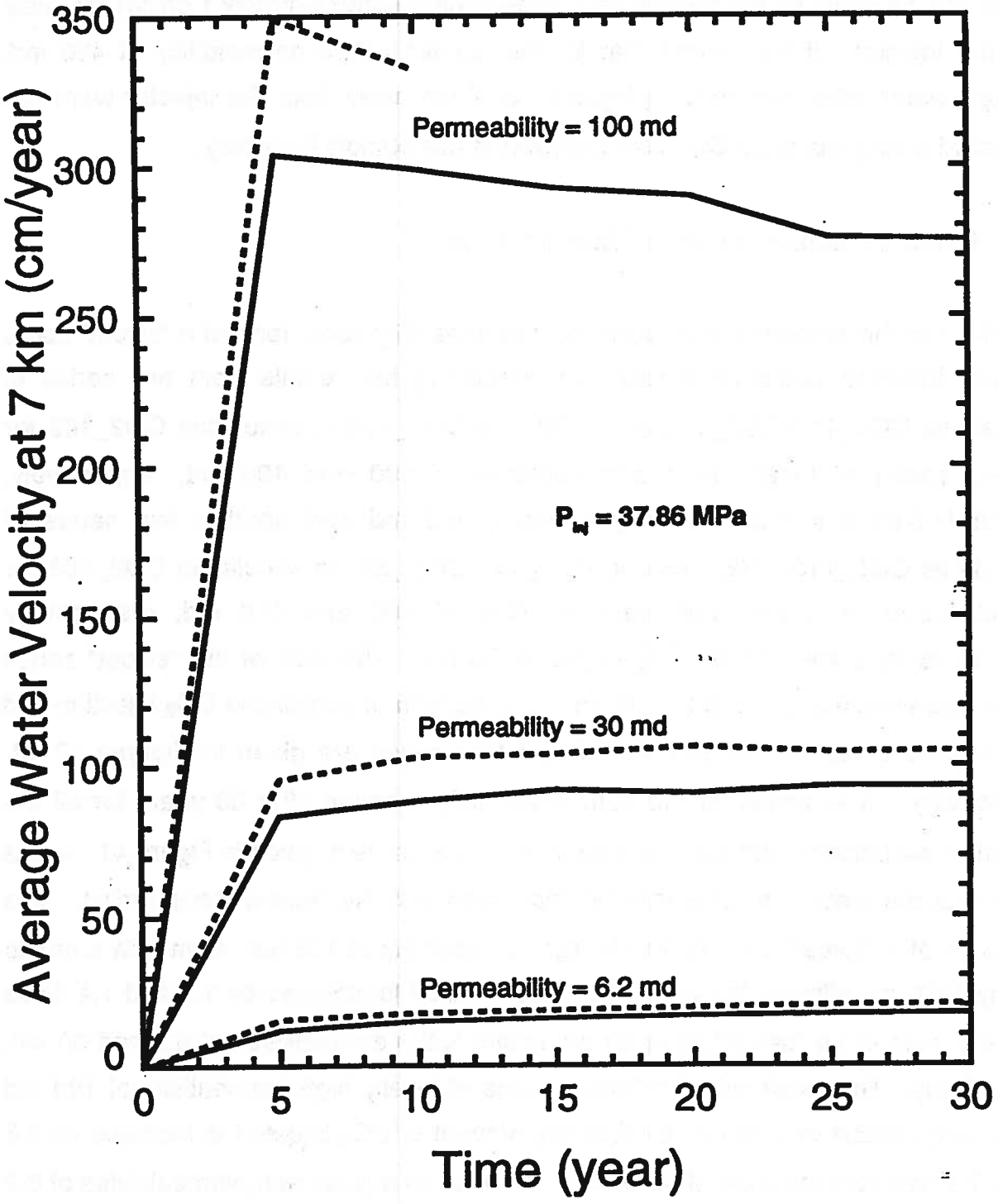

Figure 36: Average water velocity at 7 km away from injector for Nisku aquifer with different permeabilities and porosities

Nisku Aquifer

EFFECT OF 100 md ZONE RADIUS

Aquifer Porosity = 0.12 Aquifer Permeability = 6.2 md (horizontal)
Injection Pressure = 37.86 MPa

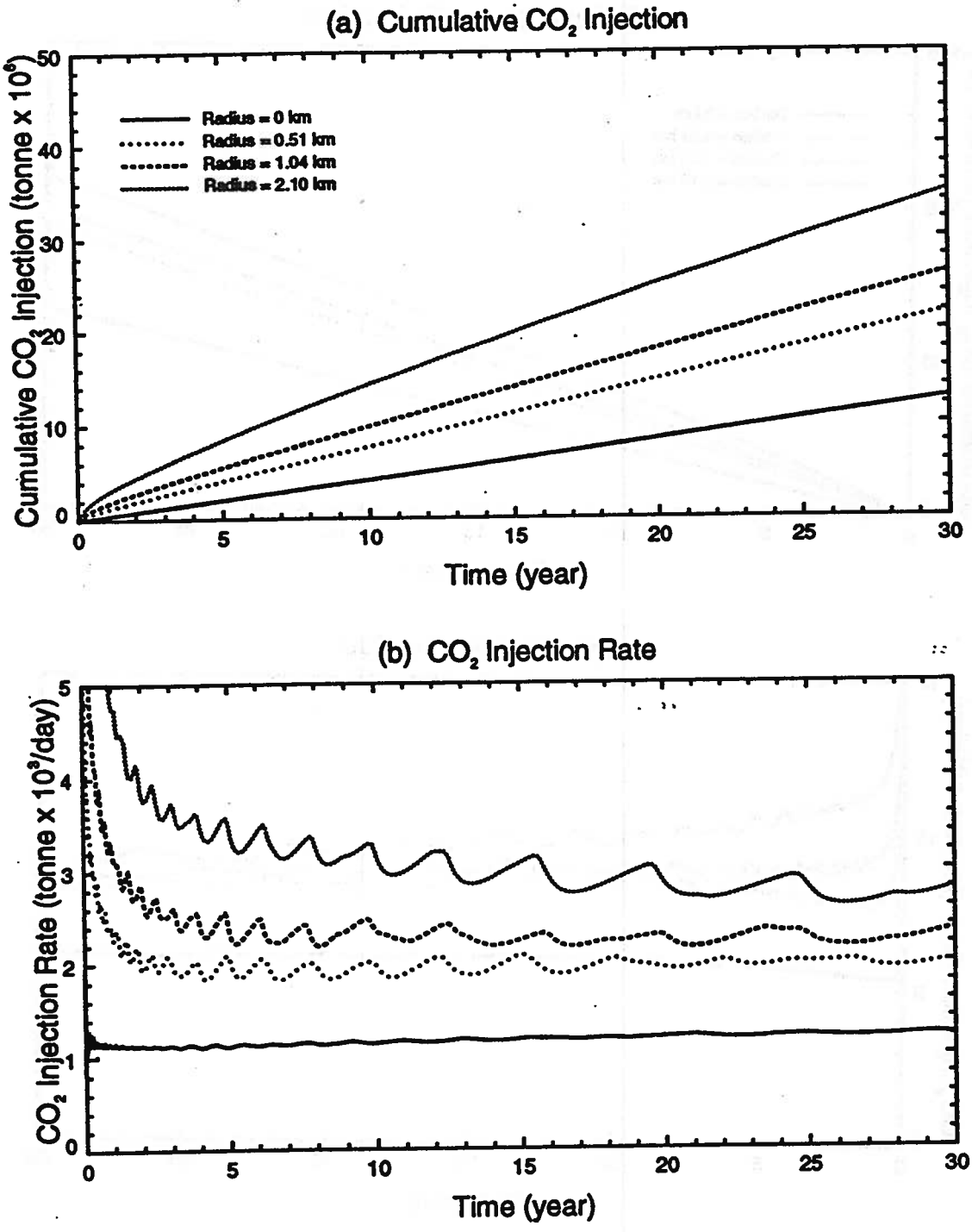

Figure 37: Effect of existence of 100 md "sweet" zone on CO_2 injection for Nisku aquifer with permeability of 6.2 md

Nisku Aquifer

EFFECT OF 100 md ZONE RADIUS

Aquifer Porosity = 0.12 Aquifer Permeability = 30 md (horizontal)
Injection Pressure = 37.86 MPa

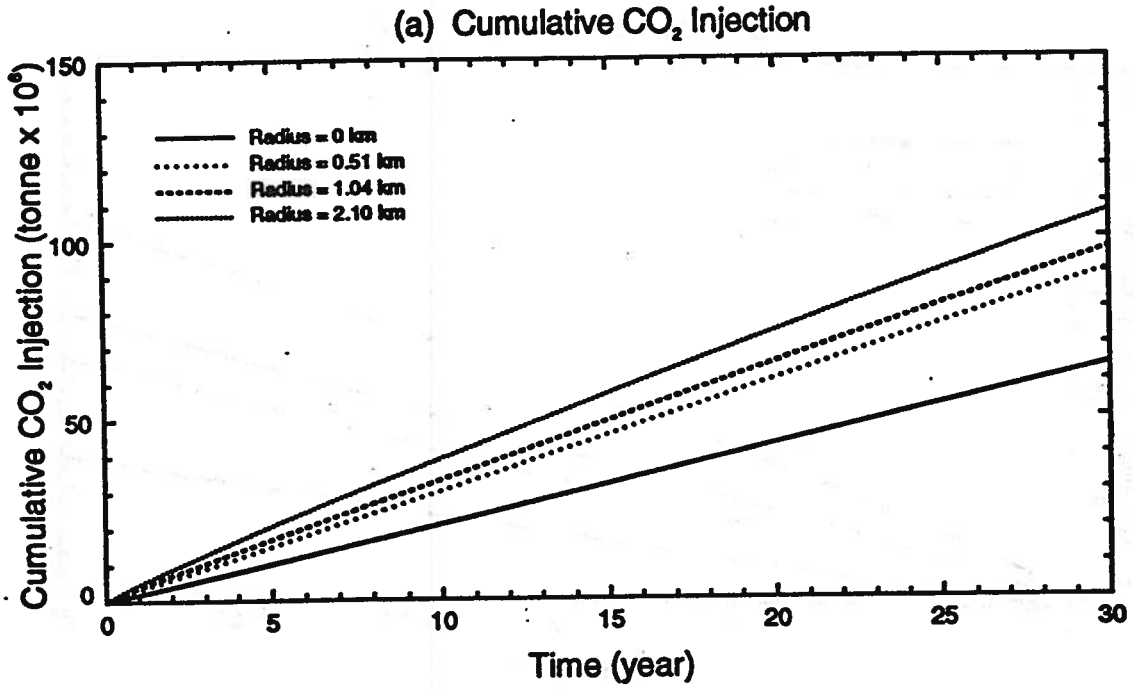

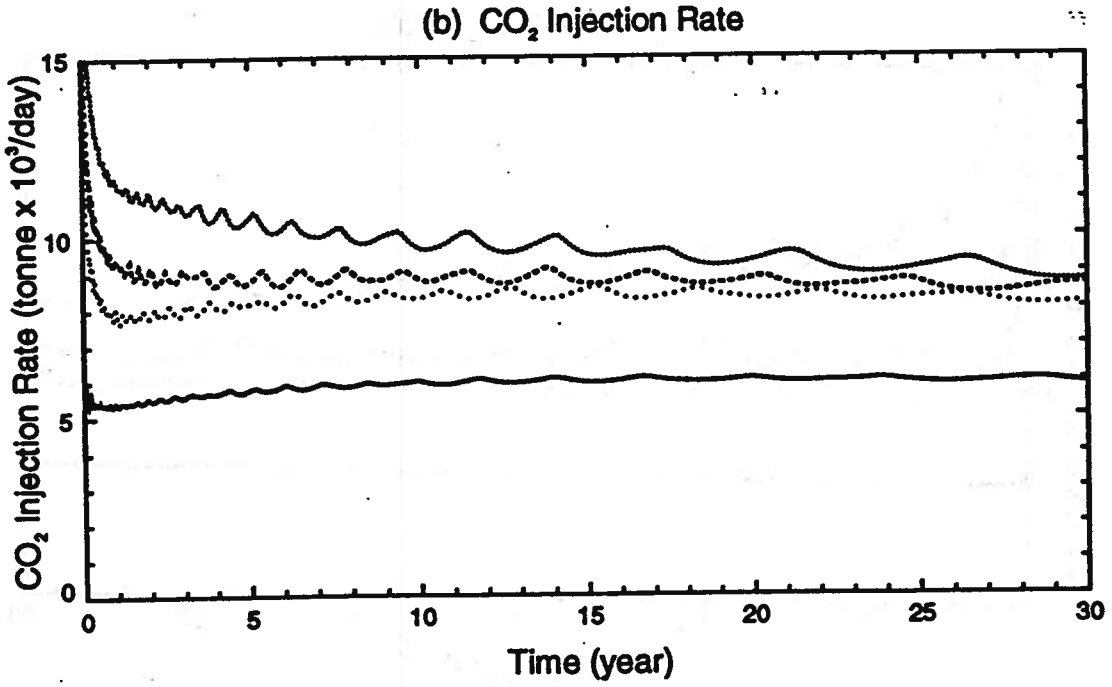

Figure 38: Effect of existence of 100 md "sweet" zone on CO_2 injection for Nisku aquifer with permeability of 30 md

Nisku Aquifer

EFFECT OF 400 md ZONE RADIUS

Aquifer Porosity = 0.12 Aquifer Permeability = 6.2 md (horizontal)
Injection Pressure = 37.86 MPa

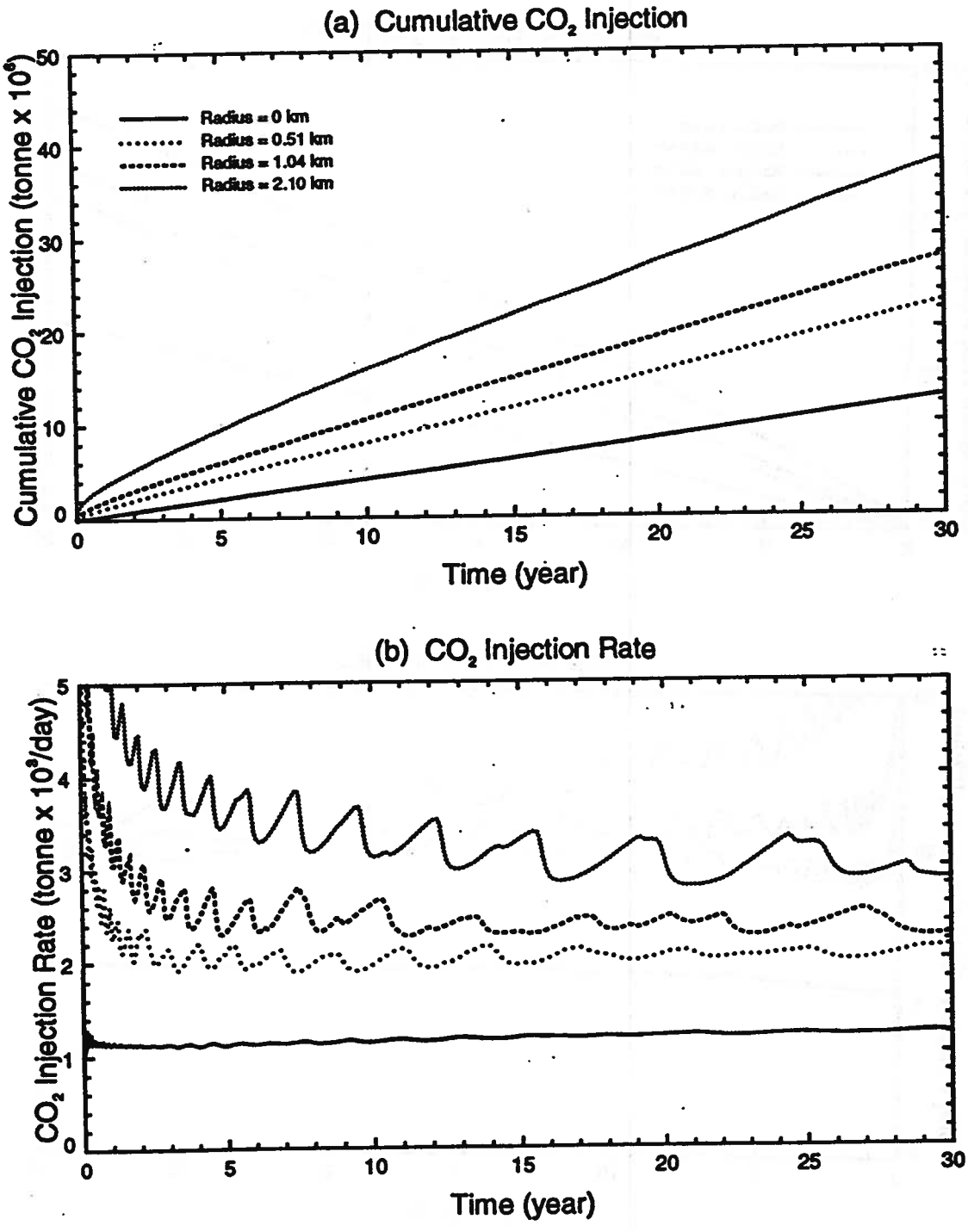

Figure 39: Effect of existence of 400 md "sweet" zone on CO_2 injection for Nisku aquifer with permeability of 6.2 md

Nisku Aquifer

EFFECT OF 400 md ZONE RADIUS

Aquifer Porosity = 0.12 Aquifer Permeability = 30 md (horizontal)
Injection Pressure = 37.86 MPa

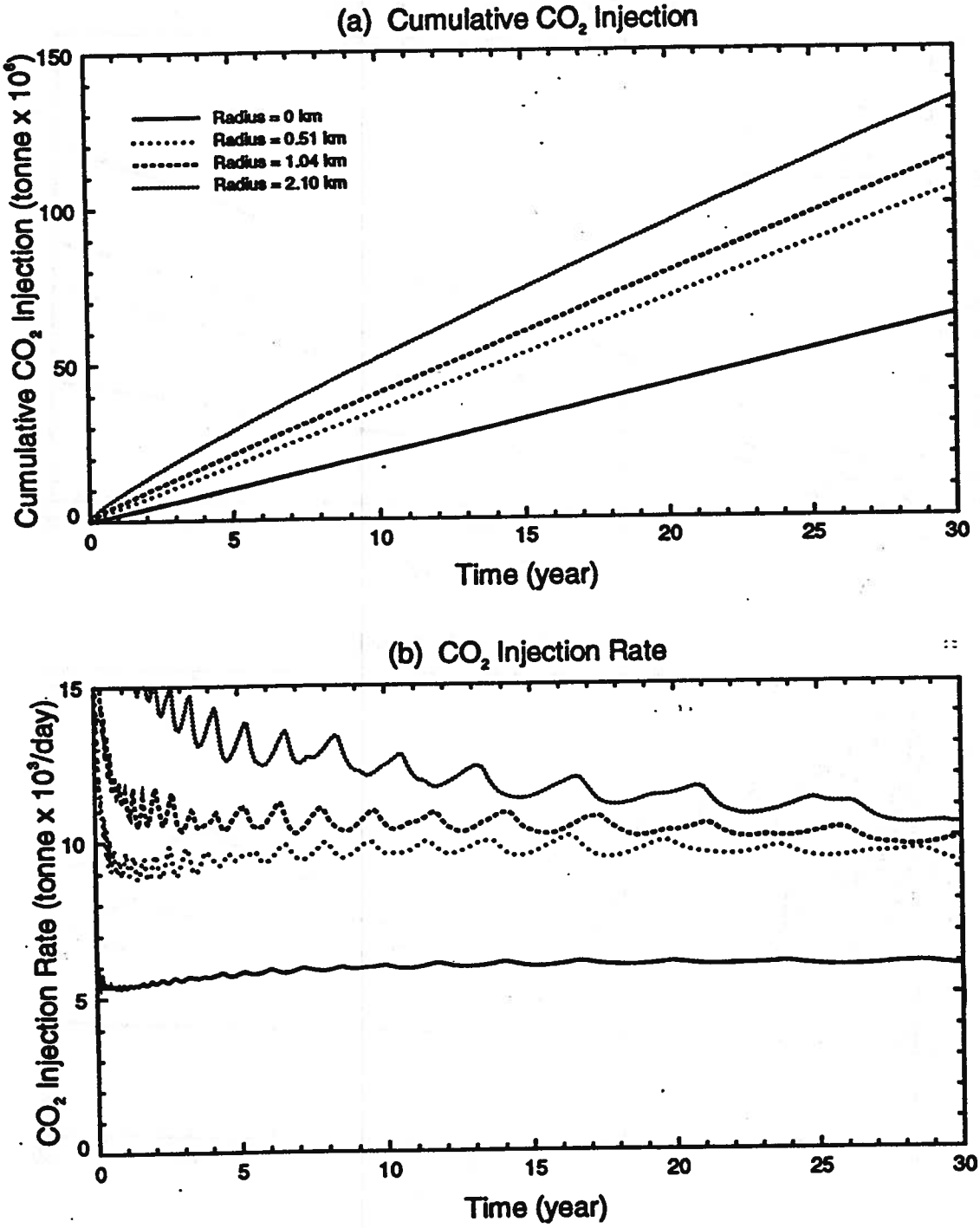

Figure 40: Effect of existence of 400 md "sweet" zone on CO_2 injection for Nisku aquifer with permeability of 30 md

Nisku Aquifer

EFFECT OF PERMEABILITY DISTRIBUTION

Closed Symbols: Permeability = 100/30 md (Circles) 400/30 md (Squares)

Open Symbols: Permeability = 100/6.2 md (Circles) 400/6.2 md (Squares)

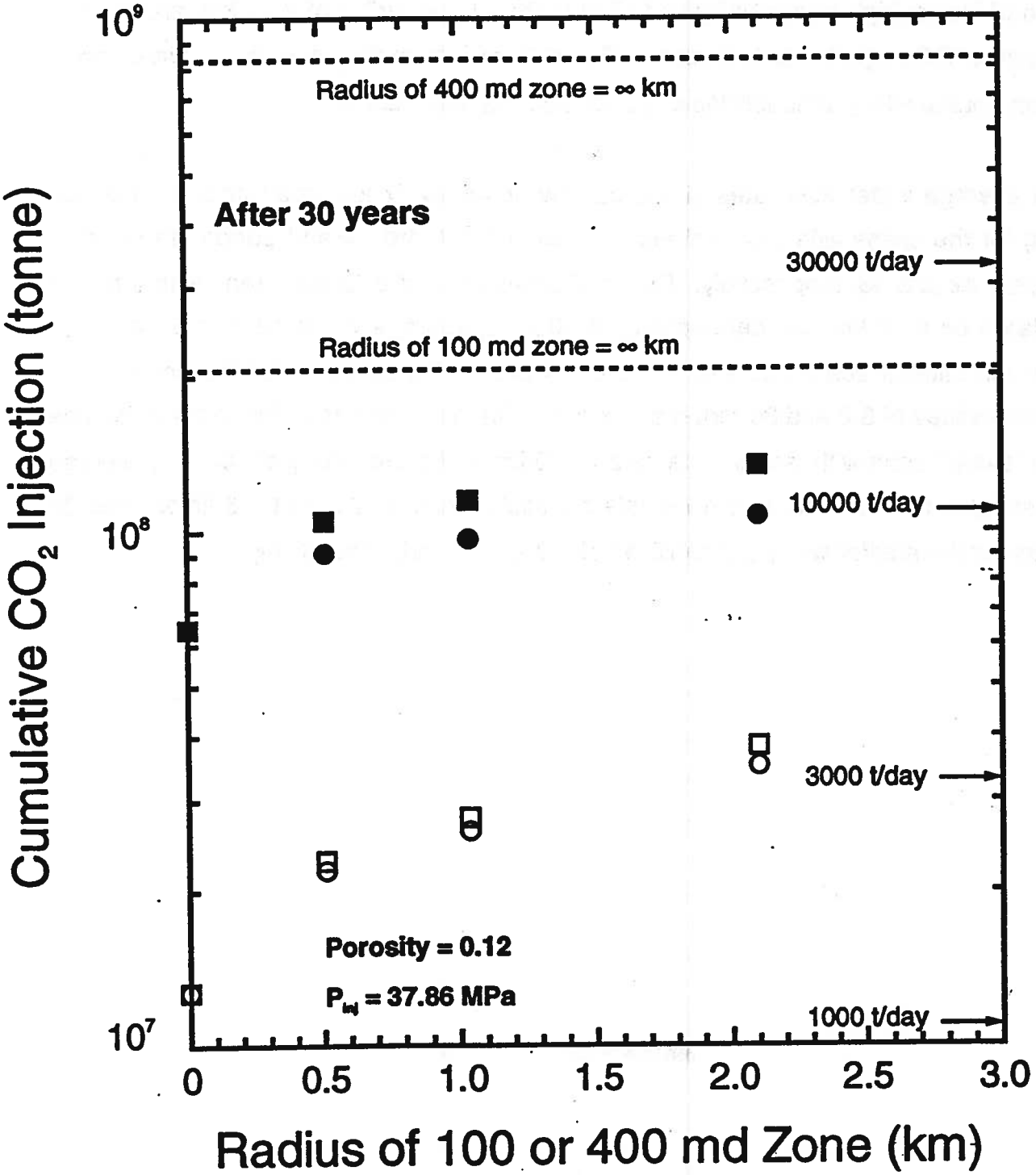

Figure 41: Cumulative CO_2 injection after 30 years for Nisku aquifer with the existence of "sweet" zone

and 30 md, respectively. On the other hand, the existence of a "sweet" zone of locally high permeability of 400 md even with a radius of only 0.51 km, allowed the amount of CO_2 injected to increase by 1.8 and 1.6 times from the case of no "sweet" zone for an aquifer with permeabilities of 6.2 and 30 md, respectively. The existence of a "sweet" zone of locally high permeability of 400 md with a large radius of 2.10 km, allowed the amount of CO_2 injected to increase by 3 and 2 times from the case of no "sweet" zone for an aquifer with permeabilities of 6.2 and 30 md, respectively.

The average water flow rates at the outflow boundary (7 km away from the injector well) for the cases with the existence of 100 and 400 md "sweet" zones are given in Figures 42 and 43, respectively. Due to the existence of a "sweet" zone with a radius as large as 2.10 km and permeability of 100 md, average water rates at 7 km away from the injector could increase 2.1 and 1.4 times after 30 years for the aquifer with permeabilities of 6.2 and 30 md, respectively. On the other hand, due to the existence of a "sweet" zone with radius as large as 2.10 km and permeability of 400 md, average water rates at 7 km away from the injector could increase 2.3 and 1.6 times after 30 years for the aquifer with permeabilities of 6.2 and 30 md, respectively.

Nisku Aquifer

EFFECT OF PERMEABILITY DISTRIBUTION

Solid Lines: homogeneous aquifer

Dashed and Dotted Lines: aquifer with 100 md zone

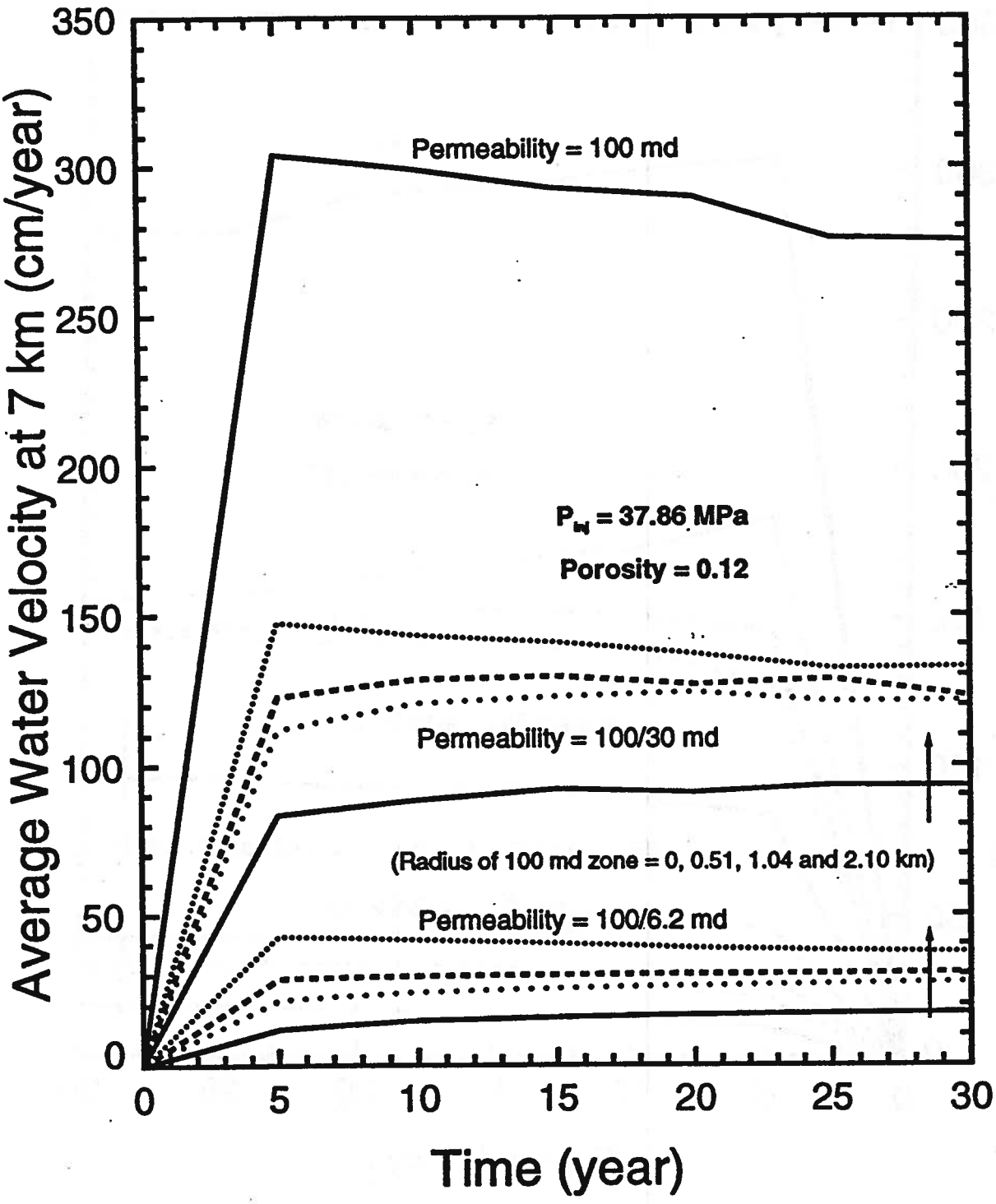

Figure 42: Average water velocity at 7 km away from injector for Nisku aquifer with the existence of 100 md "sweet" zone

Nisku Aquifer

EFFECT OF PERMEABILITY DISTRIBUTION

Solid Lines: homogeneous aquifer

Dashed and Dotted Lines: aquifer with 400 md zone

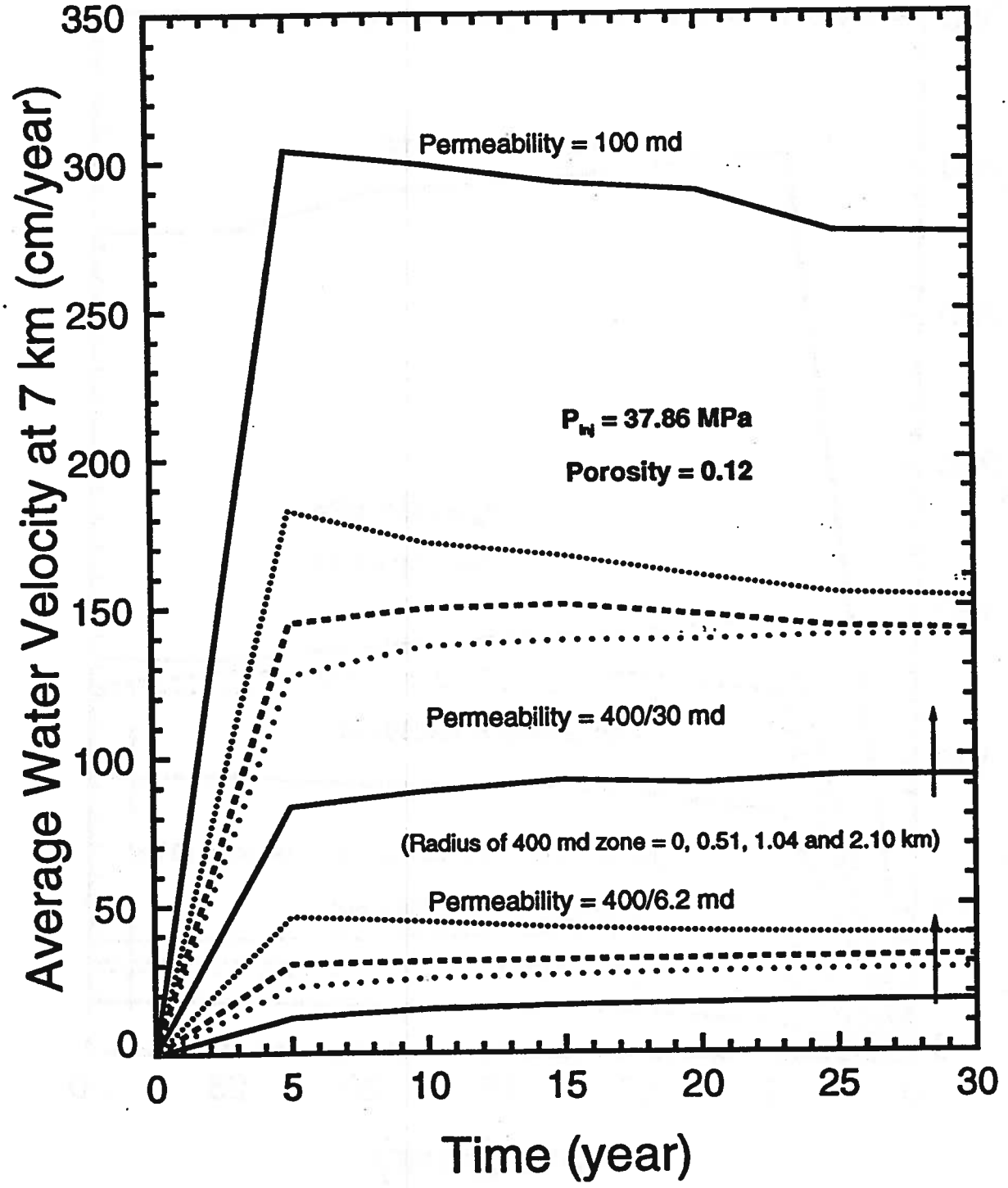

Figure 43: Average water velocity at 7 km away from injector for Nisku aquifer with the existence of 400 md "sweet" zone

8. GENERALIZATIONS FOR EXTRAPOLATION TO OTHER AQUIFERS

8.1 Homogeneous Aquifers

8.1.1 CO_2 Injectivity

Cumulative CO_2 volumes after 30 years of injection for the homogeneous Glauconitic Sandstone and Nisku aquifers as a function of horizontal absolute permeability are given in Figure 44. Also, shown in Figure 44 are the average CO_2 injection rates calculated based on these cumulative CO_2 injections. The output from 500 MW power plant, approximately 15,000 t/d of CO_2 (i.e. 1.64×10^8 tonnes over a period of 30 years) is indicated on Figure 44 for reference.

The results of the simulations on the Glauconitic Sandstone and Nisku aquifers can be used as the basis for a simple analytical model to determine CO_2 injectivity into aquifers over a wide range of conditions. According to a simple steady state, radial outflow well model (Craft and Hawkins, 1959):

$$q_{co2} = I \times p_{co2} \times (P_{inj} - P_{aq}) \qquad (3)$$

The injectivity well index is: $I = (k_r / \mu_{co2}) \times I'$, where (4)

$$I' = 2 \pi h k f / \ln (r_e / r_w) \qquad (5)$$

f: injector completion factor

h: thickness of aquifer, [m]

k: absolute permeability around the injector, [m^2]

k_r: relative permeability of CO_2

($k_r = 1$ for 100% CO_2 injection)

EFFECT OF ABSOLUTE PERMEABILITY ON HOMOGENEOUS AQUIFERS

Closed Symbols: Porosity = 0.12

Open Symbols: Porosity = 0.06

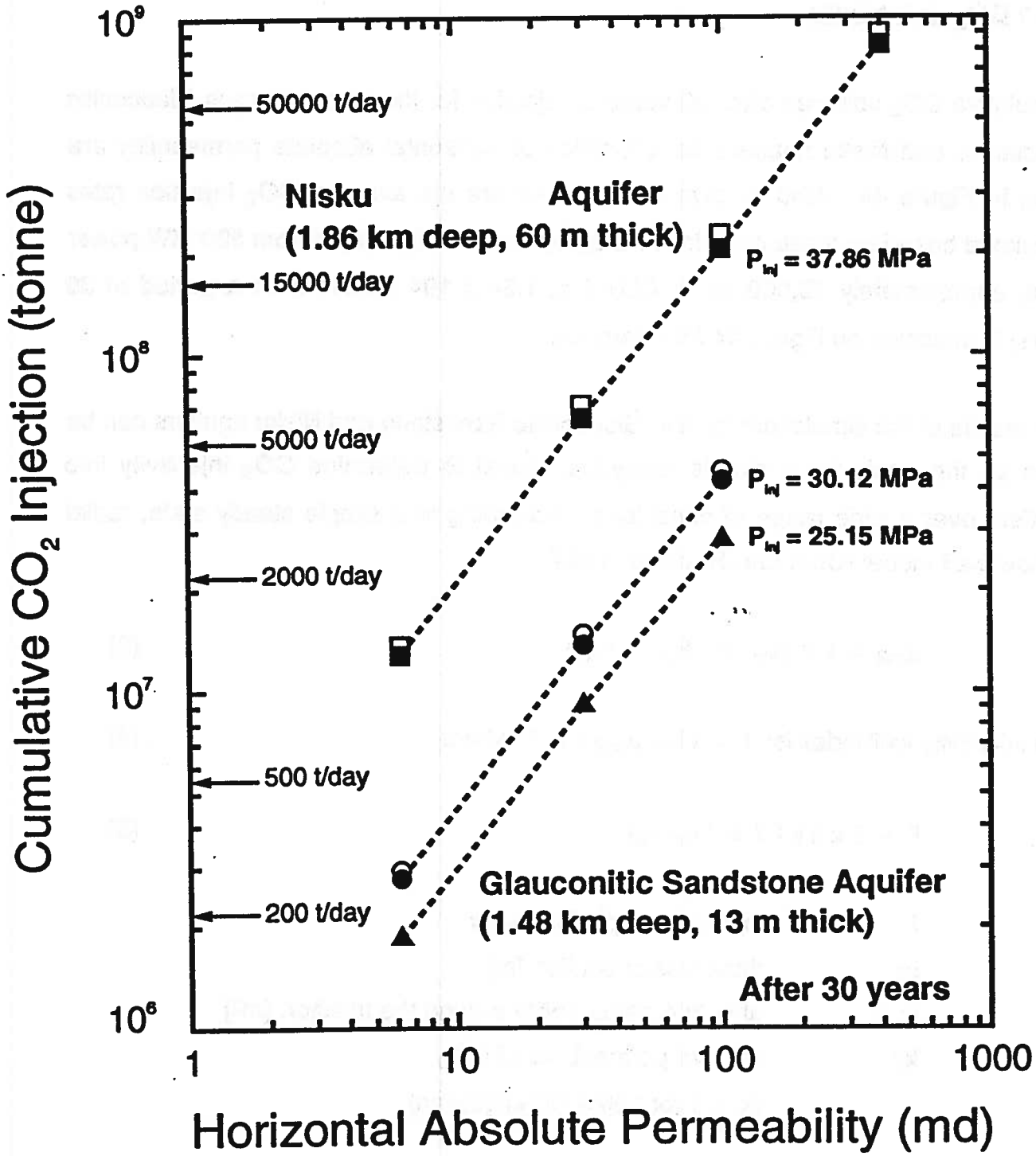

Figure 44: Cumulative CO_2 injection after 30 years in homogeneous aquifers in the Alberta sedimentary basin

P_{aq}: initial aquifer pressure at average depth, [Pa] or [kg/m-s^2]

P_{inj}: injection pressure, [Pa] or [kg/m-s^2]

q_{co2}: average mass injection rate of CO_2, [kg/s]

r_e: distance from the centre of the wellbore at P_{inj} to point where regional aquifer pressure of P_{aq} is reached, [m]

r_w: injector well radius, [m]

ρ_{co2}: density of CO_2, [kg/m^3]

μ_{co2}: viscosity of CO_2, [Pa-s] or [kg/m-s]

For an anisotropic aquifer, $k = (k_h \times k_v)^{0.5}$, where k_h and k_v are absolute permeabilities in the horizontal and vertical directions, respectively. By rearranging Equation 3 and choosing $f = 1$ (i.e. injector was completed at an interval covering the entire thickness of the aquifer), the following correlation can be obtained:

$$q_{co2} / [h \times (P_{inj} - P_a)] = [5.358 \times 10^{-4} \rho_{co2} / \ln (r_e / r_w)] \times (k k_r / \mu_{co2}) \quad (6)$$

where the units of length, permeability, pressure, injection rate, density and viscosity have been converted to [m], [md], [MPa], [tonne/day], [kg/m^3] and [mPa-s], respectively. The left-hand side of Equation 6 is defined as the CO_2 injectivity, which is the mass injection rate of CO_2 (e.g. tonne/day) per unit thickness of the aquifer (e.g. 1 m) at an injection pressure exceeding the average aquifer pressure by one unit pressure (e.g. 1 MPa). On the right-hand side of Equation 6, $(k k_r / \mu_{co2})$ is defined as the mobility of the CO_2. By assuming that both r_e and ρ_{co2} are constants (although it may not be true since r_e is a function of time and ρ_{co2} is a function of the aquifer temperature and pressure), a log-log plot of the CO_2 injectivity, $q_{co2} / [h \times (P_{inj} - P_{aq})]$, versus the CO_2 mobility, $(k k_r / \mu_{co2})$, should result in a straight line with a slope = 1.

Based on the aforementioned analysis, a log-log plot of the CO_2 injectivity for the Glauconitic Sandstone and the Nisku aquifers versus the CO_2 mobility at aquifer

conditions is given in Figure 45. The plot of the CO_2 injectivity for a hypothetical aquifer in the Lake Wabamun area obtained from the numerical study in Phase I (Gunter et al., 1993b) is also given in Figure 45. It was found that all the numerical results of the CO_2 injectivity for homogeneous aquifers could be generalized using the following correlation:

$$q_{co2} = 0.0208 \times (k_h \times k_v)^{0.5} \times h \times (P_{inj} - P_{aq}) / \mu_{co2} \qquad (7)$$

where q_{co2} is in [tonne/day], k_h and k_v are in [md], h is in [m], P_{inj} and P_{aq} are in [MPa] and μ_{co2} is in [mPa-s]. Equation 7 has average and maximum errors of 9.3% and 19.9%, respectively. The deviation of the numerical results from this simple correlation is believed to be due to the more complicated nature of the flow of injected CO_2 and aquifer water as indicated by this numerical study (e.g. the non-uniform front of CO_2 propagation due to override). Nevertheless, Equation 7 which takes into account the aquifer thickness, depth, permeability anisotropy and CO_2 properties (only the aquifer water properties were not taken into account), should provide a convenient tool for the prediction of CO_2 injection into deep aquifers other than those studied in the Lake Wabamun area (e.g. the aquifers in the North Sea area) with the assumption that the relative permeabilities curves for the CO_2-water system in these aquifers are very similar to those used in this study.

In order to use Equation 7 for predicting the average CO_2 injection rate into an aquifer, it is necessary to know the aquifer depth, thickness and absolute permeabilities in both the vertical and the horizontal directions. If the aquifer temperature is not known, the average aquifer temperature can be estimated based on the ground surface temperature and a geothermal gradient in the study area:

$$T_{aq} = T_{sur} + (dT/dz) \times [z + (h \times 10^{-3}) / 2] \qquad (8)$$

CORRELATION FOR INJECTIVITY FOR HOMOGENEOUS AQUIFERS

Closed Symbols: Porosity = 0.12

Open Symbols: Porosity = 0.06

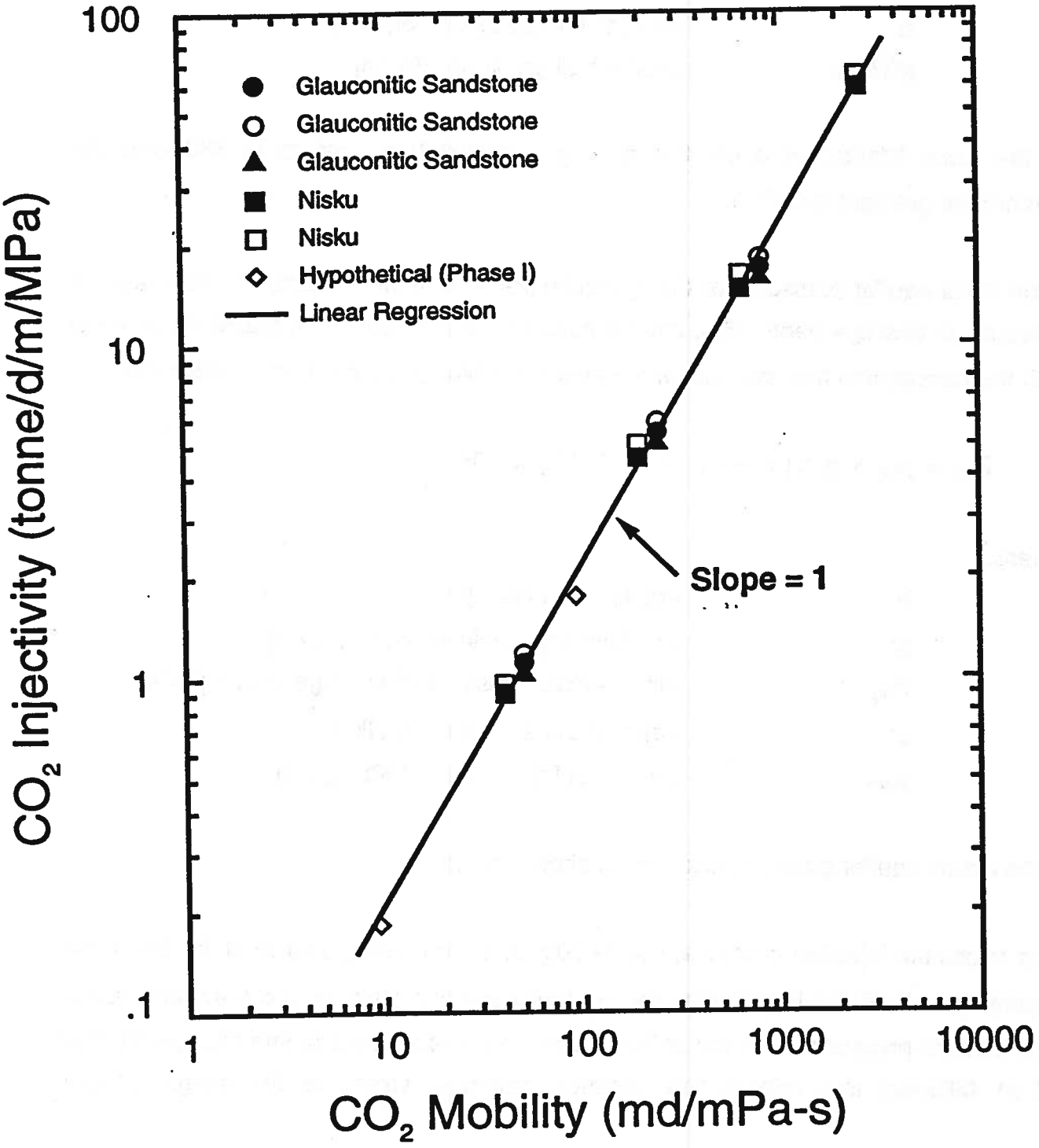

Figure 45: Correlation for CO_2 injectivity for homogeneous aquifers in the Alberta sedimentary basin

where:

h:	aquifer thickness, [m]
T_{aq}:	average aquifer temperature, [°C]
T_{sur}:	ground surface average temperature, [°C]
z:	depth to the top of aquifer, [km]
(dT/dz):	geothermal gradient, [°C/km]

In the Lake Wabamun area, the average ground temperature is 6°C and the geothermal gradient is 30°C/km.

If the initial aquifer pressure (or the hydraulic gradient) is not known, the initial aquifer pressure at average depth, P_{aq}, can be estimated based on the hydraulic head value with the assumption that the aquifer is neither overpressured nor under pressured:

$$P_{aq} = p_{aq} \times g \times [z + (h \times 10^{-3})/2] \times 10^{-3} \quad (9)$$

where:

h:	aquifer thickness, [m]
g:	gravitational acceleration, [9.8 m/s^2]
P_{aq}:	initial aquifer pressure at average depth, [MPa]
z:	depth to the top of aquifer, [km]
p_{aq}:	density of fresh water, [1000 kg/m^3]

If the actual aquifer pressure is known, it should be used.

The maximum injection pressure, P_{inj}, is 90% of the fracture pressure at the top of the aquifer (as stipulated by Alberta law, in other countries other conventions are used). The fracture pressure at the top of the aquifer can be estimated based on a gradient of 22.61 MPa/km that relates the minimum principal stress to the weight of the

overburden:

$$P_{fr} = (dP/dz) \times z \qquad (10)$$

where:

P_{fr}:	fracture pressure at the top of aquifer, [MPa]
z:	depth to the top of aquifer, [km]
(dP/dz):	pressure gradient, [MPa/km]

Figure 46 shows the initial aquifer pressure at average depth, the fracture pressure and the maximum injection pressure for aquifers with different depths and thicknesses.

The viscosity of CO_2 can be estimated based on the published data (McHugh and Krukonis, 1986) of CO_2 viscosity versus pressure at different temperatures as shown in Figure 47.

8.1.2 Average Water Velocity at Outflow Boundary

Average water velocities at the outflow boundary (7 km away from the injector well) after 30 years of CO_2 injection into the Glauconitic Sandstone and Nisku aquifers (assumed to be homogenous) as a function of horizontal absolute permeability are given in Figure 48. The average water velocity at the outflow boundary can be estimated from the CO_2 injection rate by applying conservation laws for the injected CO_2 and the outflow water in the region of the aquifer considered with the assumption that both fluids and the solid matrix are incompressible:

$$V_{aq} = 3.65 \times 10^7 \, (q_{co2} / \rho_{co2}) \, / \, (2 \pi r_{ob} h) \qquad (11)$$

where

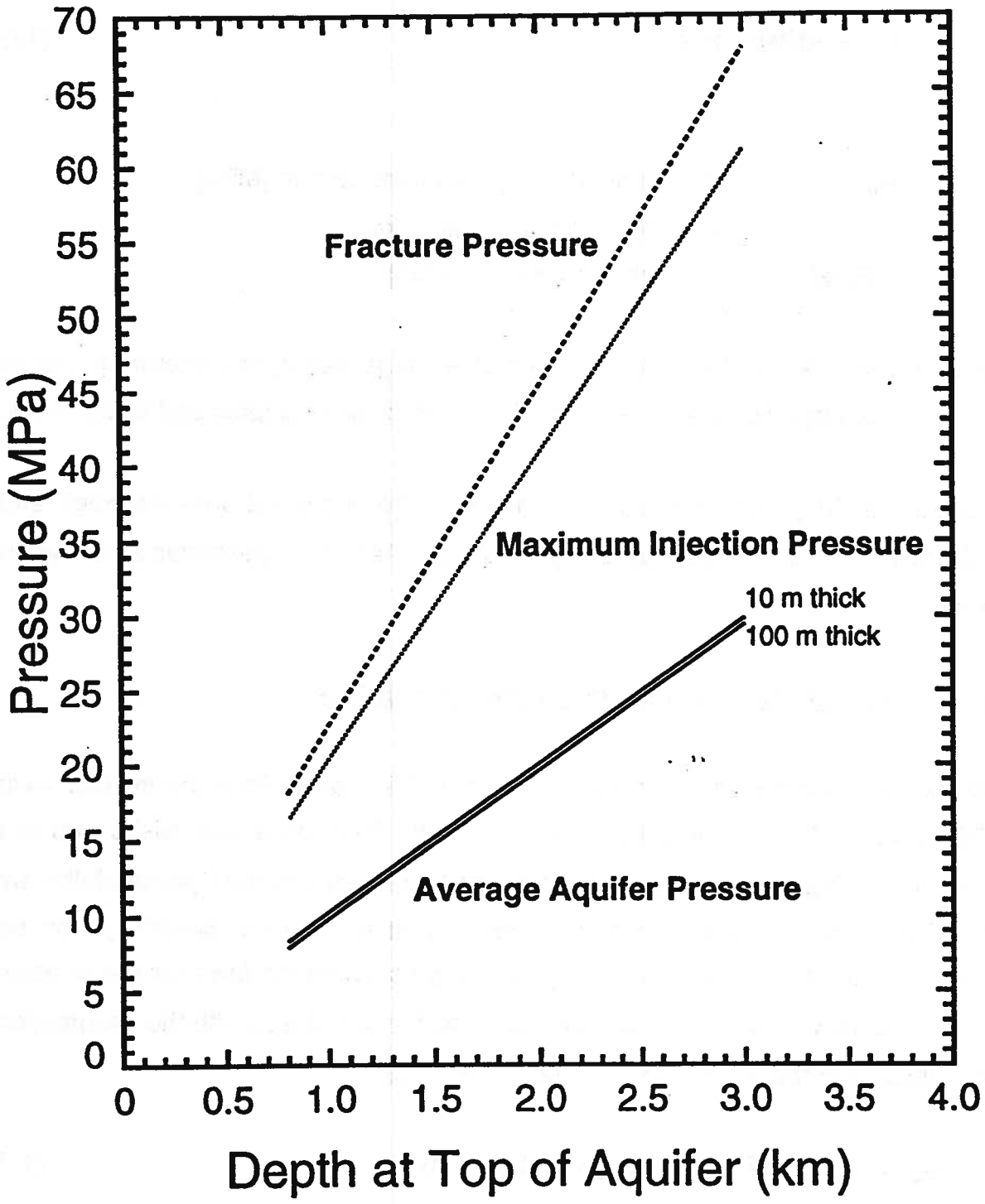

Figure 46: Fracture pressure and average pressure for aquifers in the Alberta sedimentary basin as a function of depth and thickness

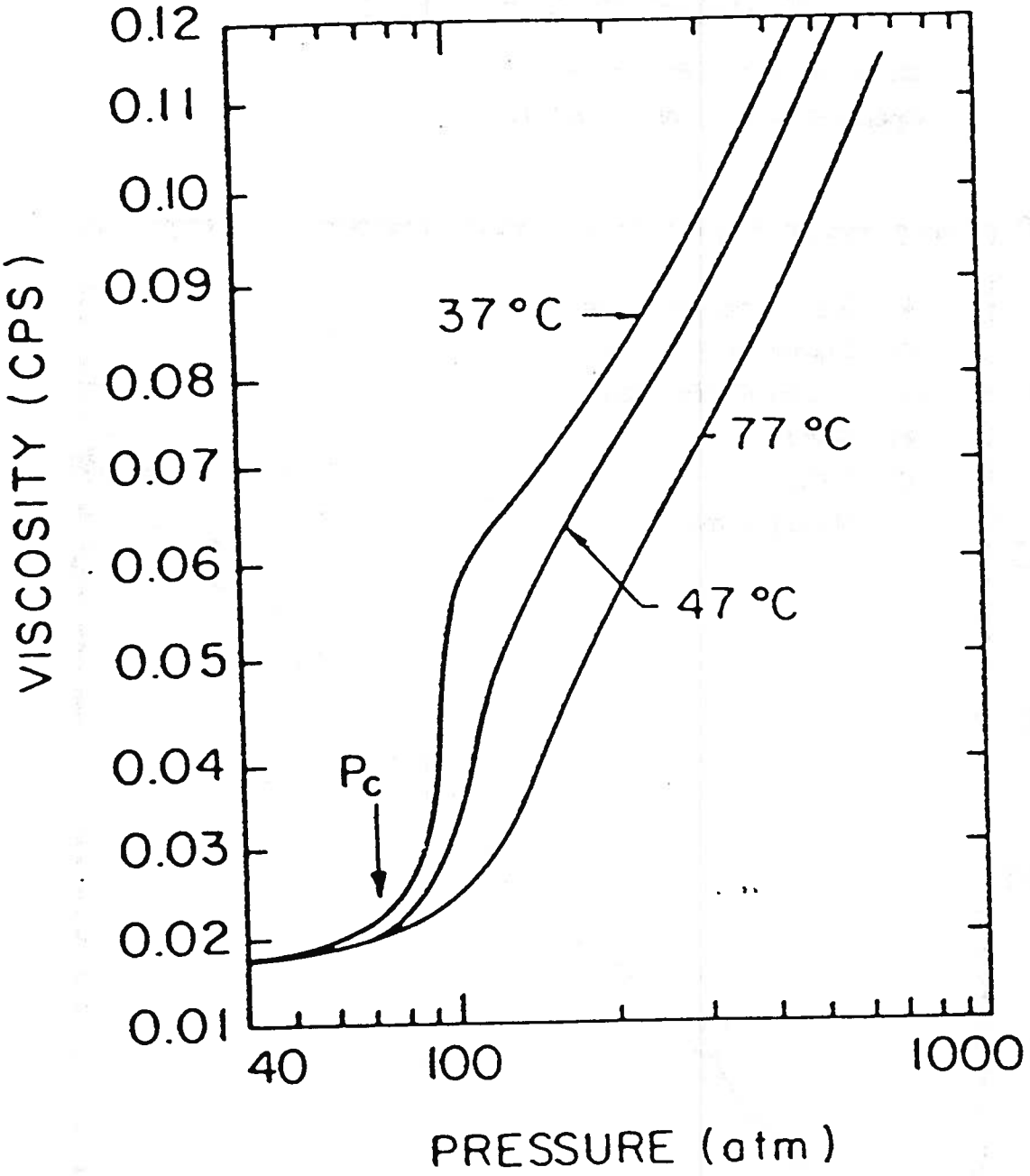

100 atm = 10.13 MPa
1 cp = 1 mPa-s

Figure 47: Viscosity of CO_2 in supercritical state

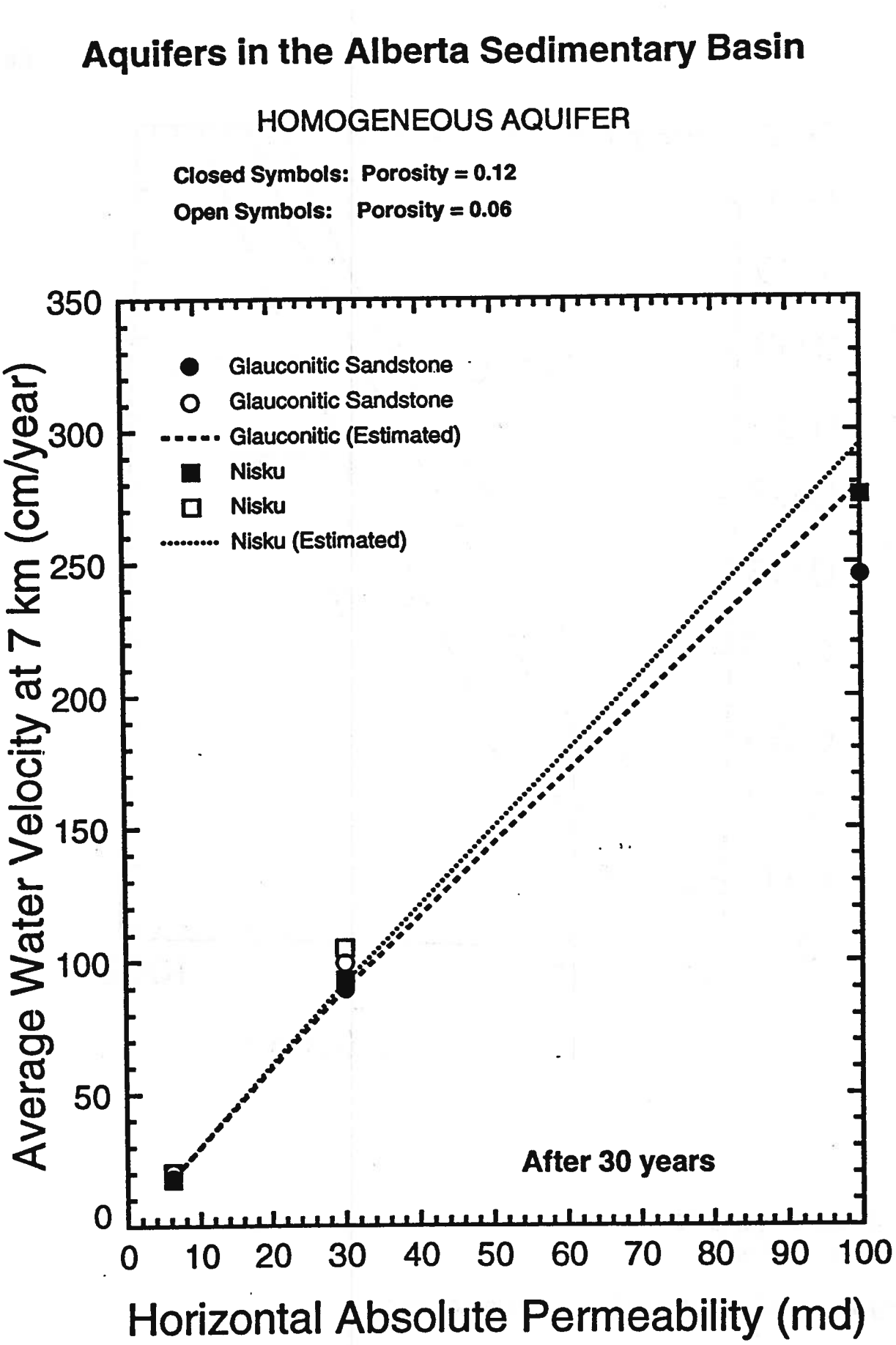

Figure 48. Average water velocity at 7 km away from injector for homogeneous aquifers in the Alberta sedimentary basin

h:	thickness of aquifer, [m]
q_{co2}:	average mass injection rate of CO_2, [tonne/day]
r_{ob}:	radius of outflow boundary, [m]
V_{aq}:	average water velocity at outflow boundary, [cm/yr]
ρ_{co2}:	density of CO_2 at injection conditions, [kg/m^3]

The predictions of average water velocities at the outflow boundary based on the numerical results of CO_2 injection in both the Glauconitic Sandstone and the Nisku aquifers with a porosity value of 0.12 are shown in Figure 48. It is noted again that porosity has very little effect on the CO_2 injectivity. In case that the CO_2 injection rate, q_{co2}, is unknown, it can be obtained from Equation 7.

Due to the compressibilities of the fluids and the solid matrix in the aquifer, Equation 11 is only valid when the outflow boundary is far away from the pressurized zone around the injector well. In this case, the average water velocity at the outflow boundary appears to increase linearly with the absolute permeability of the aquifer. However, for the case of r_{ob} = 7000 m used in this study, the discrepancy between the predictions from Equation 11 and the numerical results occurs when the aquifer is thin, the aquifer permeability is high (i.e. >100 md) and/or the aquifer porosity is low (i.e. 0.06), mainly because the pressurized zone in these cases extended farther than the location of the preset outflow boundary.

8.2 Aquifers with a "Sweet" Zone

8.2.1 CO_2 Injectivity

CO_2 injectivitiy enhancement factors due to the existence of "sweet" zones in the Glauconitic Sandstone and Nisku aquifers as a function of the size of the "sweet" zone are shown in Figure 49. The CO_2 injectivity enhancement factor is defined as the CO_2

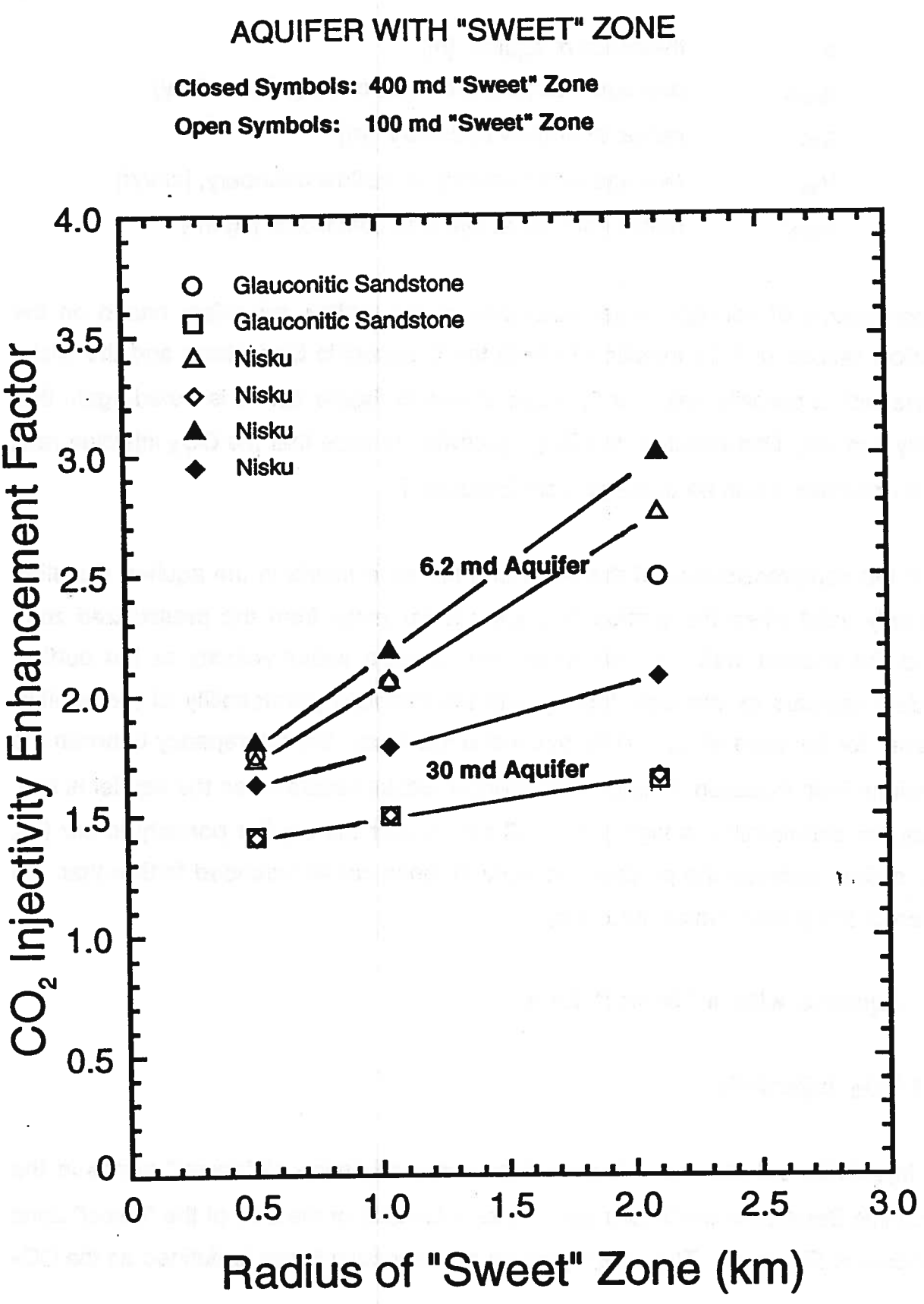

Figure 49. CO_2 injectivity enhancement factor for aquifers with "sweet" zone in the Alberta sedimentary basin

injectivity of an aquifer with the existence of a "sweet" zone of locally high permeability around the injector well divided by the CO_2 injectivity of the same aquifer with no "sweet" zone. It is found that:

- CO_2 injectivity enhancement factor varied from 1.4 to 3, depending on a wide range of "sweet" zone radius with different combinations of aquifer and "sweet" zone permeabilities;
- for a given combination of aquifer and "sweet" zone permeability values, the enhancement factor increased with the "sweet" zone radius;
- for a given combination of aquifer and "sweet" zone permeability values, the aquifer thickness appeared to have very little effect on the enhancement factor;
- for a given "sweet" zone permeability (100 or 400 md) and radius, the lower the regional aquifer permeability is (i.e. 6.2 md), the higher is the enhancement factor;
- for a given aquifer permeability (6.2 or 30 md) and "sweet" zone radius, the higher the "sweet" zone permeability is (i.e. 400 md), the higher is the enhancement factor.

Although a correlation which is taken into account the aquifer permeability, the "sweet" zone permeability and radius was not obtained, nevertheless, Figure 49 can be used as a generalized chart for the prediction of CO_2 injection into deep aquifers with a "sweet" zone other than those studied for aquifers in the Lake Wabamun area.

8.2.2 Average Water Velocity at Outflow Boundary

Average water velocity enhancement factors at the outflow boundary (7 km away from the injector well) after 30 years of injecting CO_2 into the Glauconitic Sandstone and Nisku aquifers with "sweet" zones as a function of the "sweet" zone radius are given in Figure 50. The average water velocity enhancement factor is defined as the average water velocity at the outflow boundary of an aquifer with the existence of a "sweet"

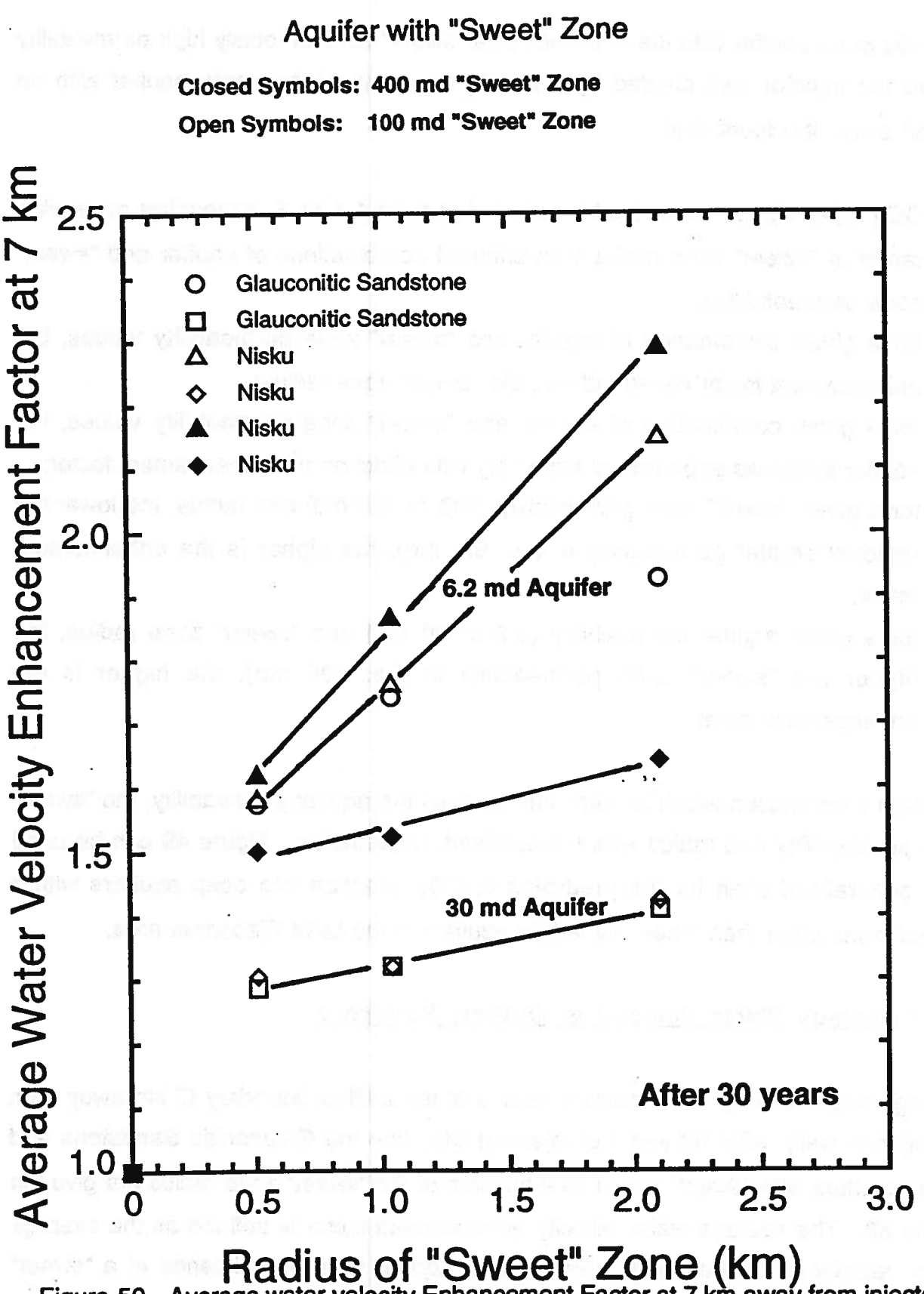

Figure 50. Average water velocity Enhancement Factor at 7 km away from injector for aquifers with "sweet" zone in the Alberta sedimentary basin

zone of locally high permeability around the injector divided by the average water velocity at the outflow boundary of the same aquifer with no "sweet" zone. It is found that:

- for a given combination of aquifer and "sweet" zone permeability values, the average water velocity enhancement factor at the outflow boundary increases with the "sweet" zone radius;
- for a given combination of aquifer and "sweet" zone permeabilities, the aquifer thickness appears to have very little effect on the average water velocity enhancement factor at the outflow boundary;
- for a given aquifer permeability (6.2 and 30 md) and "sweet" zone radius, the higher the "sweet" zone permeability is (i.e. 400 md), the higher the enhancement factor at the outflow boundary, although the increase is more significant for the aquifer having a higher permeability (i.e. 30 md).
- for a given "sweet" zone permeability (100 or 400 md) and radius, the lower the aquifer permeability is (i.e. 6.2 md), the higher the enhancement factor;

It is noted that the average water velocity at the outflow boundary for a aquifer with "sweet" zone can be estimated using Equation 11, if the CO_2 injection rate is known. For the case of aquifer with a "sweet' zone, the high pressure zone near the injector well is located in general in the "sweet" zone, as pressure drops off rather rapidly in the surrounding low permeability region of the aquifer.

9. SUMMARY

Canada is working to meet its commitment to stabilize greenhouse gas emissions at the 1990 levels by the year 2000. Alberta is an energy-rich province of Canada, and a net exporter of energy from the coal, oil and gas reserves contained in the Alberta Sedimentary Basin. As might be expected, major sources of CO_2 point emissions from energy-related industrial activities in Alberta are also located in the basin. Utilization of CO_2 for EOR (enhanced oil recovery) and disposal of CO_2 in depleted oil and gas reservoirs or aquifers in the Alberta Sedimentary Basin are considered technically viable options to reduce CO_2 emissions.

An AOSTRA survey (Bailey and MacDonald, 1993) of CO_2-emission and potential CO_2-utilization sites throughout the Alberta Sedimentary Basin was used as a basis to target sedimentary horizons that would be likely candidates for aquifer disposal of CO_2. Conclusions from examination of the stratigraphy underlying the major power plants at Lake Wabamun, the Novacor plant at Joffre, the Hanlan-Robb gas plant, the bi-provincial heavy oil upgrader at Lloydminster, and the oil fields at Carson Creek, Pembina and Redwater were that the most suitable disposal aquifers were located at Lake Wabamun, from the point of view of both CO_2 source and aquifer depth. The best siliciclastic disposal aquifer in this area is the Glauconitic Sandstone aquifer. Although the siliciclastic disposal aquifers are preferable to equivalent carbonate aquifers because of their potential for mineral trapping, the siliciclastic aquifers identified for CO_2 disposal were relatively thin, which limits their capacity for CO_2. Consequently a thicker, deeper carbonate aquifer, the Nisku aquifer, was also chosen for analysis at Lake Wabamun. The site chosen for disposal was near the southeast corner of Tp. 52, R4 W5 Mer. This is the site of a "sweet" or high permeability zone of 100 md in the Glauconitic Sandstone Aquifer. The injection strategy is to use one well to access both aquifers.

At the chosen injection site, the 13 meter thick Glauconitic Sandstone aquifer is located at an average depth of 1480 meters, with a formation temperature of 50°C and salinity of 40,000 mg/l, compared to an average depth of 1860 meters and a temperature of 60°C with a formation water salinity of 190,000 mg/l for the 60 meter thick Nisku aquifer. Regional permeabilities (6 md on average with local values up to 400 md) and porosities (6 to 12%) are similar for the two aquifers.

Injection of CO_2 was numerically modelled over a range of conditions for each aquifer. Regional permeabilities were varied from 6 to 400 md, while "sweet" zone permeabilities were varied from 100 to 400 md. The radius of the sweet zone was varied from 0.5 to 2 kilometers. Injection pressure ranged from 25 MPa for the Glauconitic Sandstone aquifer to 38 MPa for the Nisku aquifer.

For the thin siliciclastic Glauconitic Sandstone aquifer, disposal of 2.8×10^6 to 2.2×10^7 tonnes of CO_2 over a period of 30 years can be achieved realistically, which corresponds to average CO_2 injection rates ranging from 128 to 2,009 t/d/well. Approximately 17 to 22 wt% of the injected CO_2 will dissolve in the aqueous phase at the average aquifer temperature of 50°C. Even for this thin aquifer (13 m thick), there is numerical evidence of CO_2 override to the top part of the aquifer. In general, CO_2 will propagate less than 5 km away from the injector well after an injection period of 30 years except for the case of the highest permeability (i.e. 100 md) and the lowest porosity (i.e. 0.06).

For the relatively thick Nisku aquifer, disposal of 1.3×10^7 to 1.3×10^8 tonnes of CO_2 over a period of 30 years can be achieved realistically, which corresponds to average CO_2 injection rates ranging from 1,163 to 11,872 t/d/well. Approximately 16 to 25 wt% of the injected CO_2 will dissolve in the aqueous phase at the average aquifer temperature of 60°C. Due to aquifer thickness (60 m thick), CO_2 will override significantly to the top part.

In general, CO_2 will propagate less than 5 km away from the injector well after an injection period of 30 years, except for the cases of high permeabilities (i.e. 100 and 400 md).

Regional flow rates of deep aquifers in the Alberta Sedimentary Basin are in the order of 1 to 10 cm/yr. The numerical simulations have shown that the velocity of CO_2-formation water mixtures increase considerably near the injection well due to the high pressure gradients caused by CO_2 injection, but that this velocity decreases as the CO_2 and water move away from the injection well. In some cases, depending on aquifer properties, it was found that no measurable changes in the natural flow regime of formation water will take place at a distance of 7 km from the injection well, even after 30 years of continuous operation. In other cases it was found that the velocity of the CO_2-formation water mixture will increase considerably at the preset outflow boundary of 7 km (from several cm/yr to up to 300 cm/yr). However, even in these cases it is expected that the velocity will continue to decrease as the distance from the injection well increases, given the very large areal extent of the aquifers considered in this study, as opposed to CO_2 injection in depleted oil and gas reservoirs which have limited size and capacity. Thus, it is expected that the effects of injecting large quantities of CO_2 for long periods of time will not affect the natural flow regime of formation water beyond a distance of 10-15 km from the injection well, depending on aquifer properties and injection characteristics. On the other hand, the natural flow of formation water in any given aquifer will not influence the CO_2 injectivity in the near field because of the high hydraulic (pressure) gradients induced by CO_2 injection. In the far field, the CO_2-formation water mixture will flow according to the natural regime of formation water in the respective host aquifer (Bachu et al., 1994).

A correlation for the prediction of CO_2 injectivity has been established for homogeneous aquifers, which takes into account the aquifer thickness, depth, permeability anisotropy and CO_2 properties at injections conditions. A generalized chart can be used to predict the CO_2 injectivity enhancement factor due to the existence of a "sweet" zone in the aquifer. This chart takes into account the regional aquifer permeability and the size and permeability of

the "sweet" zone. The strategy is to locate near-well "sweet" zones of high permeability (100-400 md), as the existence of this "sweet" zone will allow CO_2 injectivity to improve by a factor of 1.4 to 3. This correlation for homogeneous aquifers and the generalized chart can be used as a scoping tool to target other aquifers in the Alberta Sedimentary Basin as promising candidates for CO_2 disposal and long term storage.

Other regions of the Alberta basin may be promising for aquifer disposal of CO_2. In contrast with CO_2 injection in depleted oil and gas reservoirs, CO_2 injection in deep aquifers in sedimentary basins has the advantage that it is not limited by reservoir location, size and properties. There are various aquifers in the Alberta basin suitable in places for CO_2 disposal. In particular, thin, isolated aquifers in the Cretaceous and post-Cretaceous sedimentary succession in the southwestern part of the basin near the deformed thrust and fold belt have the additional significant property that the flow of formation water is downdip, basin-inward, toward hydraulic sinks created by shale elastic rebound as a result of Tertiary-to-Recent erosion (Bachu and Underschultz, 1995). Thus, disposal of CO_2 and of any other liquid wastes in these aquifers in this area will lead practically to the permanent capture and retention of CO_2 and other wastes (on a geological time scale), as pointed out previously in a theoretical study by Neuzil (1986). Similar phenomena of basin-inward flow of formation waters was observed in a sub-Andean foreland basin in Colombia (Villegas et al., 1994). Thus, it is expected that other aquifers in various foreland sedimentary basins in the world may exhibit similar flow characteristics, enhancing the advantages of disposing of CO_2 and other waste liquids in deep aquifers. Such foreland basins are found, for example, all along the eastern side of the American Cordillera, from the Rocky Mountains in North America to the Andes Mountains in South America (from Colombia to Argentina).

There are other types of mid-continent sedimentary basins, like the intracratonic Williston basin in Canada and USA, the Michigan and Illinois basins, etc. The flow of formation waters in deep aquifers in these basins is regional-scale in nature and generally slow

(several cm/yr), like in the Alberta basin, being driven by the basin-scale topography (e.g., the Williston basin, Bachu and Hitchon, in press). These mid-continent sedimentary basins offer also the opportunity of disposing of CO_2 and other liquid wastes by deep injection. On the other hand, it is believed that intra-montane sedimentary basins have limited capacity for CO_2 disposal because of their generally small size. As for rift and coastal basins forming now, like the Beaufort basin in Canada, the Gulf coast, and along the Atlantic ocean (e.g. the Jeanne d'Arc basin in Canada), these basins are currently undergoing active compaction and subsidence. The flow of formation waters is not driven laterally by topography, which is nonexistent, but vertically by sediment loading and compaction. Thus, it is believed that these sedimentary basins are not particularly suitable for the disposal of CO_2 or other liquid wastes. The correlations found for injecting CO_2 in specific aquifers and sites in the Alberta basin may be applicable to other deep aquifers in various sedimentary basins around the world, aquifers characterized by similar properties and for similar CO_2-injection characteristics.

Through this study and its predecessors, CO_2 disposal into low permeability, deep aquifers in sedimentary basins has been shown to be technically feasible and perhaps offers the largest potential for the landlocked areas of the world. However, a preliminary financial assessment indicates that this option will be costly, due mainly to CO_2 capture, purification and compression, and secondarily due to field facilities required. Although there are many possibilities to reduce CO_2 emissions that are more economically attractive, aquifer disposal remains as one of the largest sinks available for CO_2, and may be utilized if other less expensive options are exhausted.

10. CONCLUSIONS

- The most suitable CO_2 disposal aquifers in the Alberta Sedimentary Basin are located at Lake Wabamun, from the point of view of both CO_2 source and aquifer depth.

- In the Lake Wabamun area, the best disposal aquifer for mineral trapping of CO_2 is the relatively thin (13m) siliciclastic Glauconitic Sandstone aquifer.

- In the Lake Wabamun area, the best disposal aquifer for CO_2 capacity is the thick (60m) carbonate Nisku aquifer.

- Although aquifers in the Alberta Basin have low regional permeability (in the order of 5 millidarcies), injection rates may be significantly increased by locating injection wells in areas of locally high permeability (= sweet zones).

- The site chosen for CO_2 disposal in the Lake Wabamun area is near the southeast corner of Tp. 52, R4W5Mer. This is the site of a "sweet" or high permeability zone of 100 md in the Glauconitic Sandstone aquifer.

- The injection strategy is to use one well to access both the Glauconitic Sandstone and the Nisku aquifers.

- For the thin Glauconitic Sandstone aquifer, CO_2 disposal of 128 (for the homogeneous aquifer) to 2,009 t/d/well (when a sweet zone exists) can be achieved realistically.

- For the relatively thick Nisku aquifer, CO_2 disposal of 1,163 (for the homogeneous aquifer) to 11,872 t/d/well (when a sweet zone exists) can be achieved realistically.

- In general, CO_2 will propagate less than 5 km away from the injector after an injection period of 30 years in either the Glauconitic Sandstone or Nisku aquifers.

- A generalized chart was prepared and can be used to predict the CO_2 injectivity enhancement factor due to the existence of a sweet zone in the aquifer. This chart takes into account the regional aquifer permeability and the size and permeability of the sweet zone. Injection into a sweet zone will increase CO_2 injection rates by factor of 1.4 to 3.

- A correlation for the prediction of CO_2 injectivity has been established for homogeneous aquifers, which takes into account the aquifer thickness, depth, permeability anisotropy and CO_2 properties at injection conditions. This tool can be used to target aquifers for detailed evaluation for CO_2 disposal and long term storage in other parts of the Alberta Basin or in other sedimentary basins of the world.

11. REFERENCES

Bachu, S. 1995. Synthesis and model of formation water flow in the Alberta basin. American Association of Petroleum Geologists Bulletin, in press.

Bachu, S. 1991. On the effective thermal and hydraulic conductivity of binary heterogeneous sediments. Tectonophysics, v. 2-4, p. 299-314.

Bachu, S. and Burwash, R.A. 1991. Regional-scale analysis of the geothermal regime in the Western Canada Sedimentary Basin. Geothermics, v. 20 (5/6), p. 387-407.

Bachu, S., Gunter, W.D. and Perkins, E.H. 1994. Aquifer disposal of CO_2: Hydrodynamic and mineral trapping. Energy Conversion and Management, v. 35, p. 269-279.

Bachu, S. and Hitchon, B. (in press) Regional-scale flow of formation waters in the Williston Basin. Amer. Ass. Petroleum Geol. Bull.

Bachu S. and Underschultz, J.R. 1995. Large-scale underpressuring in the Mississippian-Cretaceous succession, Southwestern Alberta Basin. Amer. Assoc. Petroleum Geol. Bull., v. 79, (in press)

Bailey, R.T. and McDonald, M.M. 1993. CO_2 capture and use for EOR in Western Canada 1. General Overview. Energy Conversion and Management, v. 35, p. 1145-1150.

Clark, S.P. 1966. Handbook of physical constants. The Geological Society of America, Inc., New York, p. 382-383.

Craft, B.C. and Hawkins, M.F. 1959. Applied petroleum engineering. Prentice-Hall Inc., Englewood Cliffs, New Jersey, p. 283-285.

Desbarats, A.J. and Bachu, S. 1994. Geostatistical analysis of aquifer heterogeneity from the core scale to the basin scale. Water Resources Research, v. 30(3), p. 673-684.

Gunter, W.D., Perkins, E.H. and McCann, T.J. 1993a. Aquifer disposal of CO_2-rich gases: Reaction design for added capacity. Energy Conversion and Management, v. 34, p. 941-948.

Gunter, W.D., Perkins, E.H., Bachu, S., Law, D.H.-S., Wiwchar, B. and Zhou, Z. 1993b. Aquifer disposal of CO_2-rich gases - Phase I, In the vicinity of the Sundance and Genesee power plants, Injectivity, chemical reactions, and proof of concept. Alberta Geological Survey Open File Report no. 1994-16.

Gunter, W.D., Bachu, B., Perkins, E.H., Underschultz, J.R., Wiwchar, B., Yuan, L.P., Berhane, M. and Cotterill, D. 1994. Central Alberta: CO_2 disposal into Alberta basin aquifers - Phase II, Hydrogeoloical and mineralogical characterization of Mannville Group strata in the Lake Wabamun area & water-rock reactions due to CO_2 injection into the Glauconitic Sandstone aquifer. Alberta Geological Survey Open File Report no. 1994-17.

Hitchon, B. and Brulotte, M. 1994. Culling criteria for "standard" formation water analyses. Applied Geochemistry, v. 9, p. 637-645.

Kestin, J., Khalifa, H.E., and Correia, R.J. 1981. Tables of the dynamic and kinematic viscosity of aqueous NaCl solutions in the temperature range 20-150°C and the pressure range 0.1-35 MPa. J. Physical & Chemical Ref. Data, v. 10, #1, p. 71-87.

McHugh, M.A. and Krukonis, V.J. 1986. Supercritical fluid extraction, principles and practice. Butterworths, Boston, p. 10.

Neuzil, C.E. 1986. Groundwater flow in low permeability environments. Water Resources Research, v. 22, p. 1163-1195

Rowe, A.M. and Chou, J.C.S. 1970. Pressure-volume-temperature-concentration relation of aqueous NaCl solutions. J. Chem. Eng. Data, v. 15, #1, p. 61-66.

STARS Technical Manual, Version 4.0 1990. Computer Modelling Group, Calgary, Alberta.

Todd, M.R. and Grand, G.W. 1993. Enhanced oil recovery using carbon dioxide. Energy Conversion and Management, v. 34, p. 1157-1164.

van der Meer, L.G.H. 1992. Investigations regarding the storage of carbon dioxide in aquifers in the Netherlands. Energy Conversion and Management v. 33, p. 611-618.

Villegas, M.E., Bachu, S., Ramon, J.C. and Underschultz, J.R. 1994. Flow of formation waters in the Cretaceous-Miocene succession of the Llanos Basin, Columbia. Amer. Assoc. Petroleum Geol. Bull., v. 78, p. 1843-1862.

APPENDIX I

FORMATION WATER ANALYSES

AGSWDB WATER ANALYSIS REPORT

AGSWDB Well site identifier (SITID): 80748 Chemistry number: 1
AGSWDB Hard copy number (HRDCPNO): 44552

CHEMICAL & GEOLOGICAL LAB LTD Lab. Sample ID. C78-3515-3

Well identifier	Well name	KB elev.	Gr. elev
0515040805000	ANDEX ET AL HIGHVALE 5-8-51-4	757.30	753.20

Interval Sampled from: 1927.56 to: 1935.18 meters KB

Formation Sampled: WINT. Formation code: 6700

Sample produced by: DST # 1 Sampling point:BOTTOM

DST Recovery
94.50 M MUD
72.90 M WATER
91.40 M SULPHUROUS SALT WATER

Date: Sampled: 1978/06/16 Received: 1978/08/14 Analyzed: 1978/08/23

CATIONS

ION	mg/l	%MEQ	MEQ/L
Na+K	44176.		
Ca	8909.	14.409	444.6
Mg	1665.	4.441	137.0

ANIONS

ION	mg/l	%MEQ	MEQ/L
Cl	87400.	79.905	2465.2
HCO3	616.	0.327	10.1
SO4	1360.	0.918	28.3

Specific gravity 1.1010 @ 16. C
PH 8.00 @ 22. C
Hydrogen Sulfide Description:
Organics Description :
Calculated sodium: 44194.
TDS by Evapor. @ 110 C: 165500.

Refractive Index 1.35740 @ 25. C
Resistivity ohm/m 0.06900 @ 25. C
Calculated TDS : 143831.
TDS at Ignition : 137400.

Sample appearance:

PALE YELLOW FILTRATE REC'D FROM A SAMPLE CONTAINING APPROX. 10% SED. AND H2S.

Remarks:

FE TRACE.

AGSWDB WATER ANALYSIS REPORT

AGSWDB Well site identifier (SITID): 80755 Chemistry number: 1
AGSWDB Hard copy number (HRDCPNO): 44567

CHEMICAL & GEOLOGICAL LAB LTD Lab. Sample ID. E82-2343

Well identifier	Well name	KB elev.	Gr. elev
0515040912000	ANDEX ET AL HIGHVALE 12-9-51-4	799.10	795.00

Interval Sampled from: 1594.00 to: 1595.70 meters KB

Formation Sampled: OST 3120 Formation code: 3120

Sample produced by: Sampling point:

CATIONS

ION	mg/l	%MEQ	MEQ/L
K	482.	1.024	12.3

ANIONS

ION	mg/l	%MEQ	MEQ/L
Cl	42100.	98.600	1187.5
SO4	218.	0.377	4.5

Sample appearance:

THE SAMPLE CONSISTED OF 54% FREE, SALT WATER, 46% OIL LAYER.

AGSWDB WATER ANALYSIS REPORT

AGSWDB Well site identifier (SITID): 80827 Chemistry number: 1
AGSWDB Hard copy number (HRDCPNO): 44628

CHEMICAL & GEOLOGICAL LAB LTD Lab. Sample ID. E78-3618-5

Well identifier	Well name	KB elev.	Gr. elev
0515043401000	ANDEX ET AL HIGHVALE 1-34-51-4	802.20	798.10

Interval Sampled from: 1948.00 to: 1956.00 meters KB

Formation Sampled: WINT. Formation code: 6700

Sample produced by: DST # 1 Sampling point:BOTTOM

DST Recovery

60.00 M	MUD
280.00 M	GAS-CUT MUD
1320.00 M	GAS-CUT SALT WATER

Date: Sampled: 1978/11/13 Received: 1978/11/15 Analyzed: 1978/11/29

CATIONS

ION	mg/l	%MEQ	MEQ/L
Na+K	48818.		
Ca	11490.	15.514	573.4
Mg	2582.	5.749	212.5

ANIONS

ION	mg/l	%MEQ	MEQ/L
Cl	102500.	78.231	2891.2
HCO3	437.	0.194	7.2
SO4	553.	0.312	11.5

Specific gravity 1.1240 @ 25. C Refractive Index 1.36300 @ 25. C
PH 6.90 @ 21. C Resistivity ohm/m 0.05700 @ 25. C
Hydrogen Sulfide Description:
Organics Description :
Calculated sodium: 48838. Calculated TDS : 166178.
TDS by Evapor. @ 110 C: 185100. TDS at Ignition : 163700.

Sample appearance:

THE SAMPLE CONSISTED OF MURKY SALT WATER.

Remarks:

FE TRACE. E78-3618-1 - TOP RESIS OF THE FILTRATE: .125, MUD. -2 - 1000 FT. FRO M THE TOP RESIS: .057, MURKY WATER, H2S PRES. -3 - 150 FT. FROM THE TOP RESIS: .061, SAME AS -2. 4 - 57 FT. FROM TOP RESIS: .097, WATERY MUD. TRACE OF H2S. ALL RESIS OHM/M @ 25 C.

APPENDIX II

GLAUCONITIC SANDSTONE AQUIFER CO_2 MODEL INJECTION RESULTS

Glauconitic Sandstone Aquifer

NUMERICAL RUN (CO2_60)

Aquifer Porosity = 0.12 Aquifer Permeability = 6.2 md (horizontal)
Injection Pressure = 25.15 MPa

(a) Cumulative CO_2 Injection

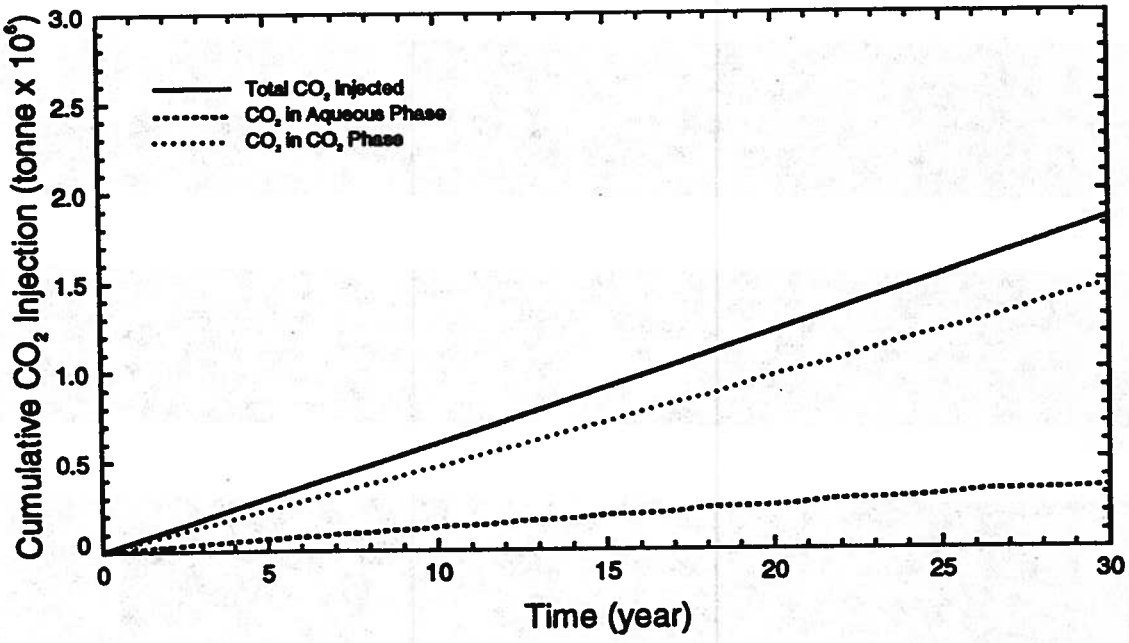

(b) CO_2 Injection Rate

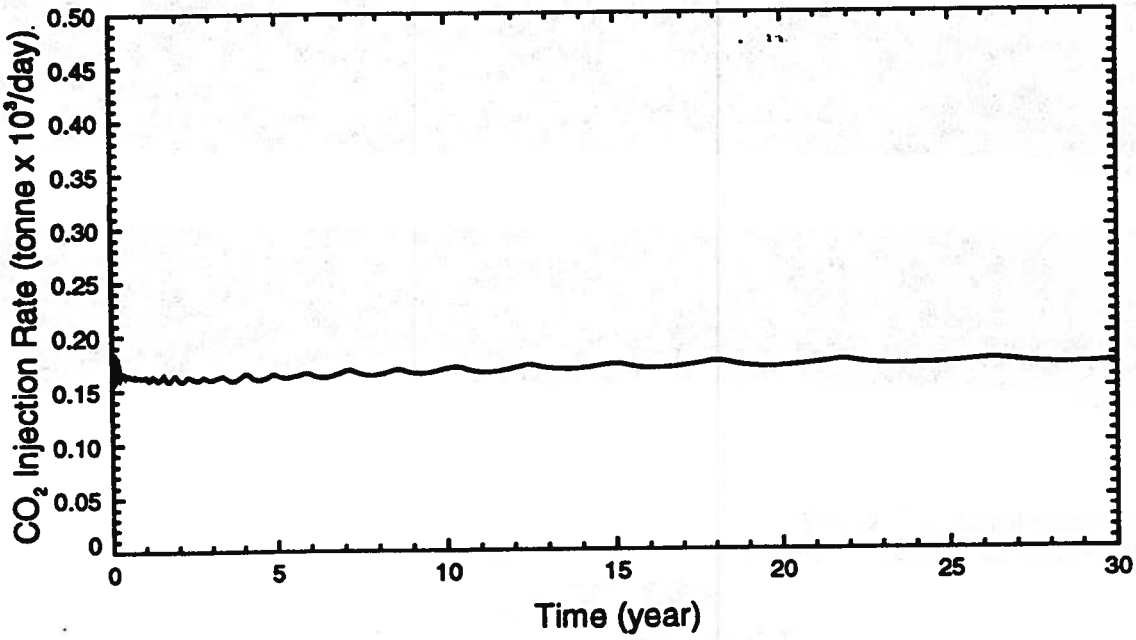

Carbon Dioxide Saturation (Run CO2_60)

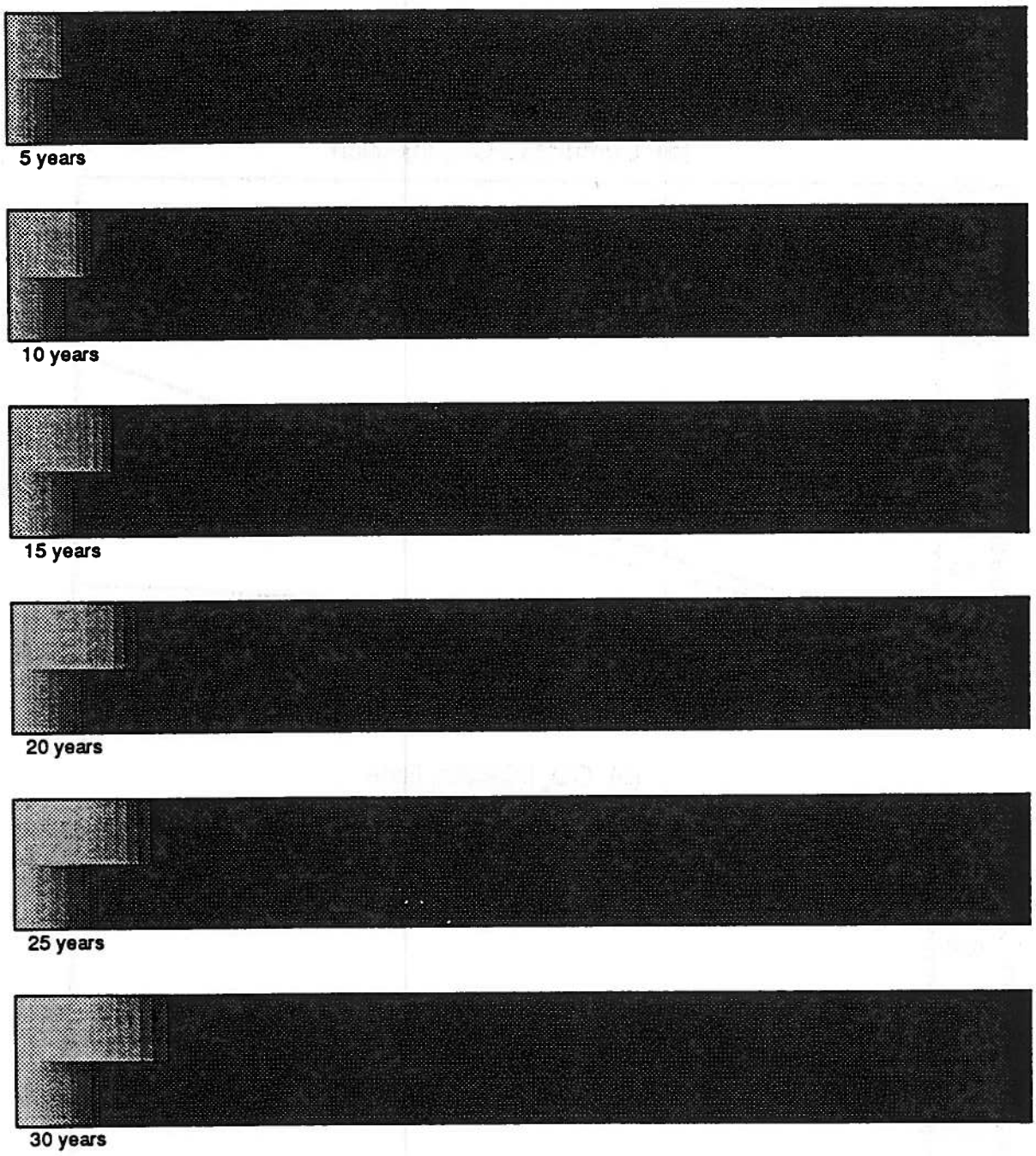

Vertical scale factor = 70.000
Field dimensions: 6999. (horiz.), 13.00 (vert.)

Glauconitic Sandstone Aquifer

NUMERICAL RUN (CO2_60)

Aquifer Porosity = 0.12 Aquifer Permeability = 6.2 md (horizontal)
Injection Pressure = 25.15 MPa

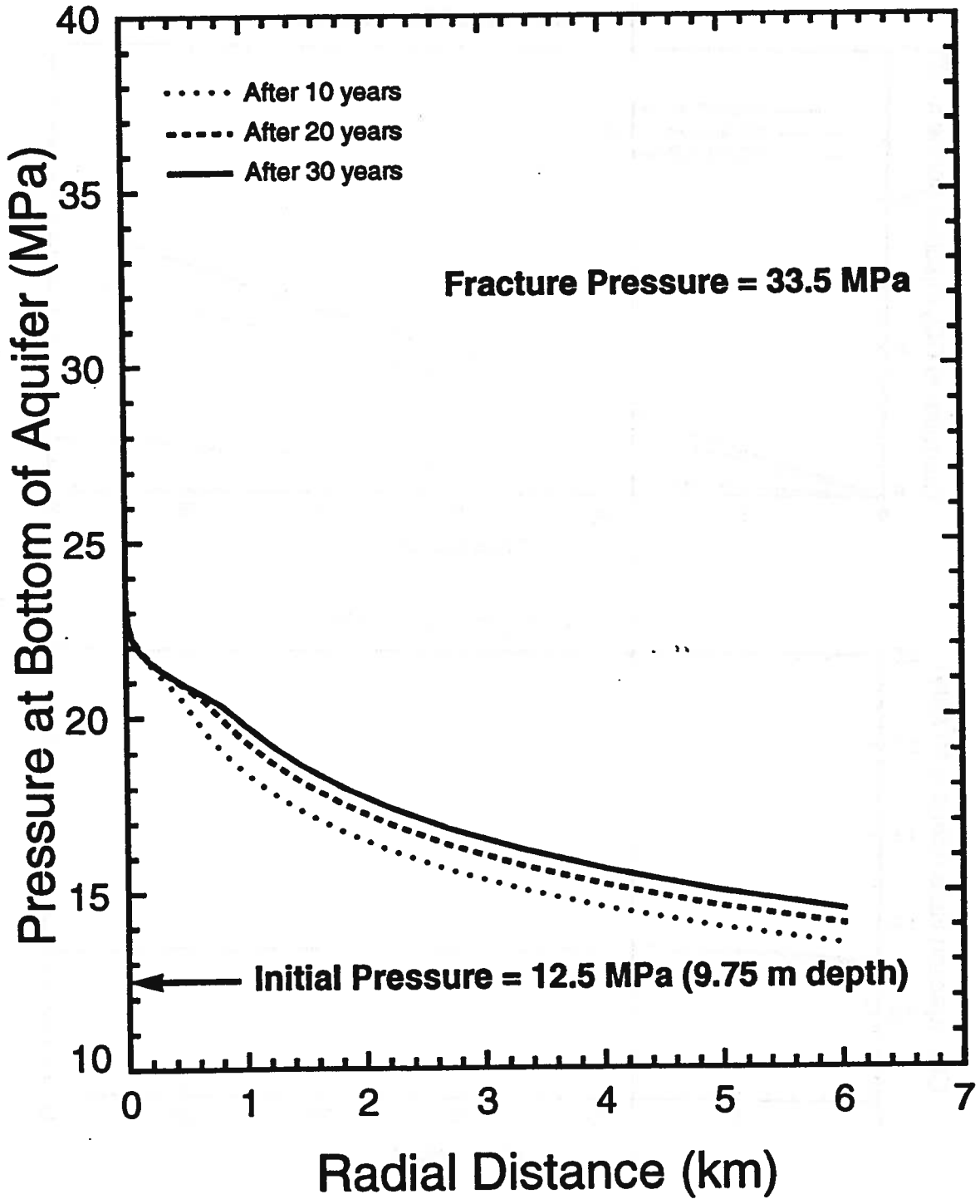

Glauconitic Sandstone Aquifer

NUMERICAL RUN (CO2_61)

Aquifer Porosity = 0.12 Aquifer Permeability = 30 md (horizontal)
Injection Pressure = 25.15 MPa

(a) Cumulative CO_2 Injection

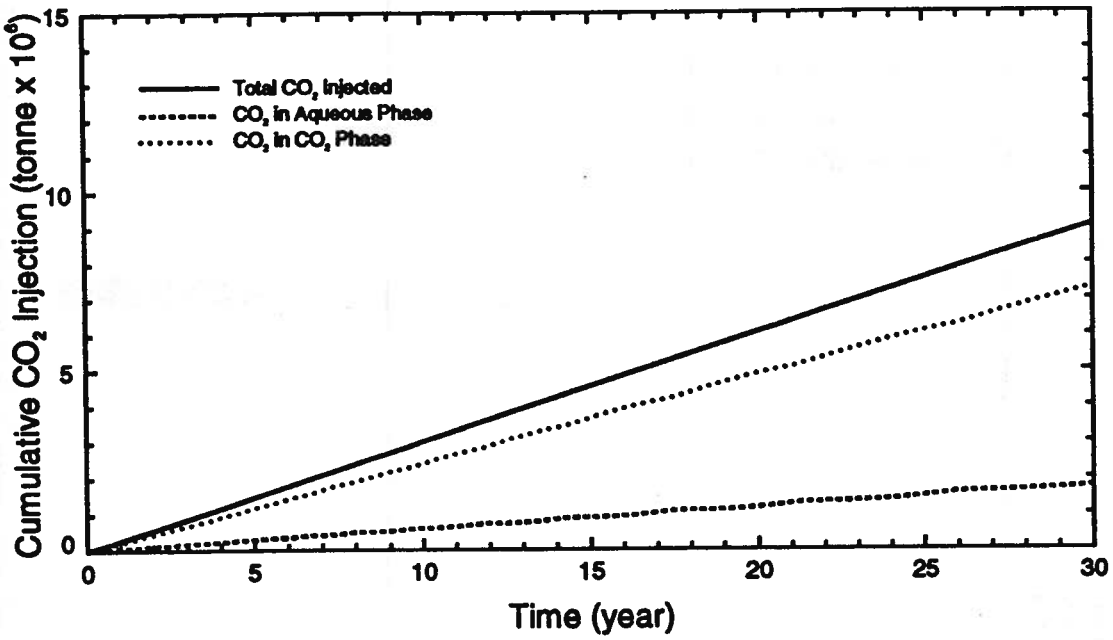

(b) CO_2 Injection Rate

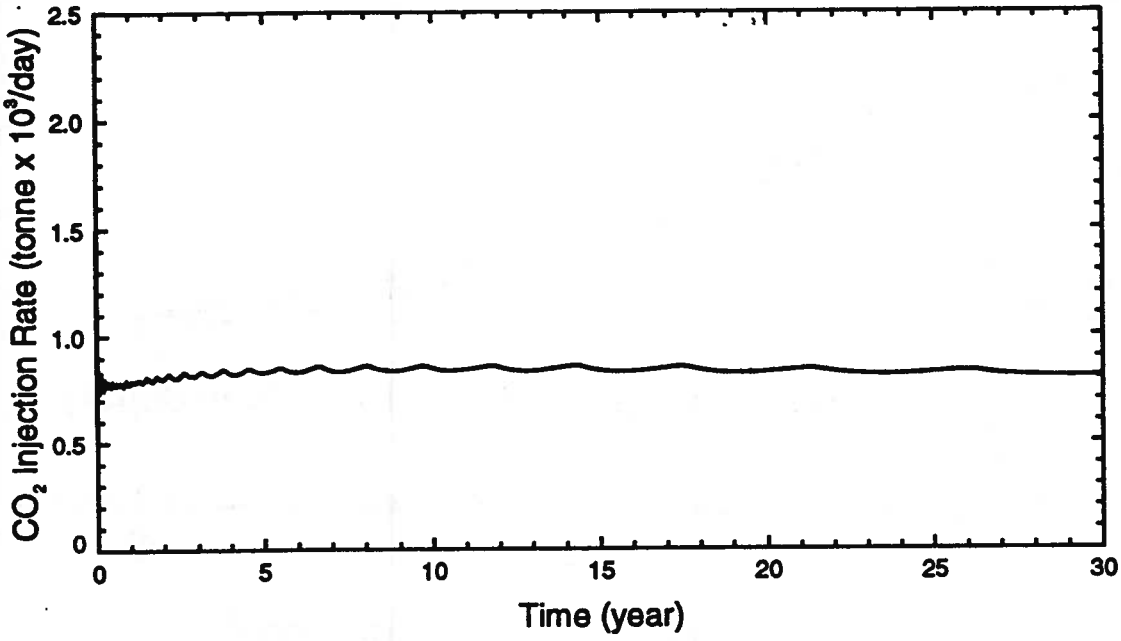

Carbon Dioxide Saturation (Run CO2_61)

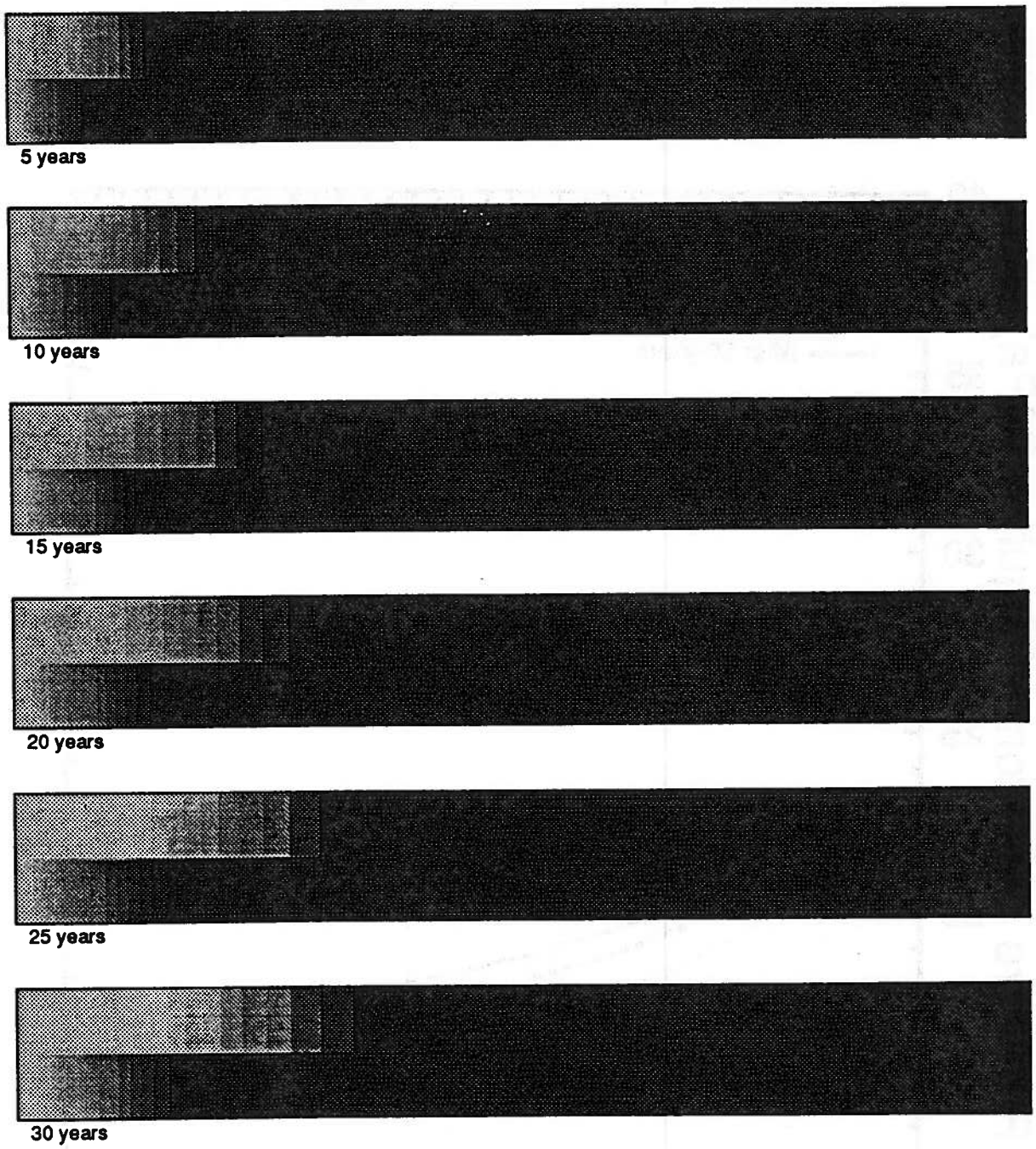

Vertical scale factor = 70.000
Field dimensions: 6999. (horiz.), 13.00 (vert.)

Glauconitic Sandstone Aquifer

NUMERICAL RUN (CO2_61)

Aquifer Porosity = 0.12 Aquifer Permeability = 30 md (horizontal)
Injection Pressure = 25.15 MPa

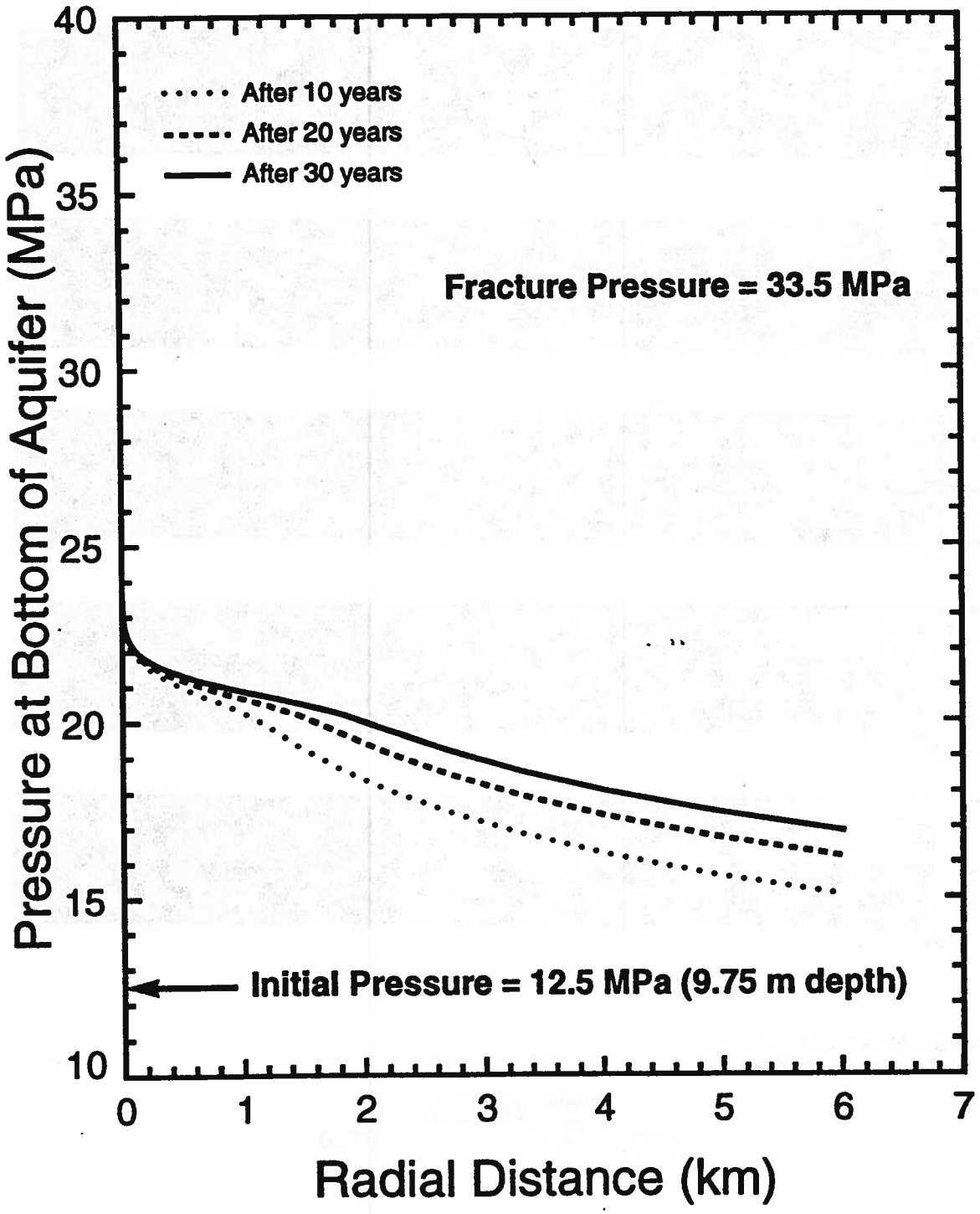

Glauconitic Sandstone Aquifer

NUMERICAL RUN (CO2_62)

Aquifer Porosity = 0.12 Aquifer Permeability = 100 md (horizontal)
Injection Pressure = 25.15 MPa

(a) Cumulative CO_2 Injection

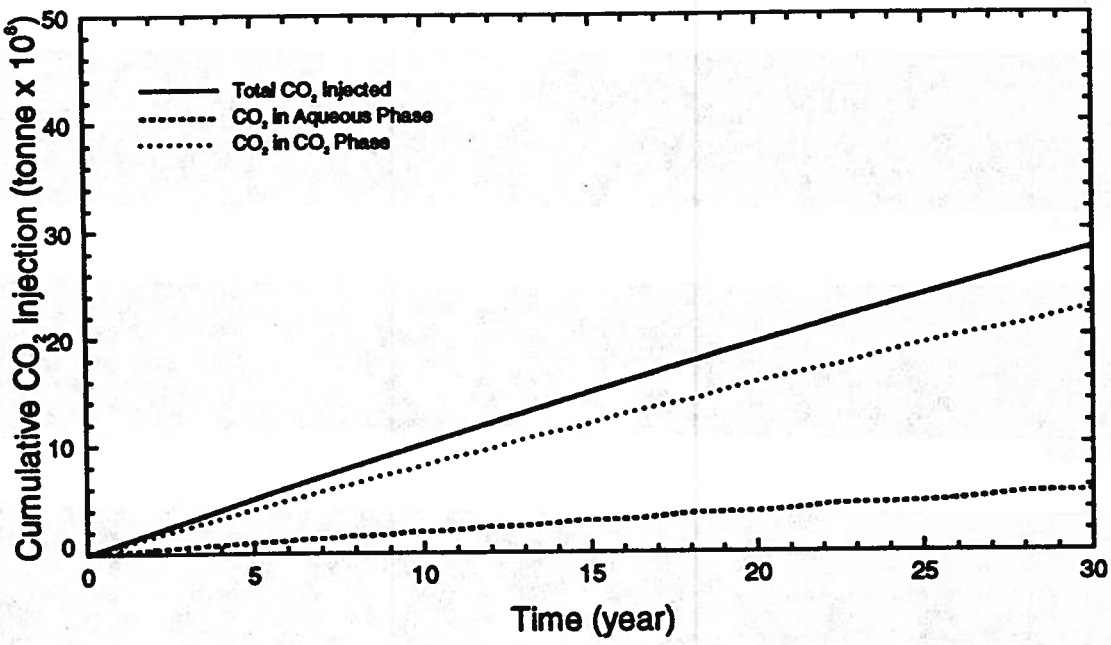

(b) CO_2 Injection Rate

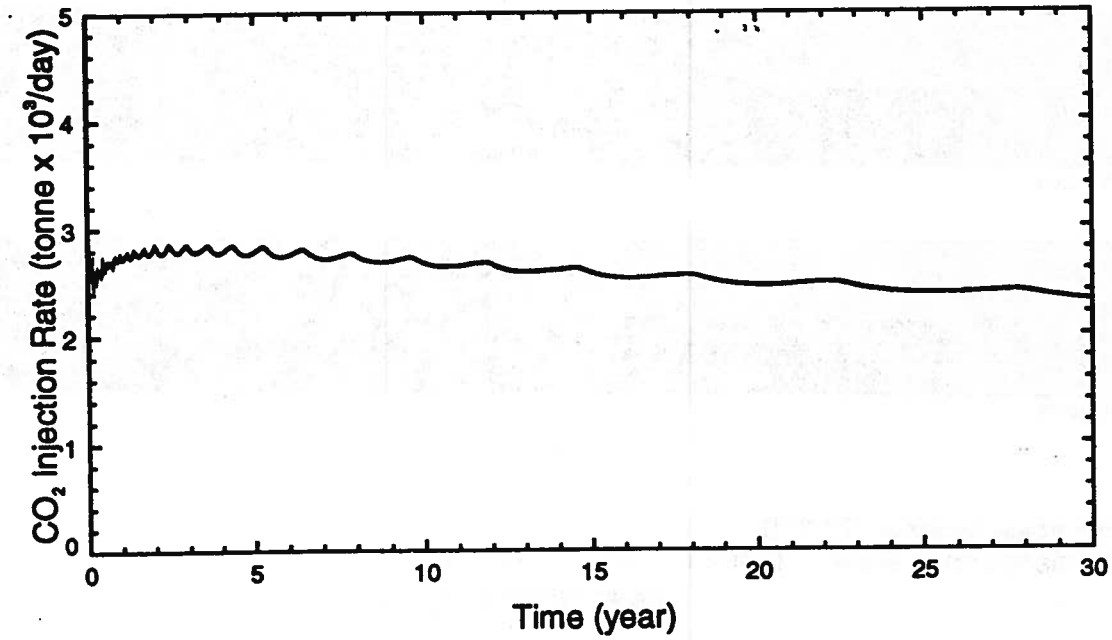

Carbon Dioxide Saturation (Run CO2_62)

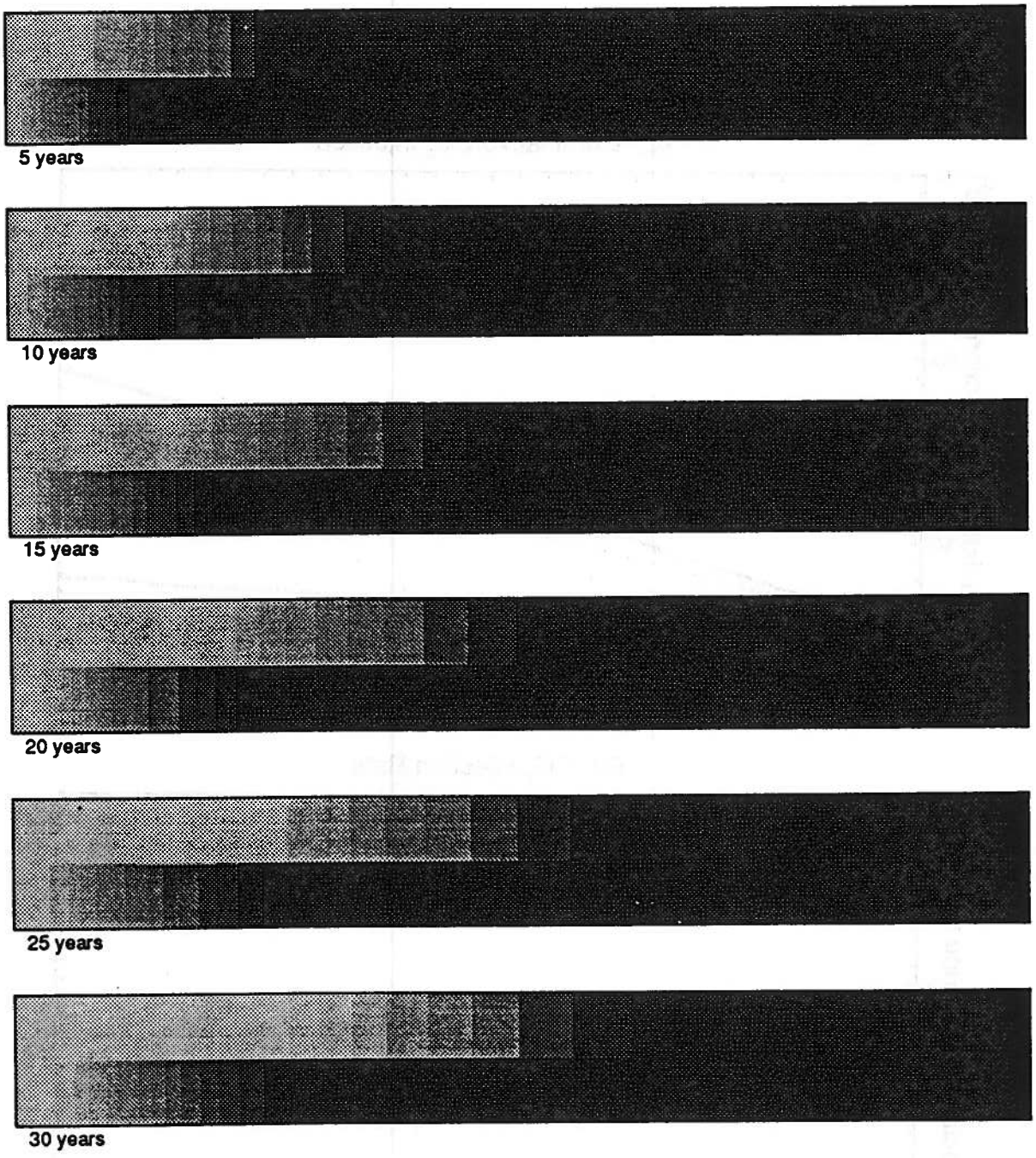

Vertical scale factor = 70.000
Field dimensions: 6999. (horiz.), 13.00 (vert.)

Glauconitic Sandstone Aquifer

NUMERICAL RUN (CO2_62)

Aquifer Porosity = 0.12 Aquifer Permeability = 100 md (horizontal)
Injection Pressure = 25.15 MPa

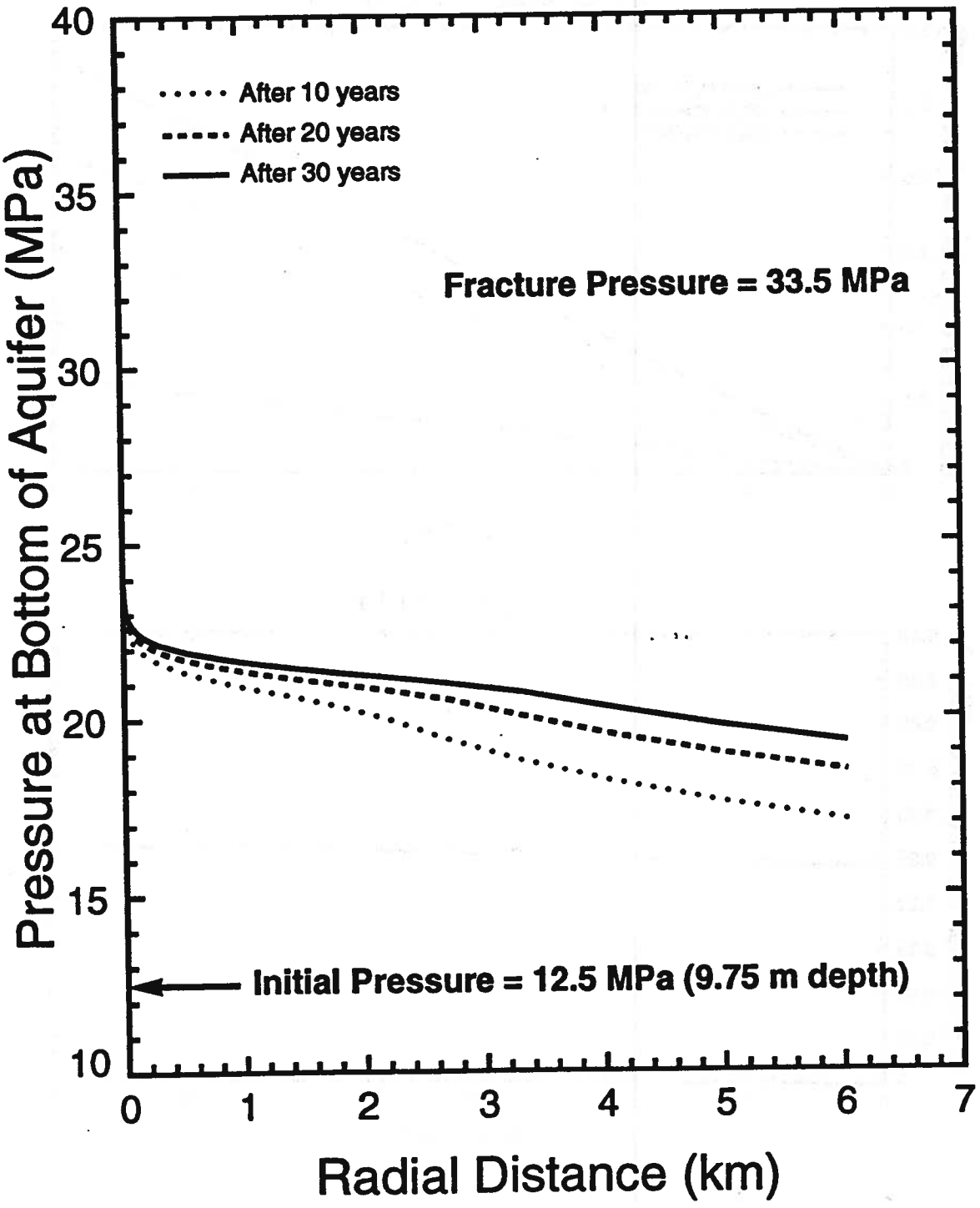

Glauconitic Sandstone Aquifer

NUMERICAL RUN (CO2_71)

Aquifer Porosity = 0.12 Aquifer Permeability = 6.2 md (horizontal)
Injection Pressure = 30.12 MPa

(a) Cumulative CO_2 Injection

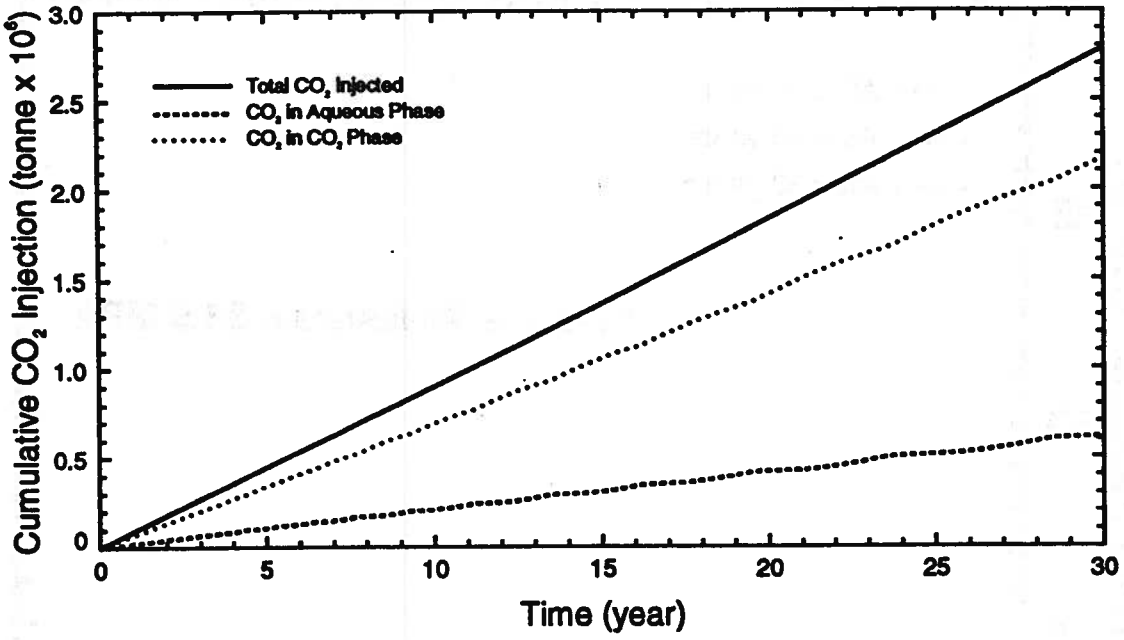

(b) CO_2 Injection Rate

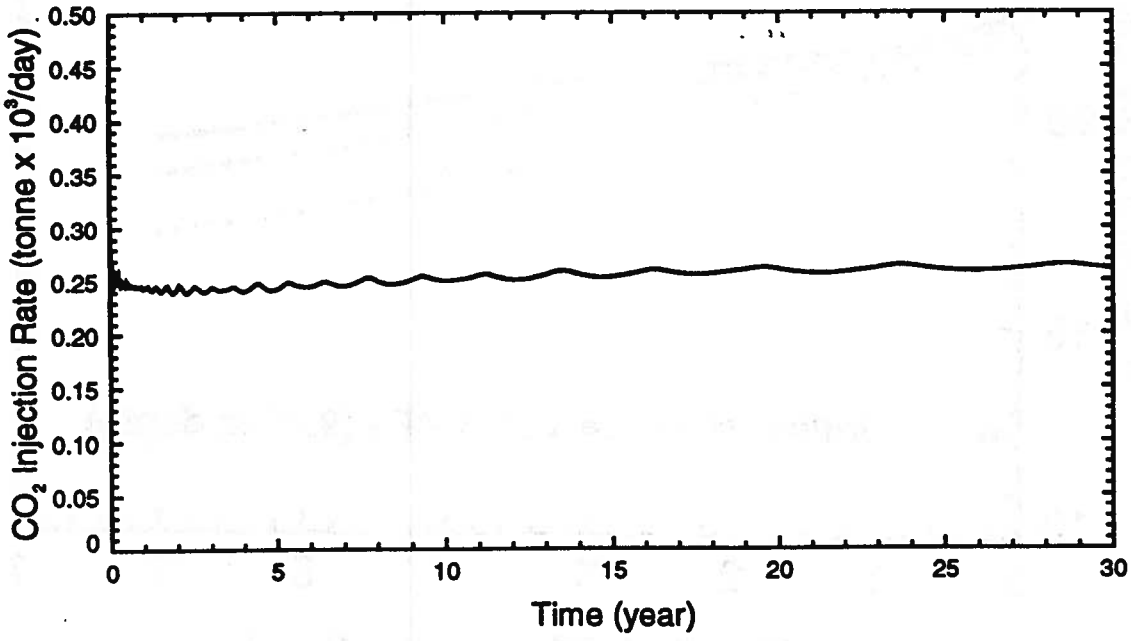

Carbon Dioxide Saturation (Run CO2_71)

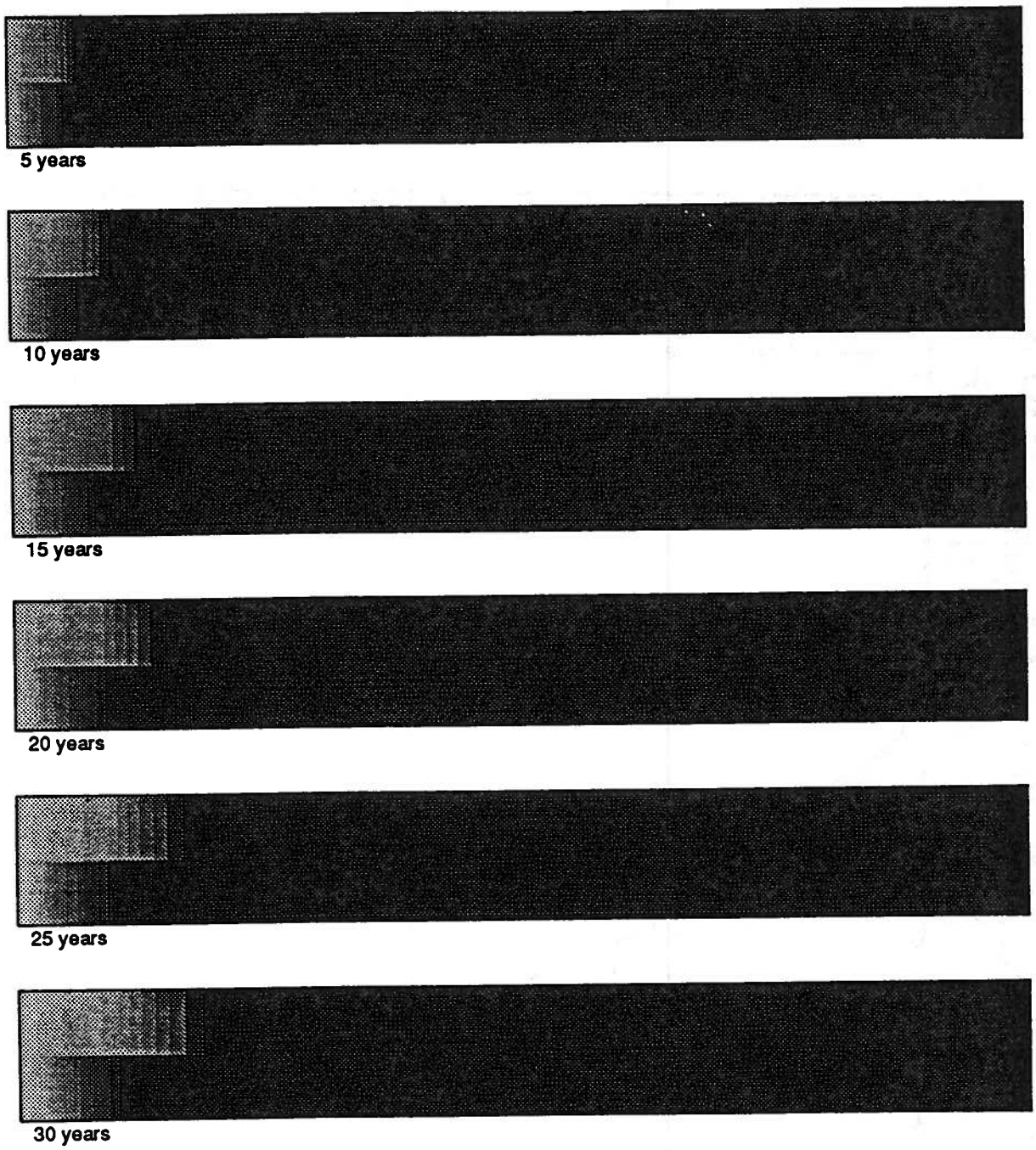

Vertical scale factor = 70.000
Field dimensions: 6999. (horiz.), 13.00 (vert.)

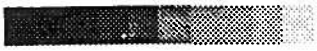

Glauconitic Sandstone Aquifer

NUMERICAL RUN (CO2_71)

Aquifer Porosity = 0.12 Aquifer Permeability = 6.2 md (horizontal)
Injection Pressure = 30.12 MPa

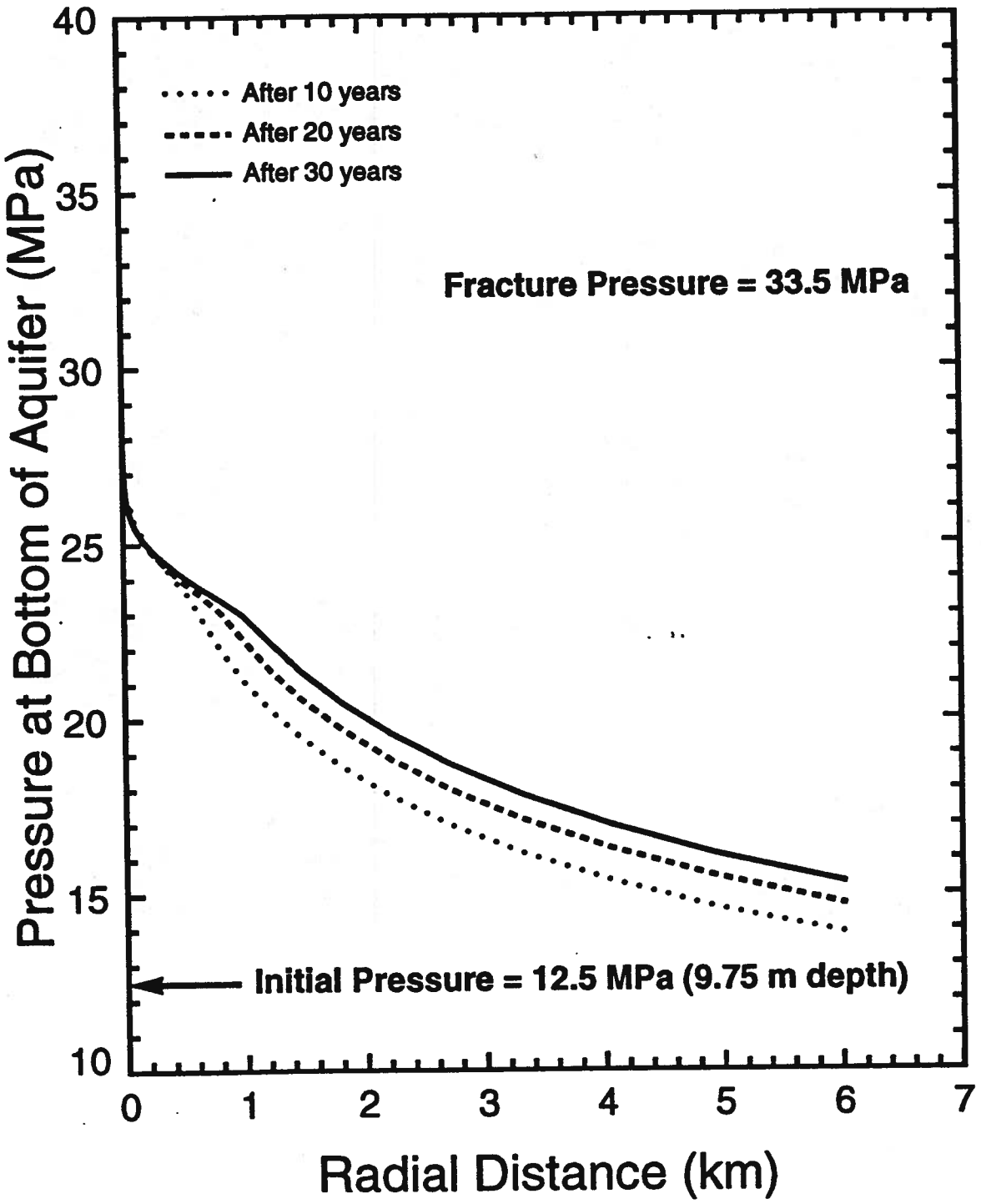

Glauconitic Sandstone Aquifer

NUMERICAL RUN (CO2_72)

Aquifer Porosity = 0.12 Aquifer Permeability = 30 md (horizontal)
Injection Pressure = 30.12 MPa

(a) Cumulative CO_2 Injection

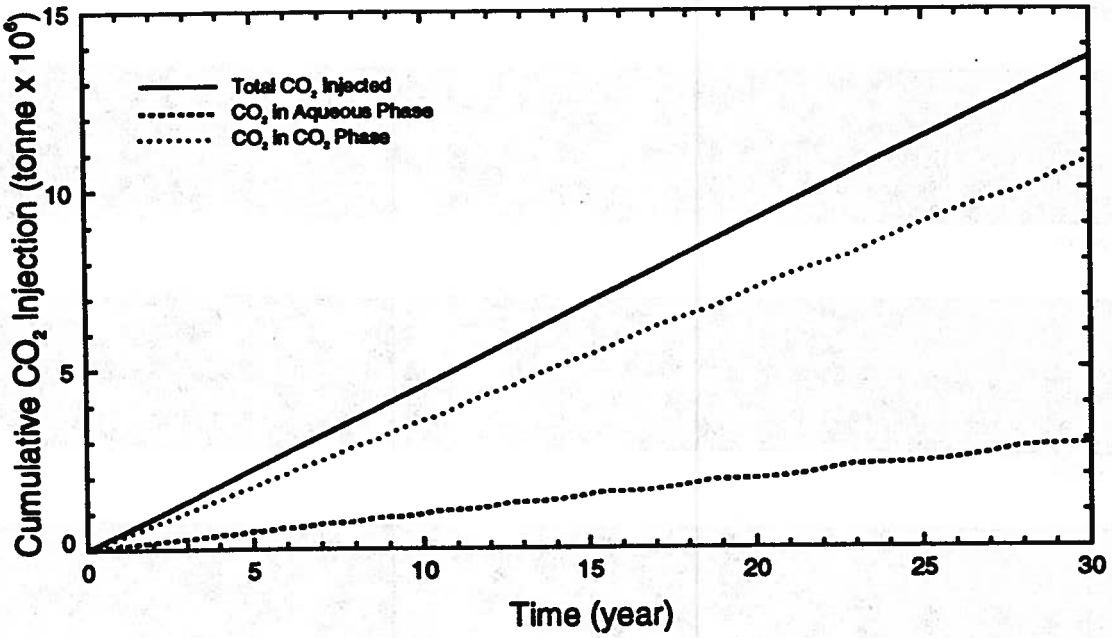

(b) CO_2 Injection Rate

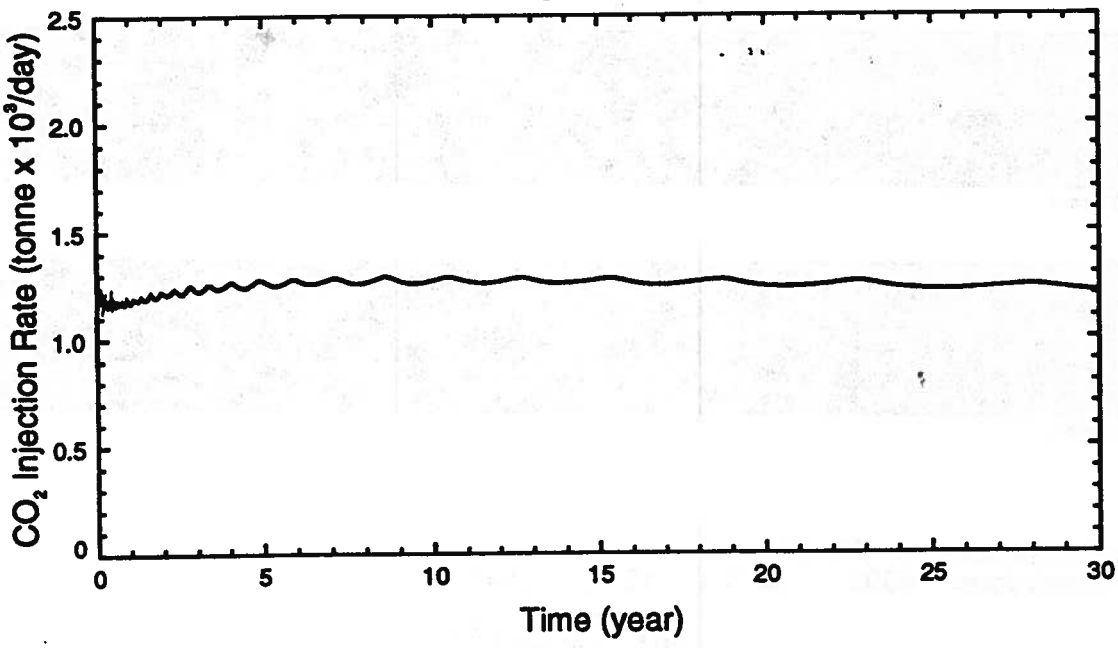

Carbon Dioxide Saturation (Run CO2_72)

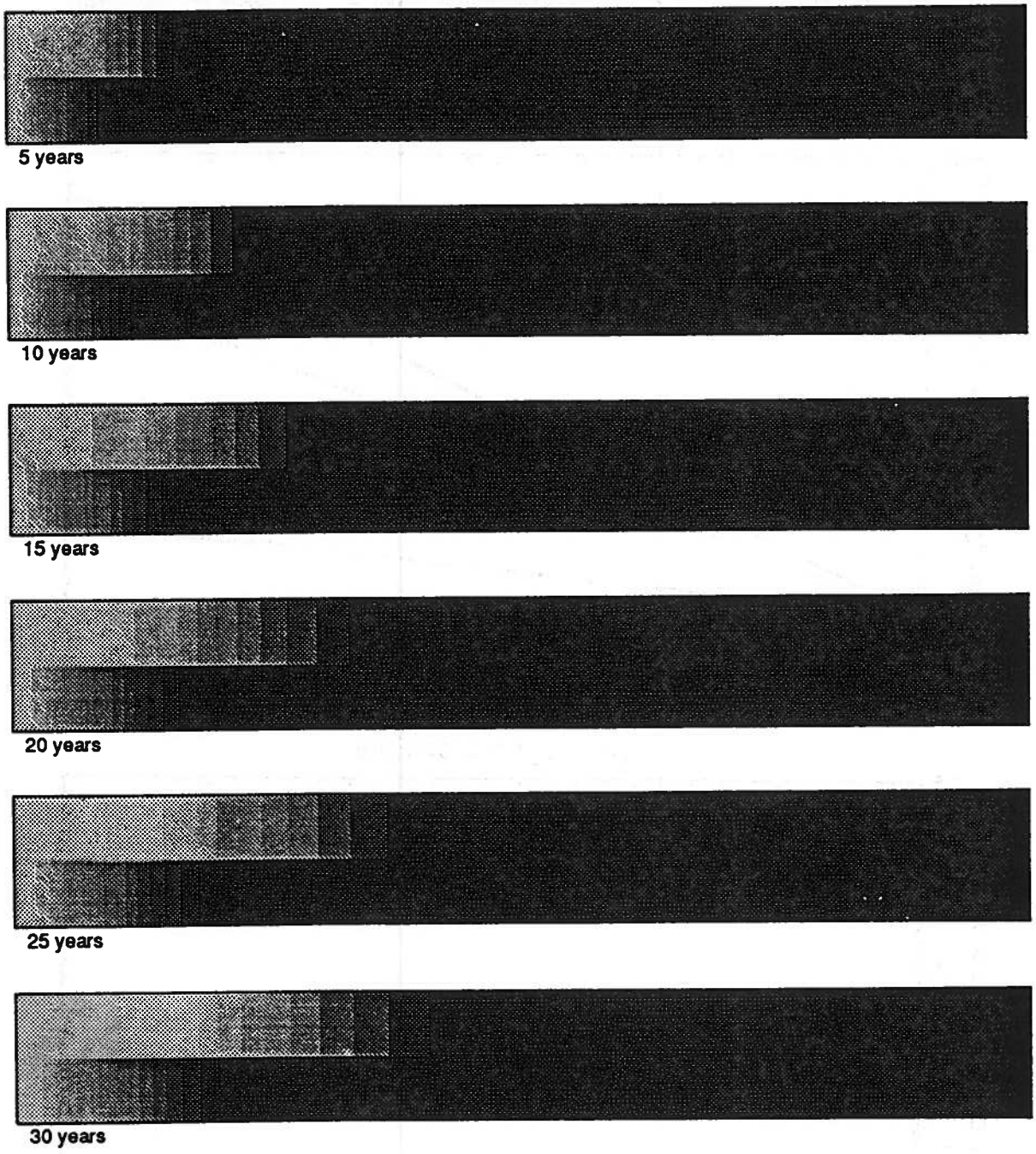

Vertical scale factor = 70.000
Field dimensions: 6999. (horiz.), 13.00 (vert.)

Glauconitic Sandstone Aquifer

NUMERICAL RUN (CO2_72)

Aquifer Porosity = 0.12 Aquifer Permeability = 30 md (horizontal)
Injection Pressure = 30.12 MPa

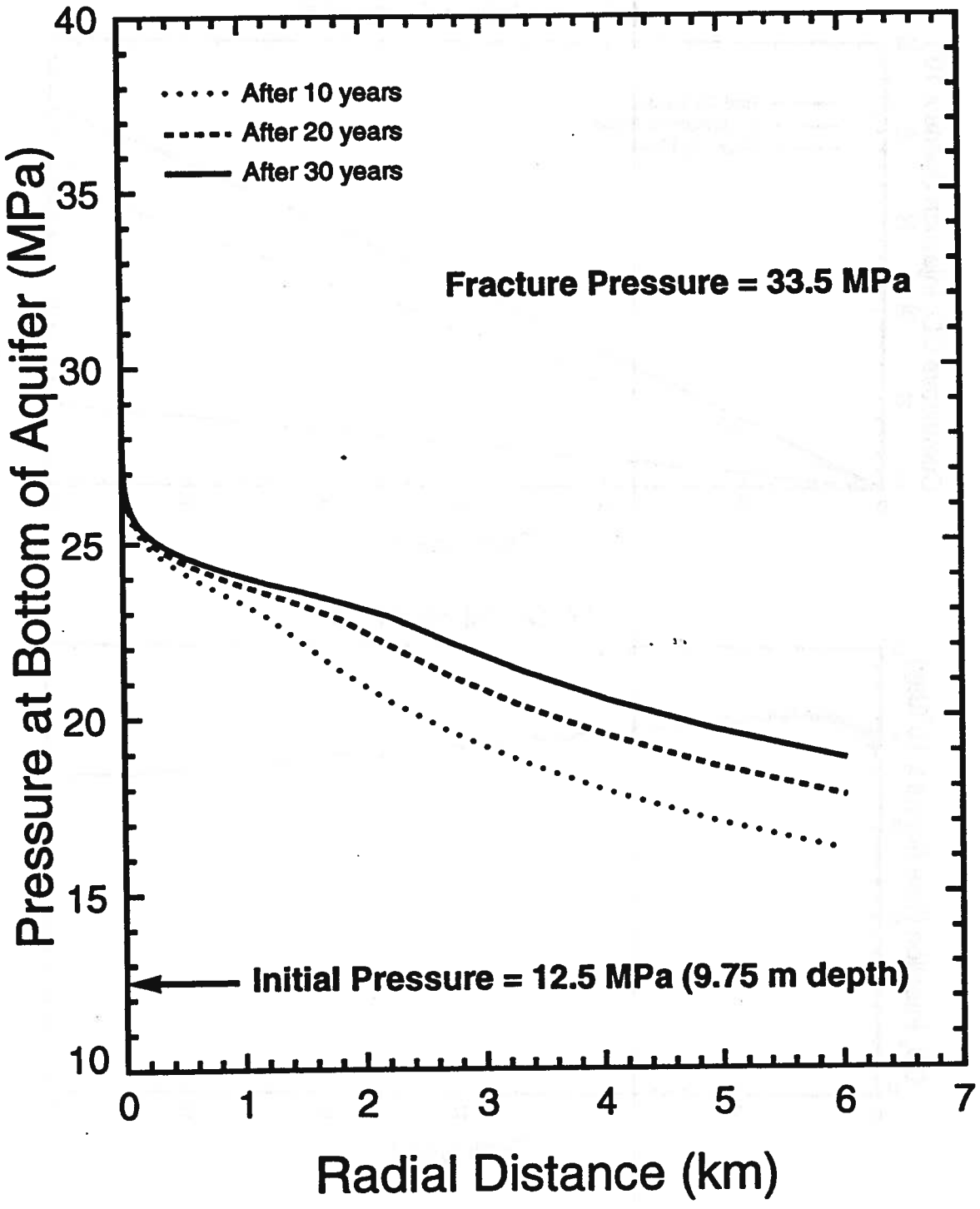

Glauconitic Sandstone Aquifer

NUMERICAL RUN (CO2_73)

Aquifer Porosity = 0.12 Aquifer Permeability = 100 md (horizontal)
Injection Pressure = 30.12 MPa

(a) Cumulative CO_2 Injection

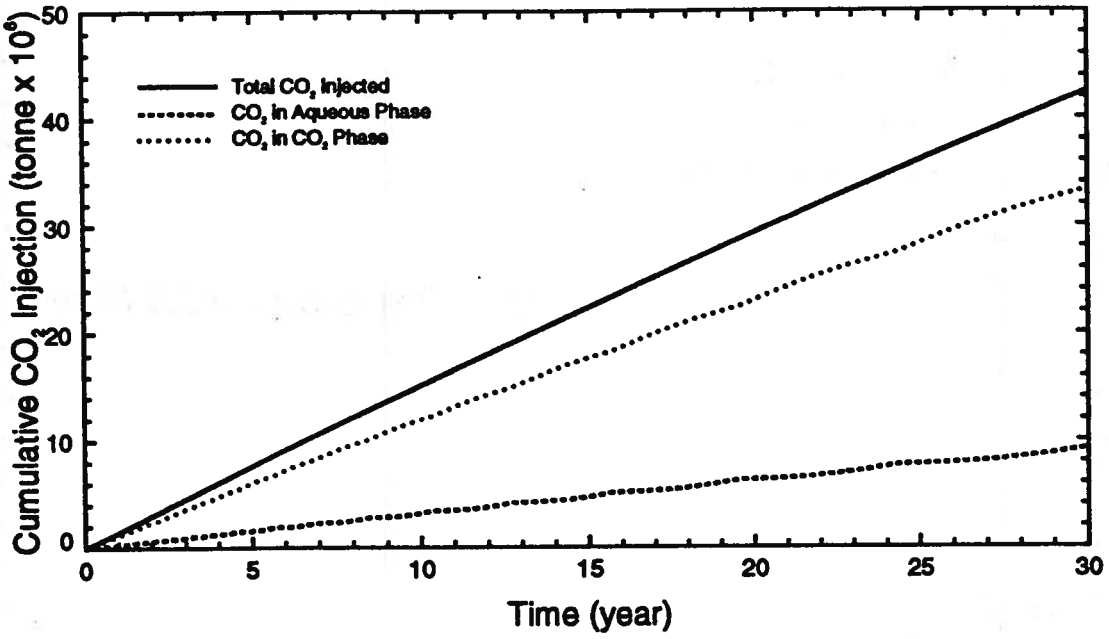

(b) CO_2 Injection Rate

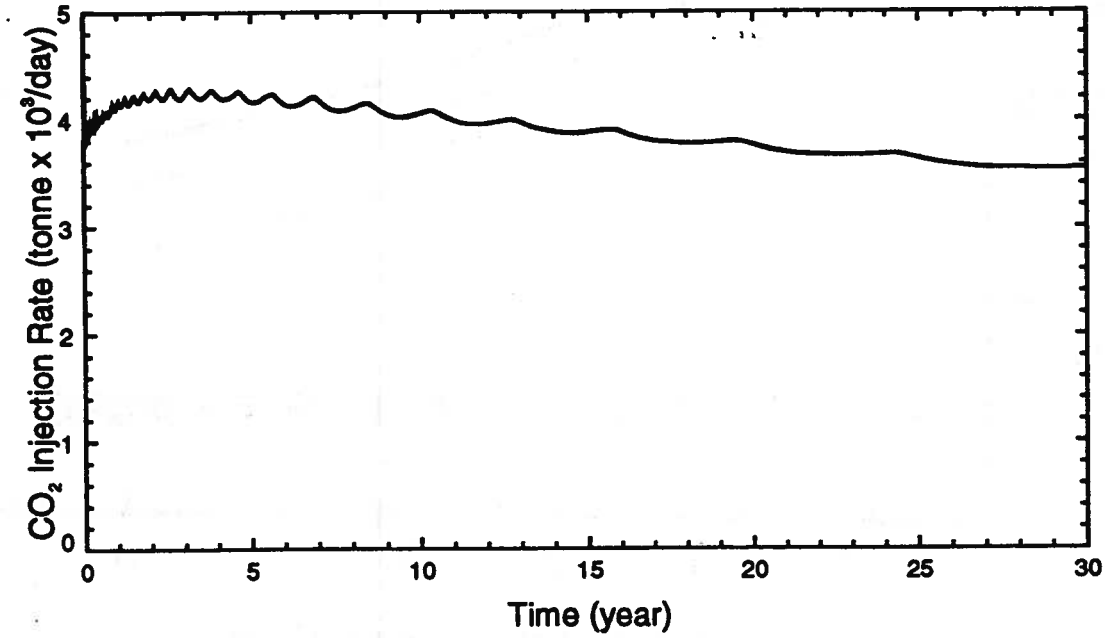

Carbon Dioxide Saturation (Run CO2_73)

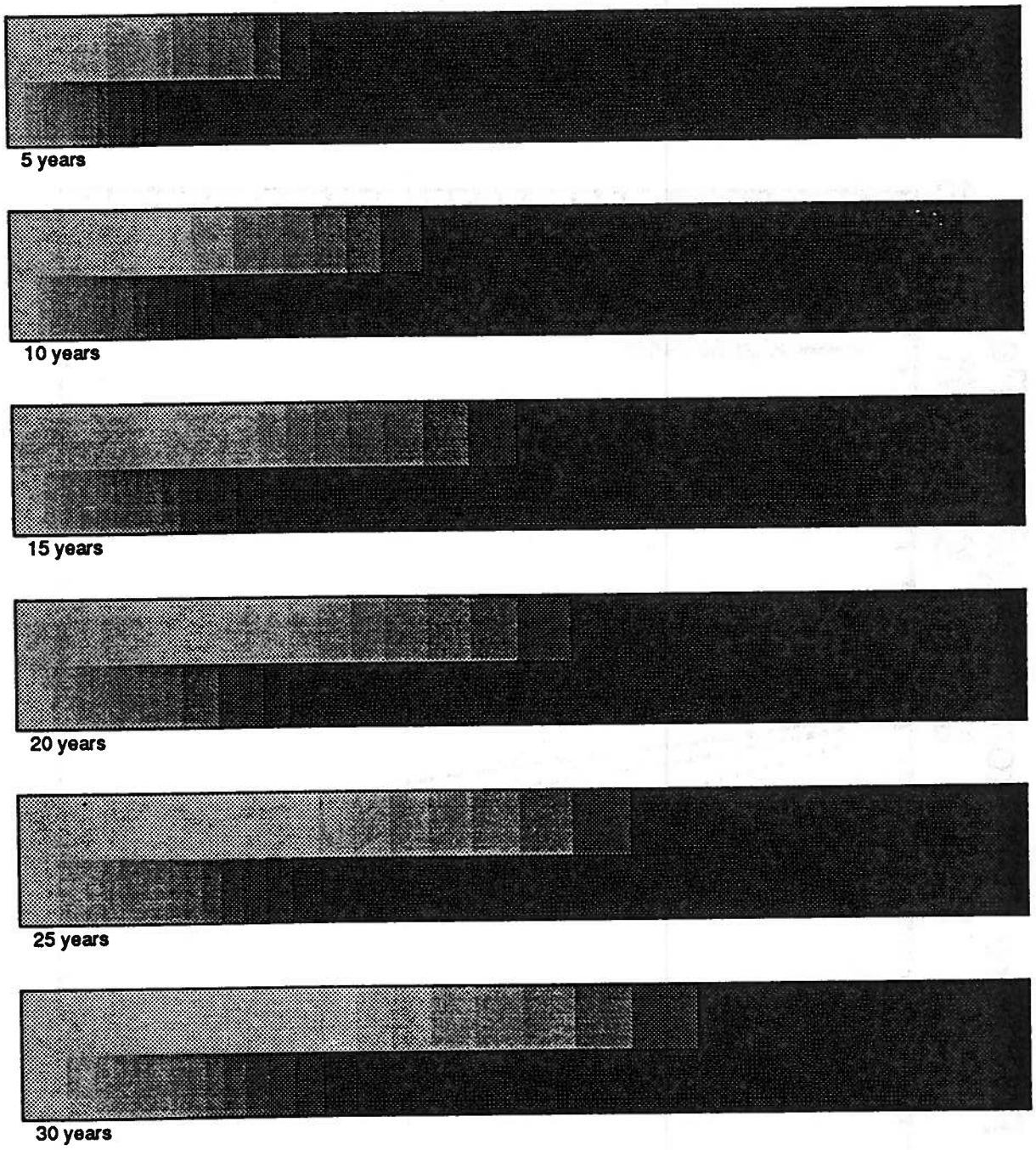

Vertical scale factor = 70.000
Field dimensions: 6999. (horiz.), 13.00 (vert.)

Glauconitic Sandstone Aquifer

NUMERICAL RUN (CO2_73)

Aquifer Porosity = 0.12 Aquifer Permeability = 100 md (horizontal)
Injection Pressure = 30.12 MPa

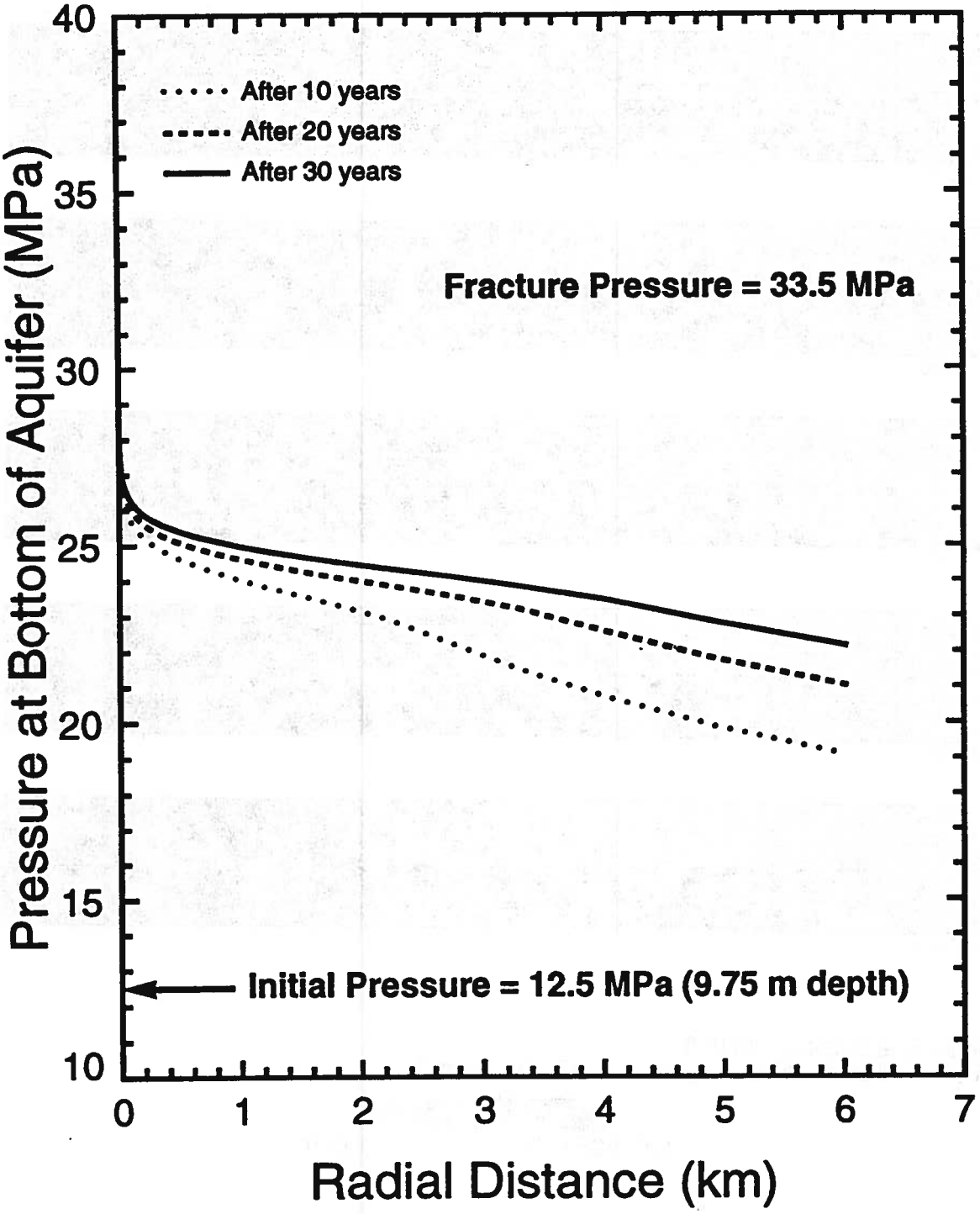

Glauconitic Sandstone Aquifer

NUMERICAL RUN (CO2_74)

Aquifer Porosity = 0.06 Aquifer Permeability = 6.2 md (horizontal)
Injection Pressure = 30.12 MPa

(a) Cumulative CO_2 Injection

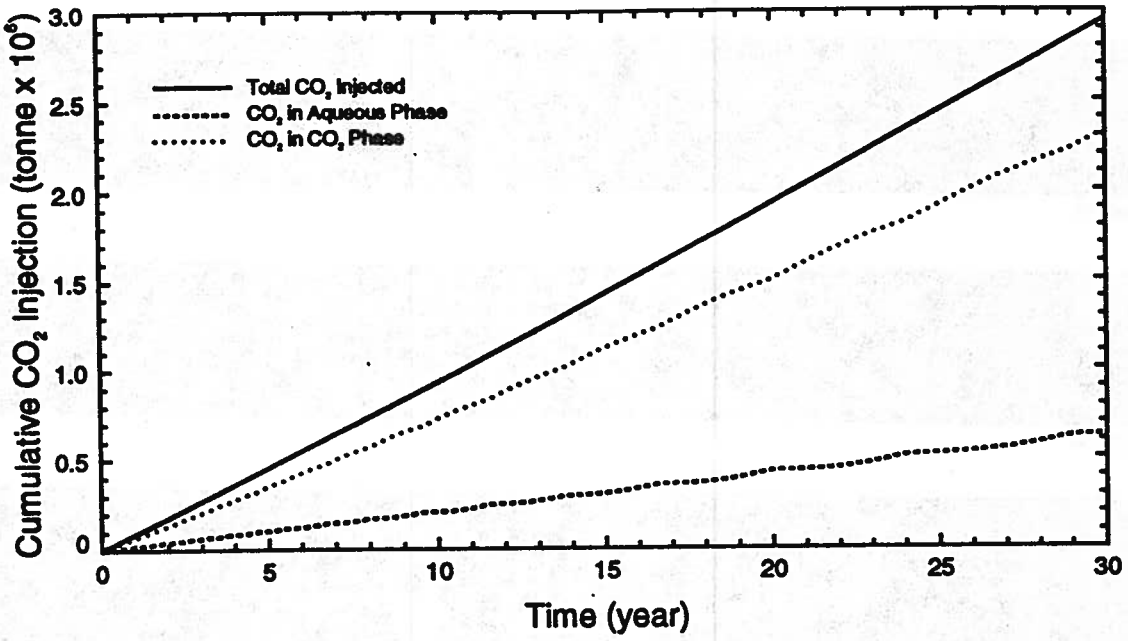

(b) CO_2 Injection Rate

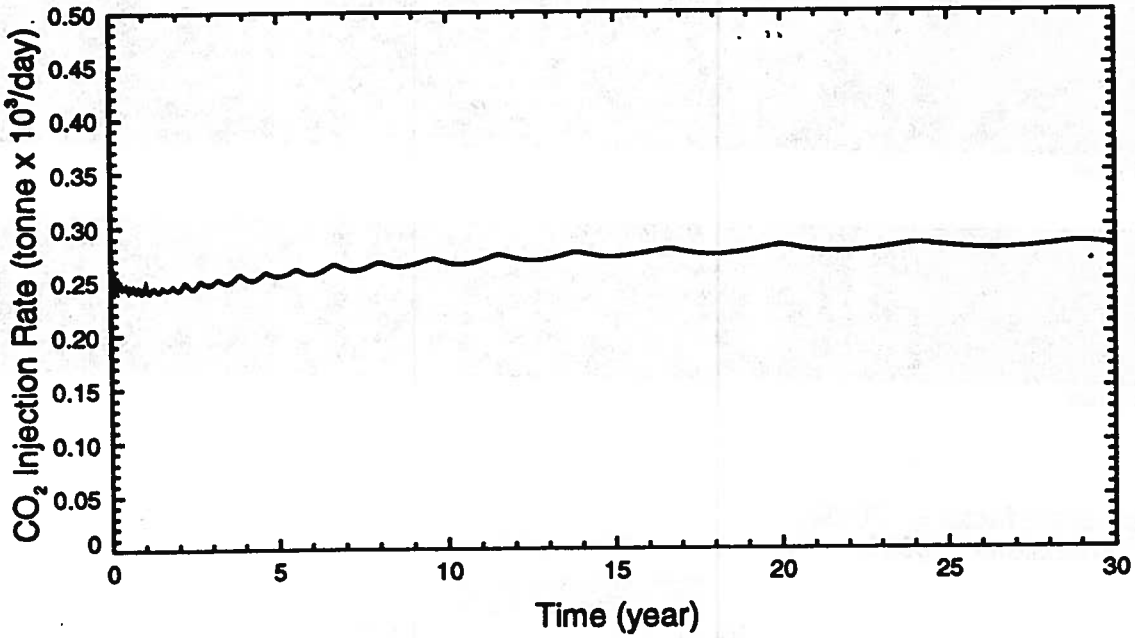

Carbon Dioxide Saturation (Run CO2_74)

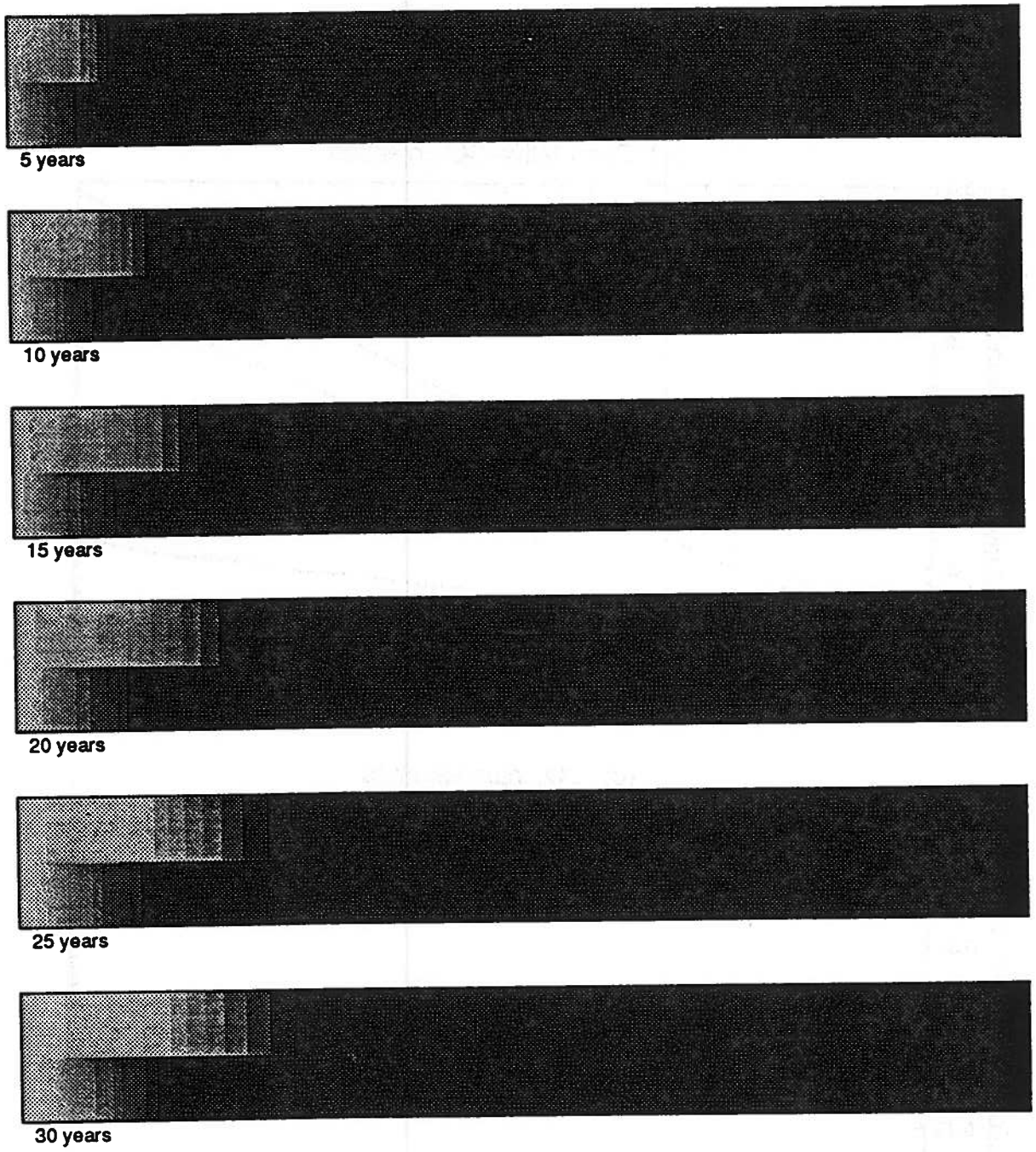

Vertical scale factor = 70.000
Field dimensions: 6999. (horiz.), 13.00 (vert.)

Glauconitic Sandstone Aquifer

NUMERICAL RUN (CO2_74)

Aquifer Porosity = 0.06 Aquifer Permeability = 6.2 md (horizontal)
Injection Pressure = 30.12 MPa

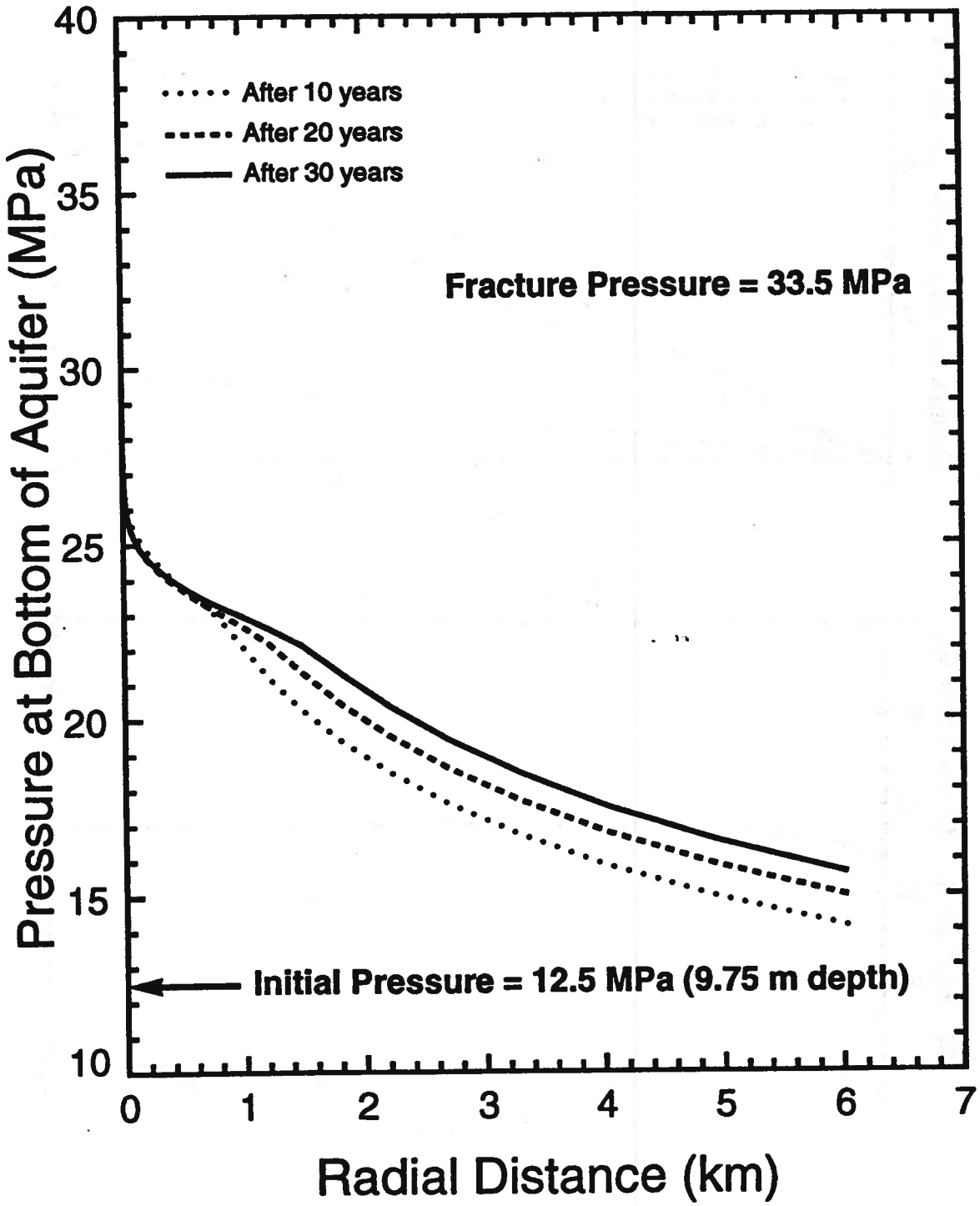

Glauconitic Sandstone Aquifer

NUMERICAL RUN (CO2_75)

Aquifer Porosity = 0.06 Aquifer Permeability = 30 md (horizontal)
Injection Pressure = 30.12 MPa

(a) Cumulative CO_2 Injection

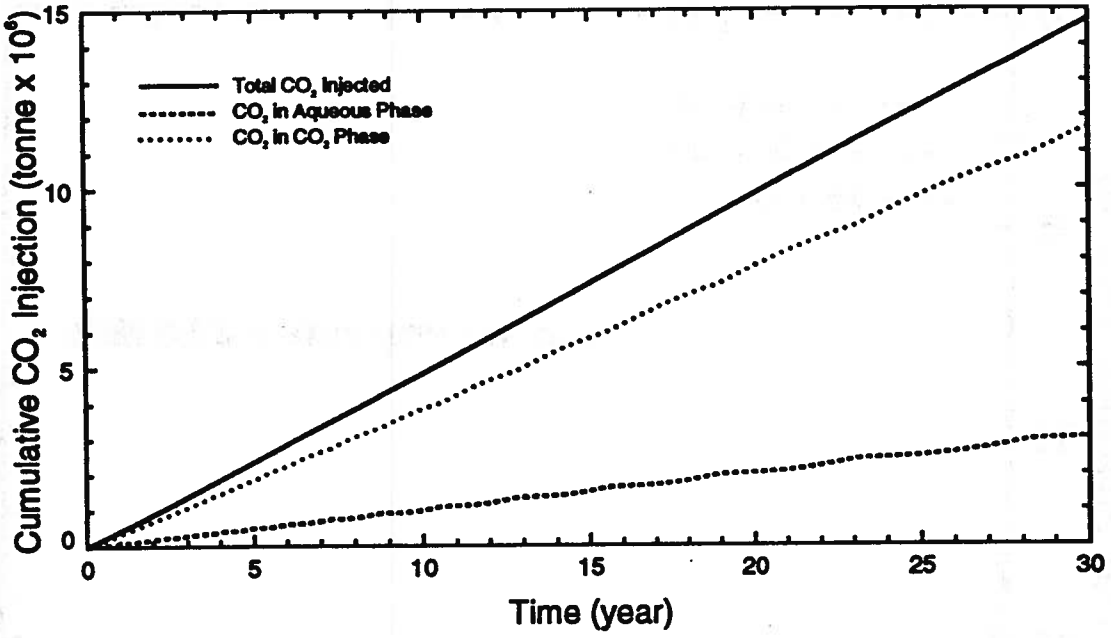

(b) CO_2 Injection Rate

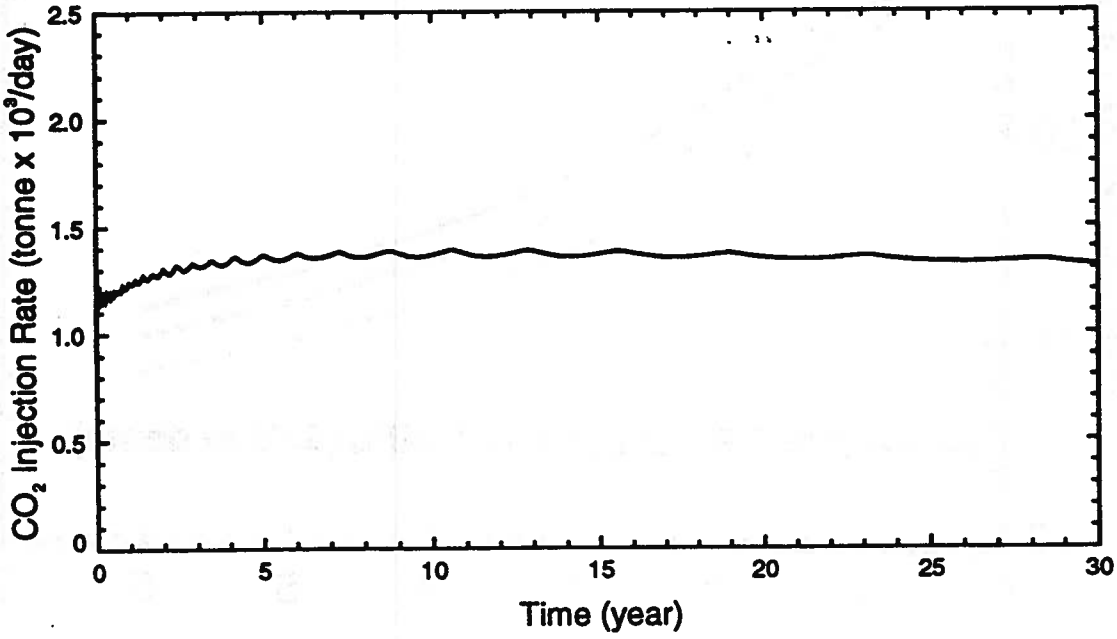

Carbon Dioxide Saturation (Run CO2_75)

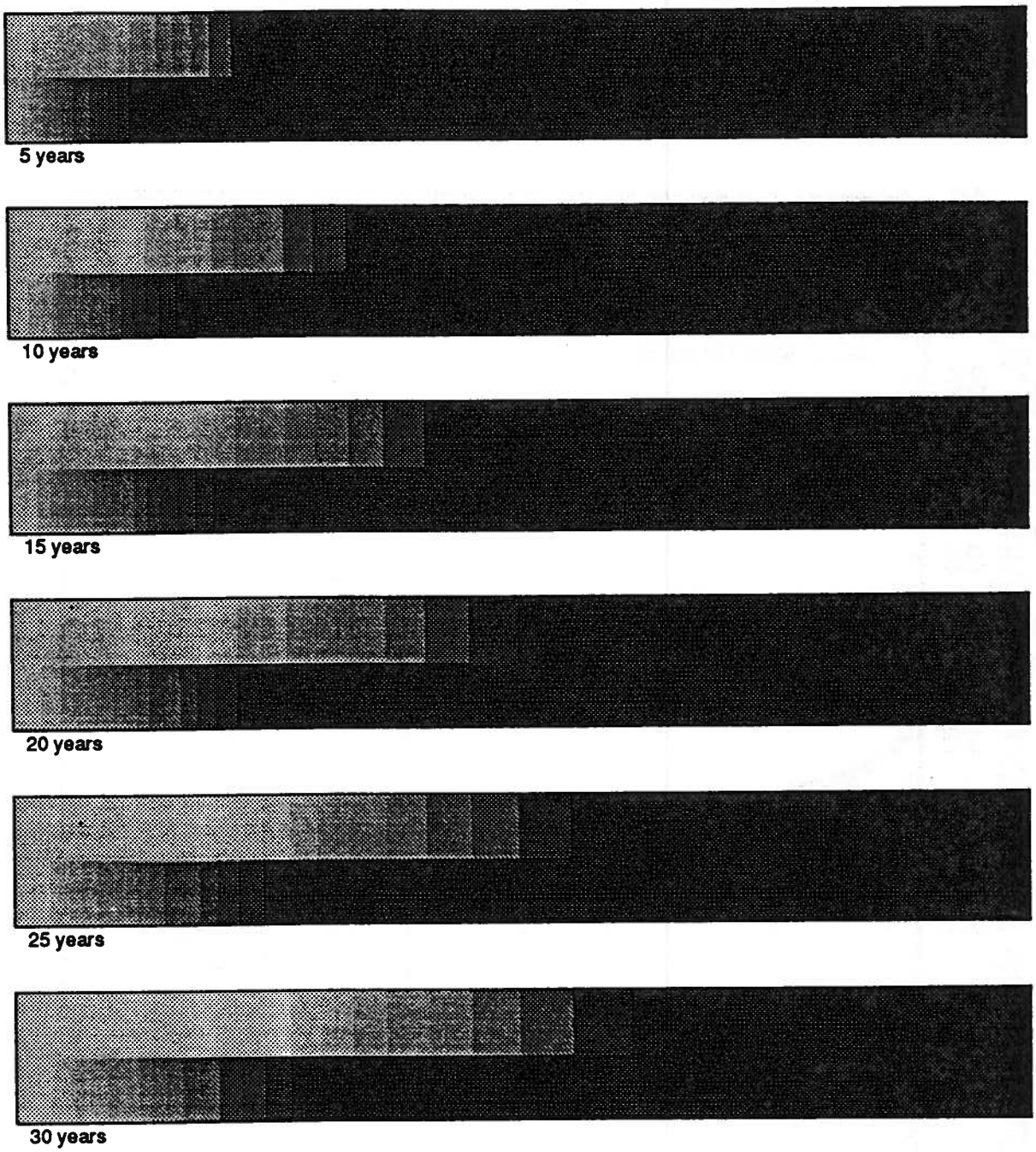

Vertical scale factor = 70.000
Field dimensions: 6999. (horiz.), 13.00 (vert.)

Glauconitic Sandstone Aquifer

NUMERICAL RUN (CO2_75)

Aquifer Porosity = 0.06 Aquifer Permeability = 30 md (horizontal)
Injection Pressure = 30.12 MPa

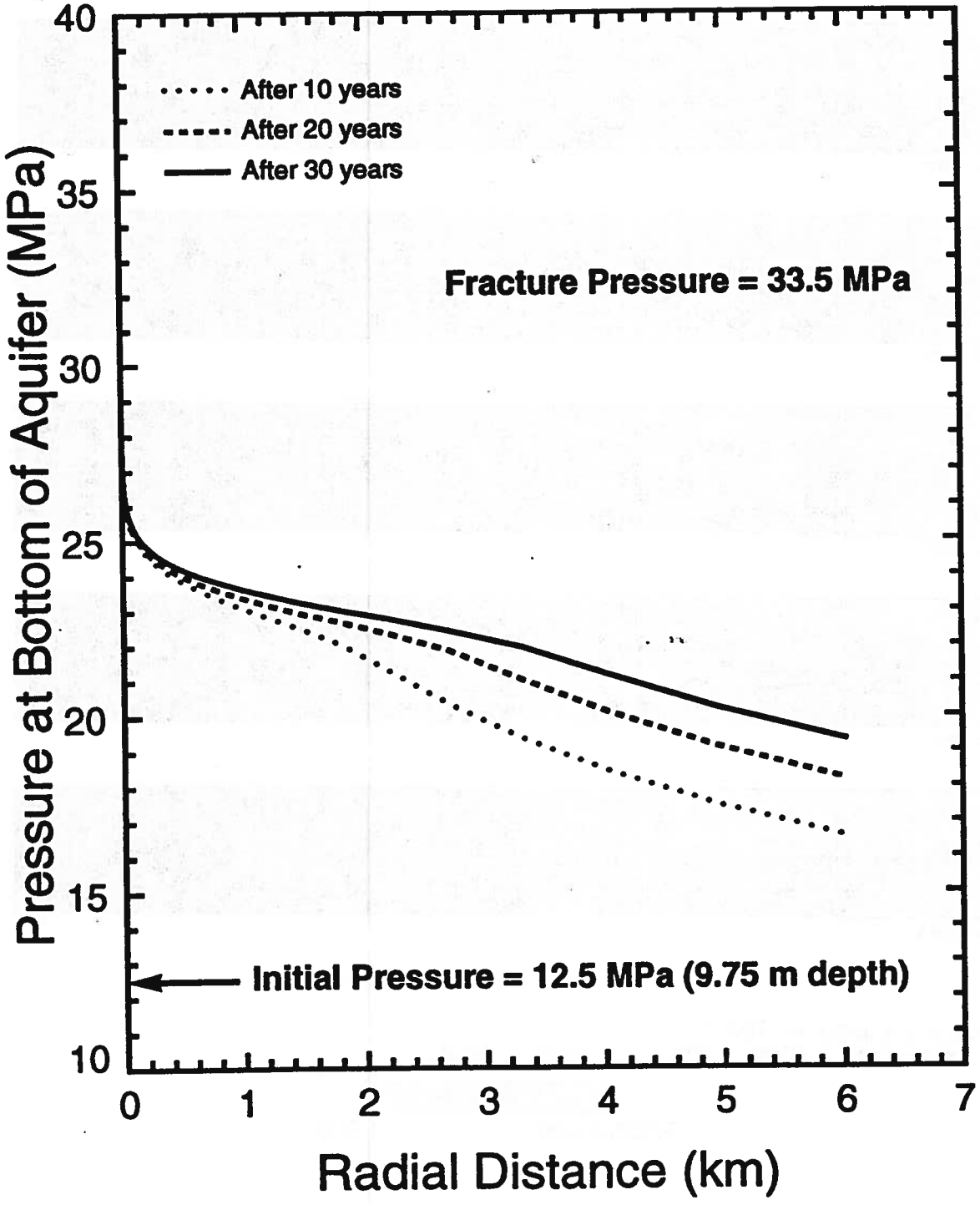

Glauconitic Sandstone Aquifer

NUMERICAL RUN (CO2_76)

Aquifer Porosity = 0.06 Aquifer Permeability = 100 md (horizontal)
Injection Pressure = 30.12 MPa

(a) Cumulative CO_2 Injection

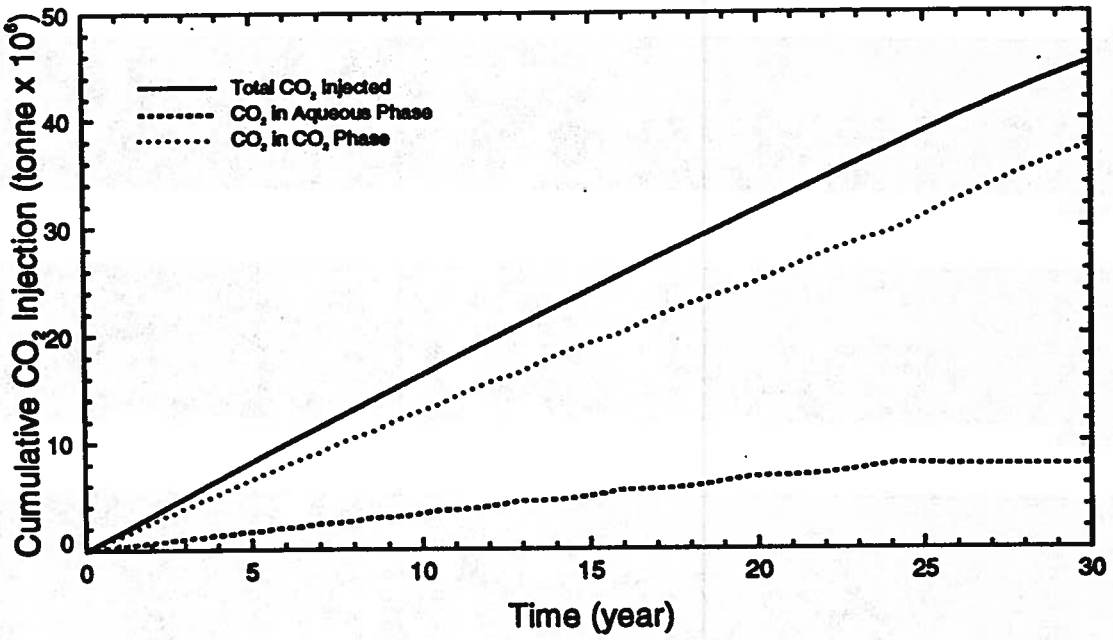

(b) CO_2 Injection Rate

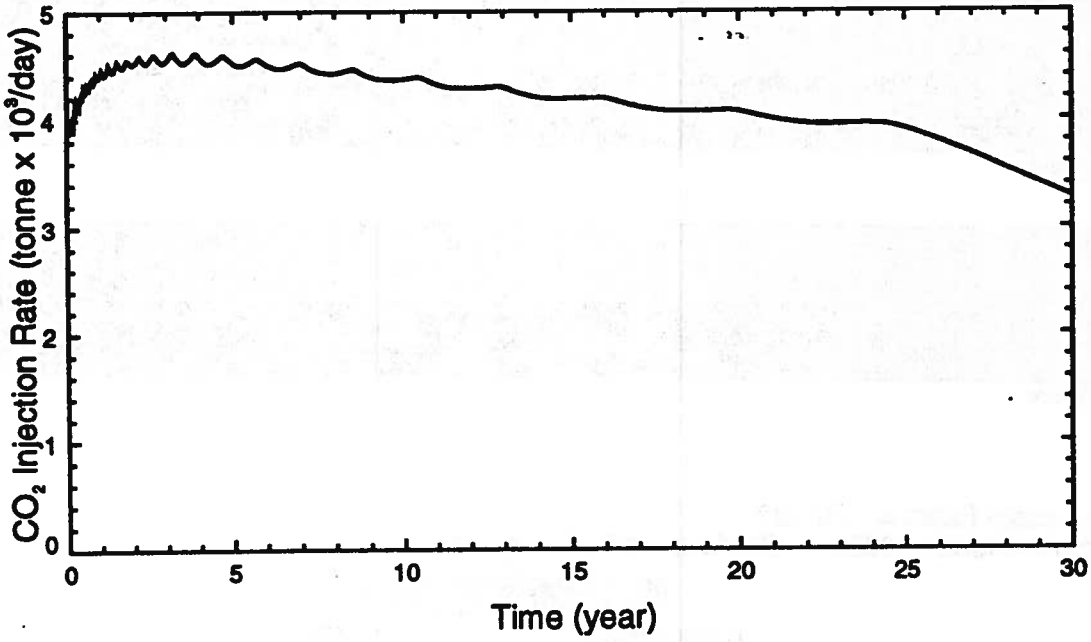

Carbon Dioxide Saturation (Run CO2_76)

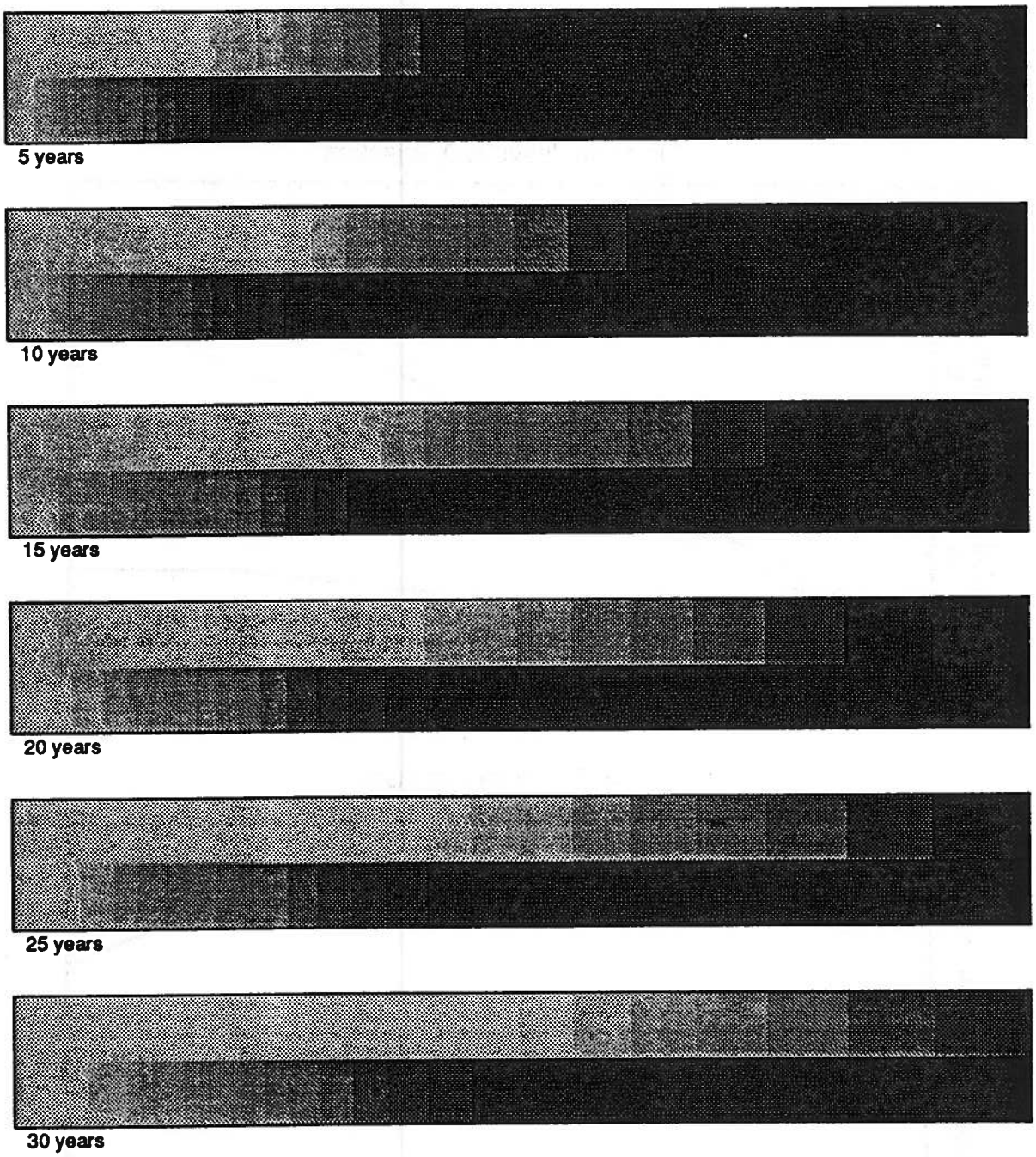

Vertical scale factor = 70.000
Field dimensions: 6999. (horiz.), 13.00 (vert.)

Glauconitic Sandstone Aquifer

NUMERICAL RUN (CO2_76)

Aquifer Porosity = 0.06 Aquifer Permeability = 100 md (horizontal)
Injection Pressure = 30.12 MPa

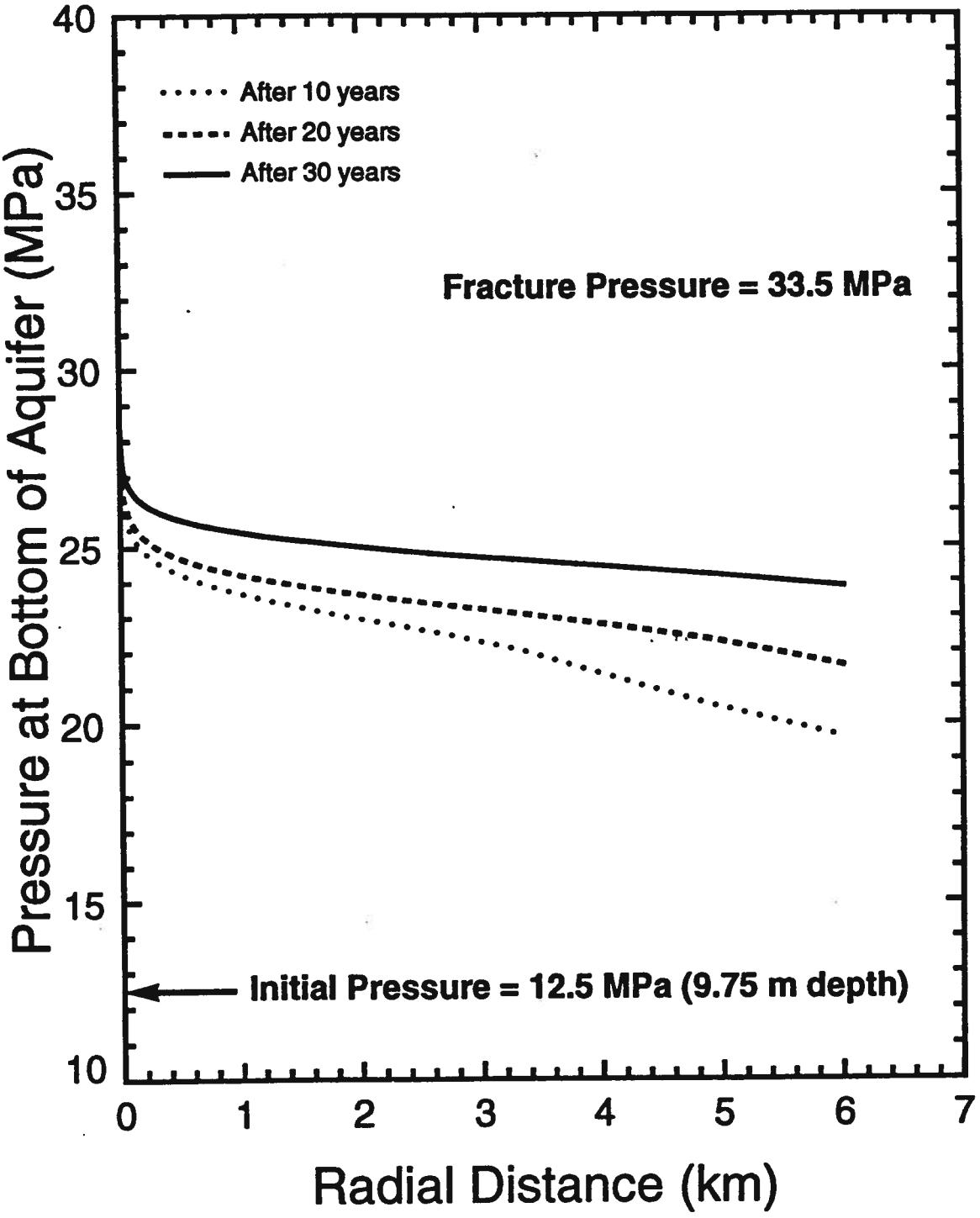

Glauconitic Sandstone Aquifer

NUMERICAL RUN (CO2_80)

Aquifer Porosity = 0.12 Aquifer Permeability = 100/6.2 md (horizontal)
Injection Pressure = 30.12 MPa

(a) Cumulative CO_2 Injection

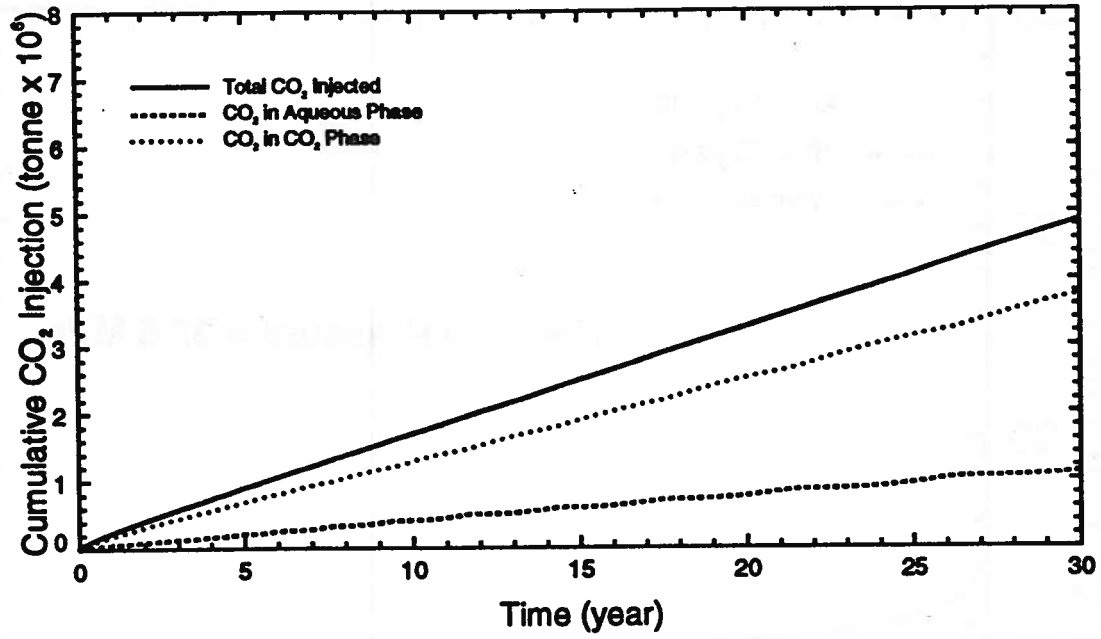

(b) CO_2 Injection Rate

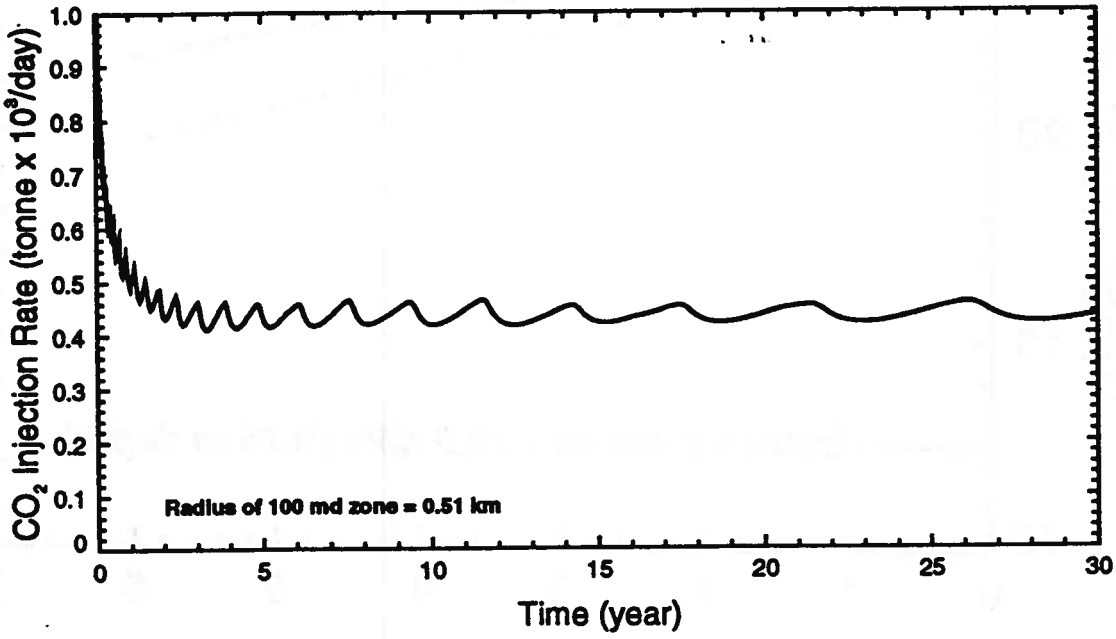

Carbon Dioxide Saturation (Run CO2_80)

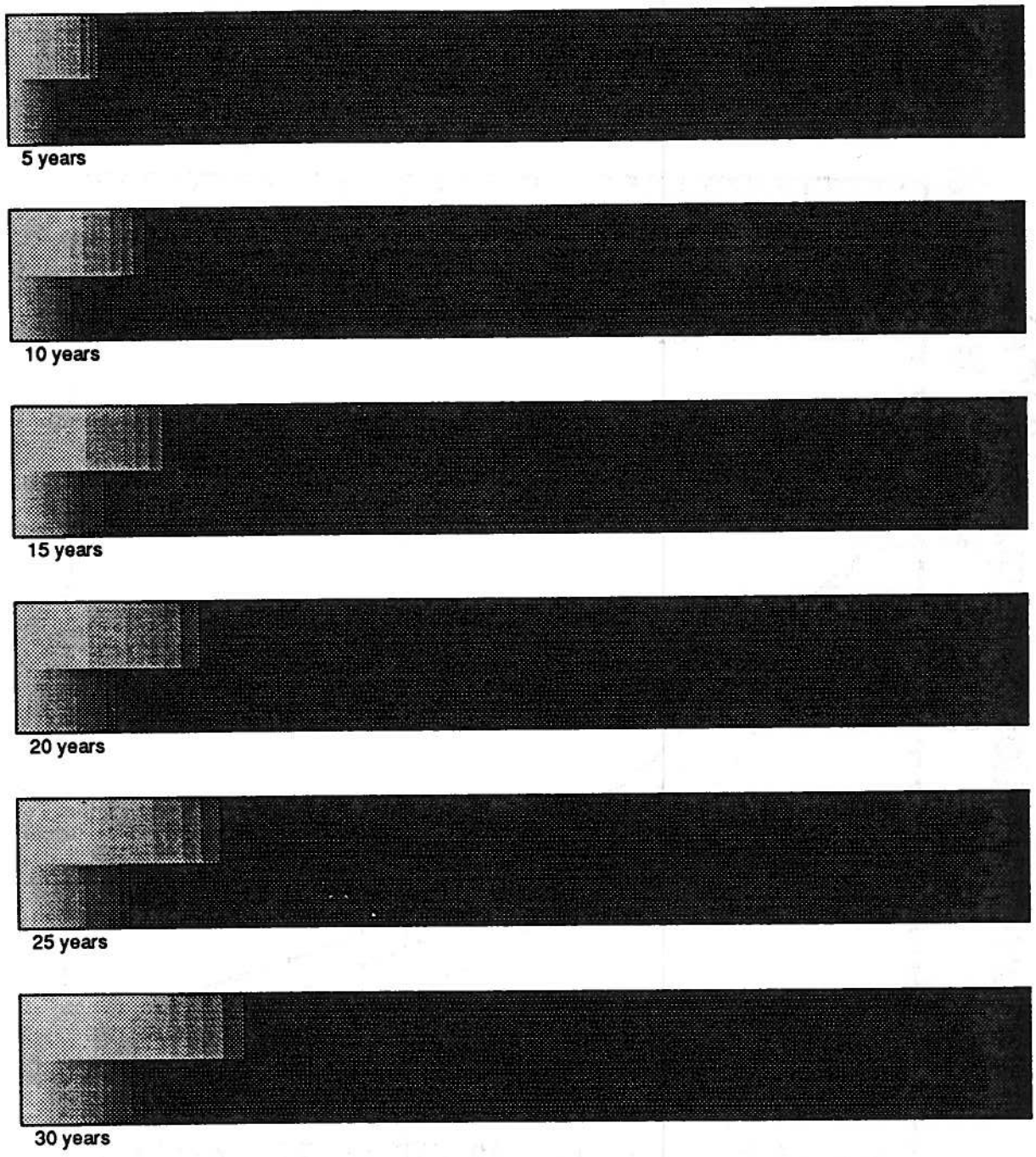

Vertical scale factor = 70.000
Field dimensions: 6999. (horiz.), 13.00 (vert.)

Glauconitic Sandstone Aquifer

NUMERICAL RUN (CO2_80)

Aquifer Porosity = 0.12 Aquifer Permeability = 100/6.2 md (horizontal)
Injection Pressure = 30.12 MPa Radius of 100 md zone = 0.51 km

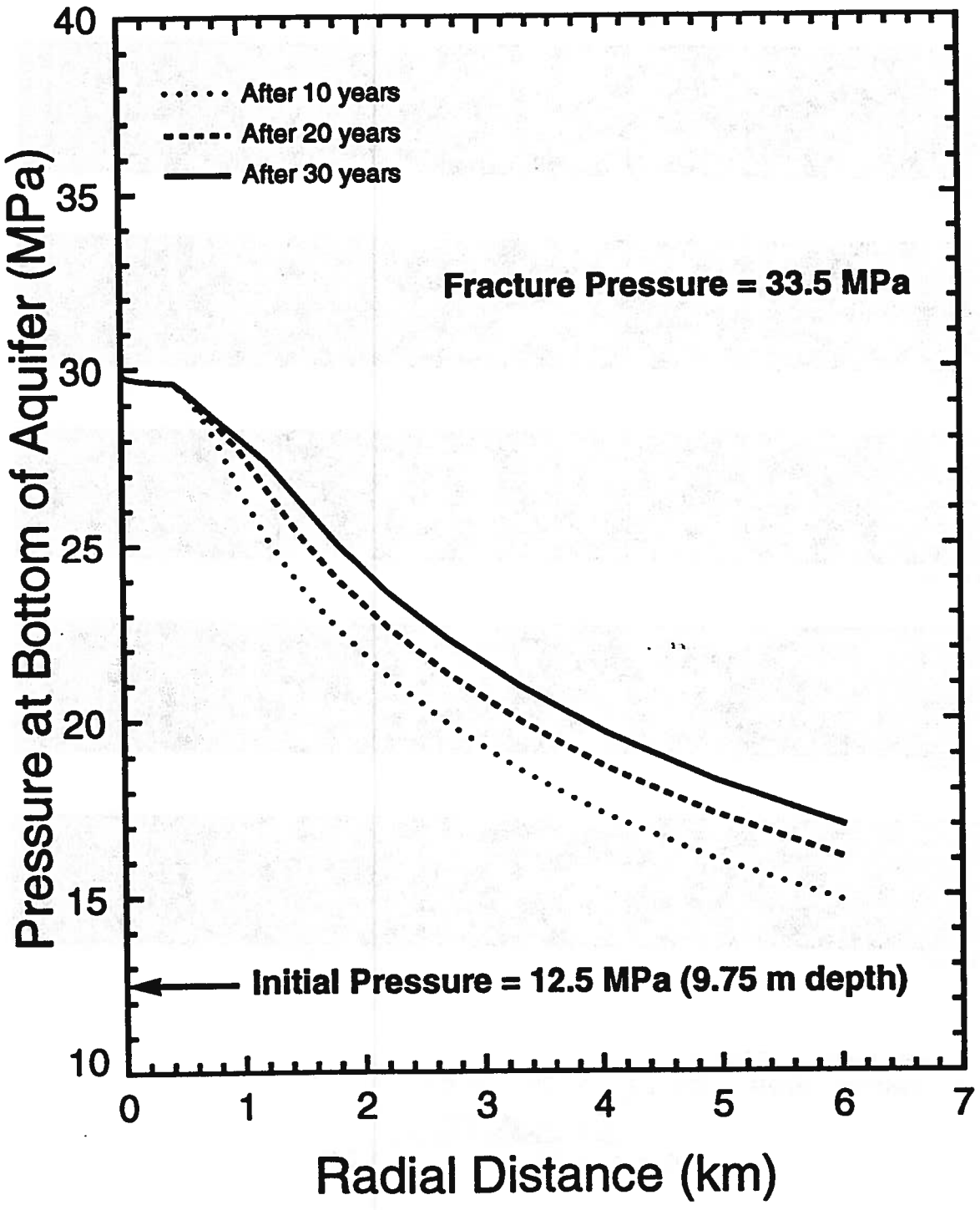

Glauconitic Sandstone Aquifer

NUMERICAL RUN (CO2_81)

Aquifer Porosity = 0.12 Aquifer Permeability = 100/6.2 md (horizontal)
Injection Pressure = 30.12 MPa

(a) Cumulative CO_2 Injection

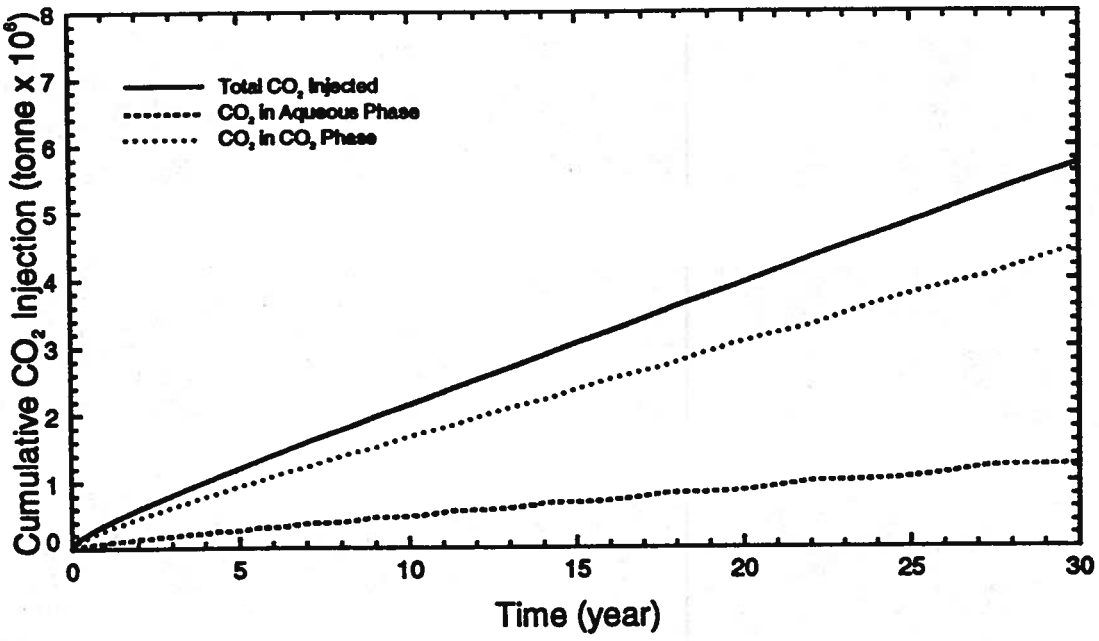

(b) CO_2 Injection Rate

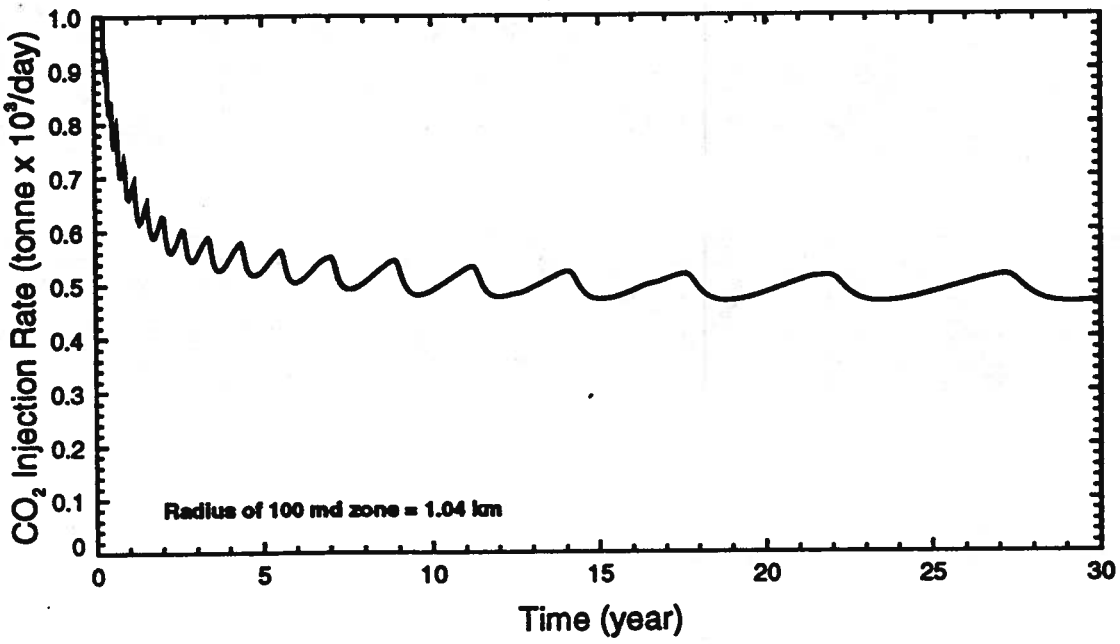

Carbon Dioxide Saturation (Run CO2_81)

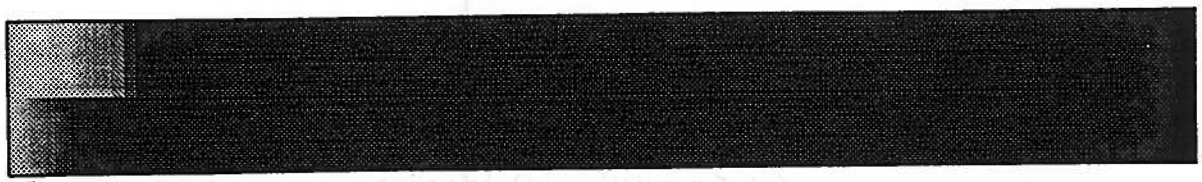

5 years

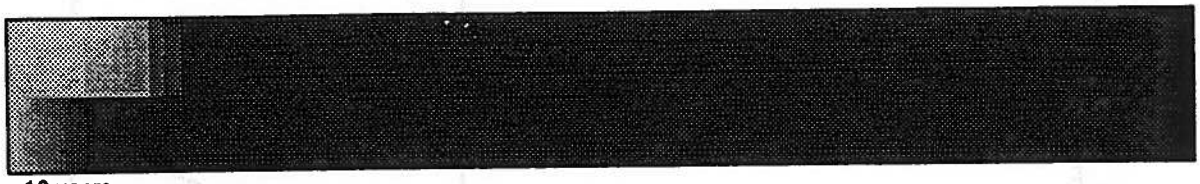

10 years

15 years

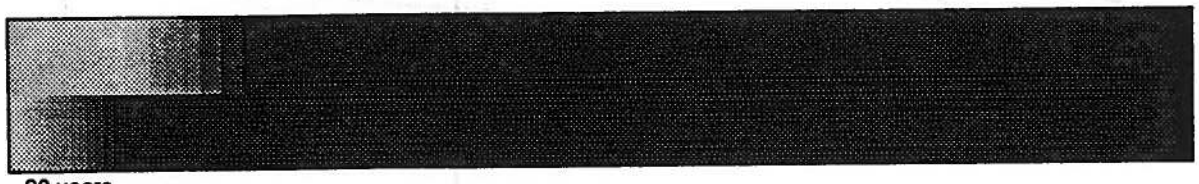

20 years

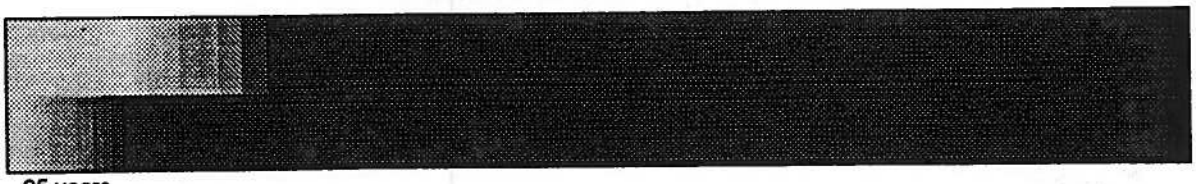

25 years

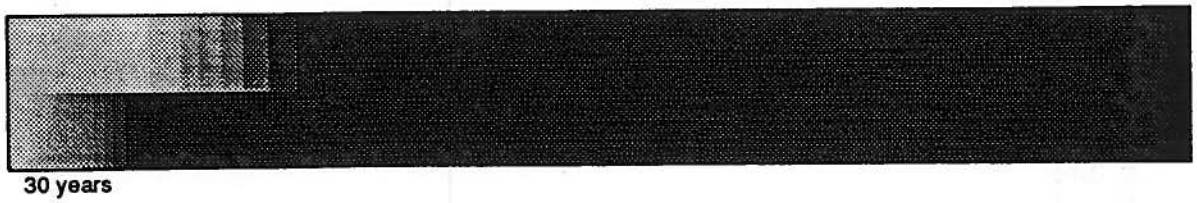

30 years

Vertical scale factor = 70.000
Field dimensions: 6999. (horiz.), 13.00 (vert.)

0.0000E+00 1.000

Glauconitic Sandstone Aquifer

NUMERICAL RUN (CO2_81)

Aquifer Porosity = 0.12 Aquifer Permeability = 100/6.2 md (horizontal)
Injection Pressure = 30.12 MPa Radius of 100 md zone = 1.04 km

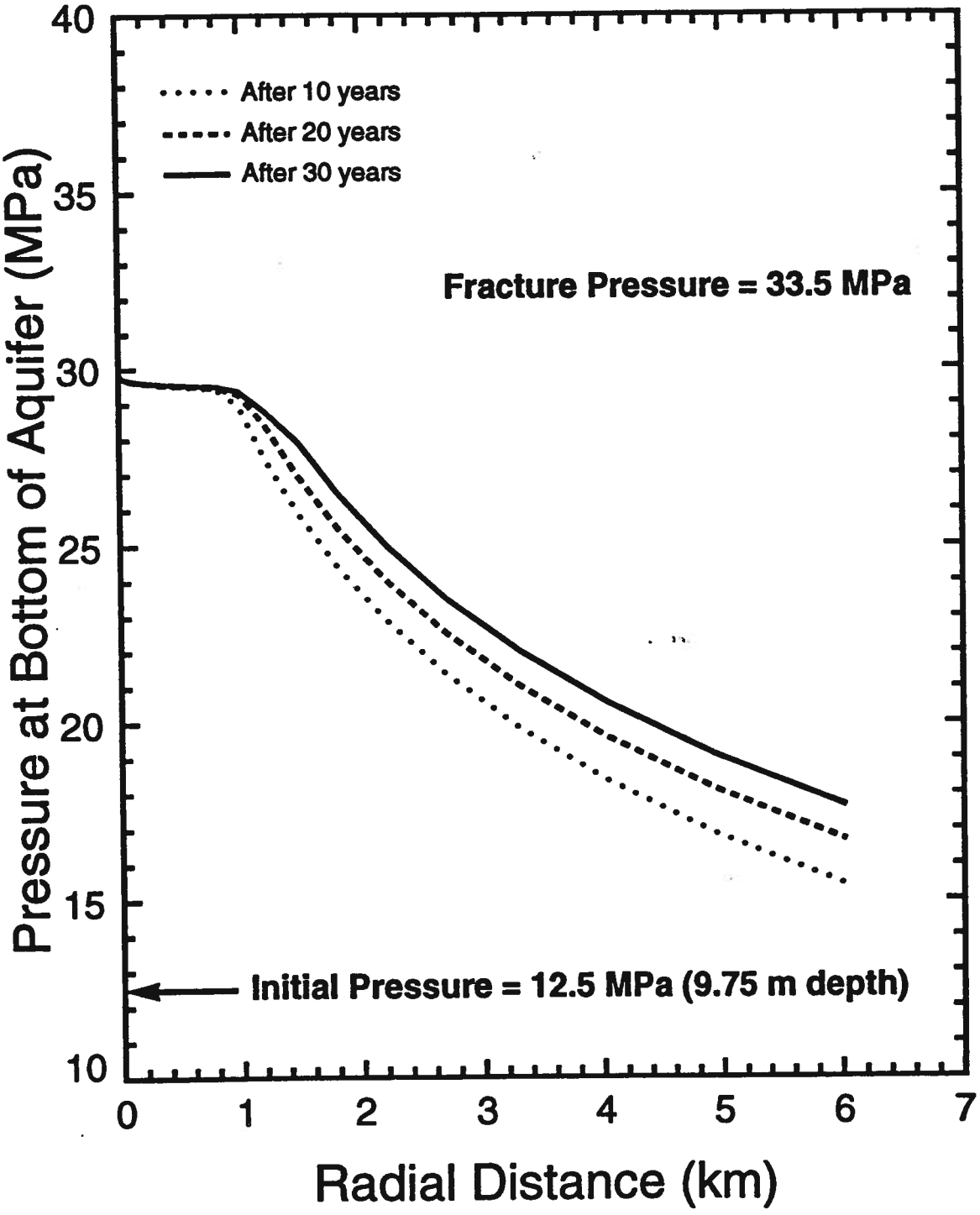

Glauconitic Sandstone Aquifer

NUMERICAL RUN (CO2_82)

Aquifer Porosity = 0.12 Aquifer Permeability = 100/6.2 md (horizontal)
Injection Pressure = 30.12 MPa

(a) Cumulative CO_2 Injection

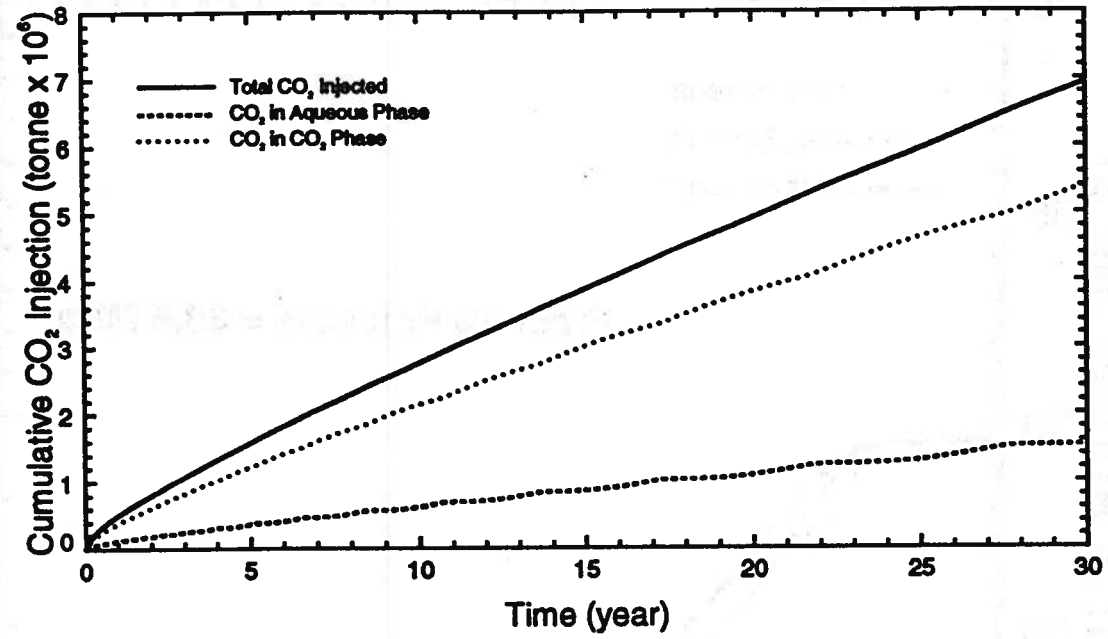

(b) CO_2 Injection Rate

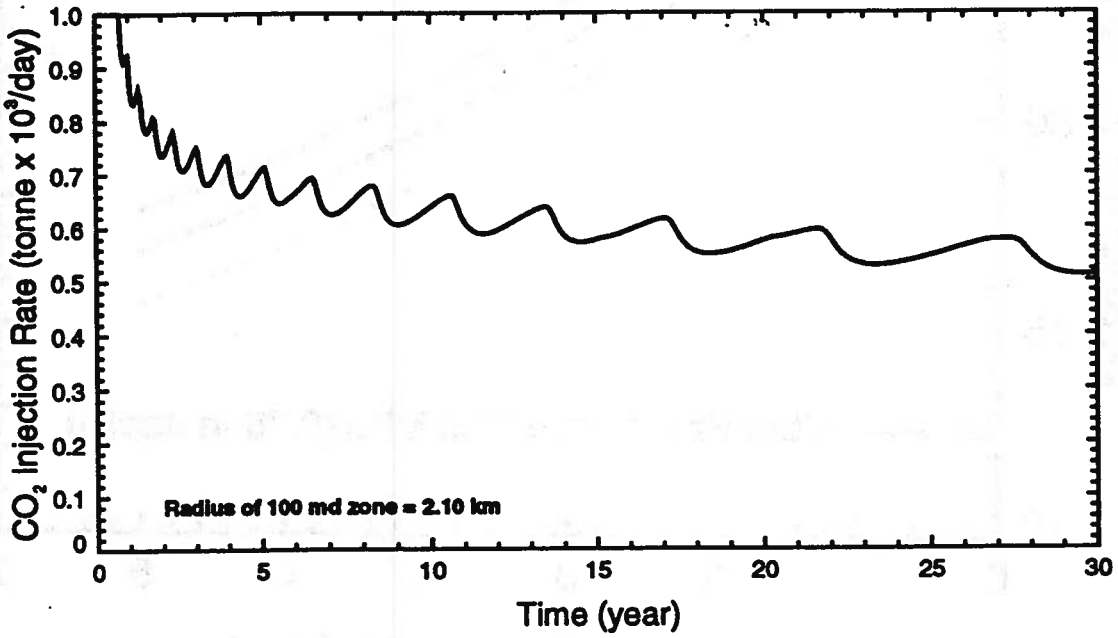

Carbon Dioxide Saturation (Run CO2_82)

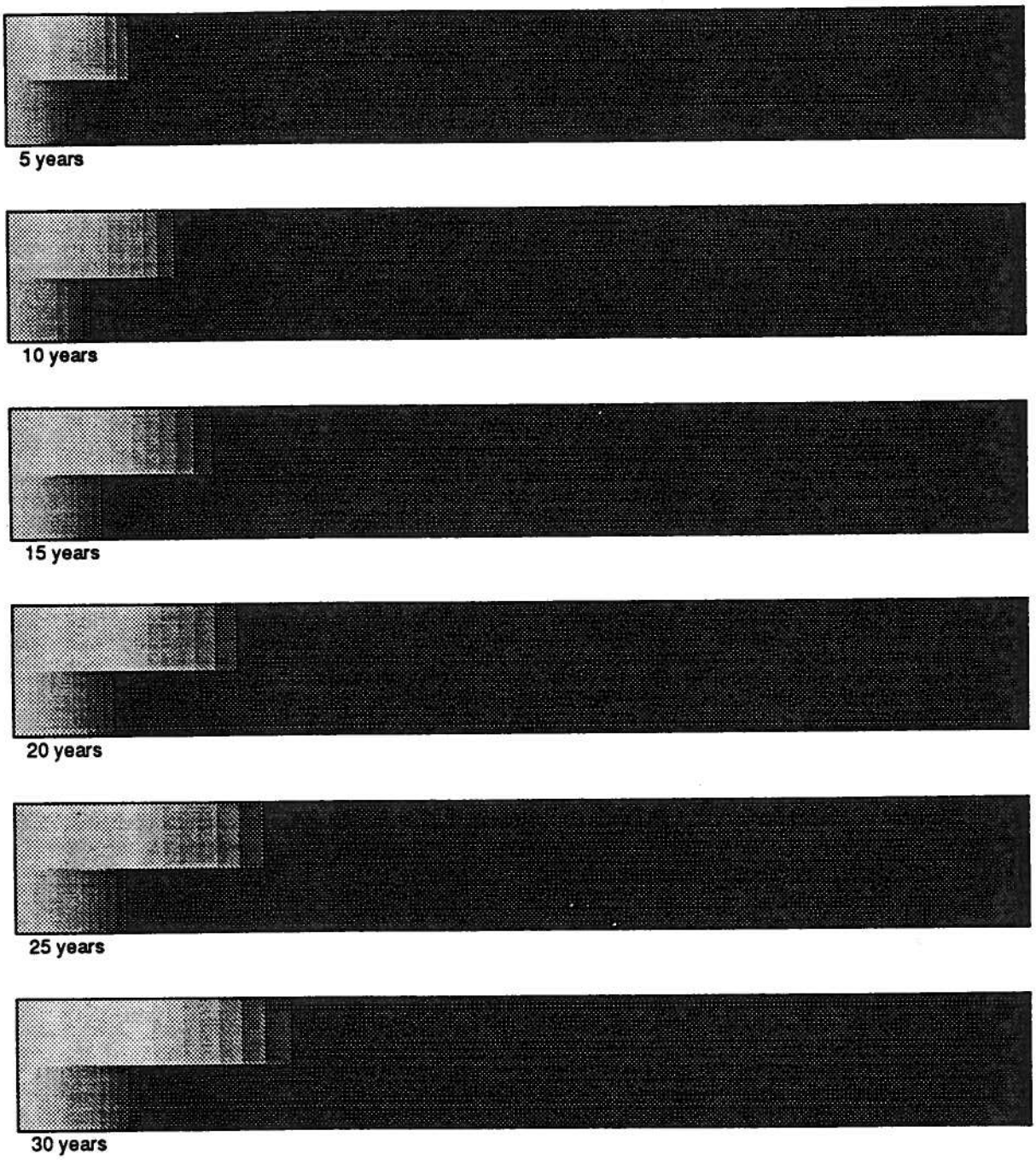

Vertical scale factor = 70.000
Field dimensions: 6999. (horiz.), 13.00 (vert.)

Glauconitic Sandstone Aquifer

NUMERICAL RUN (CO2_82)

Aquifer Porosity = 0.12 Aquifer Permeability = 100/6.2 md (horizontal)
Injection Pressure = 30.12 MPa Radius of 100 md zone = 2.10 km

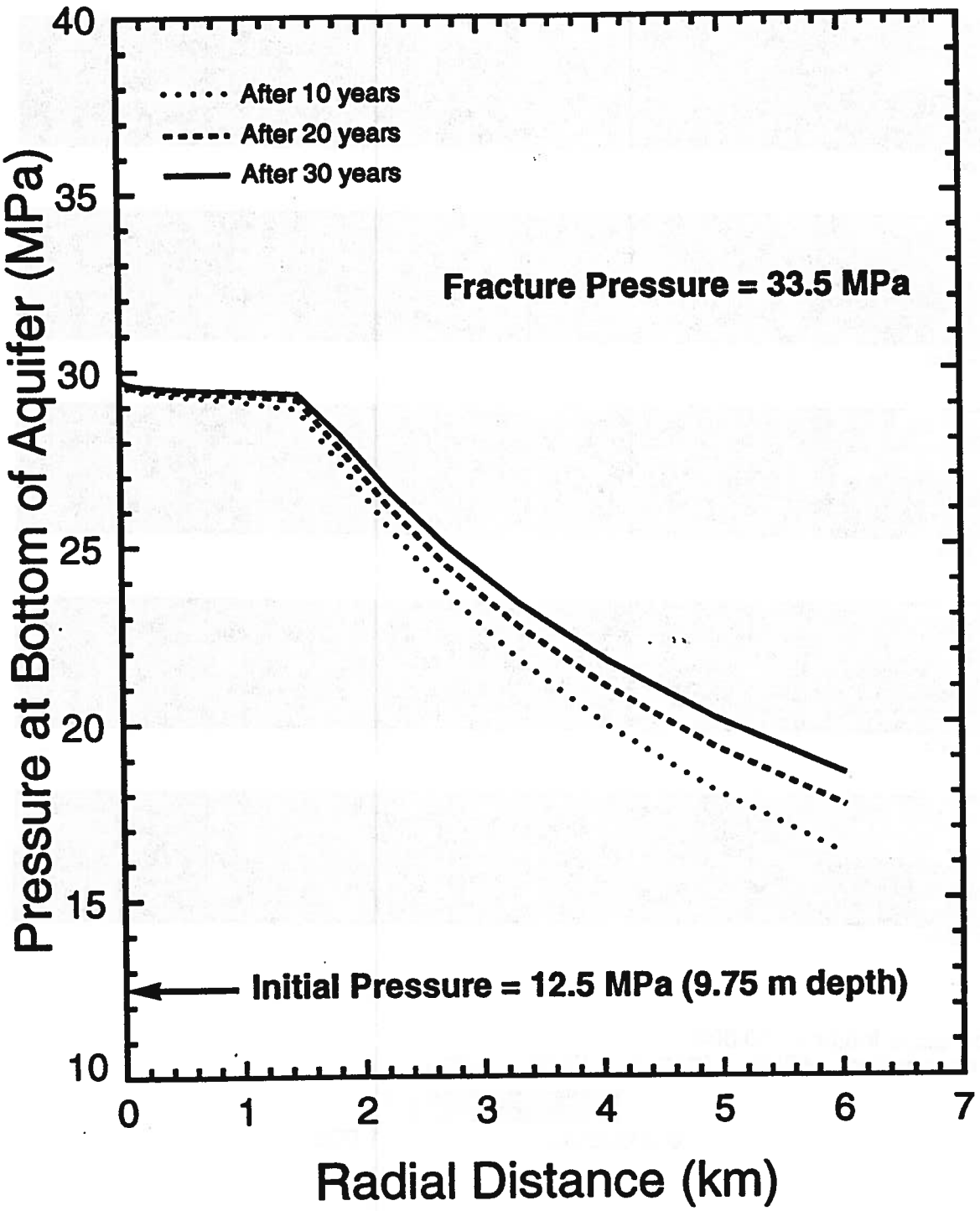

Glauconitic Sandstone Aquifer

NUMERICAL RUN (CO2_83)

Aquifer Porosity = 0.12 Aquifer Permeability = 100/30 md (horizontal)
Injection Pressure = 30.12 MPa

(a) Cumulative CO_2 Injection

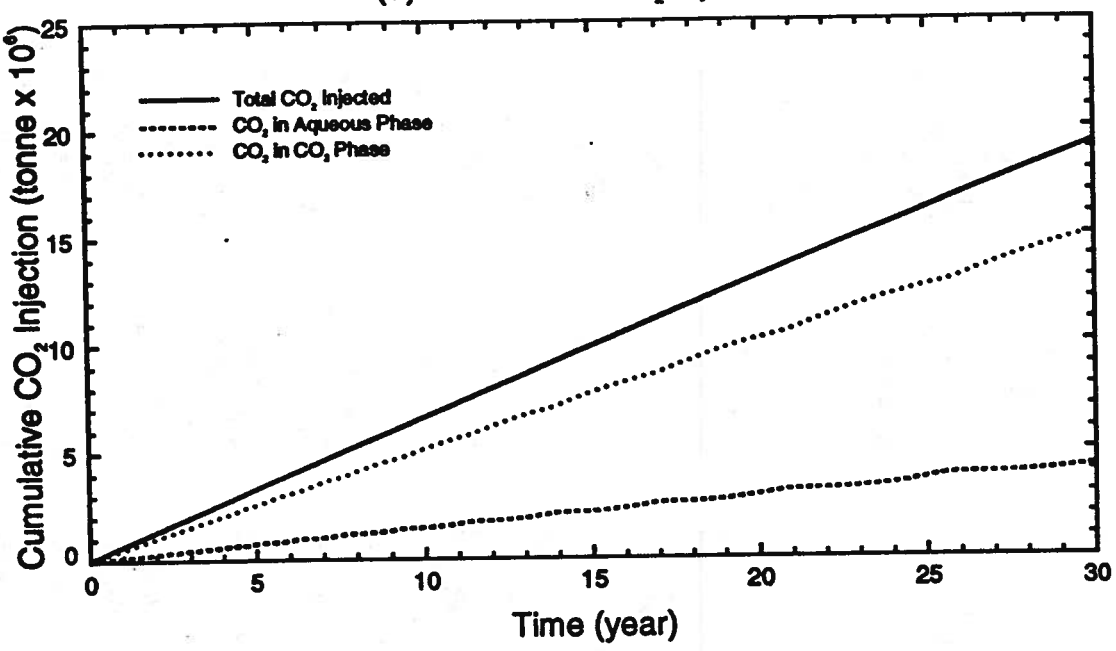

(b) CO_2 Injection Rate

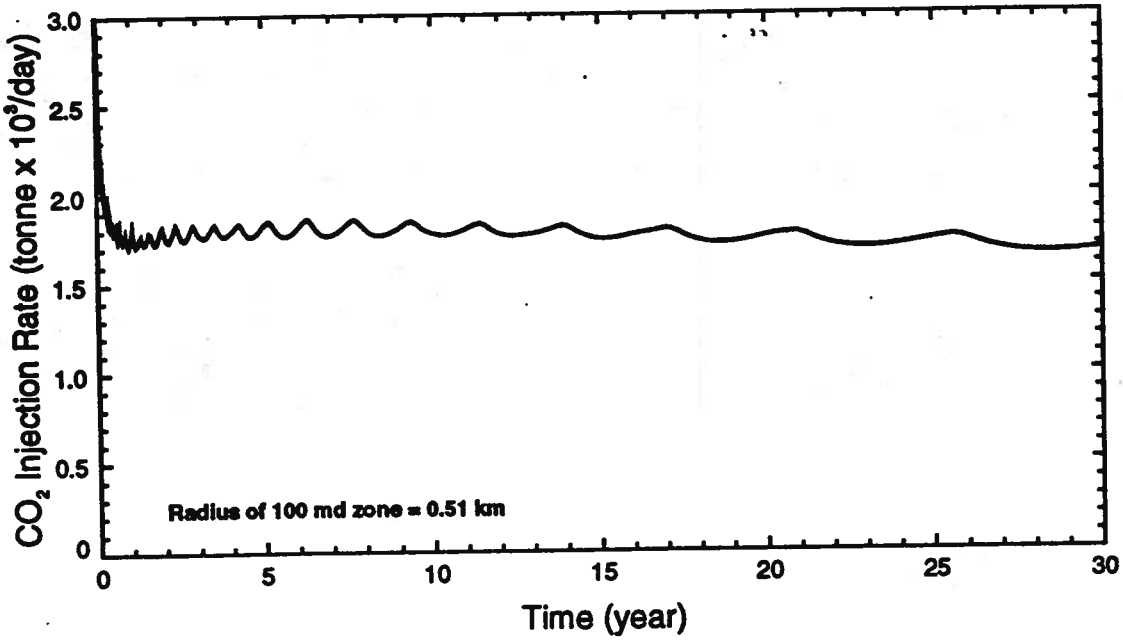

Carbon Dioxide Saturation (Run CO2_83)

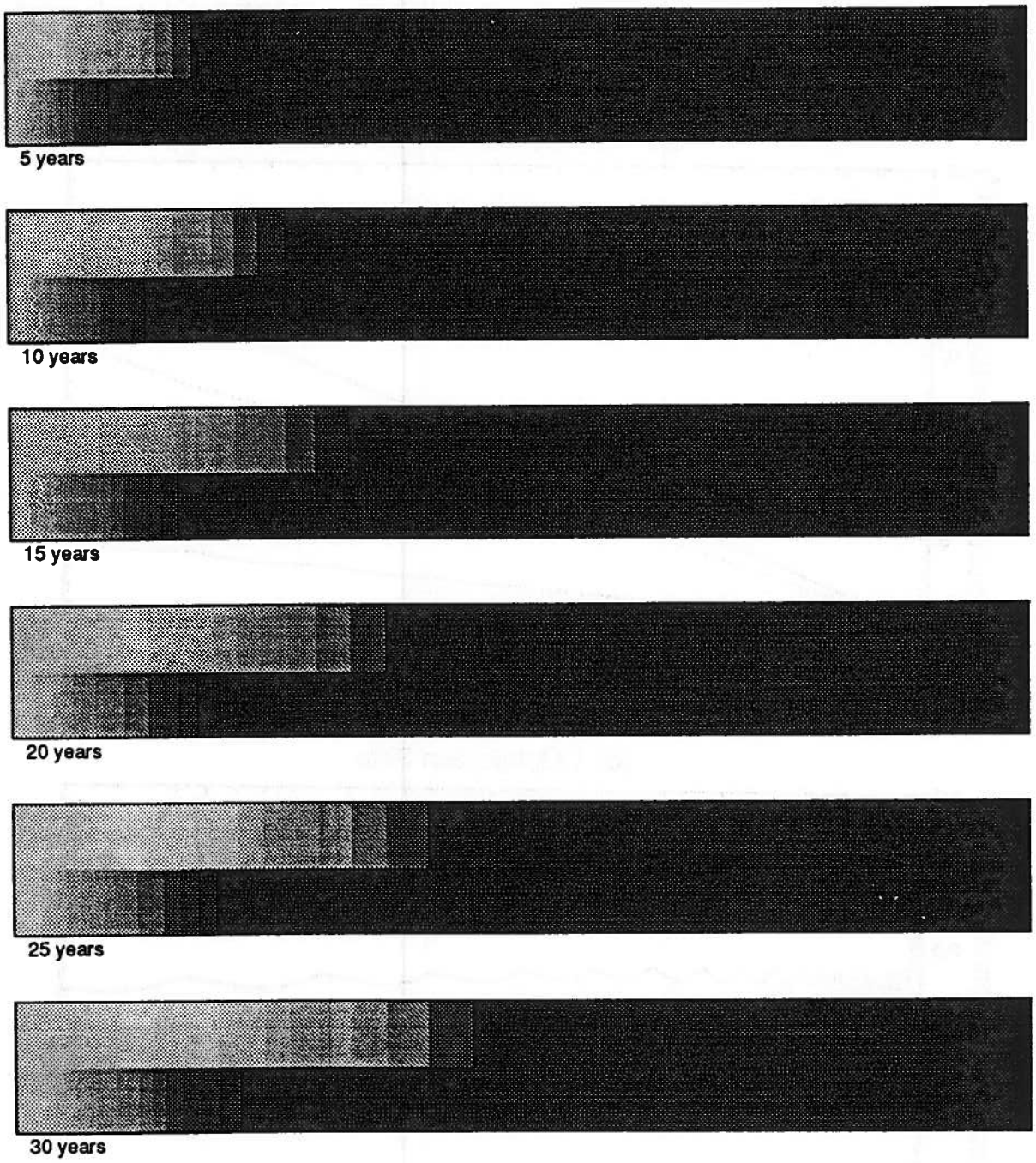

Vertical scale factor = 70.000
Field dimensions: 6999. (horiz.), 13.00 (vert.)

Glauconitic Sandstone Aquifer

NUMERICAL RUN (CO2_83)

Aquifer Porosity = 0.12 Aquifer Permeability = 100/30 md (horizontal)
Injection Pressure = 30.12 MPa Radius of 100 md zone = 0.51 km

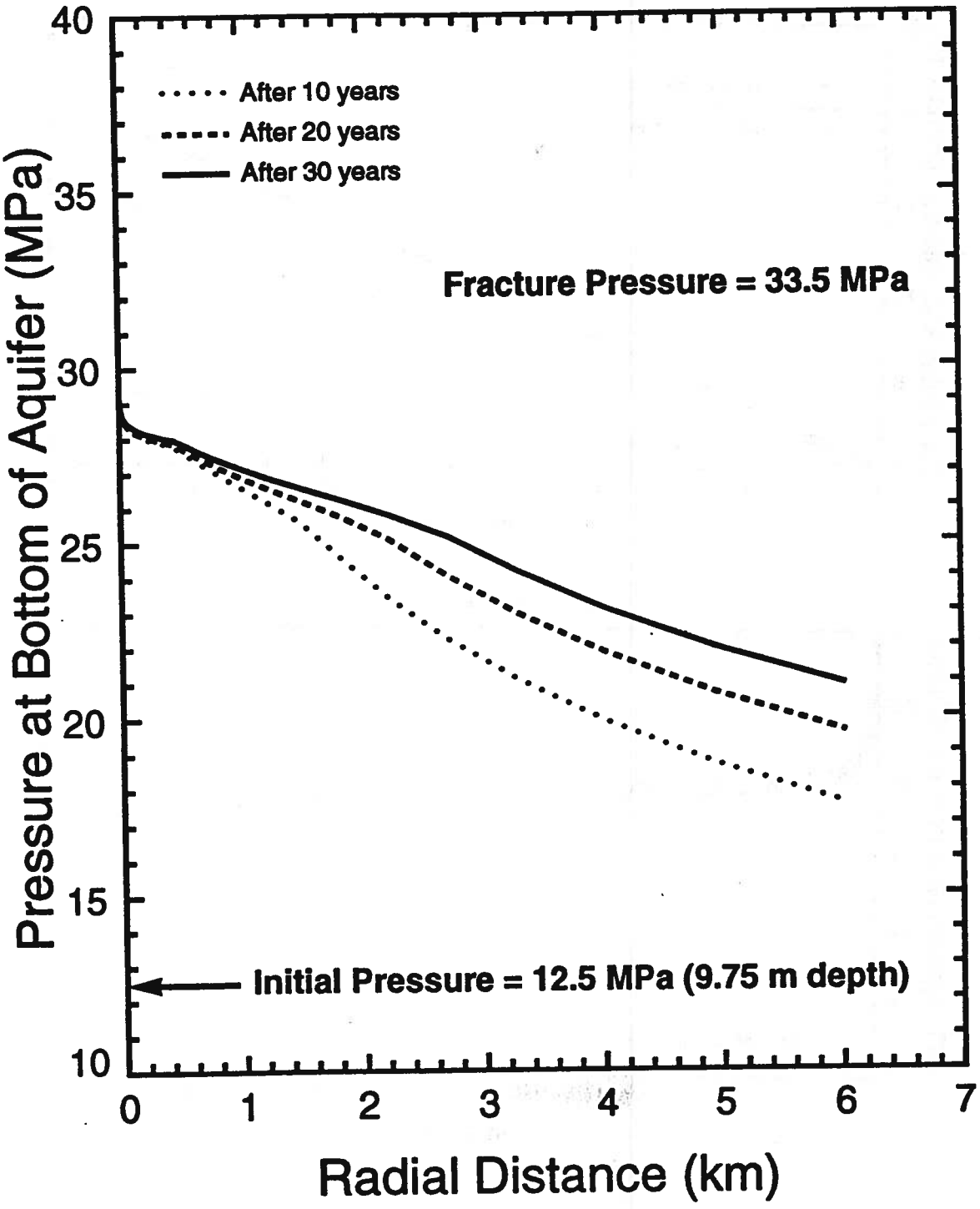

Glauconitic Sandstone Aquifer

NUMERICAL RUN (CO2_84)

Aquifer Porosity = 0.12 Aquifer Permeability = 100/30 md (horizontal)
Injection Pressure = 30.12 MPa

(a) Cumulative CO_2 Injection

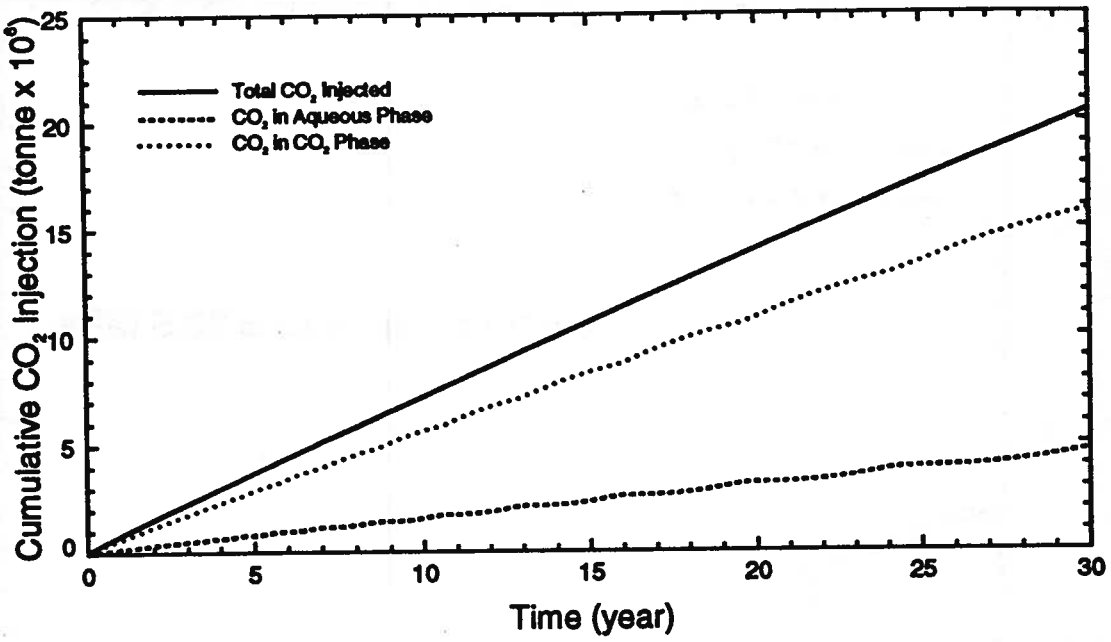

(b) CO_2 Injection Rate

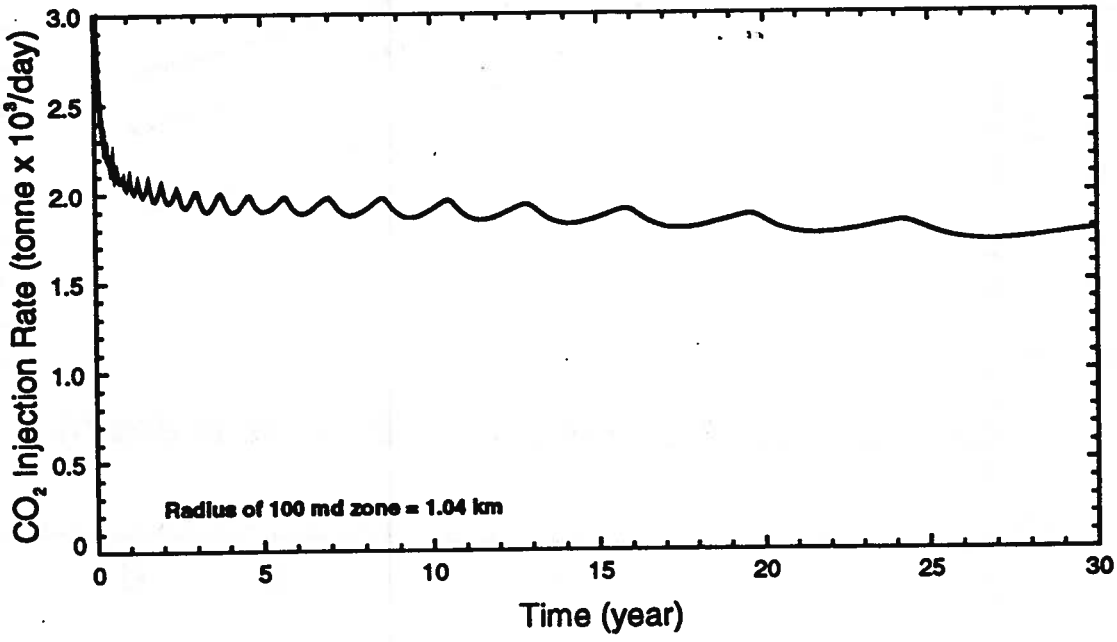

Carbon Dioxide Saturation (Run CO2_84)

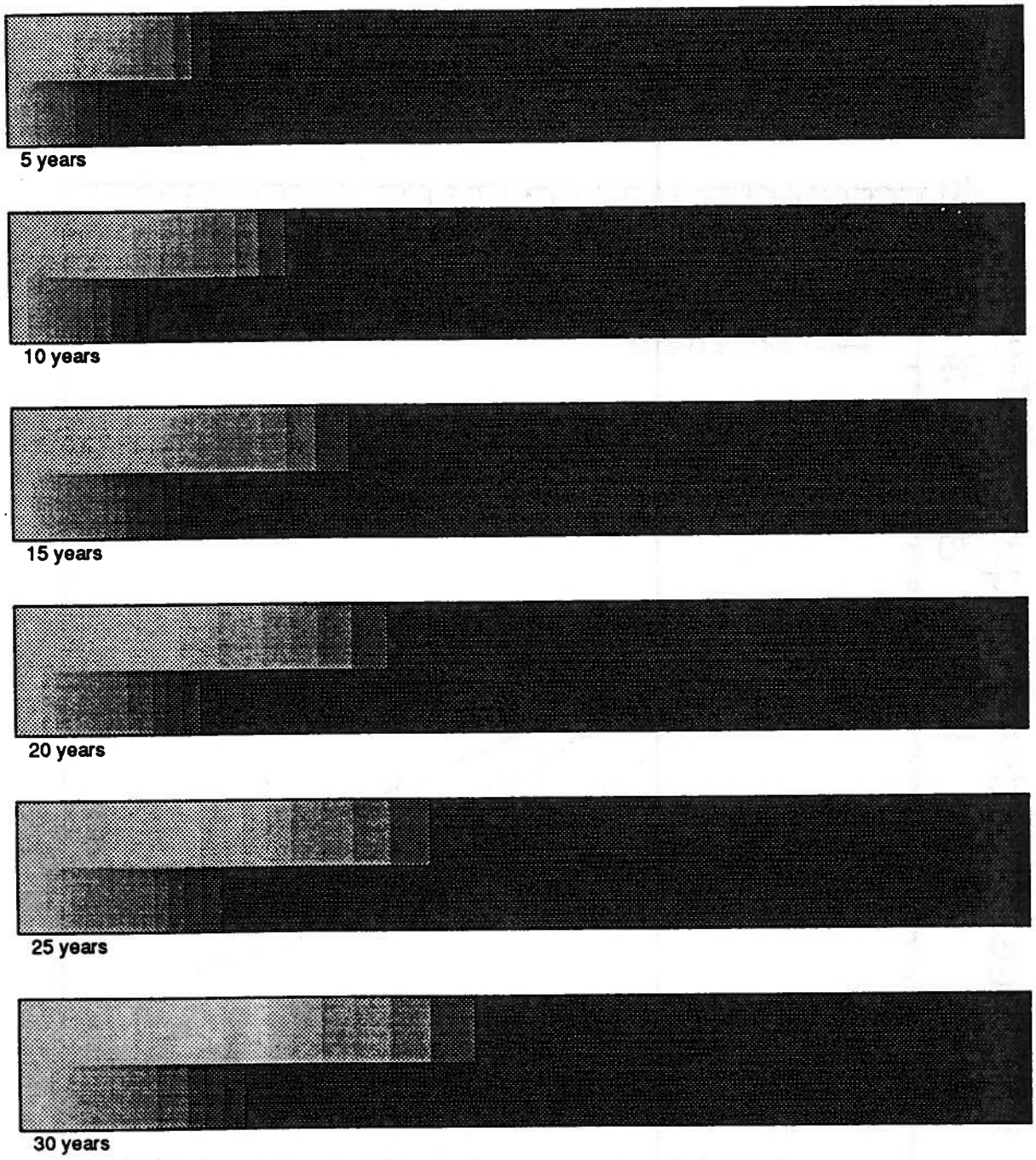

Vertical scale factor = 70.000
Field dimensions: 6999. (horiz.), 13.00 (vert.)

Glauconitic Sandstone Aquifer

NUMERICAL RUN (CO2_84)

Aquifer Porosity = 0.12 Aquifer Permeability = 100/30 md (horizontal)
Injection Pressure = 30.12 MPa Radius of 100 md zone = 1.04 km

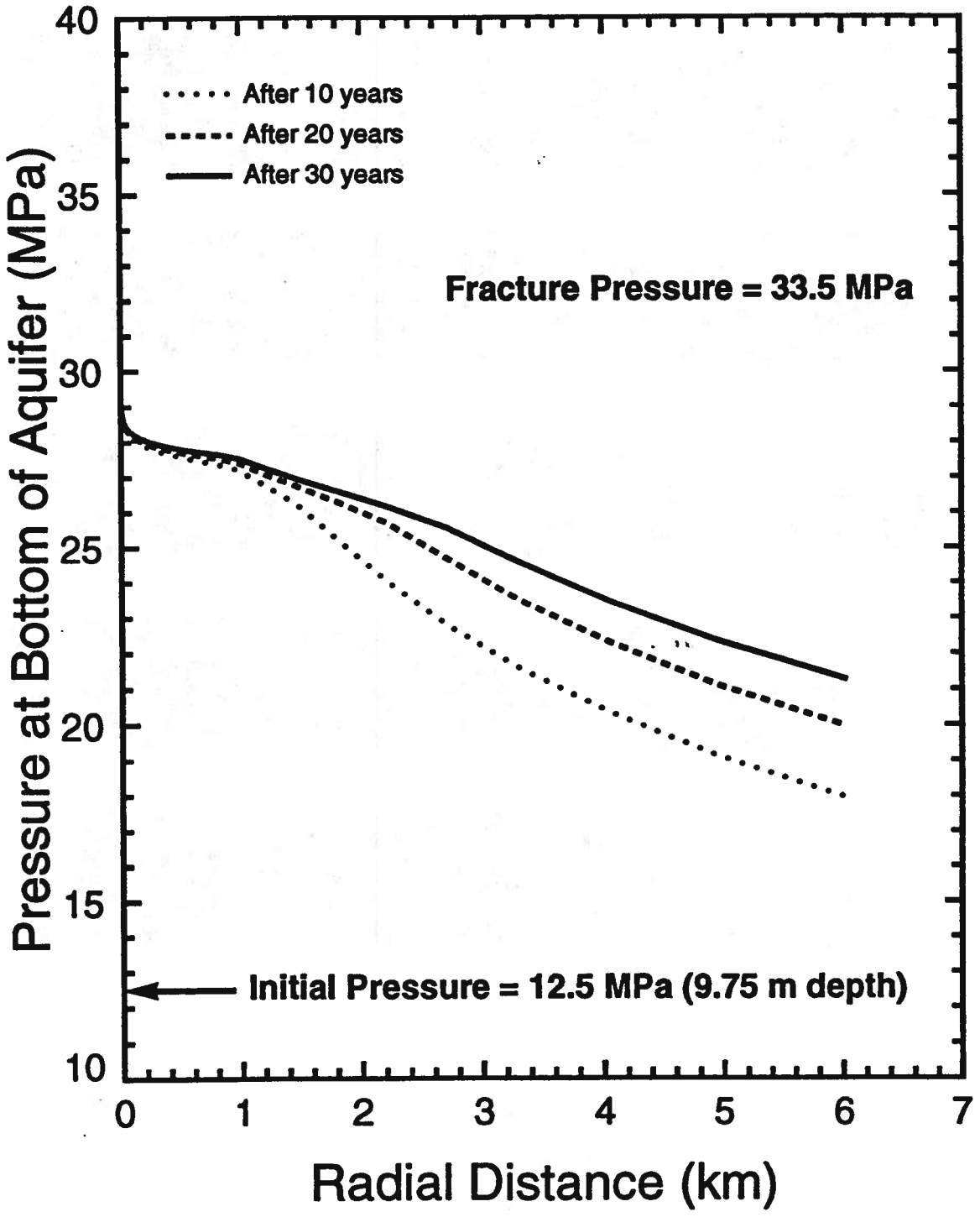

Glauconitic Sandstone Aquifer

NUMERICAL RUN (CO2_85)

Aquifer Porosity = 0.12 Aquifer Permeability = 100/30 md (horizontal)
Injection Pressure = 30.12 MPa

(a) Cumulative CO_2 Injection

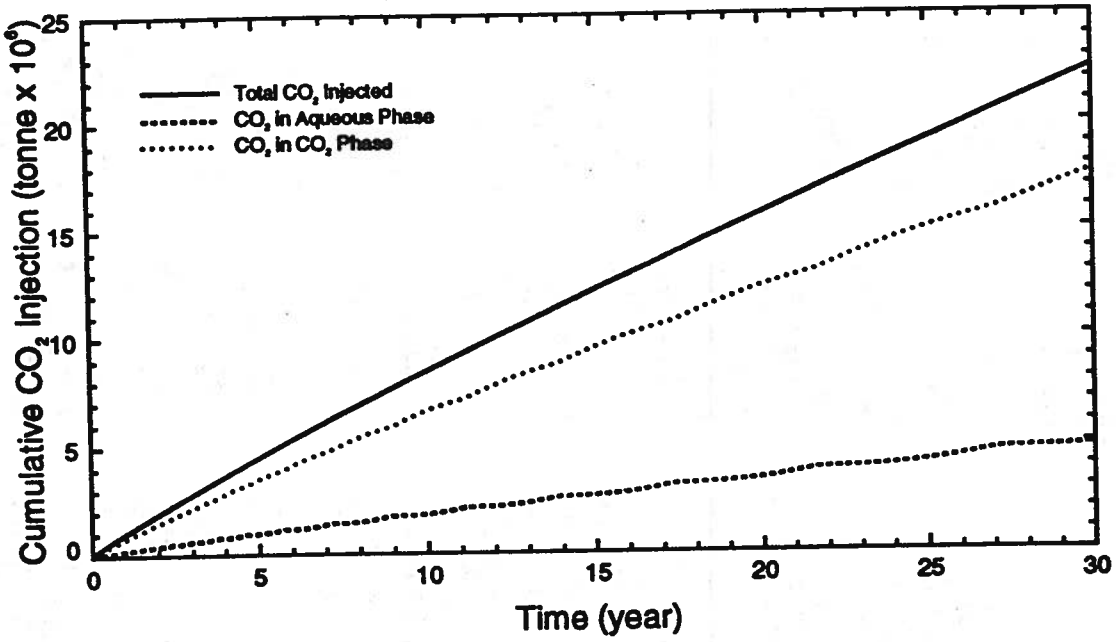

(b) CO_2 Injection Rate

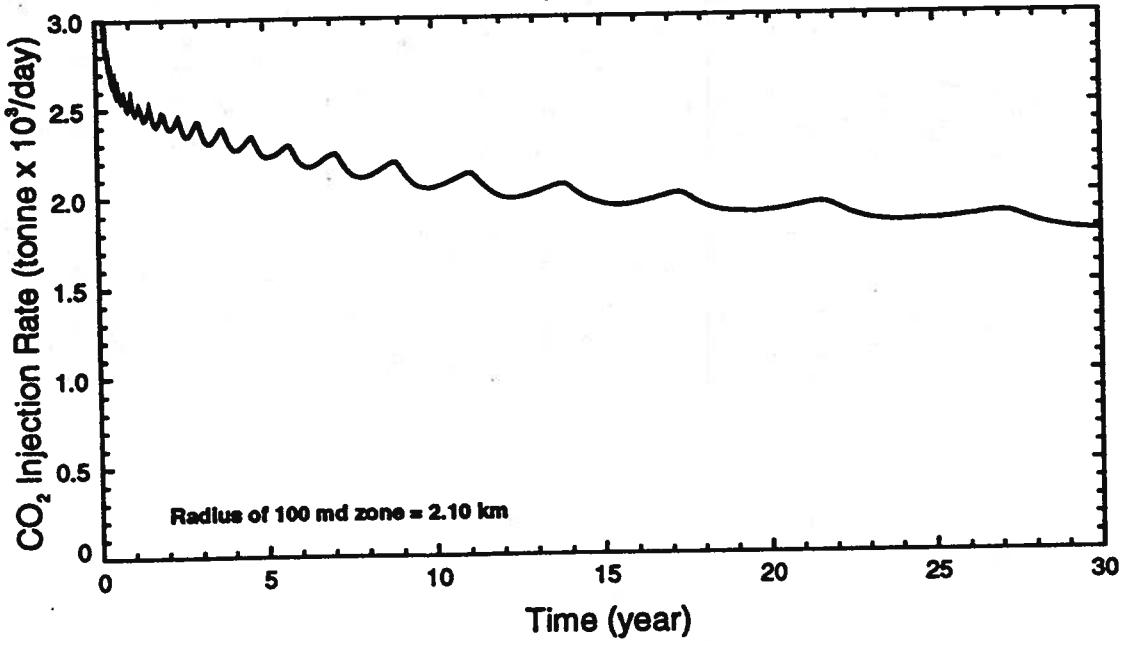

Carbon Dioxide Saturation (Run CO2_85)

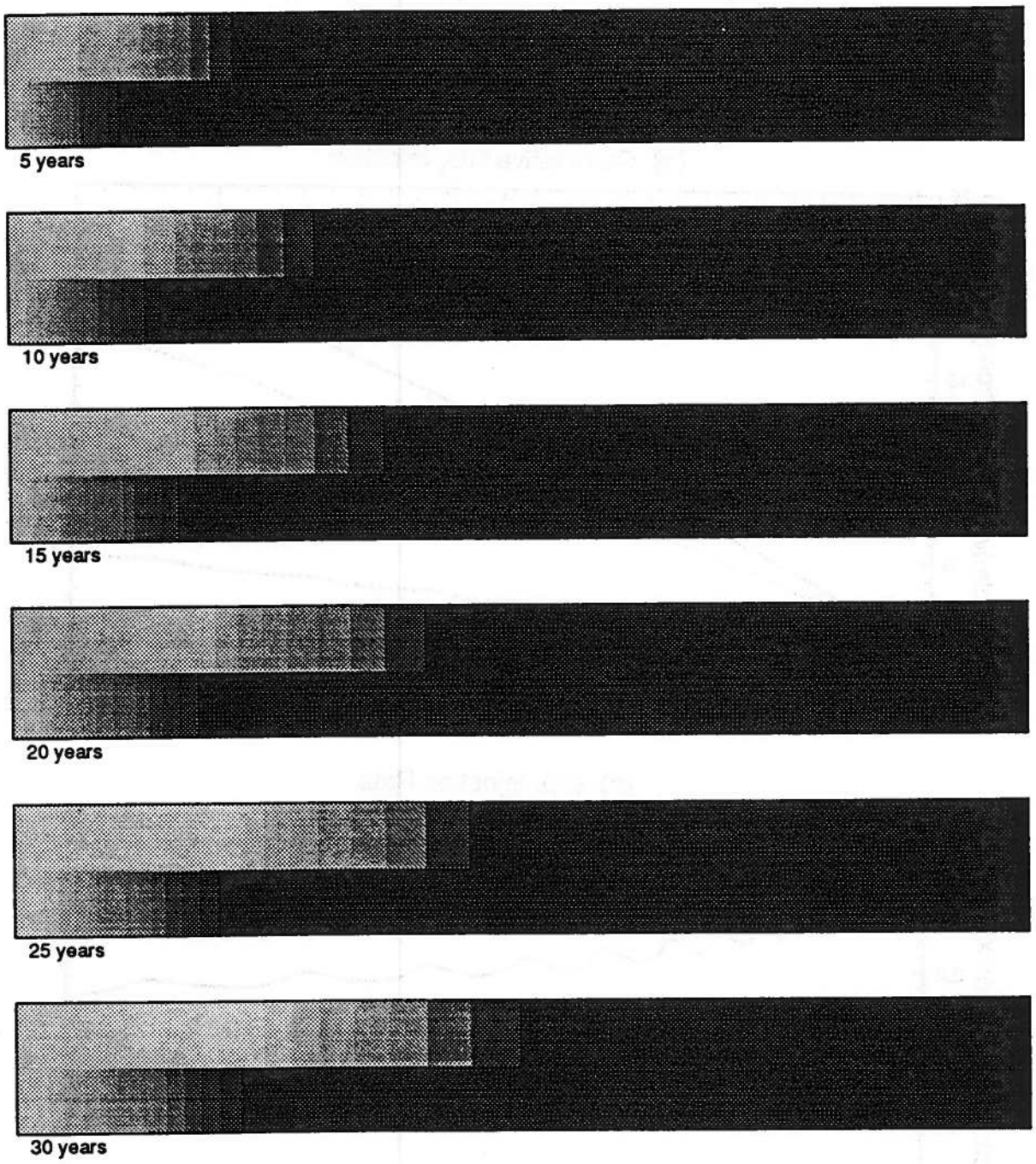

Vertical scale factor = 70.000
Field dimensions: 6999. (horiz.), 13.00 (vert.)

Glauconitic Sandstone Aquifer

NUMERICAL RUN (CO2_85)

Aquifer Porosity = 0.12 Aquifer Permeability = 100/30 md (horizontal)
Injection Pressure = 30.12 MPa Radius of 100 md zone = 2.10 km

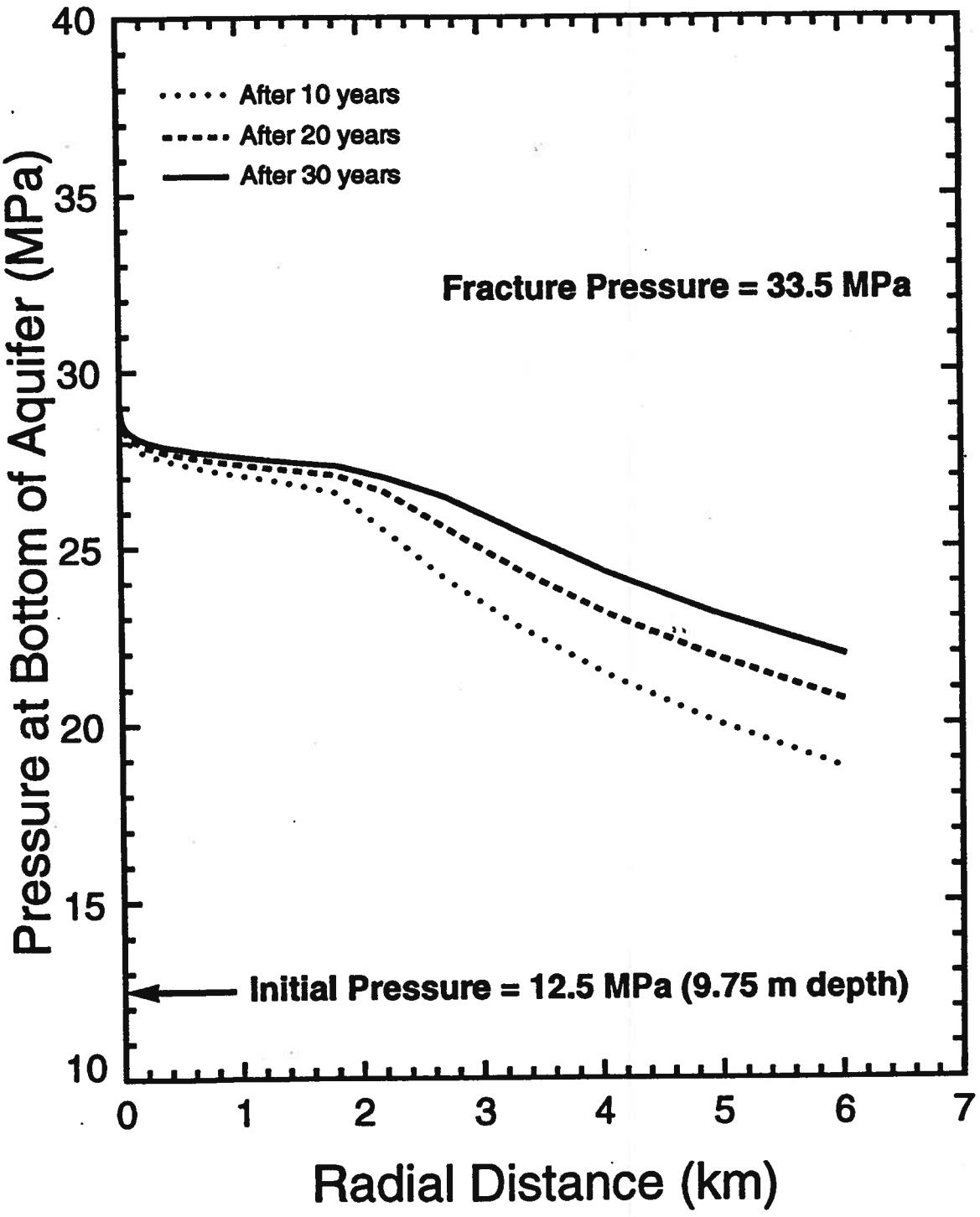

APPENDIX III

NISKU CARBONATE AQUIFER CO_2 MODEL INJECTION RESULTS

Nisku Carbonate Aquifer

NUMERICAL RUN (CO2_101)

Aquifer Porosity = 0.06 Aquifer Permeability = 6.2 md (horizontal)
Injection Pressure = 37.86 MPa Well Completion = 13 m

(a) Cumulative CO_2 Injection

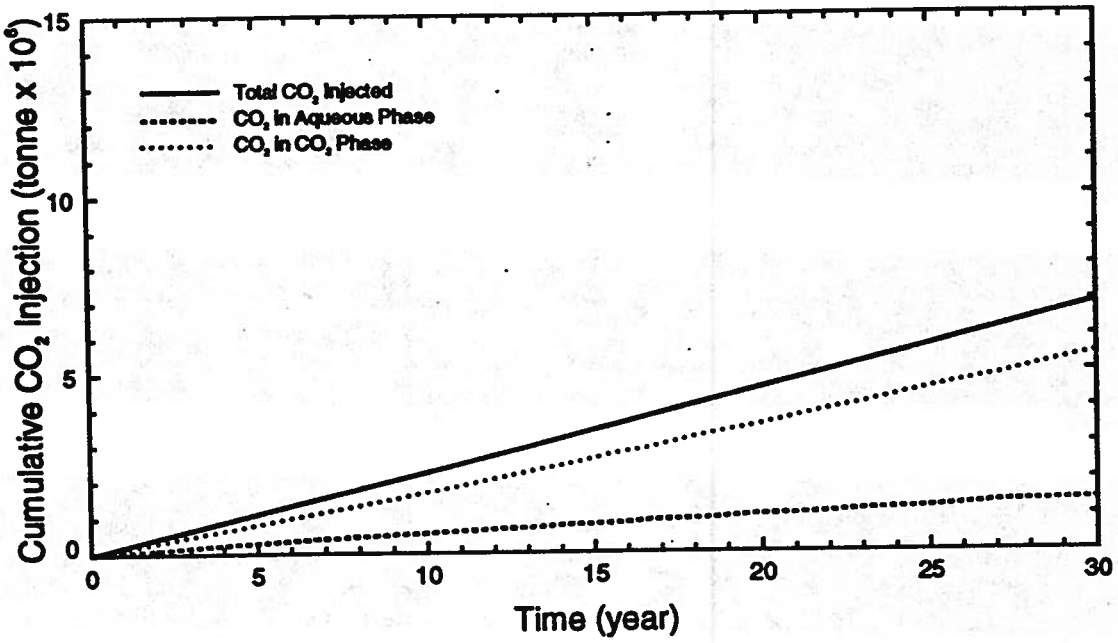

(b) CO_2 Injection Rate

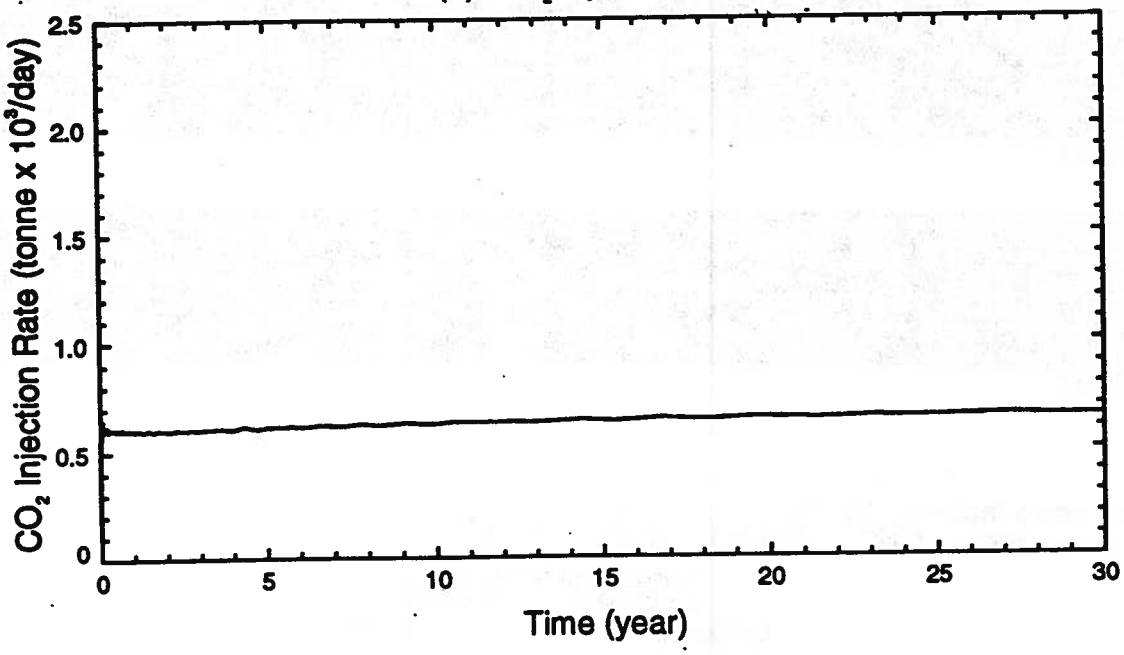

Carbon Dioxide Saturation (Run CO2_101)

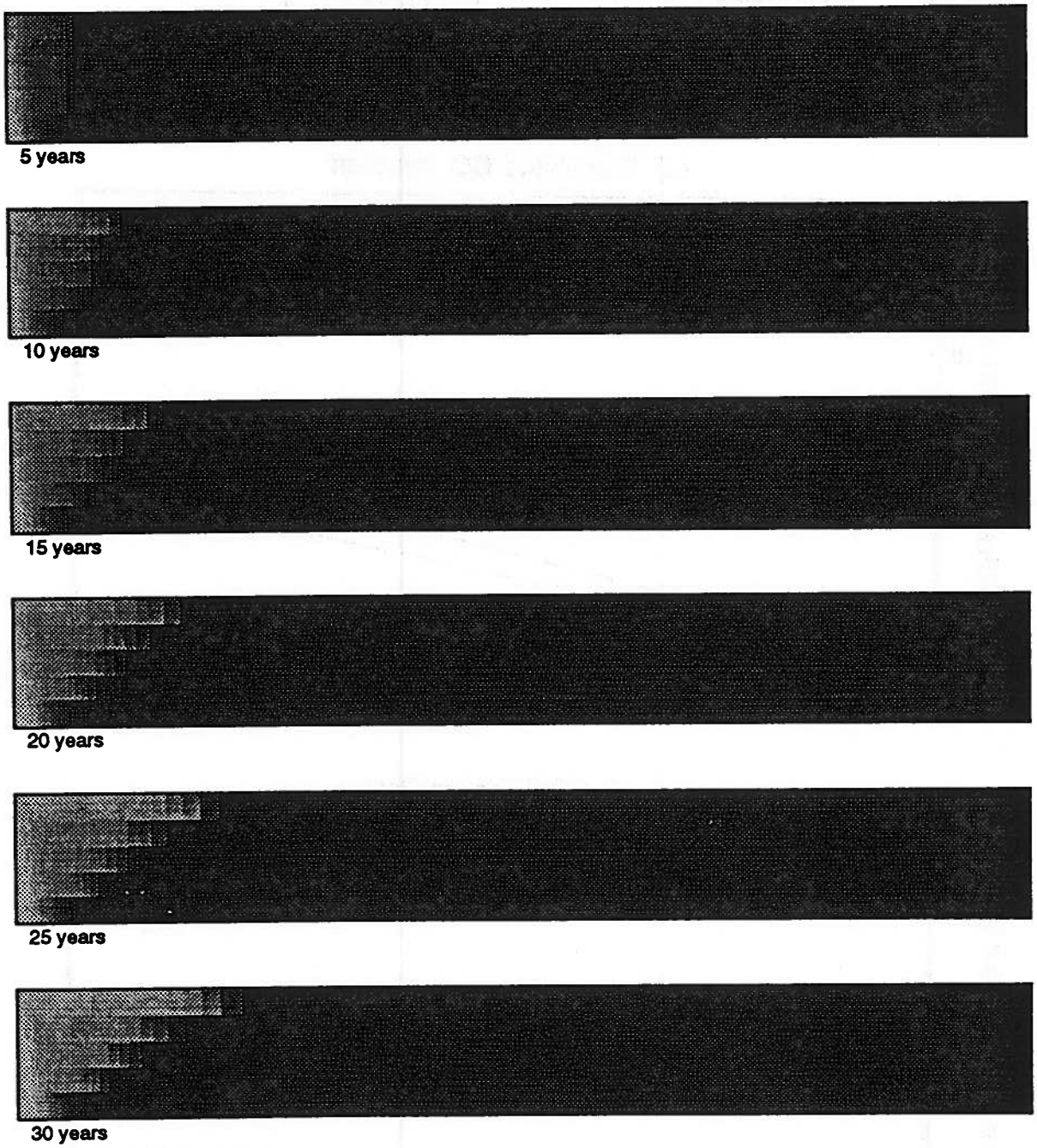

Vertical scale factor = 15.000
Field dimensions: 6999. (horiz.), 60.00 (vert.)

Nisku Carbonate Aquifer

NUMERICAL RUN (CO2_101)

Aquifer Porosity = 0.06 Aquifer Permeability = 6.2 md (horizontal)
Injection Pressure = 37.86 MPa Well Completion = 13 m

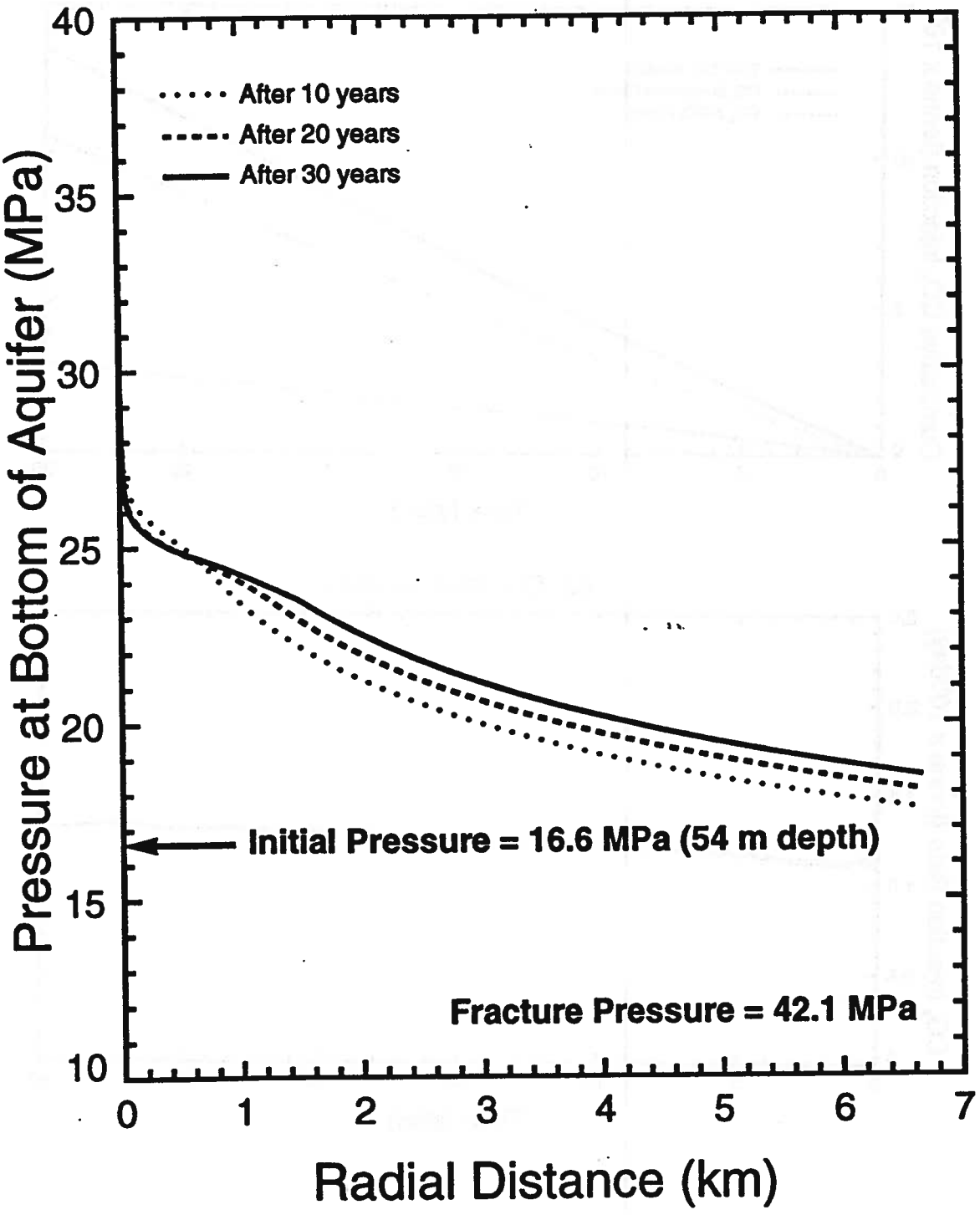

Nisku Carbonate Aquifer

NUMERICAL RUN (CO2_102)

Aquifer Porosity = 0.06 Aquifer Permeability = 6.2 md (horizontal)
Injection Pressure = 37.86 MPa

(a) Cumulative CO_2 Injection

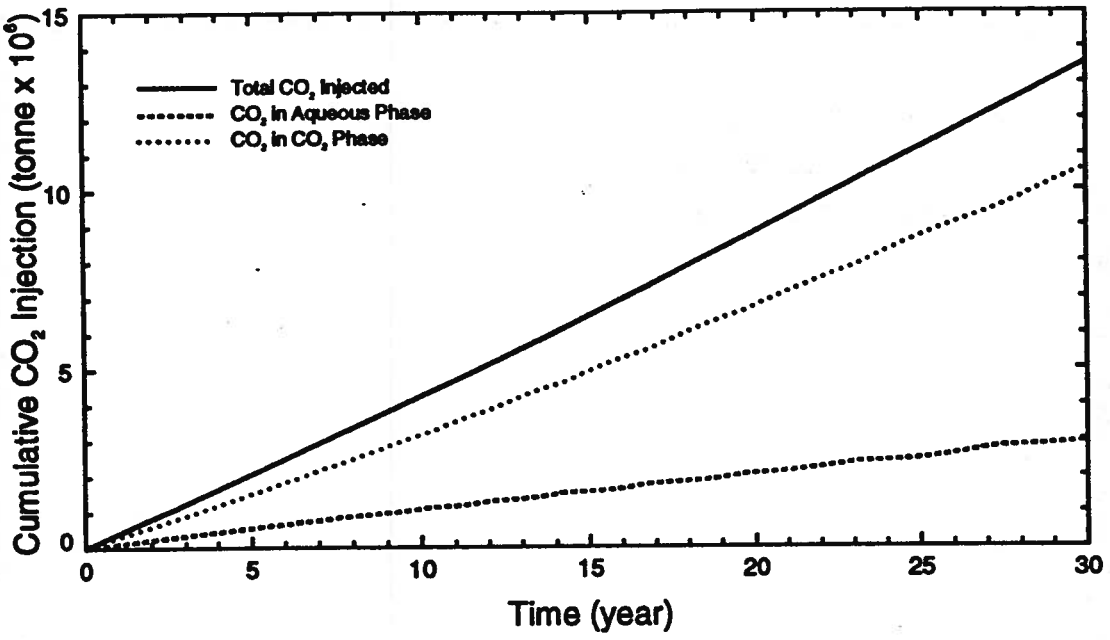

(b) CO_2 Injection Rate

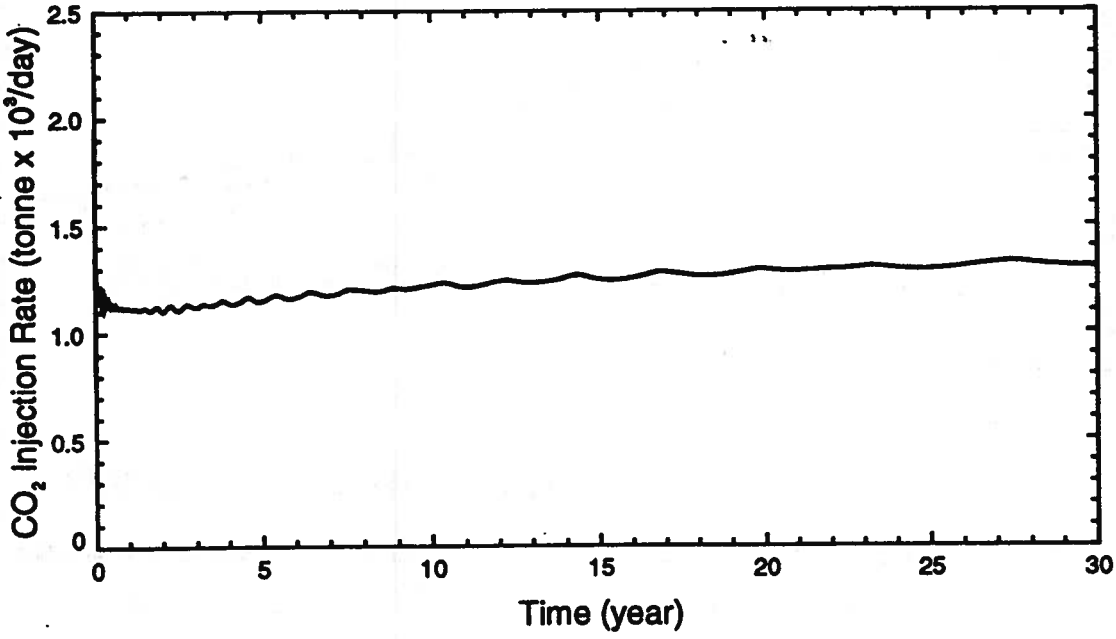

Carbon Dioxide Saturation (Run CO2_102)

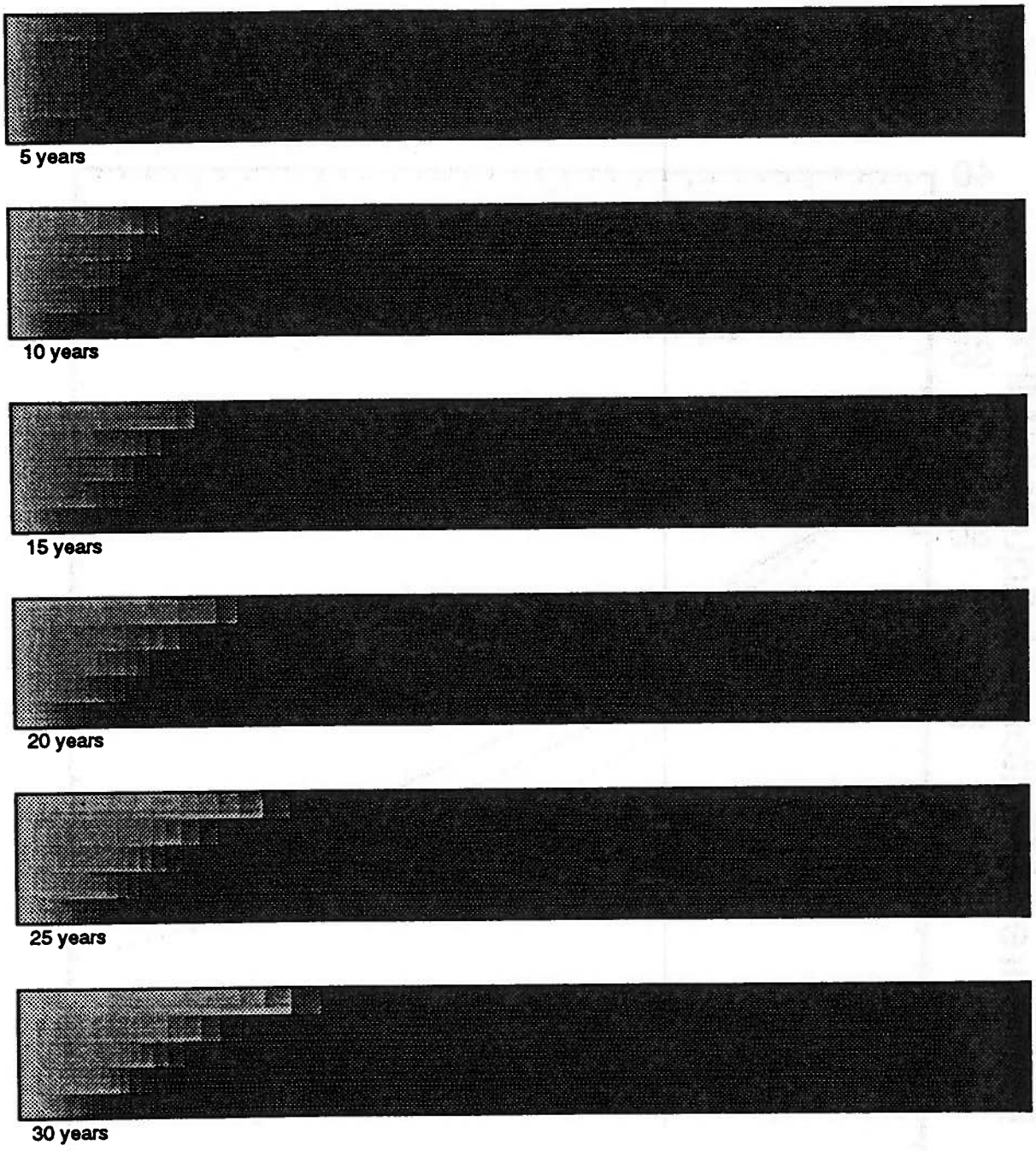

Vertical scale factor = 15.000
Field dimensions: 6999. (horiz.), 60.00 (vert.)

Nisku Carbonate Aquifer

NUMERICAL RUN (CO2_102)

Aquifer Porosity = 0.06 Aquifer Permeability = 6.2 md (horizontal)
Injection Pressure = 37.86 MPa

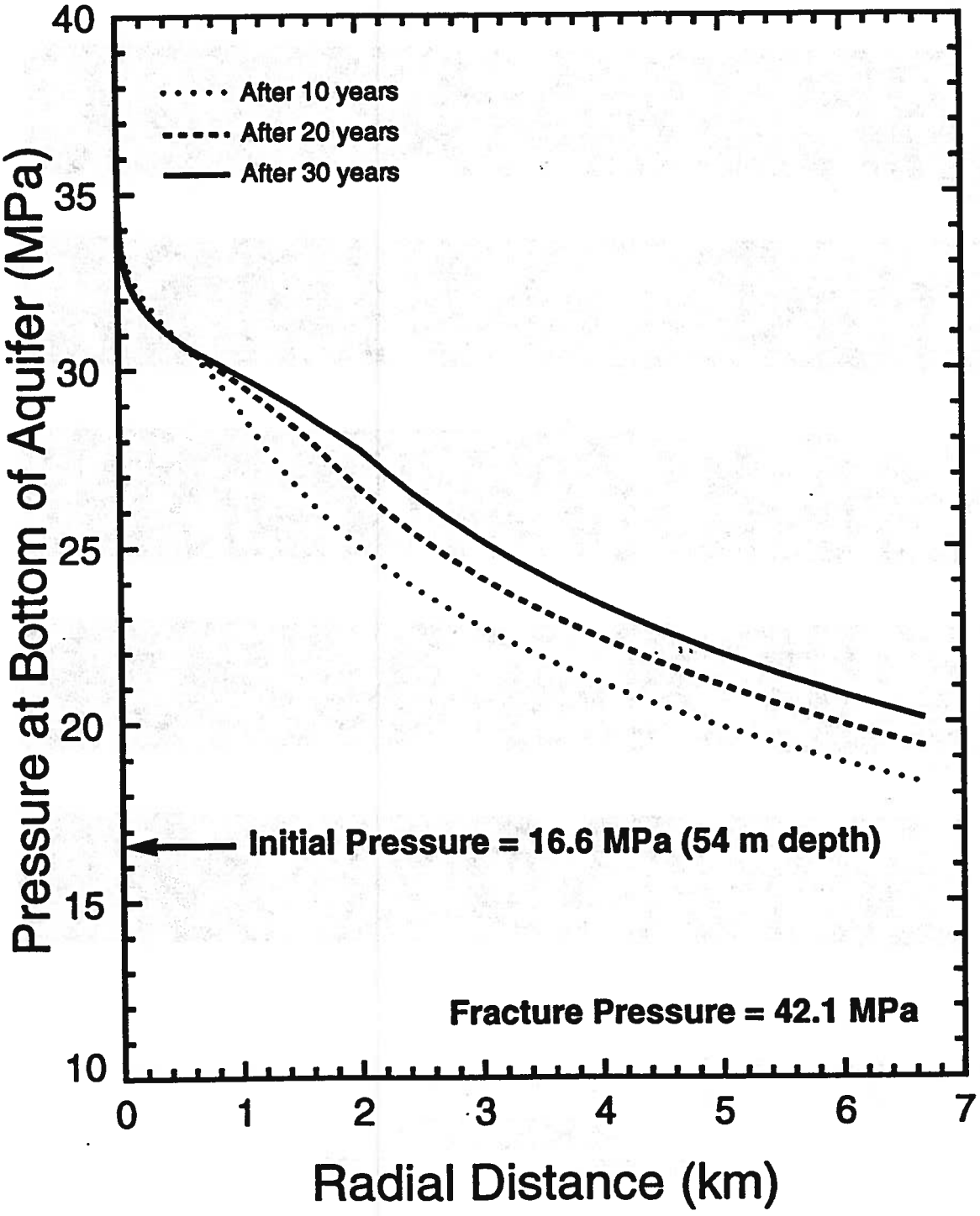

Nisku Carbonate Aquifer

NUMERICAL RUN (CO2_103)

Aquifer Porosity = 0.06 Aquifer Permeability = 30 md (horizontal)
Injection Pressure = 37.86 MPa

(a) Cumulative CO_2 Injection

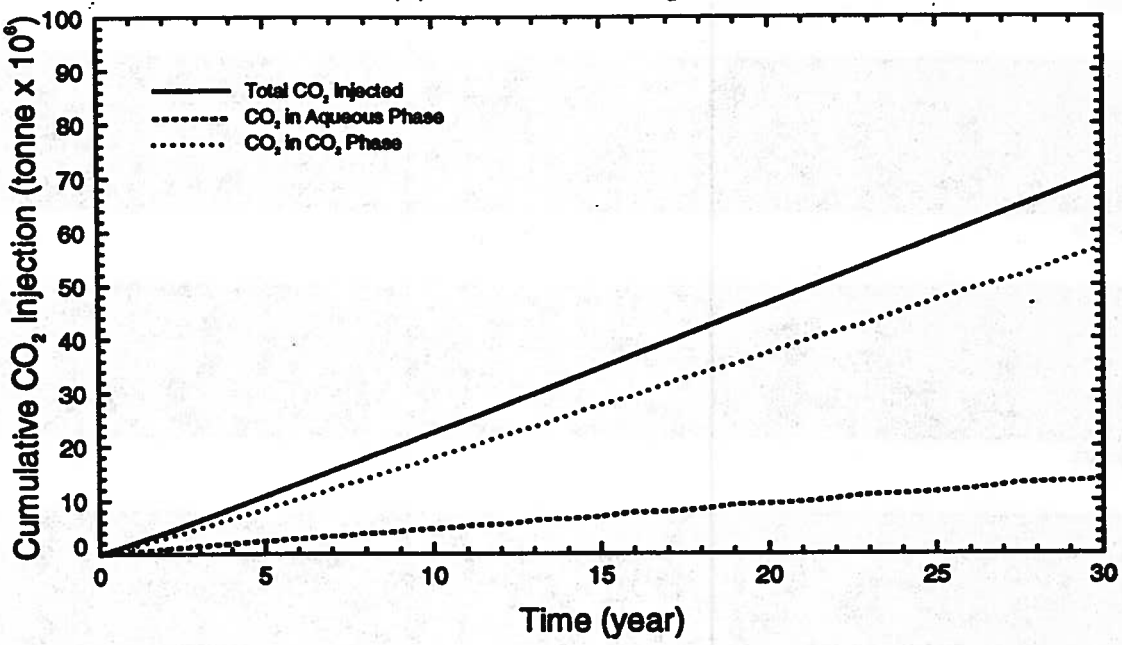

(b) CO_2 Injection Rate

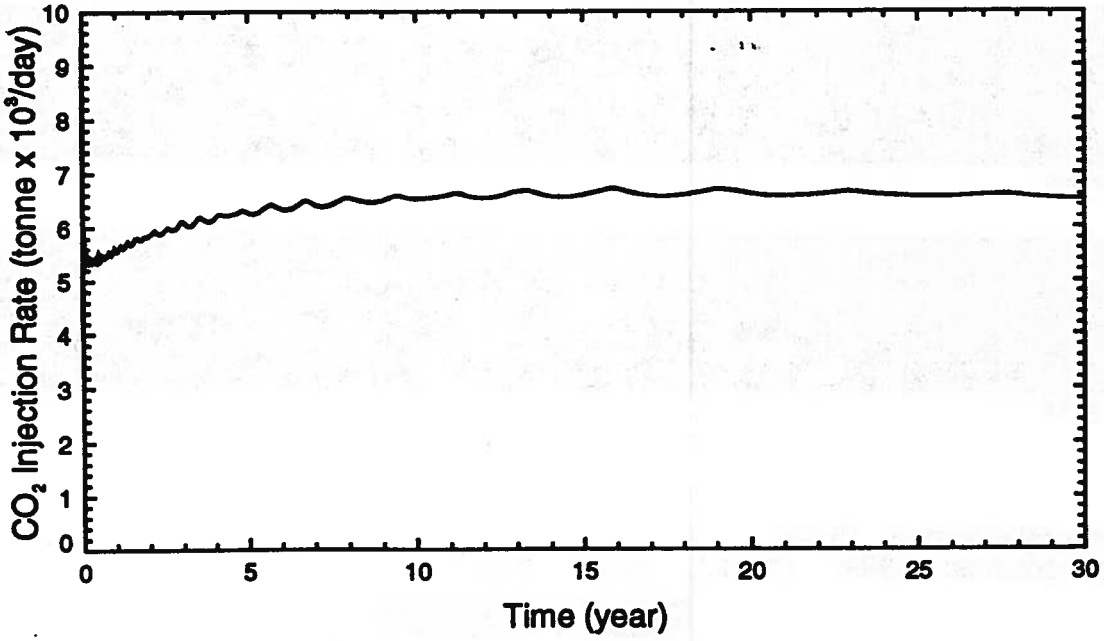

Carbon Dioxide Saturation (Run CO2_103)

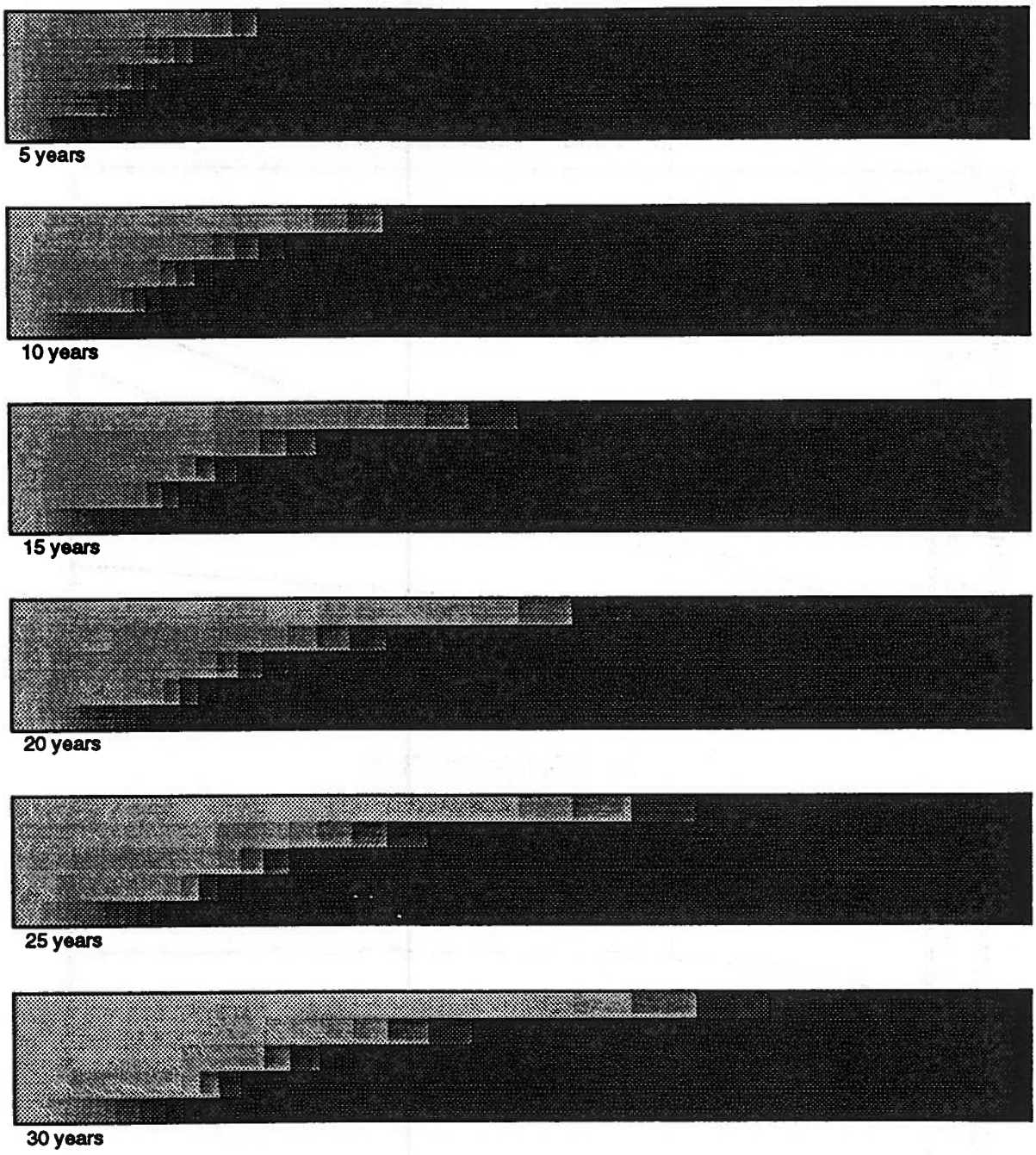

Vertical scale factor = 15.000
Field dimensions: 6999. (horiz.), 60.00 (vert.)

Nisku Carbonate Aquifer

NUMERICAL RUN (CO2_103)

Aquifer Porosity = 0.06 Aquifer Permeability = 30 md (horizontal)
Injection Pressure = 37.86 MPa

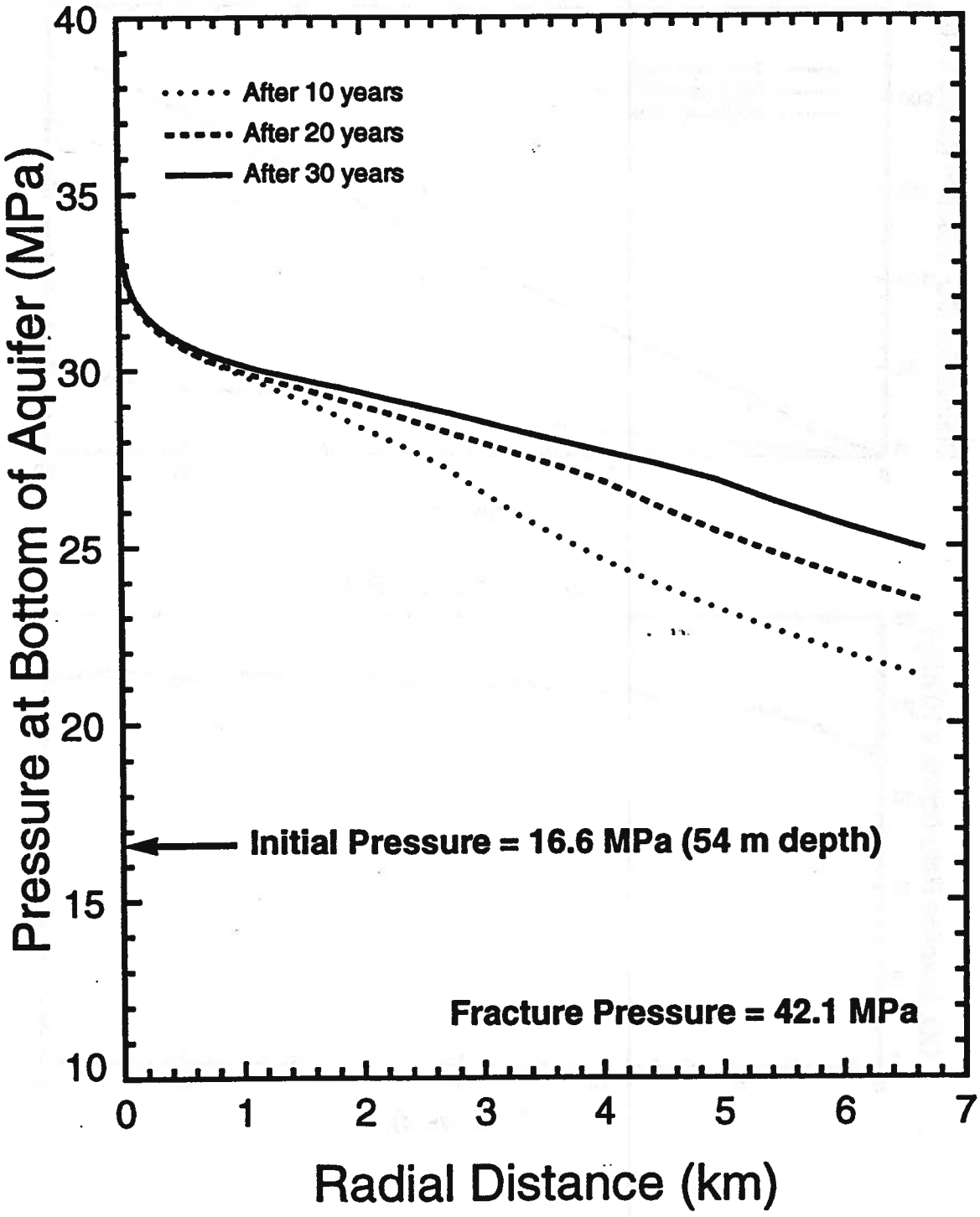

Nisku Carbonate Aquifer

NUMERICAL RUN (CO2_104)

Aquifer Porosity = 0.06 Aquifer Permeability = 100 md (horizontal)
Injection Pressure = 37.86 MPa

(a) Cumulative CO_2 Injection

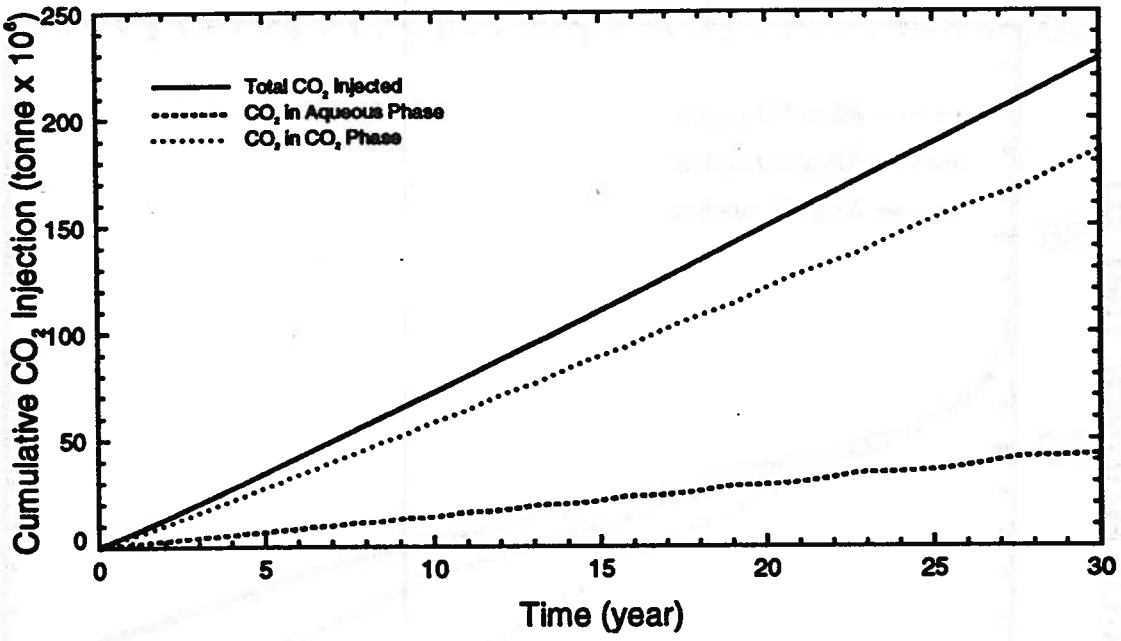

(b) CO_2 Injection Rate

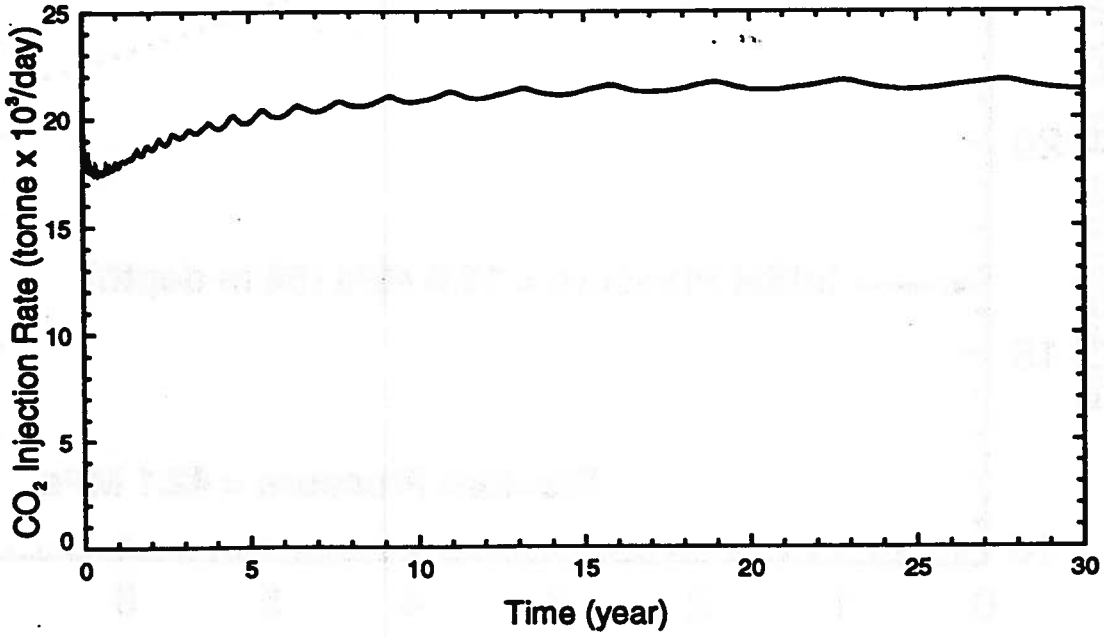

Carbon Dioxide Saturation (Run CO2_104)

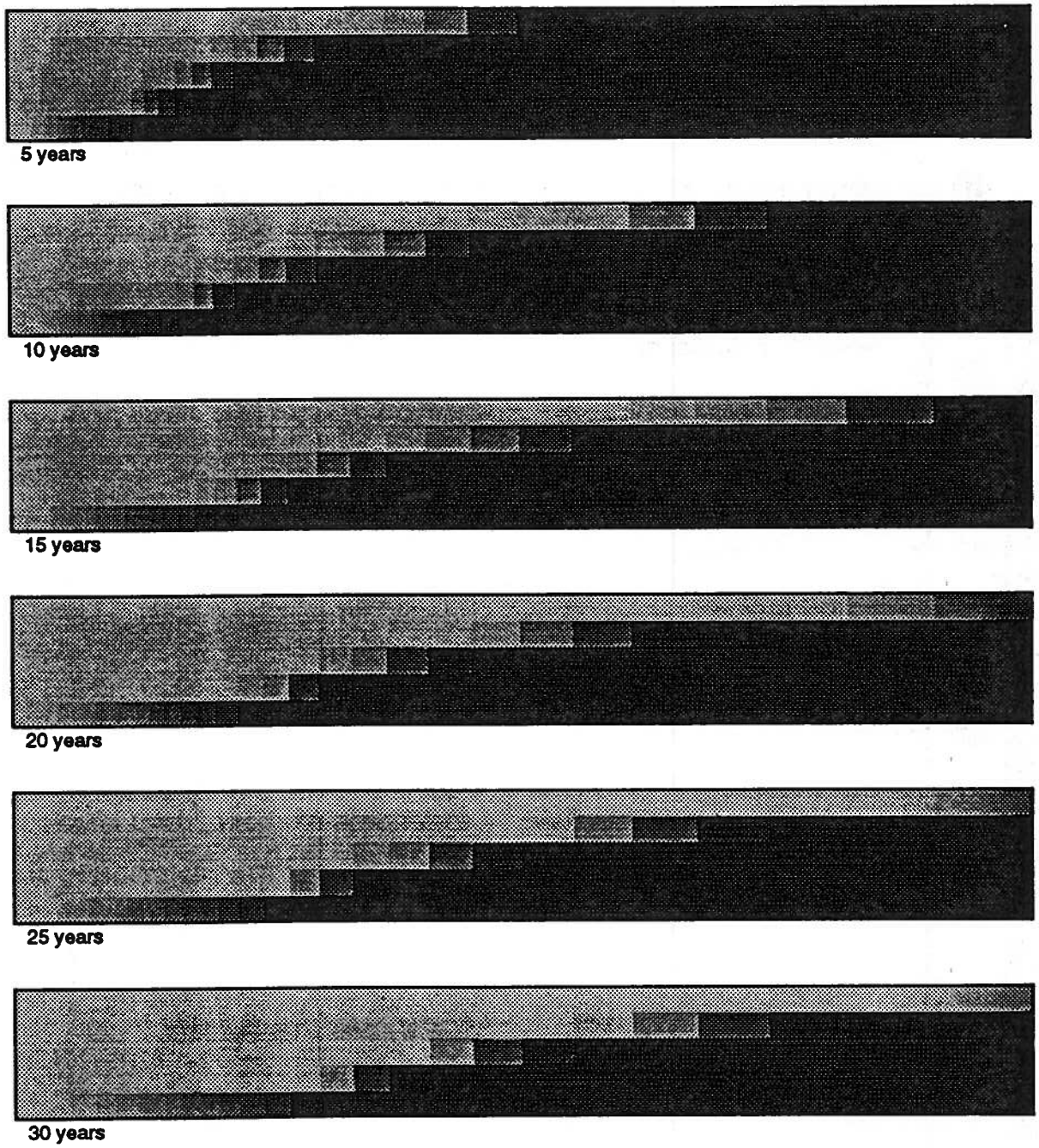

Vertical scale factor = 15.000
Field dimensions: 6999. (horiz.), 60.00 (vert.)

Nisku Carbonate Aquifer

NUMERICAL RUN (CO2_104)

Aquifer Porosity = 0.06 Aquifer Permeability = 100 md (horizontal)
Injection Pressure = 37.86 MPa

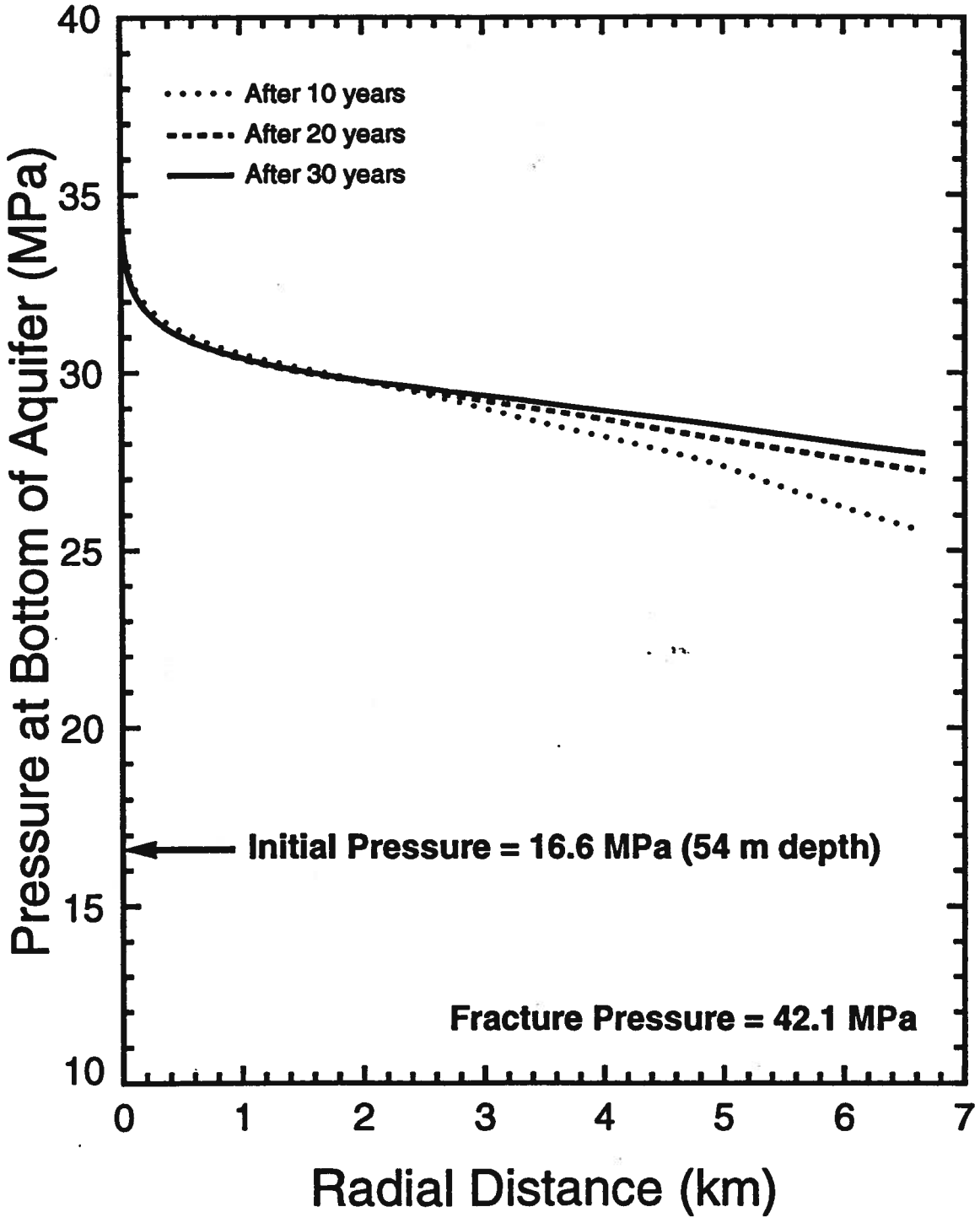

Nisku Carbonate Aquifer

NUMERICAL RUN (CO2_105)

Aquifer Porosity = 0.06 Aquifer Permeability = 400 md (horizontal)
Injection Pressure = 37.86 MPa

(a) Cumulative CO_2 Injection

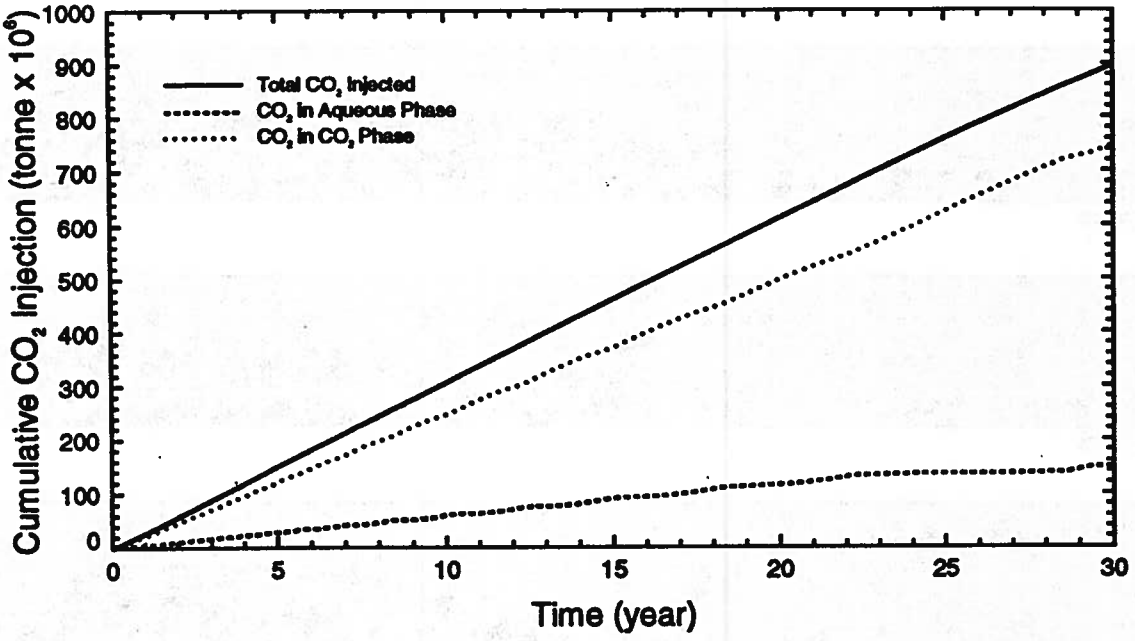

(b) CO_2 Injection Rate

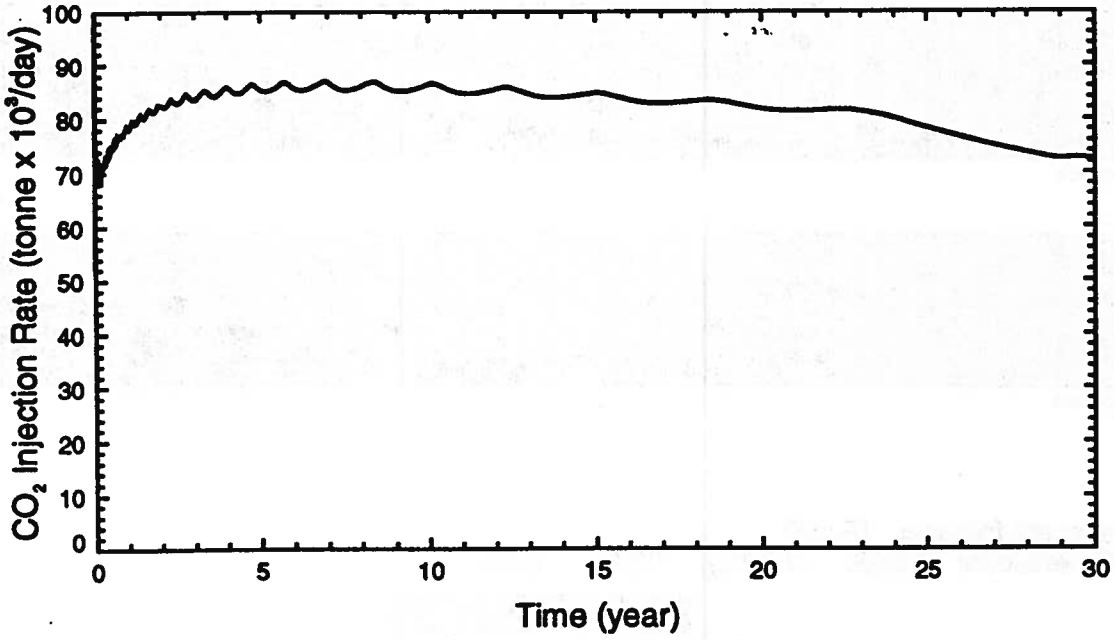

Carbon Dioxide Saturation (Run CO2_105)

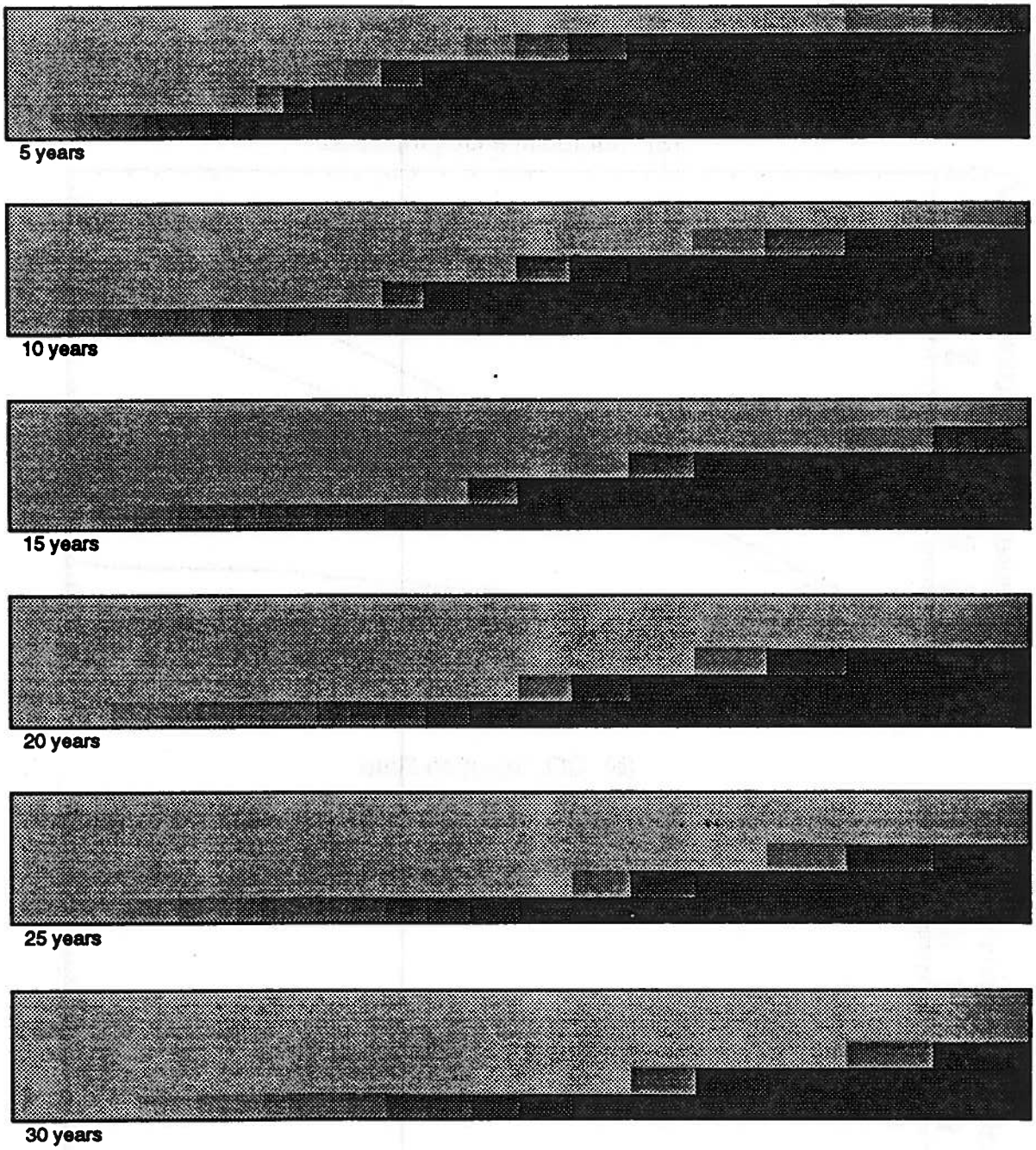

Vertical scale factor = 15.000
Field dimensions: 6999. (horiz.), 60.00 (vert.)

Nisku Carbonate Aquifer

NUMERICAL RUN (CO2_105)

Aquifer Porosity = 0.06 Aquifer Permeability = 400 md (horizontal)
Injection Pressure = 37.86 MPa

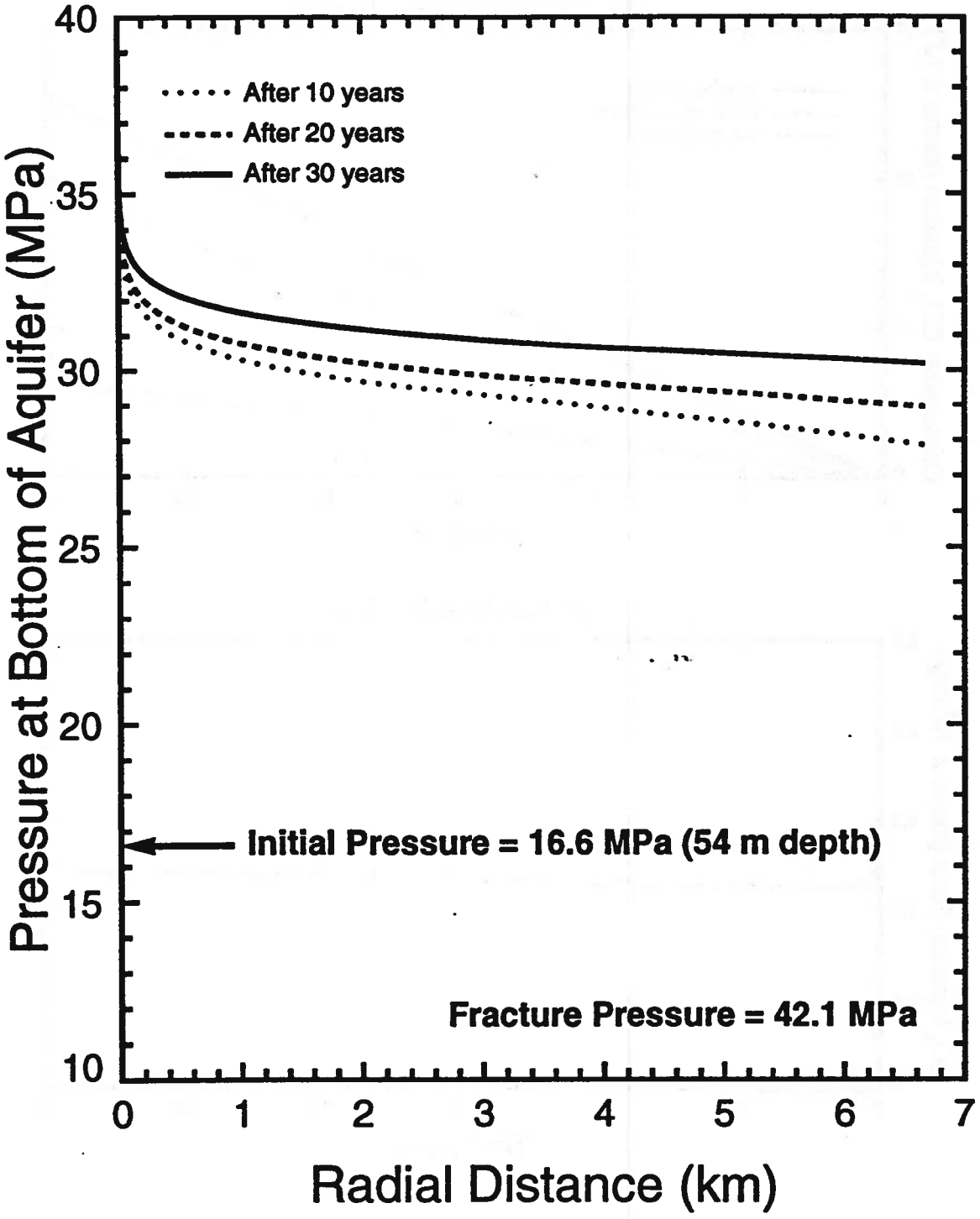

Nisku Carbonate Aquifer

NUMERICAL RUN (CO2_109)

Aquifer Porosity = 0.12 Aquifer Permeability = 6.2 md (horizontal)
Injection Pressure = 37.86 MPa

(a) Cumulative CO_2 Injection

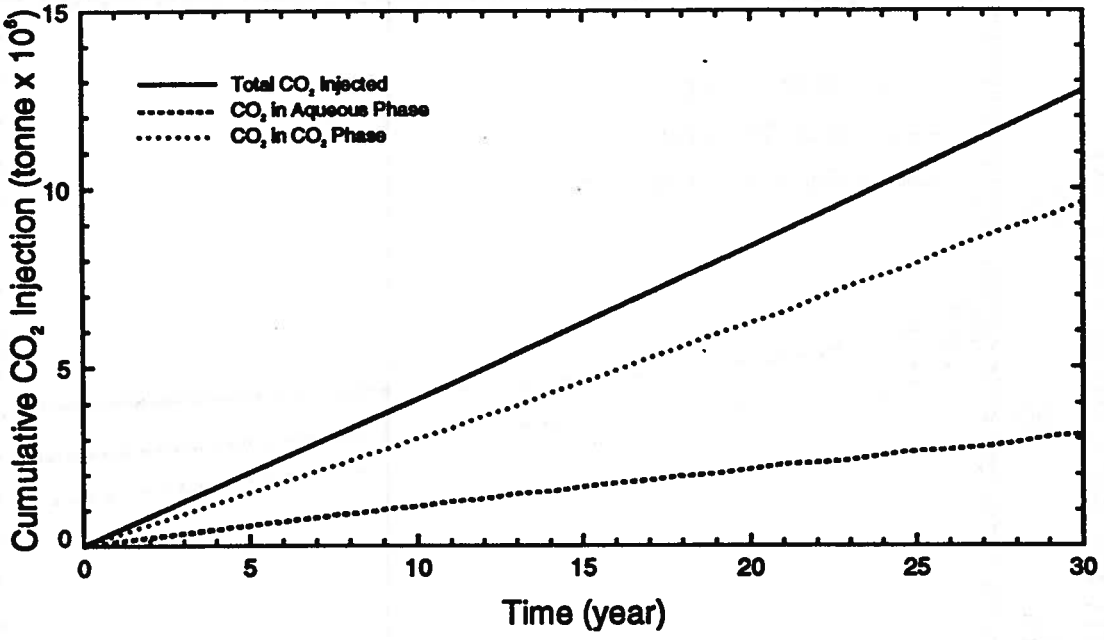

(b) CO_2 Injection Rate

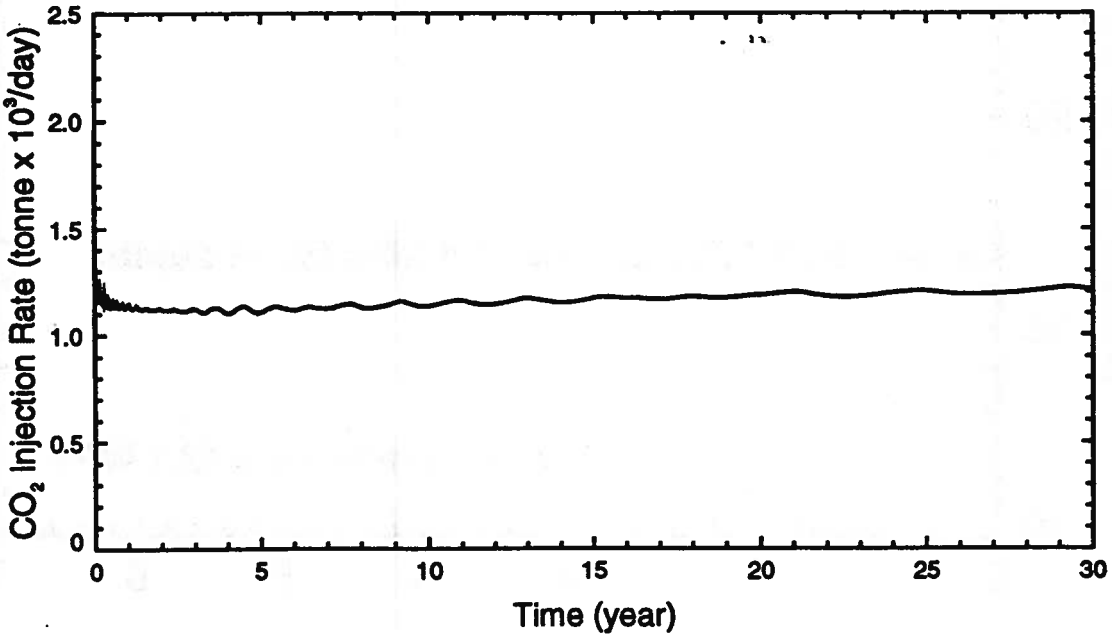

Carbon Dioxide Saturation (Run CO2_109)

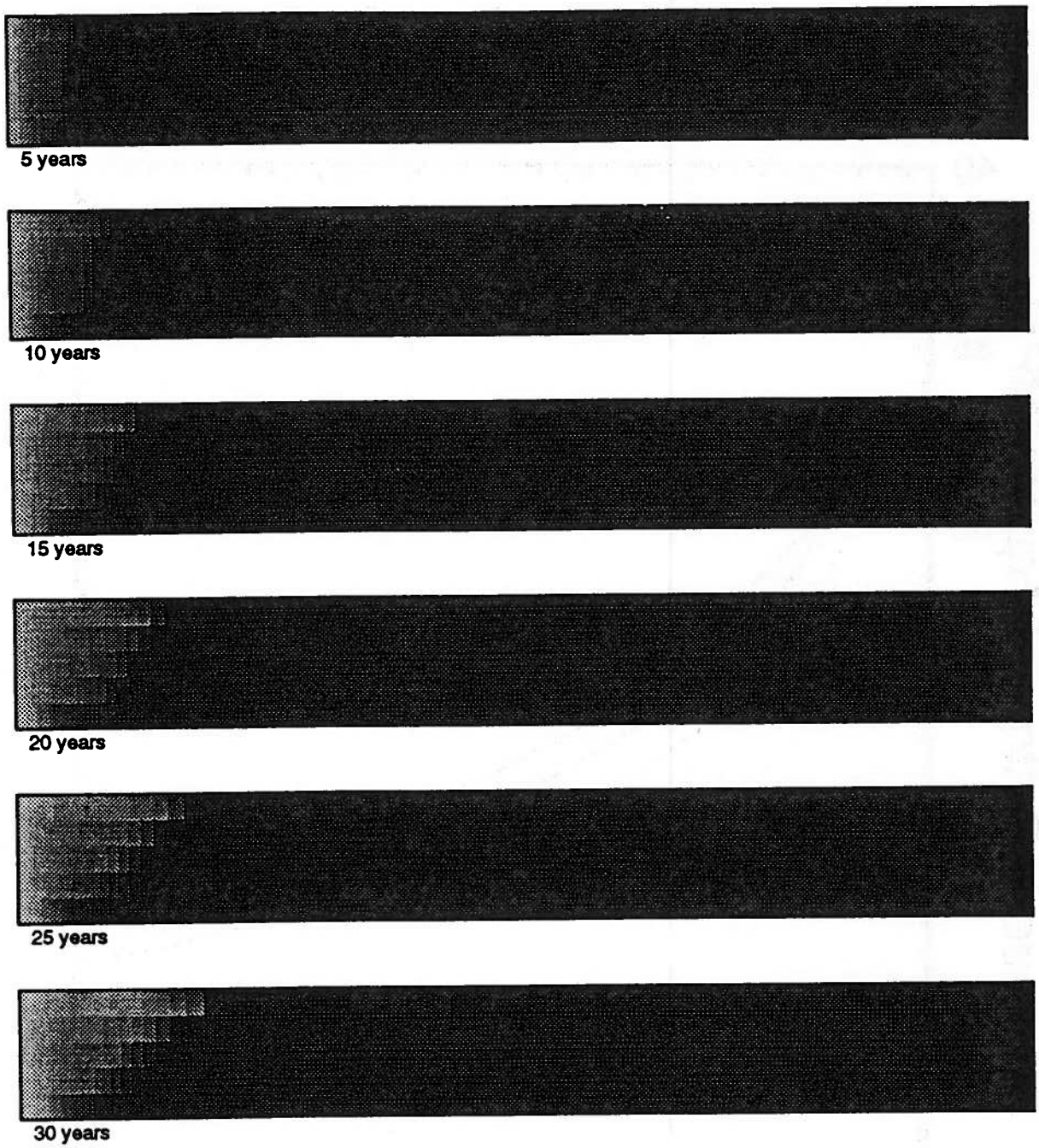

Vertical scale factor = 15.000
Field dimensions: 6999. (horiz.), 60.00 (vert.)

Nisku Carbonate Aquifer

NUMERICAL RUN (CO2_109)

Aquifer Porosity = 0.12 Aquifer Permeability = 6.2 md (horizontal)
Injection Pressure = 37.86 MPa

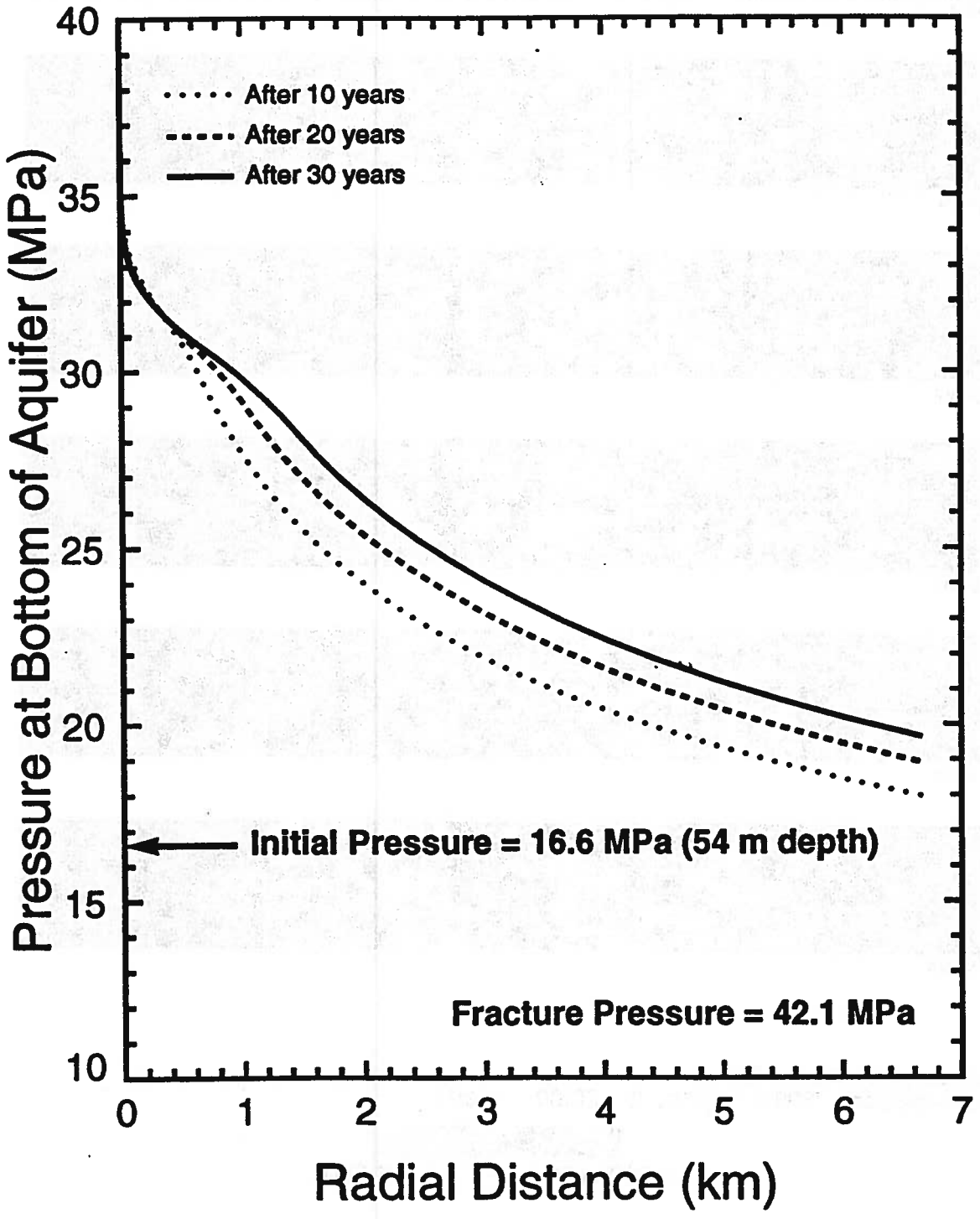

Nisku Carbonate Aquifer

NUMERICAL RUN (CO2_108)

Aquifer Porosity = 0.12 Aquifer Permeability = 30 md (horizontal)
Injection Pressure = 37.86 MPa

(a) Cumulative CO_2 Injection

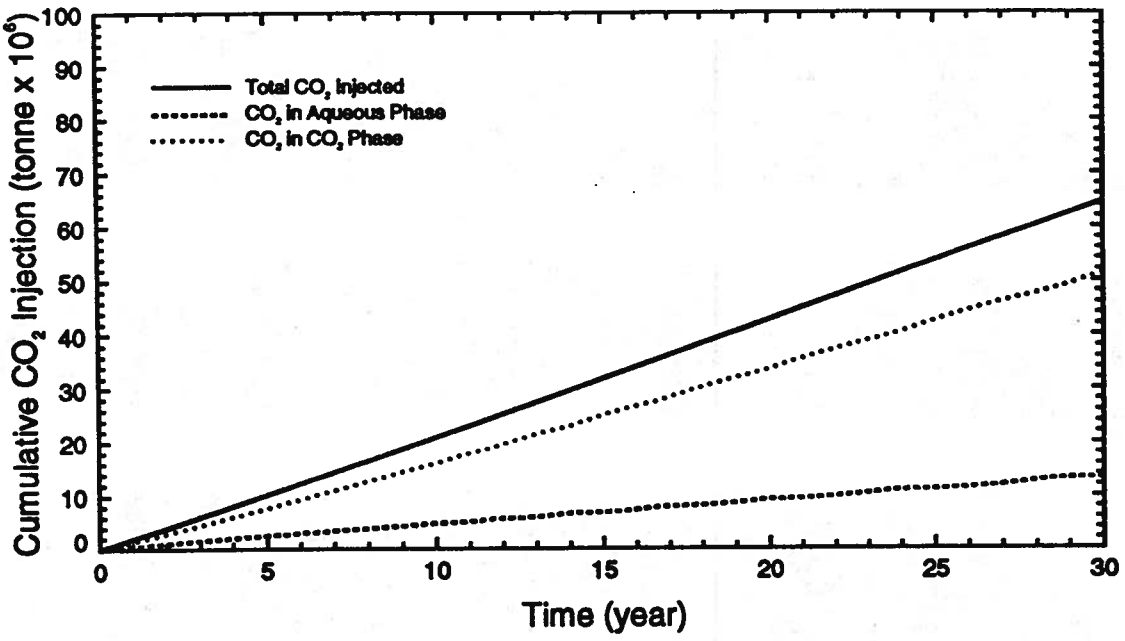

(b) CO_2 Injection Rate

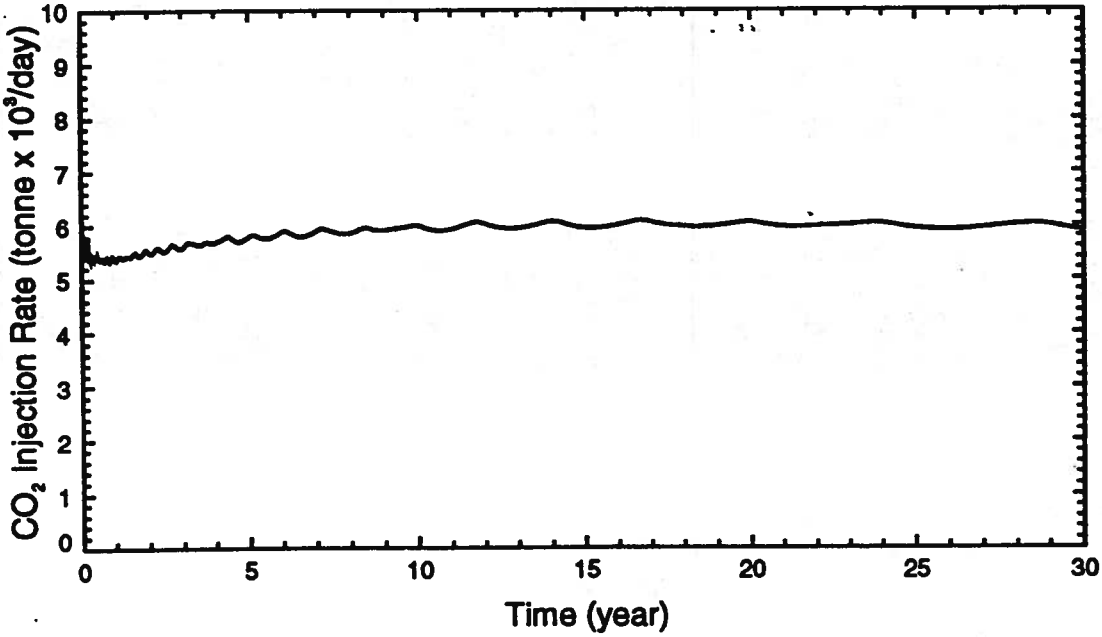

Carbon Dioxide Saturation (Run CO2_108)

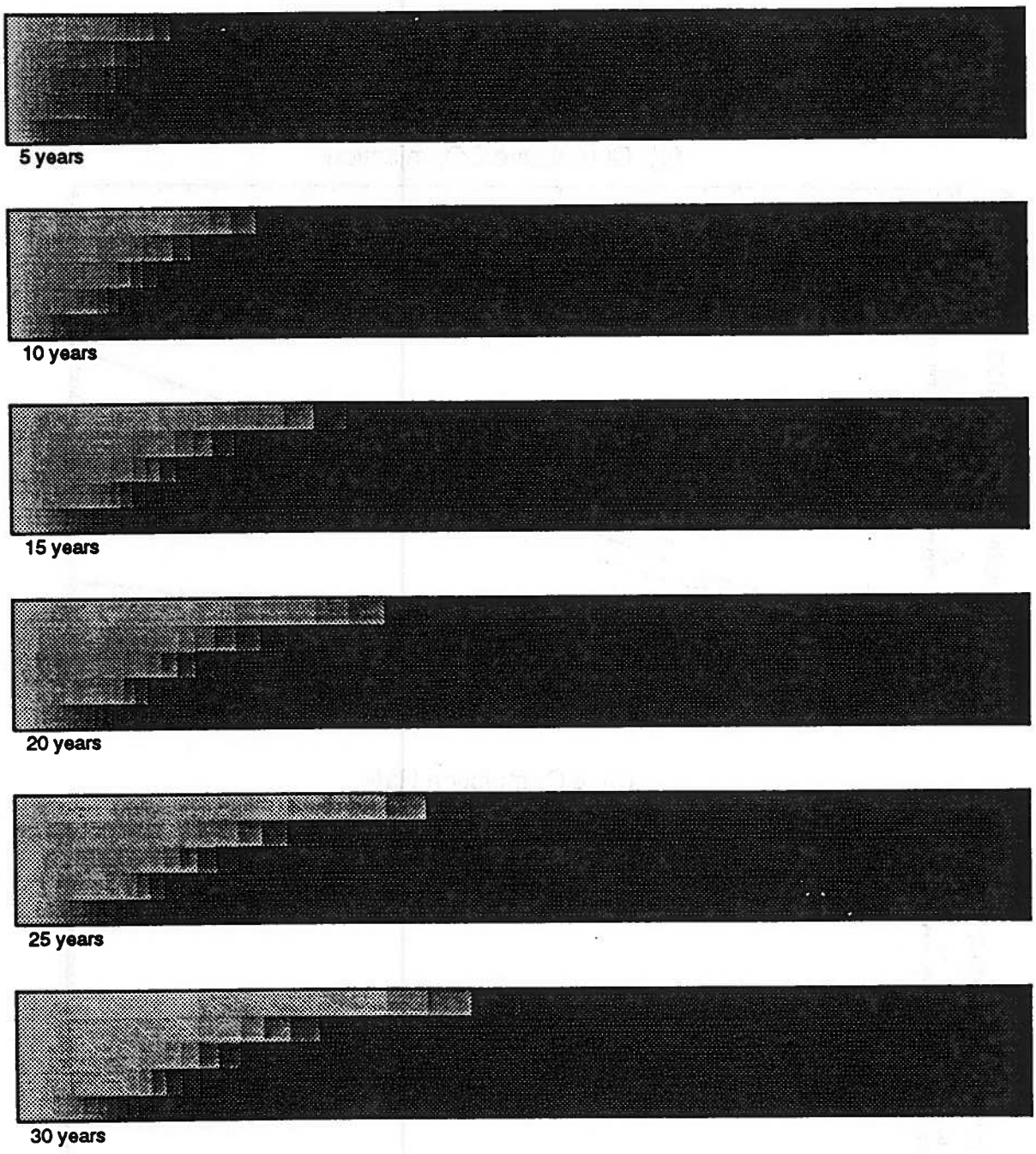

Vertical scale factor = 15.000
Field dimensions: 6999. (horiz.), 60.00 (vert.)

Nisku Carbonate Aquifer

NUMERICAL RUN (CO2_108)

Aquifer Porosity = 0.12 Aquifer Permeability = 30 md (horizontal)
Injection Pressure = 37.86 MPa

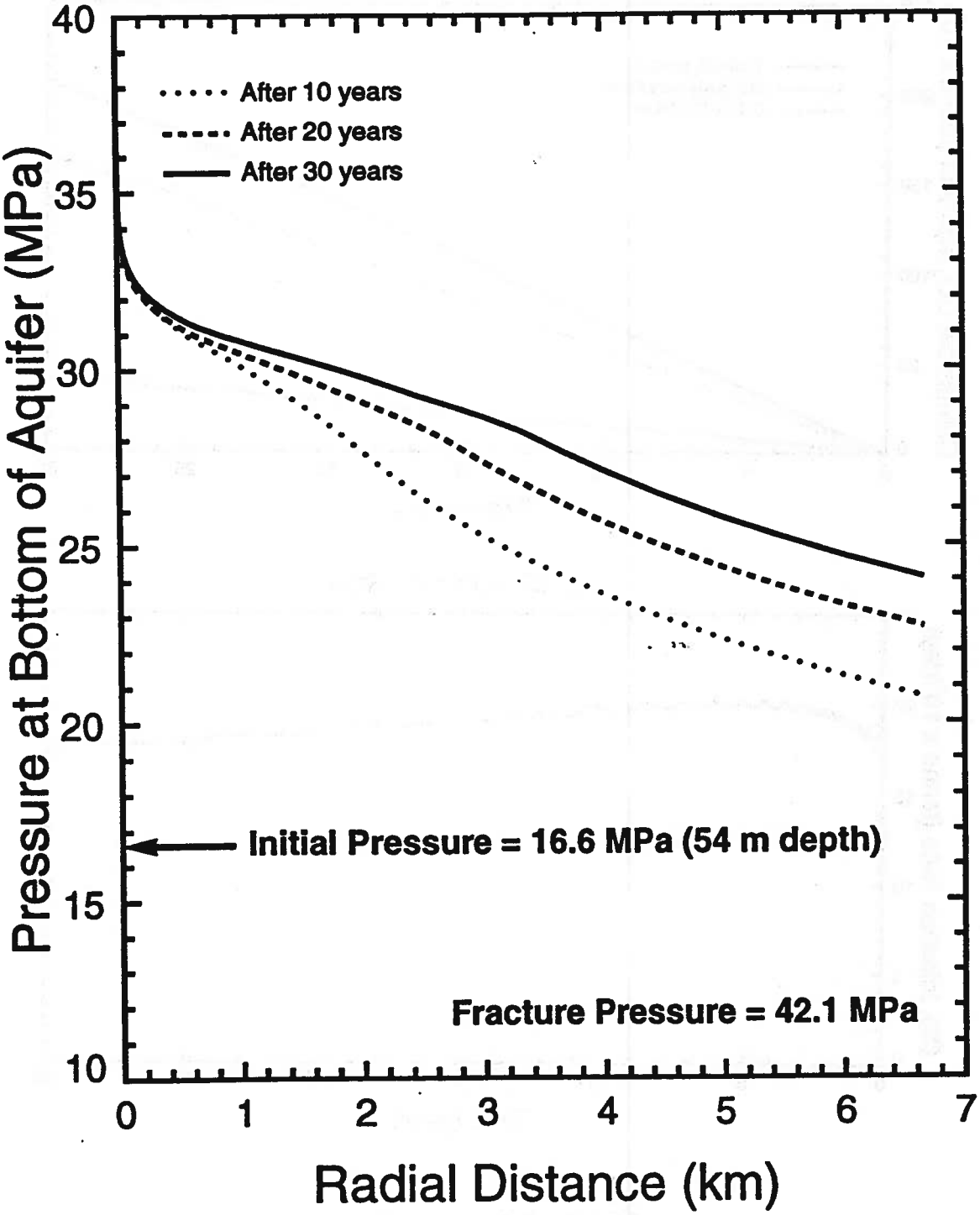

Nisku Carbonate Aquifer

NUMERICAL RUN (CO2_107)

Aquifer Porosity = 0.12 Aquifer Permeability = 100 md (horizontal)
Injection Pressure = 37.86 MPa

(a) Cumulative CO_2 Injection

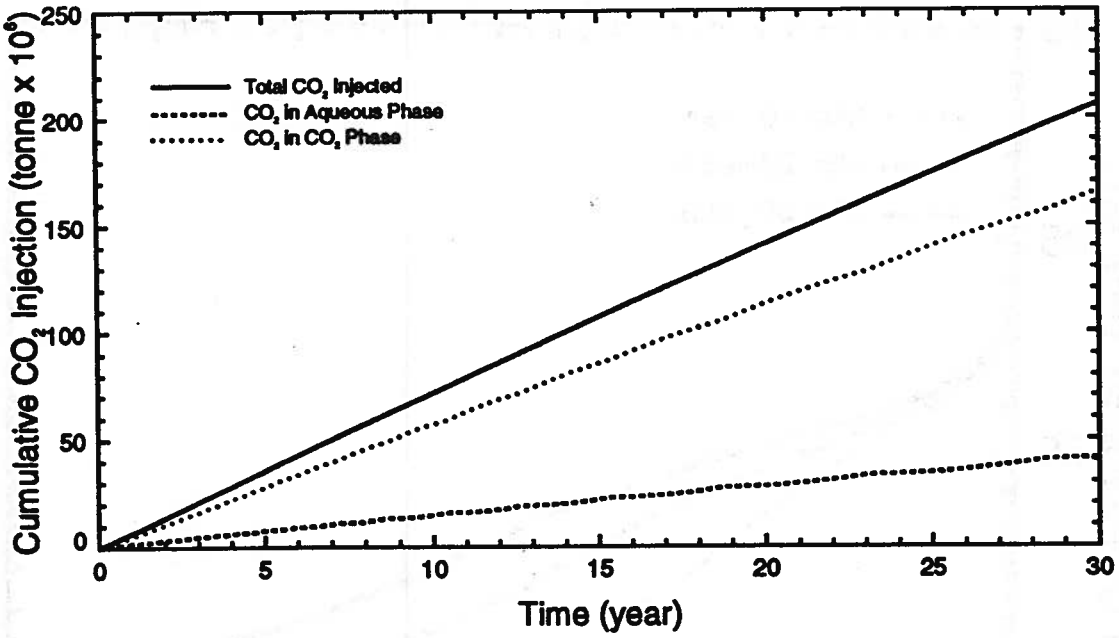

(b) CO_2 Injection Rate

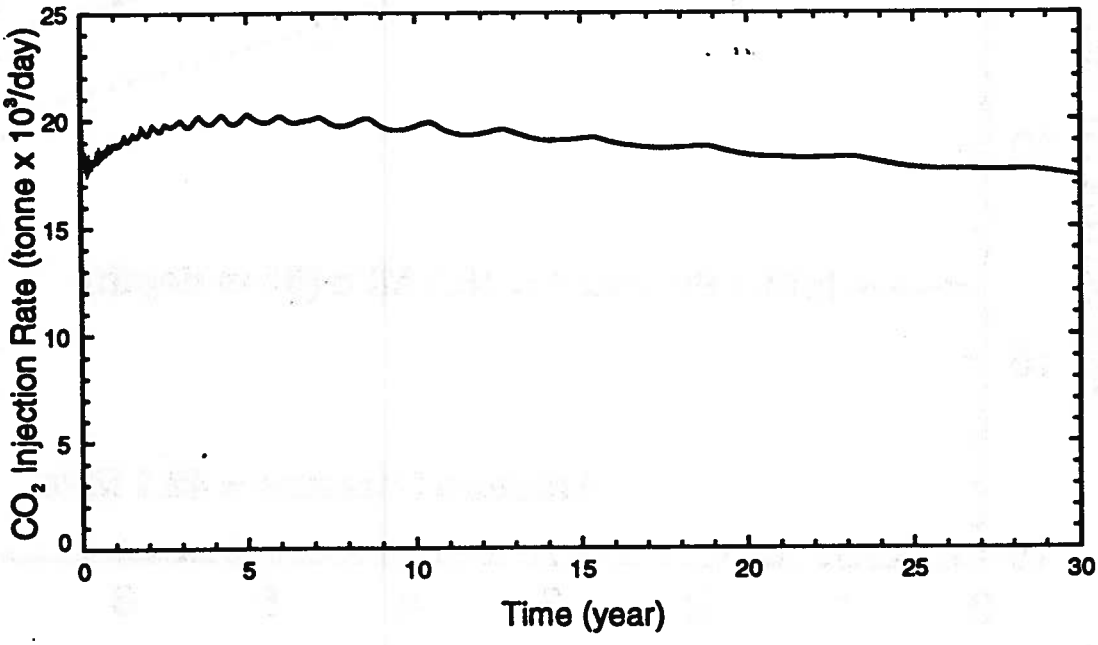

Carbon Dioxide Saturation (Run CO2_107)

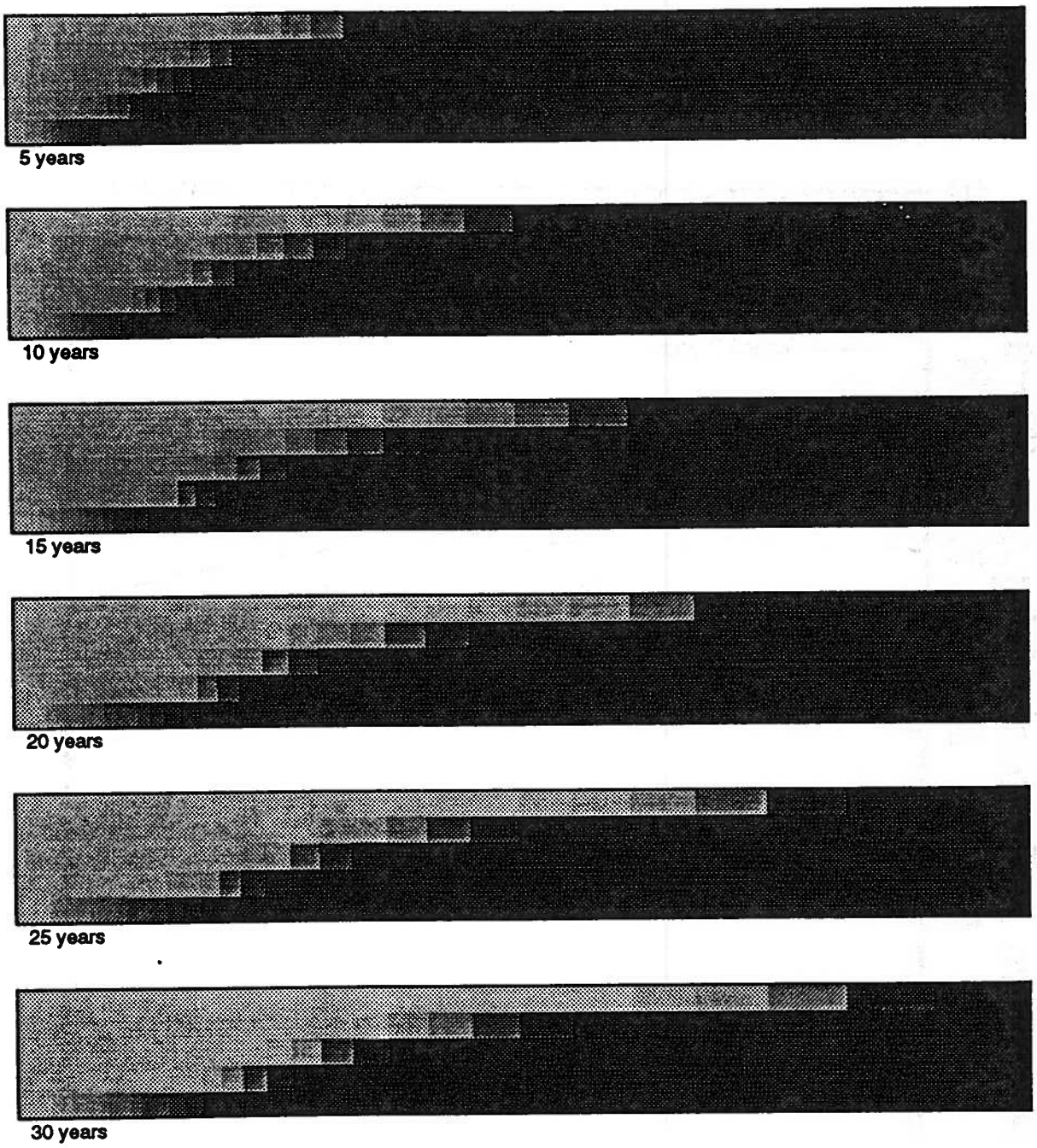

Vertical scale factor = 15.000
Field dimensions: 6999. (horiz.), 60.00 (vert.)

Nisku Carbonate Aquifer

NUMERICAL RUN (CO2_107)

Aquifer Porosity = 0.12 Aquifer Permeability = 100 md (horizontal)
Injection Pressure = 37.86 MPa

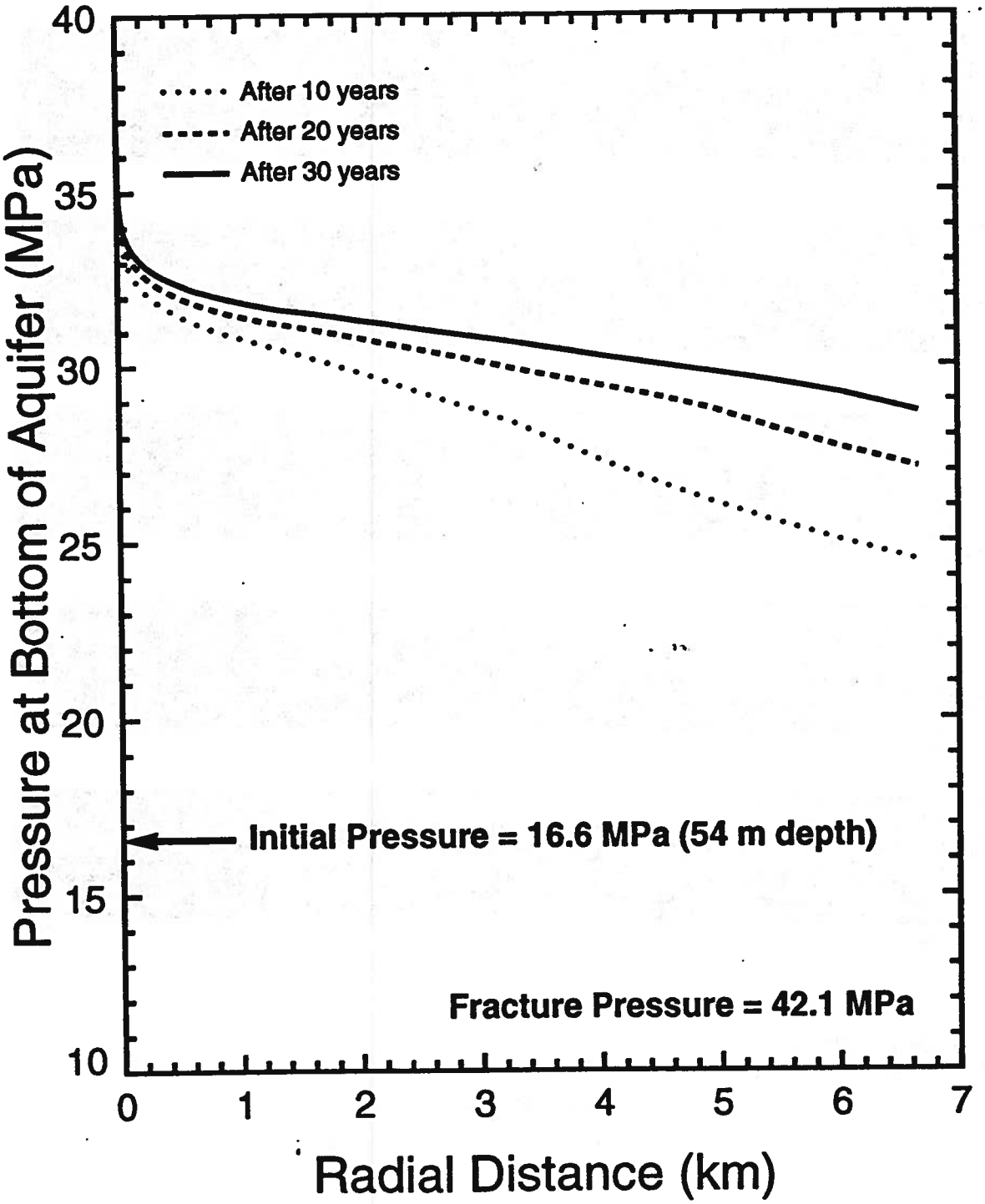

Nisku Carbonate Aquifer

NUMERICAL RUN (CO2_106)

Aquifer Porosity = 0.12 Aquifer Permeability = 400 md (horizontal)
Injection Pressure = 37.86 MPa

(a) Cumulative CO_2 Injection

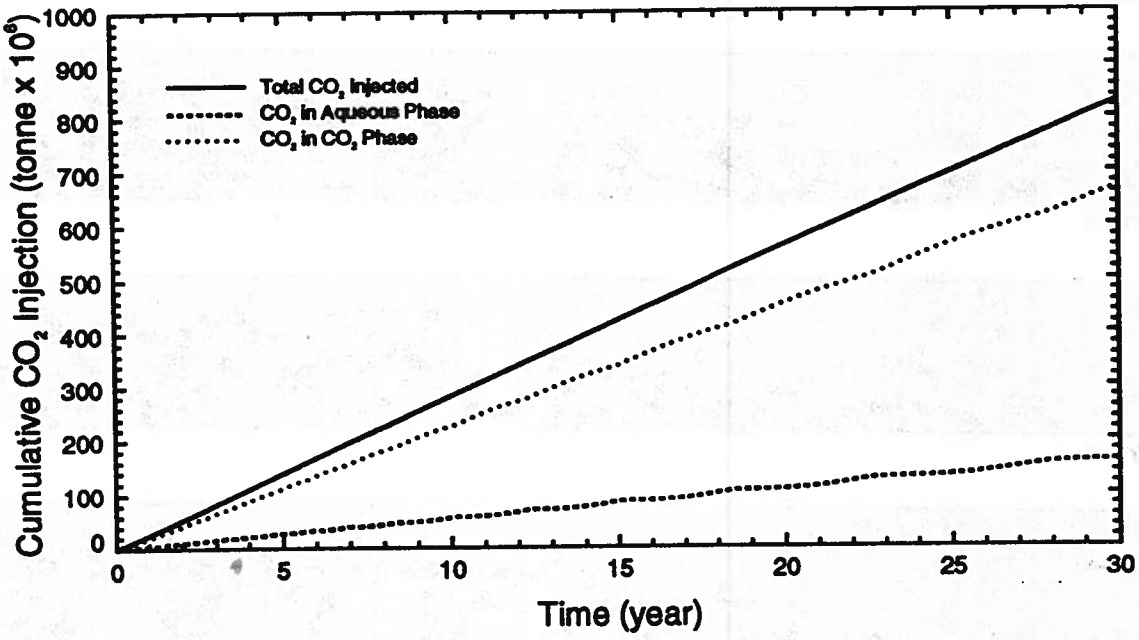

(b) CO_2 Injection Rate

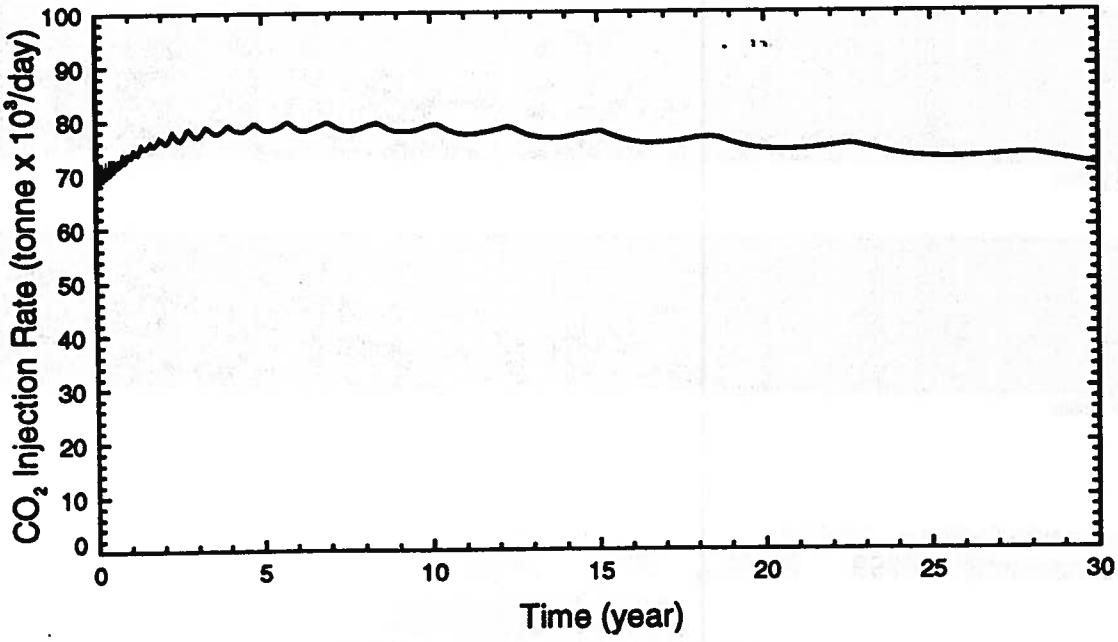

Carbon Dioxide Saturation (Run CO2_106)

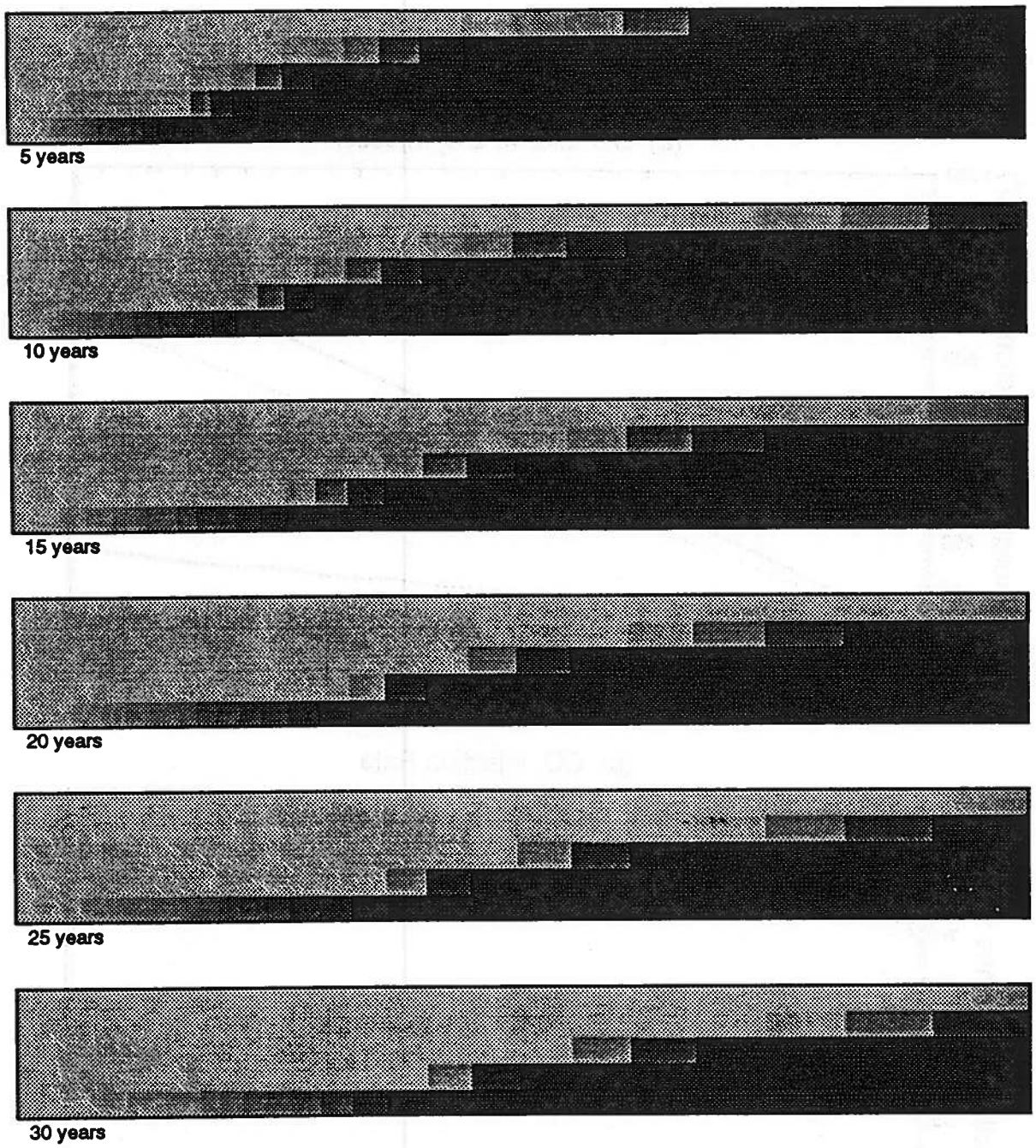

Vertical scale factor = 15.000
Field dimensions: 6999. (horiz.), 60.00 (vert.)

Nisku Carbonate Aquifer

NUMERICAL RUN (CO2_106)

Aquifer Porosity = 0.12 Aquifer Permeability = 400 md (horizontal)
Injection Pressure = 37.86 MPa

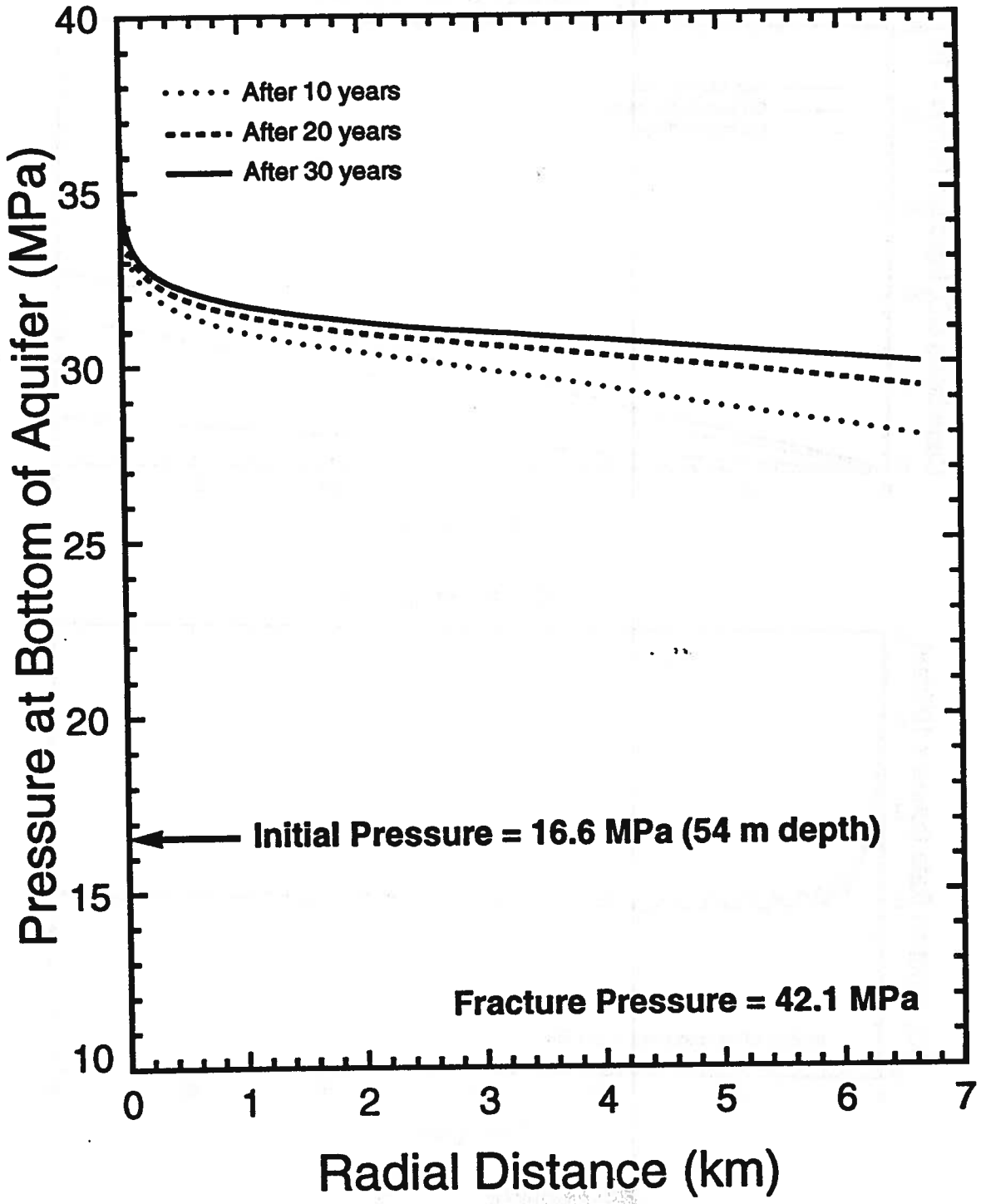

Nisku Carbonate Aquifer

NUMERICAL RUN (CO2_110)

Aquifer Porosity = 0.12 Aquifer Permeability = 100/6.2 md (horizontal)
Injection Pressure = 37.86 MPa

(a) Cumulative CO_2 Injection

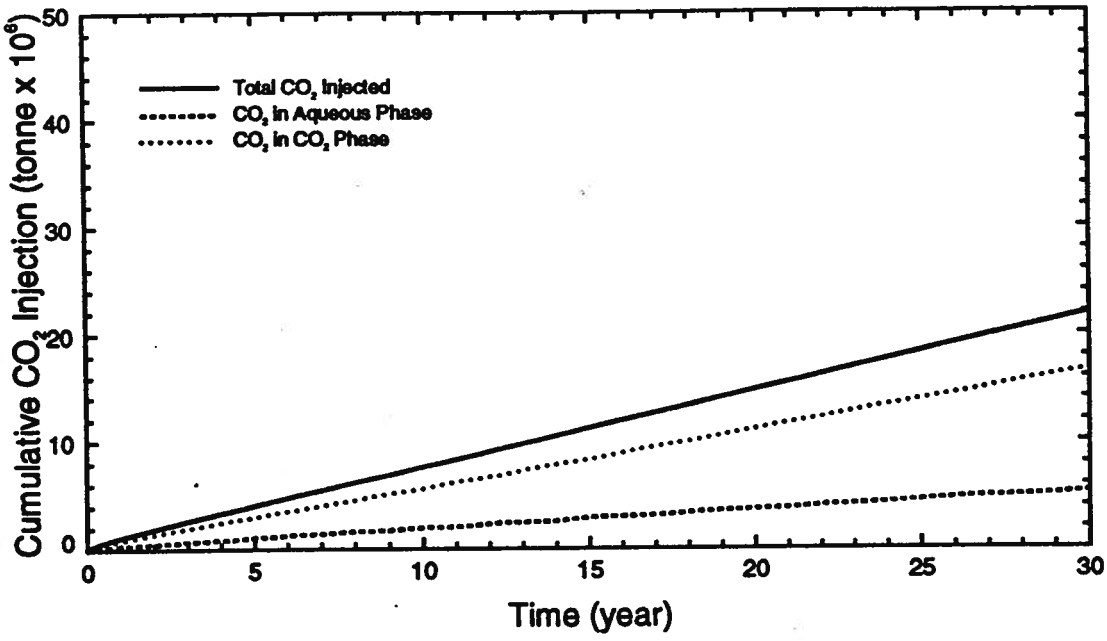

(b) CO_2 Injection Rate

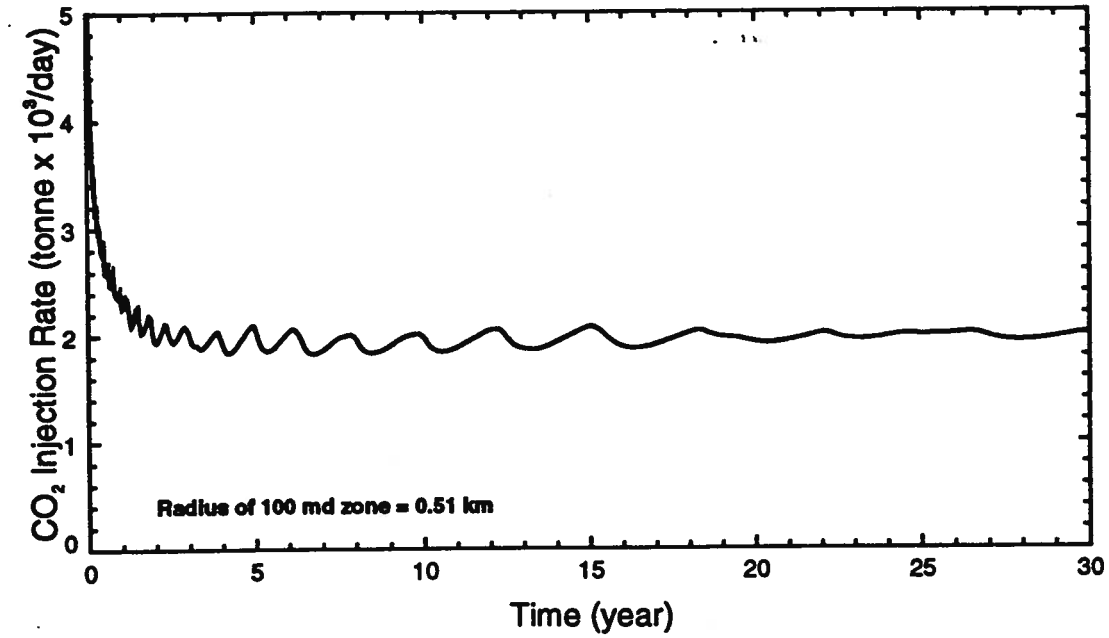

Carbon Dioxide Saturation (Run CO2_110)

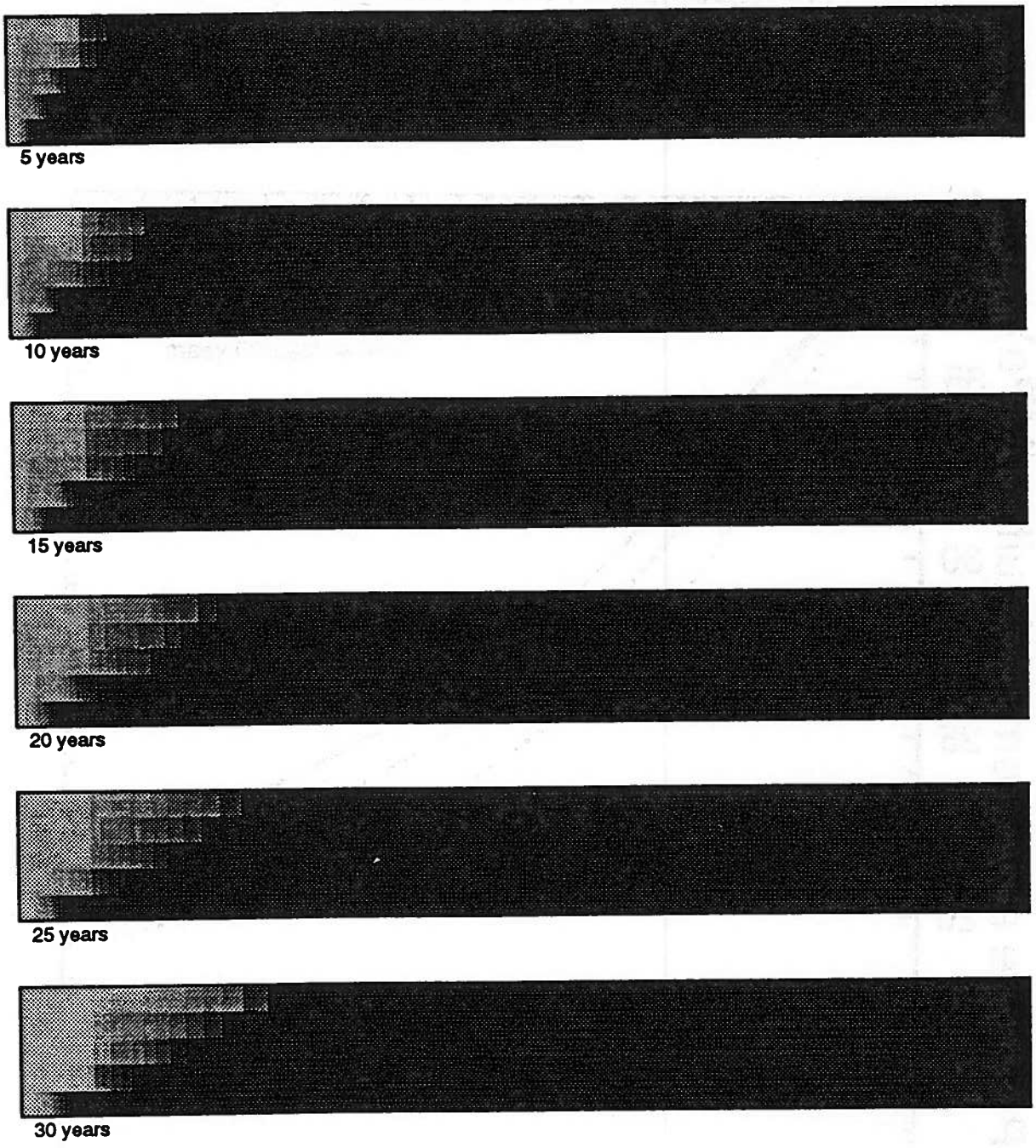

Vertical scale factor = 15.000
Field dimensions: 6999. (horiz.), 60.00 (vert.)

Nisku Carbonate Aquifer

NUMERICAL RUN (CO2_110)

Aquifer Porosity = 0.12 Aquifer Permeability = 100/6.2 md (horizontal)
Injection Pressure = 37.86 MPa Radius of 100 md zone = 0.51 km

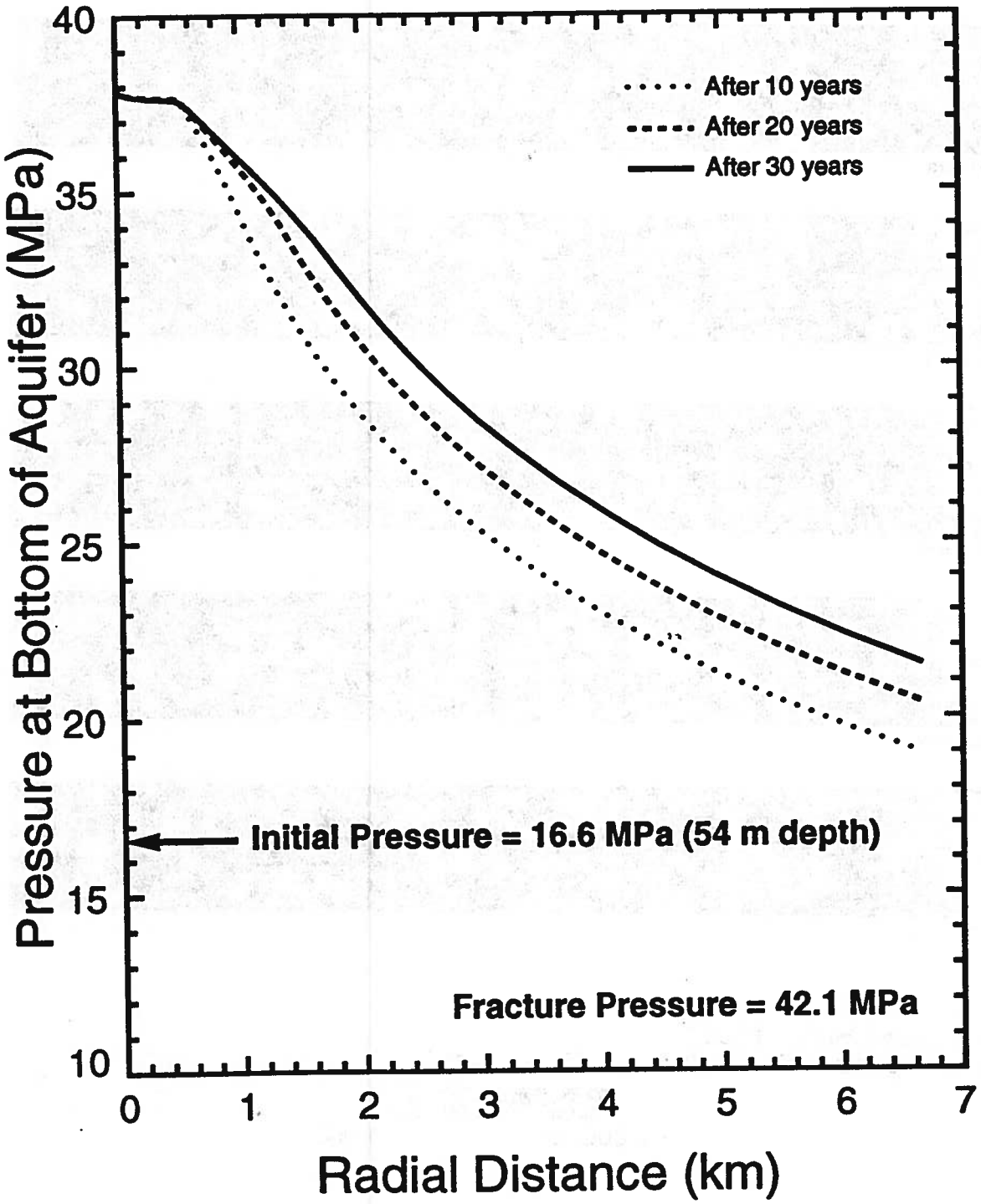

Nisku Carbonate Aquifer

NUMERICAL RUN (CO2_111)

Aquifer Porosity = 0.12 Aquifer Permeability = 100/6.2 md (horizontal)
Injection Pressure = 37.86 MPa

(a) Cumulative CO_2 Injection

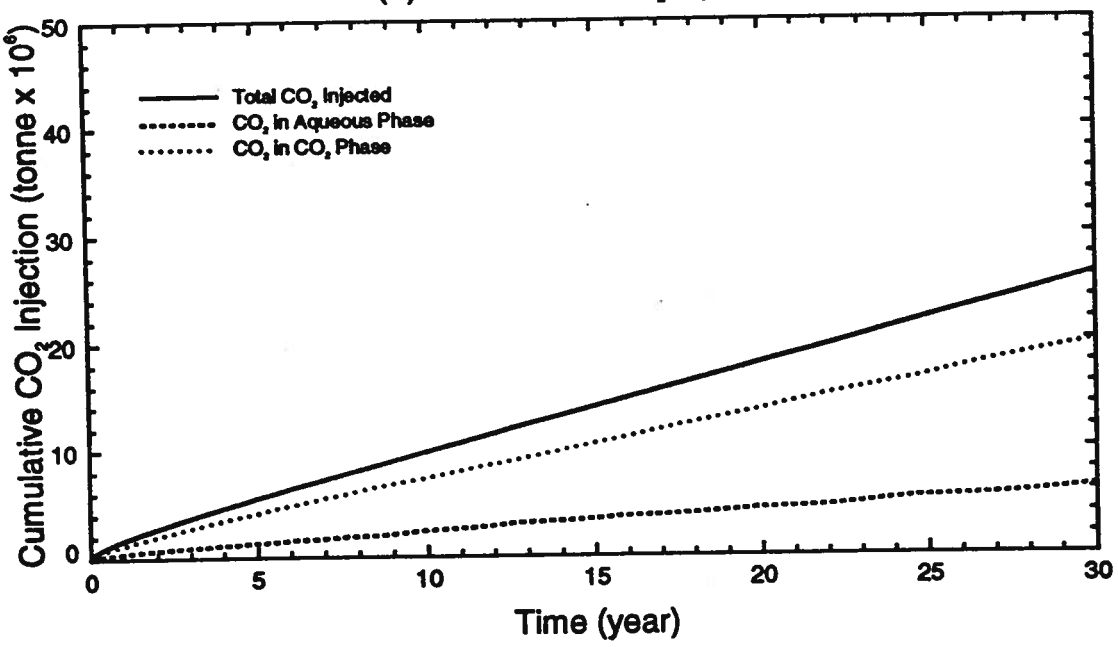

(b) CO_2 Injection Rate

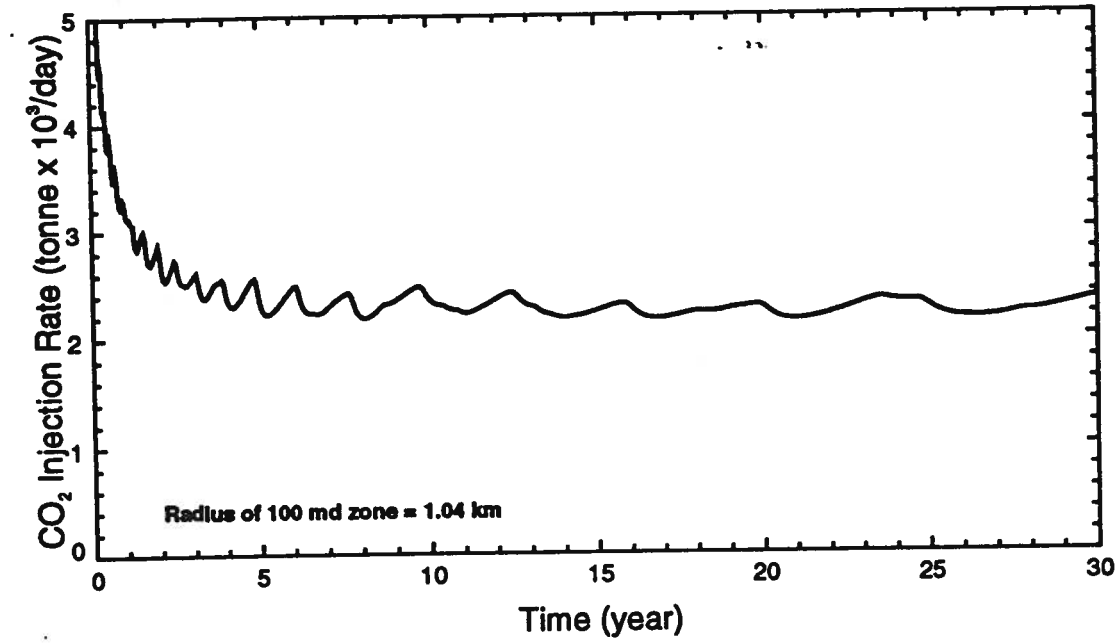

Carbon Dioxide Saturation (Run CO2_111)

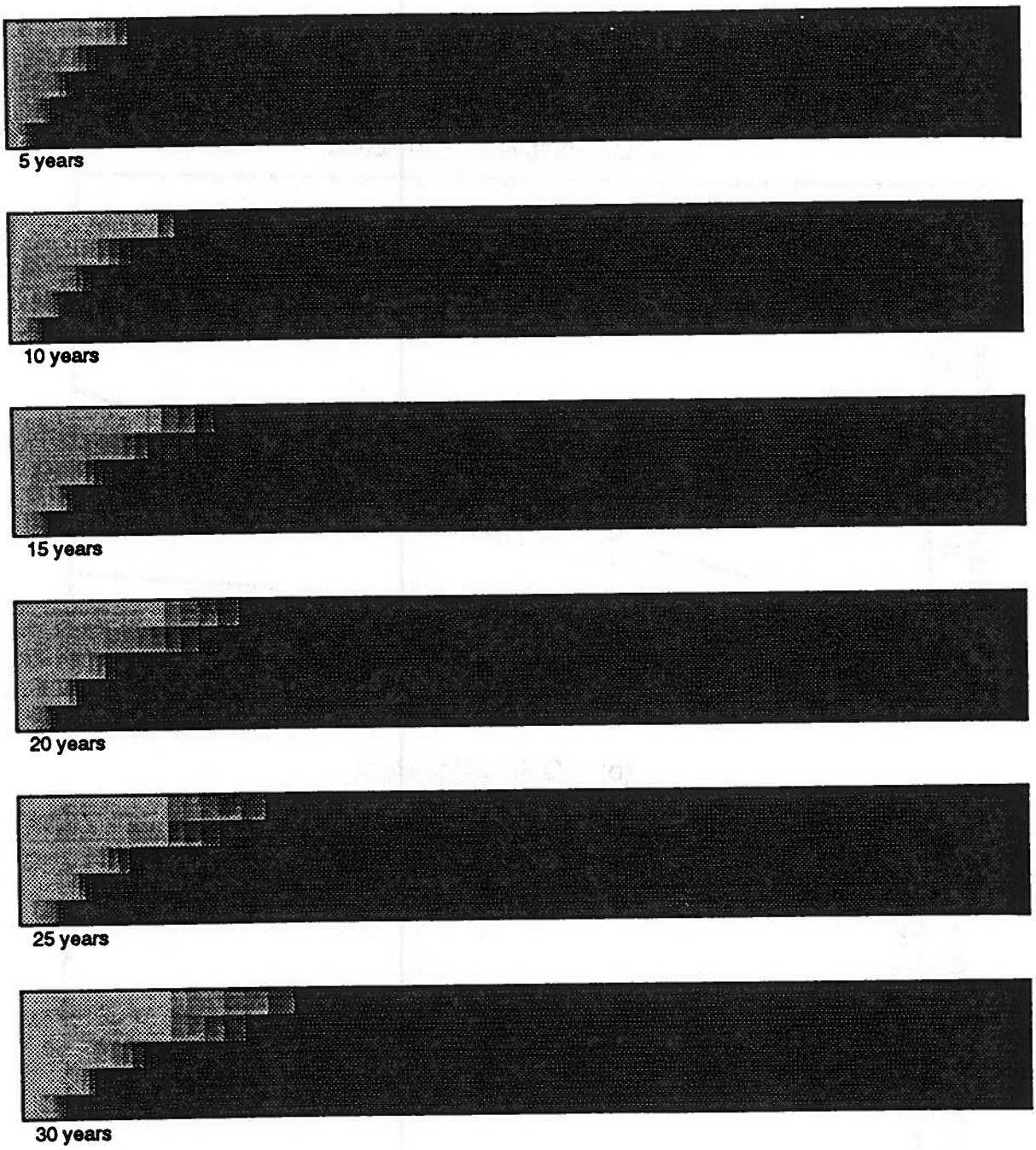

Vertical scale factor = 15.000
Field dimensions: 6999. (horiz.), 60.00 (vert.)

Nisku Carbonate Aquifer

NUMERICAL RUN (CO2_111)

Aquifer Porosity = 0.12 Aquifer Permeability = 100/6.2 md (horizontal)
Injection Pressure = 37.86 MPa Radius of 100 md zone = 1.04 km

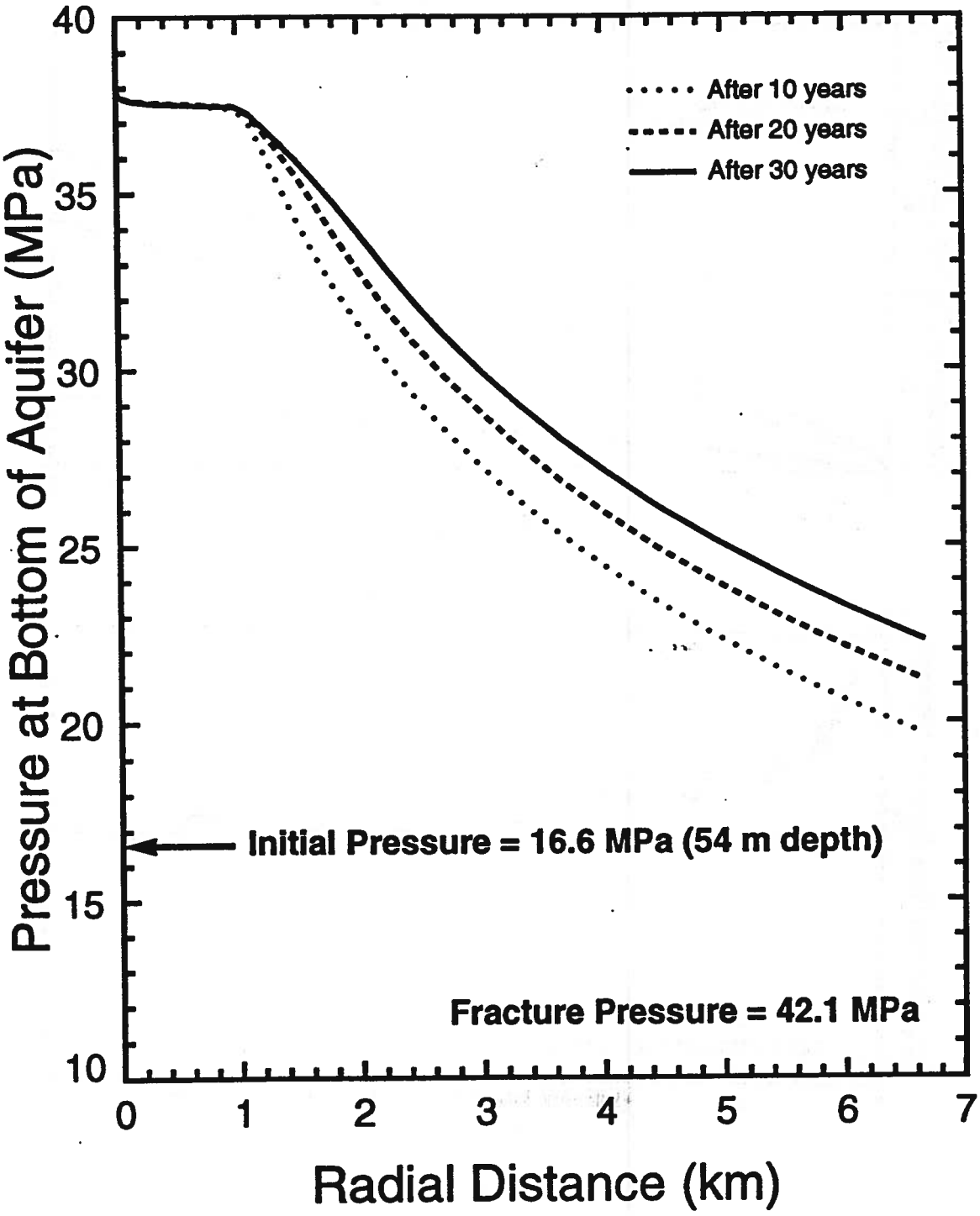

Nisku Carbonate Aquifer

NUMERICAL RUN (CO2_112)

Aquifer Porosity = 0.12 Aquifer Permeability = 100/6.2 md (horizontal)
Injection Pressure = 37.86 MPa

(a) Cumulative CO_2 Injection

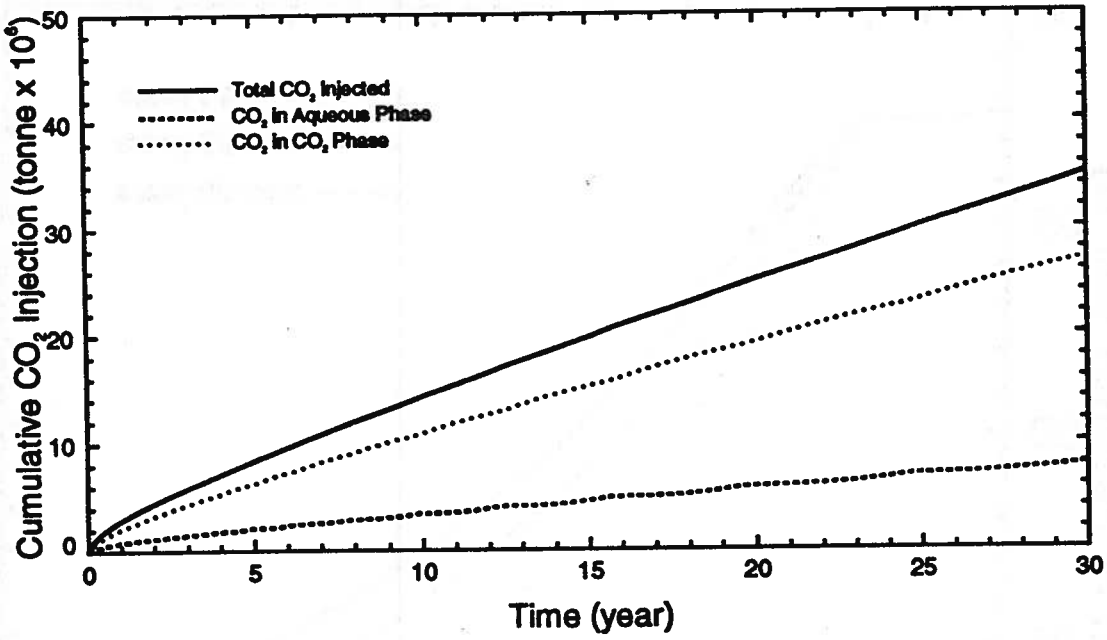

(b) CO_2 Injection Rate

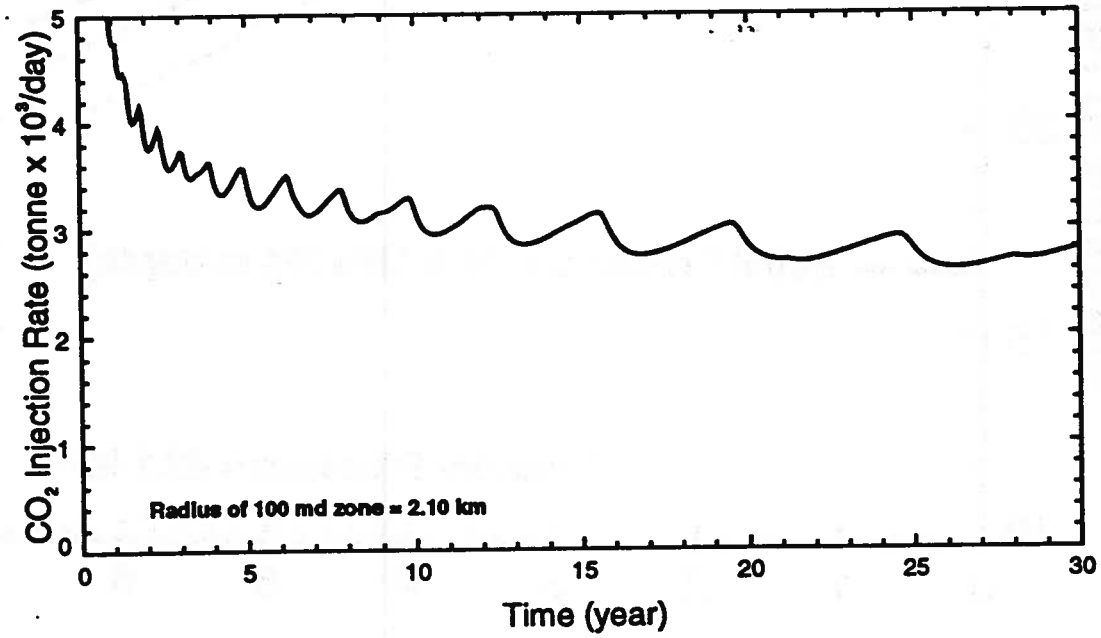

Carbon Dioxide Saturation (Run CO2_112)

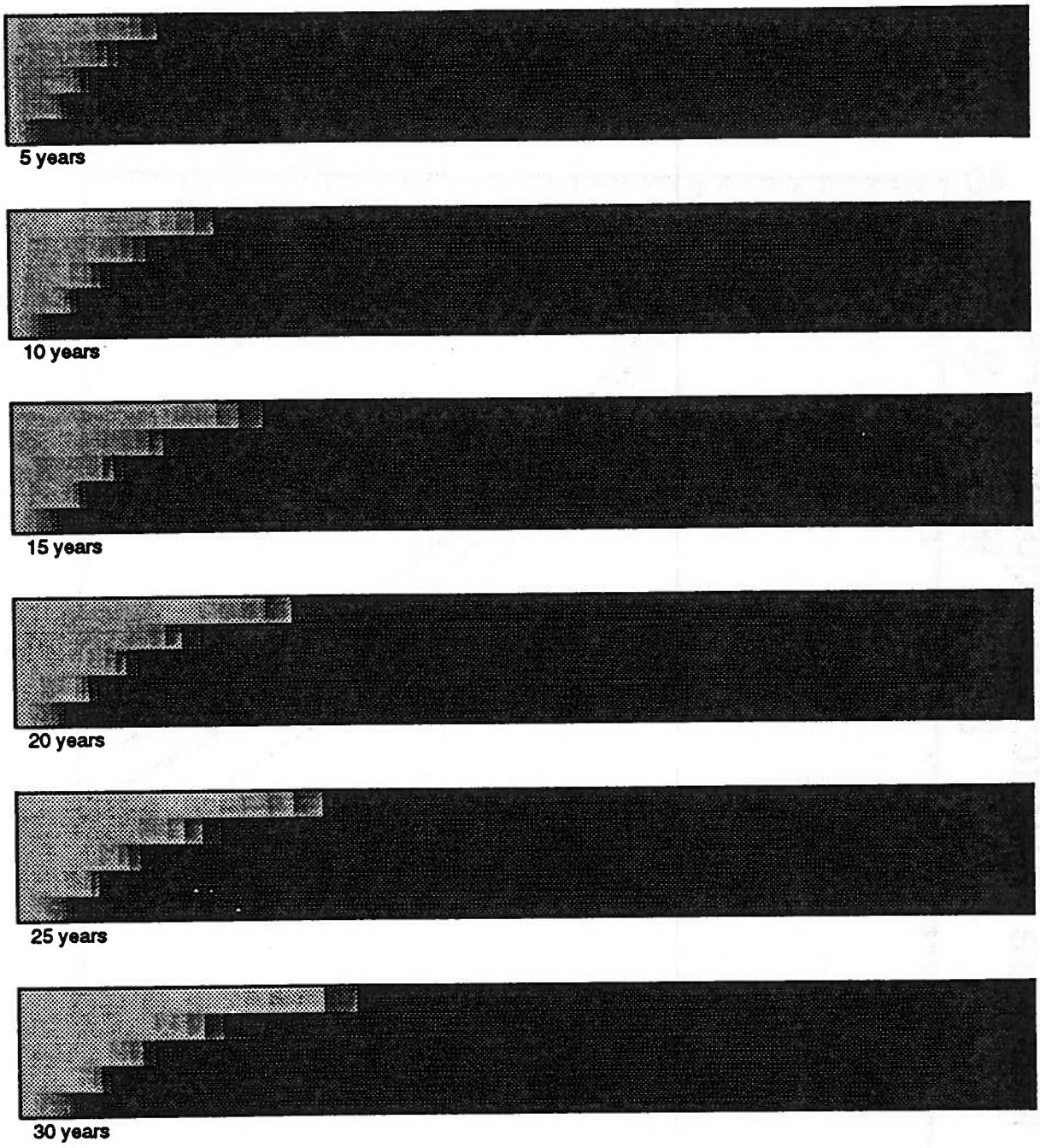

Vertical scale factor = 15.000
Field dimensions: 6999. (horiz.), 60.00 (vert.)

Nisku Carbonate Aquifer

NUMERICAL RUN (CO2_112)

Aquifer Porosity = 0.12 Aquifer Permeability = 100/6.2 md (horizontal)
Injection Pressure = 37.86 MPa Radius of 100 md zone = 2.10 km

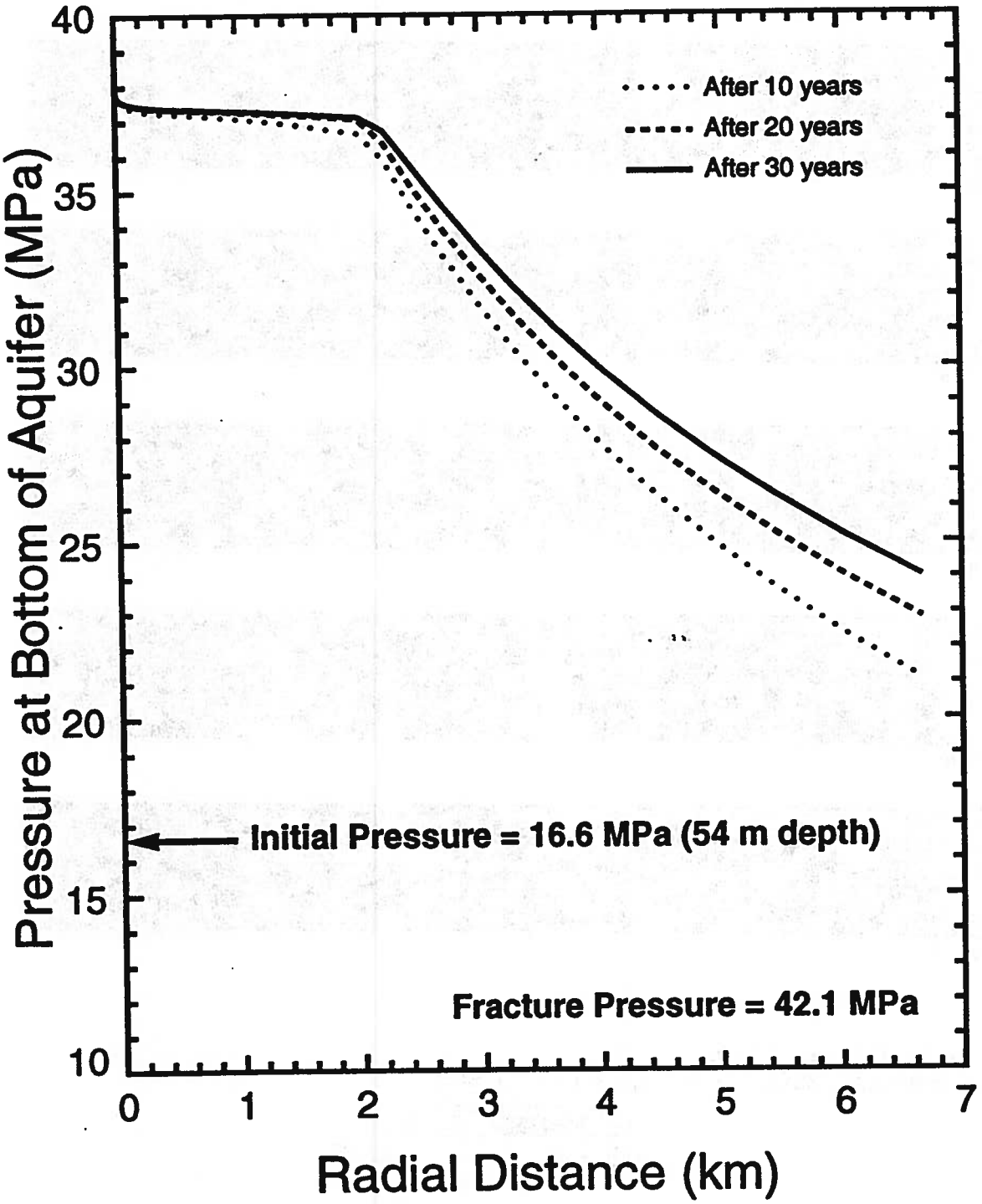

Nisku Carbonate Aquifer

NUMERICAL RUN (CO2_116)

Aquifer Porosity = 0.12 Aquifer Permeability = 400/6.2 md (horizontal)
Injection Pressure = 37.86 MPa

(a) Cumulative CO_2 Injection

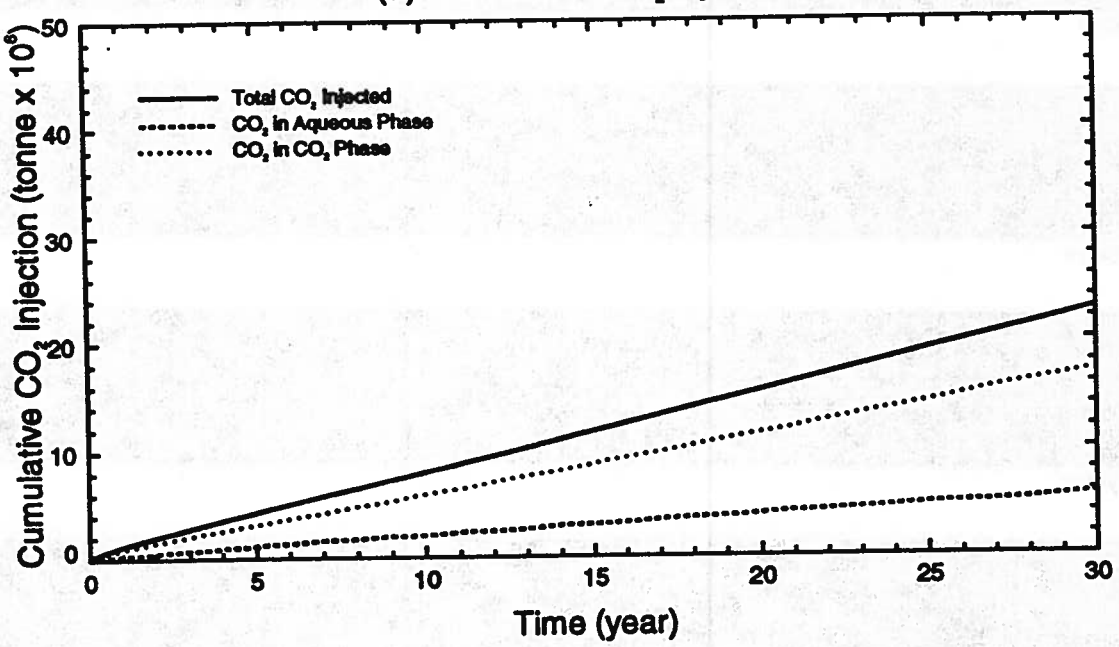

(b) CO_2 Injection Rate

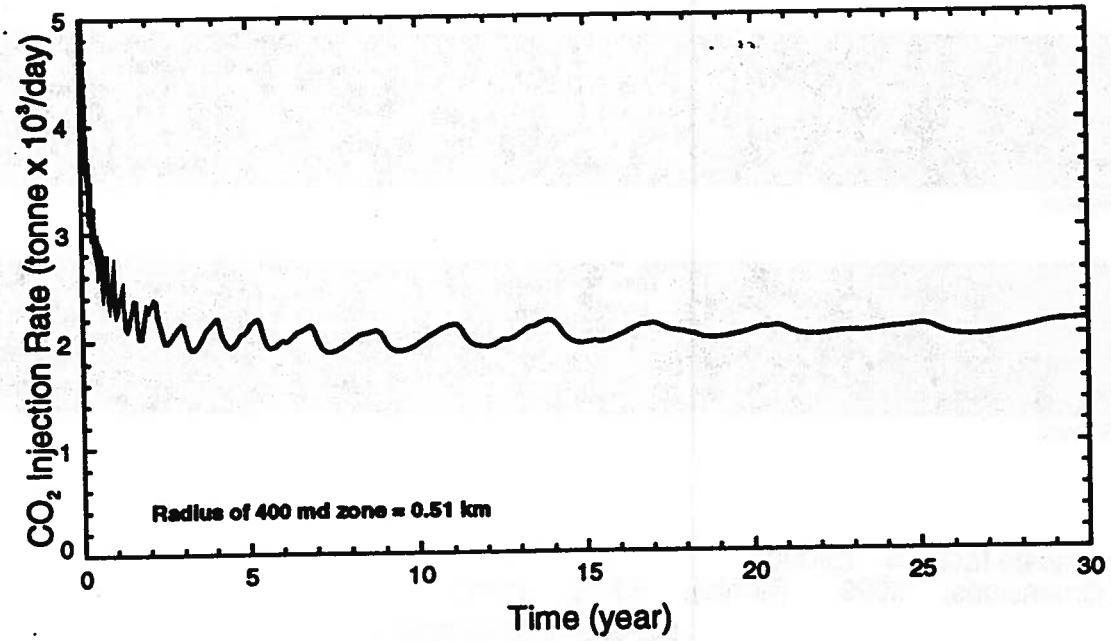

Carbon Dioxide Saturation (Run CO2_116)

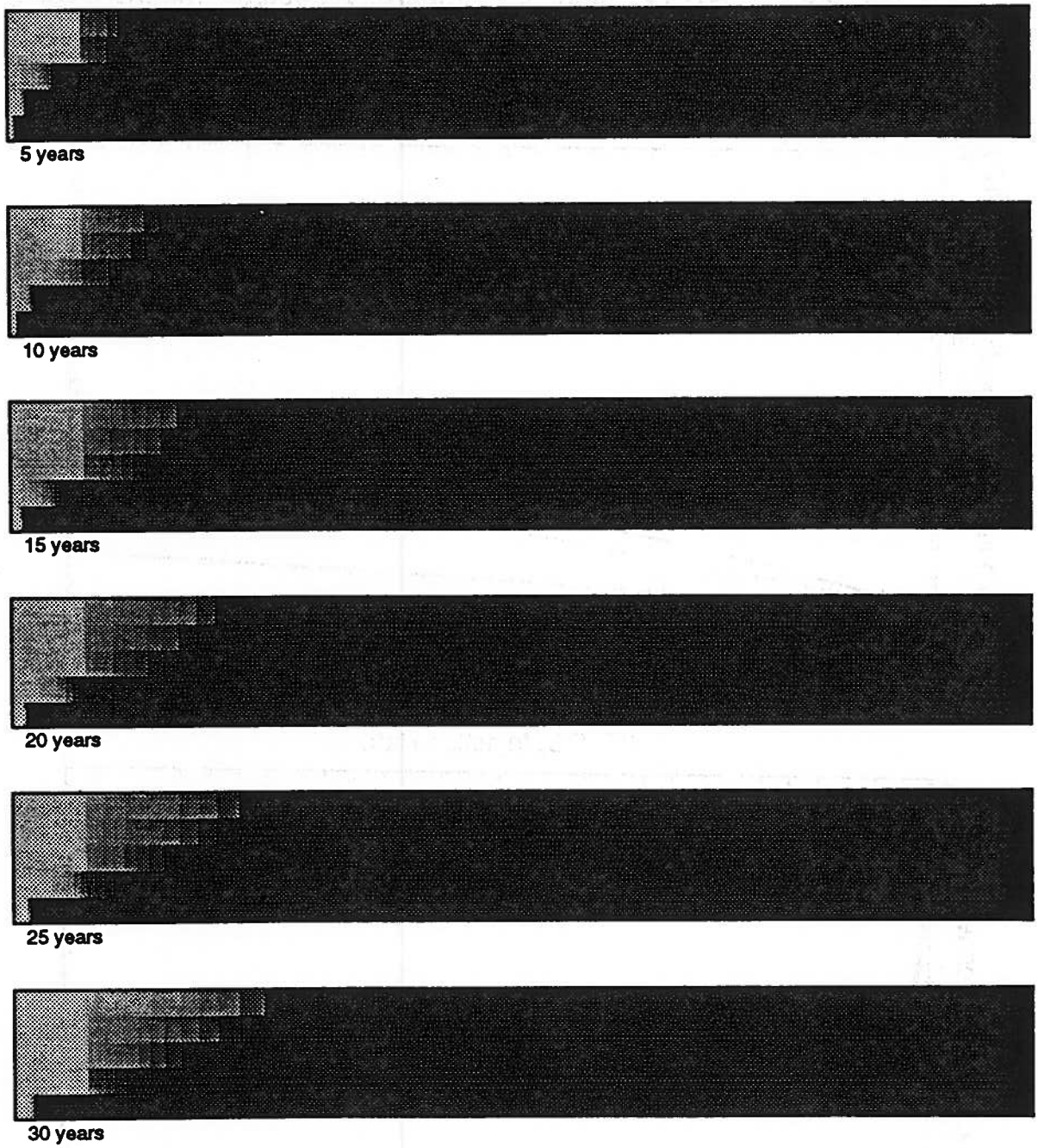

Vertical scale factor = 15.000
Field dimensions: 6999. (horiz.), 60.00 (vert.)

Nisku Carbonate Aquifer

NUMERICAL RUN (CO2_116)

Aquifer Porosity = 0.12 Aquifer Permeability = 400/6.2 md (horizontal)
Injection Pressure = 37.86 MPa Radius of 400 md zone = 0.51 km

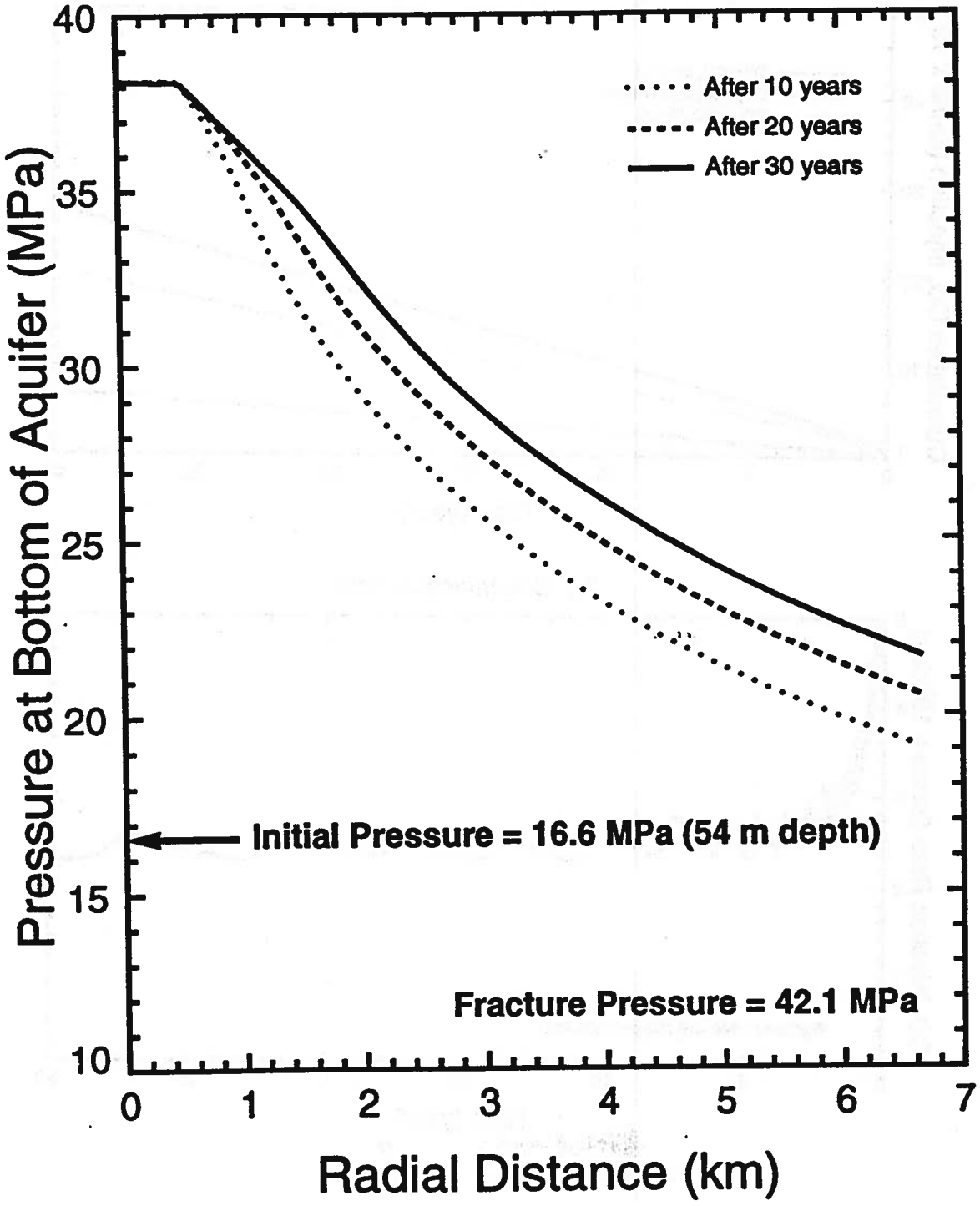

Nisku Carbonate Aquifer

NUMERICAL RUN (CO2_117)

Aquifer Porosity = 0.12 Aquifer Permeability = 400/6.2 md (horizontal)
Injection Pressure = 37.86 MPa

(a) Cumulative CO_2 Injection

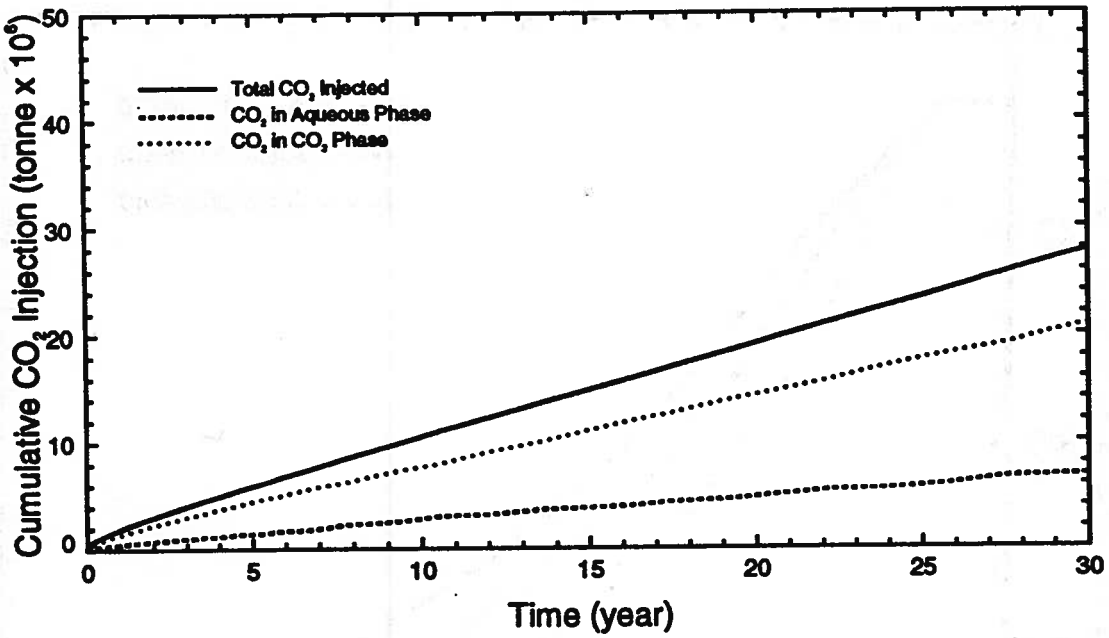

(b) CO_2 Injection Rate

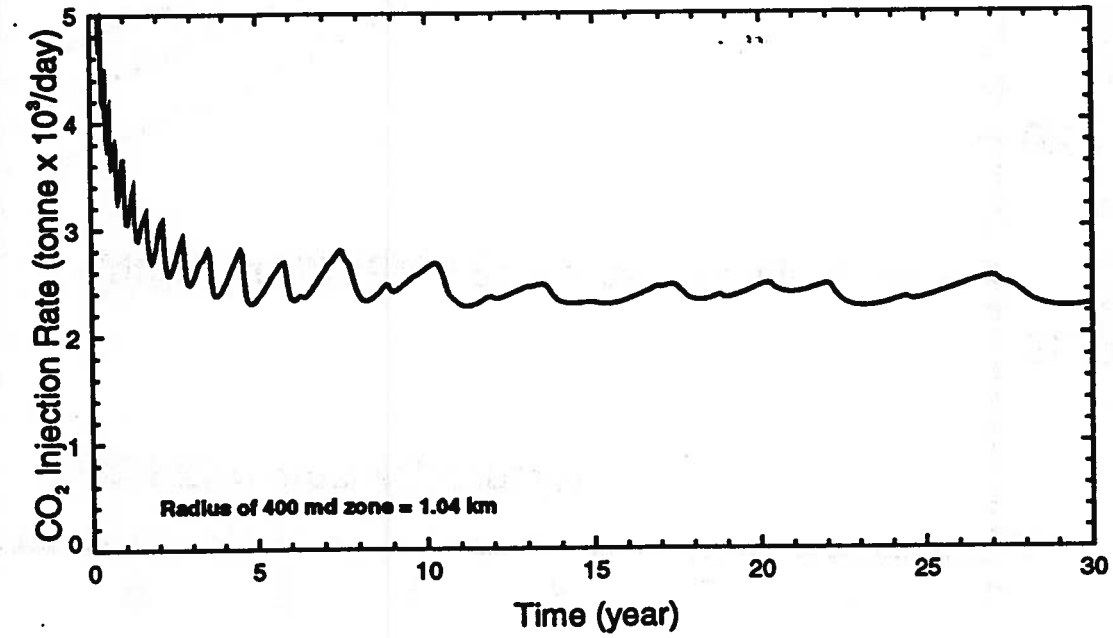

Carbon Dioxide Saturation (Run CO2_117)

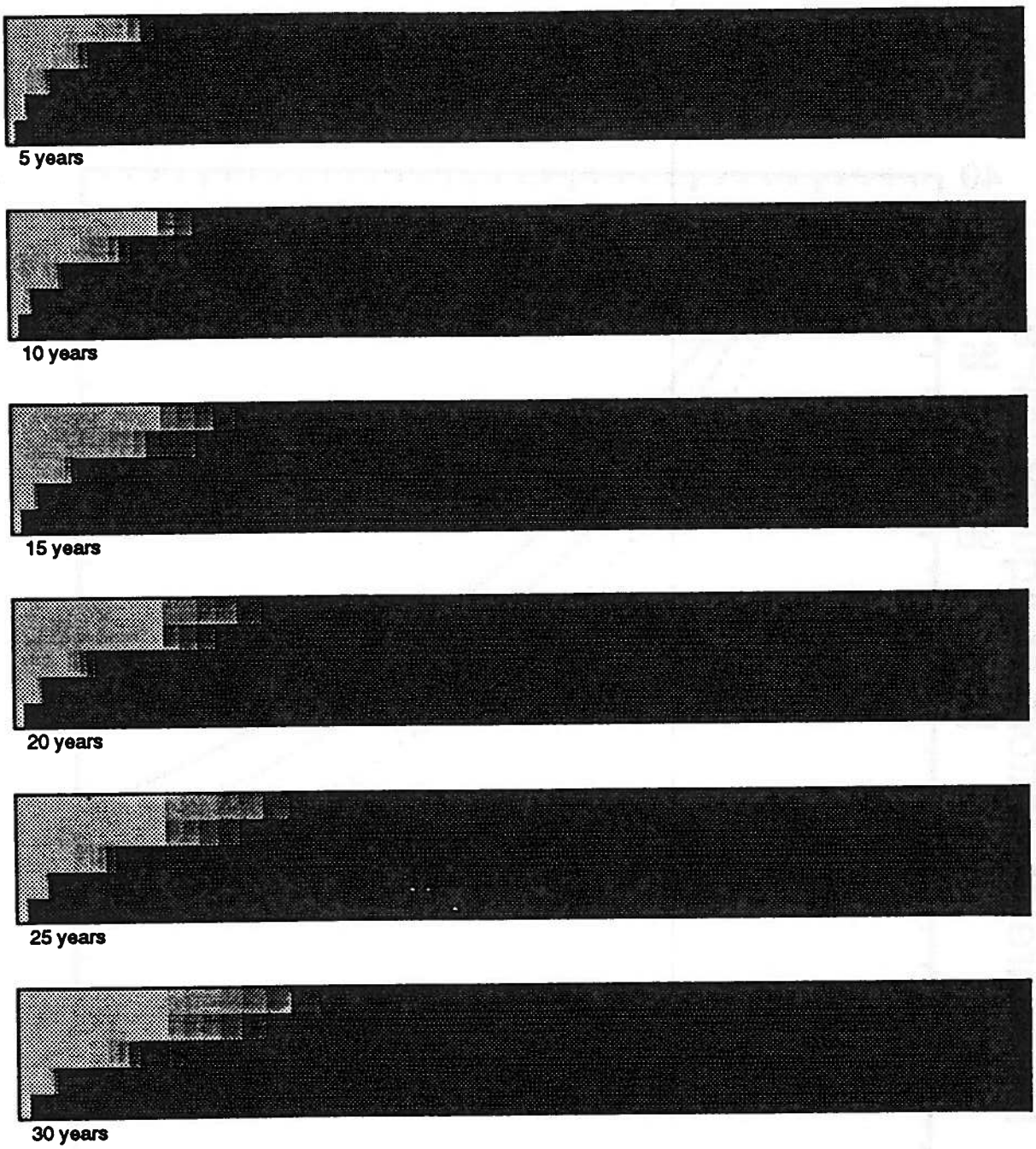

Vertical scale factor = 15.000
Field dimensions: 6999. (horiz.), 60.00 (vert.)

Nisku Carbonate Aquifer

NUMERICAL RUN (CO2_117)

Aquifer Porosity = 0.12 Aquifer Permeability = 400/6.2 md (horizontal)
Injection Pressure = 37.86 MPa Radius of 400 md zone = 1.04 km

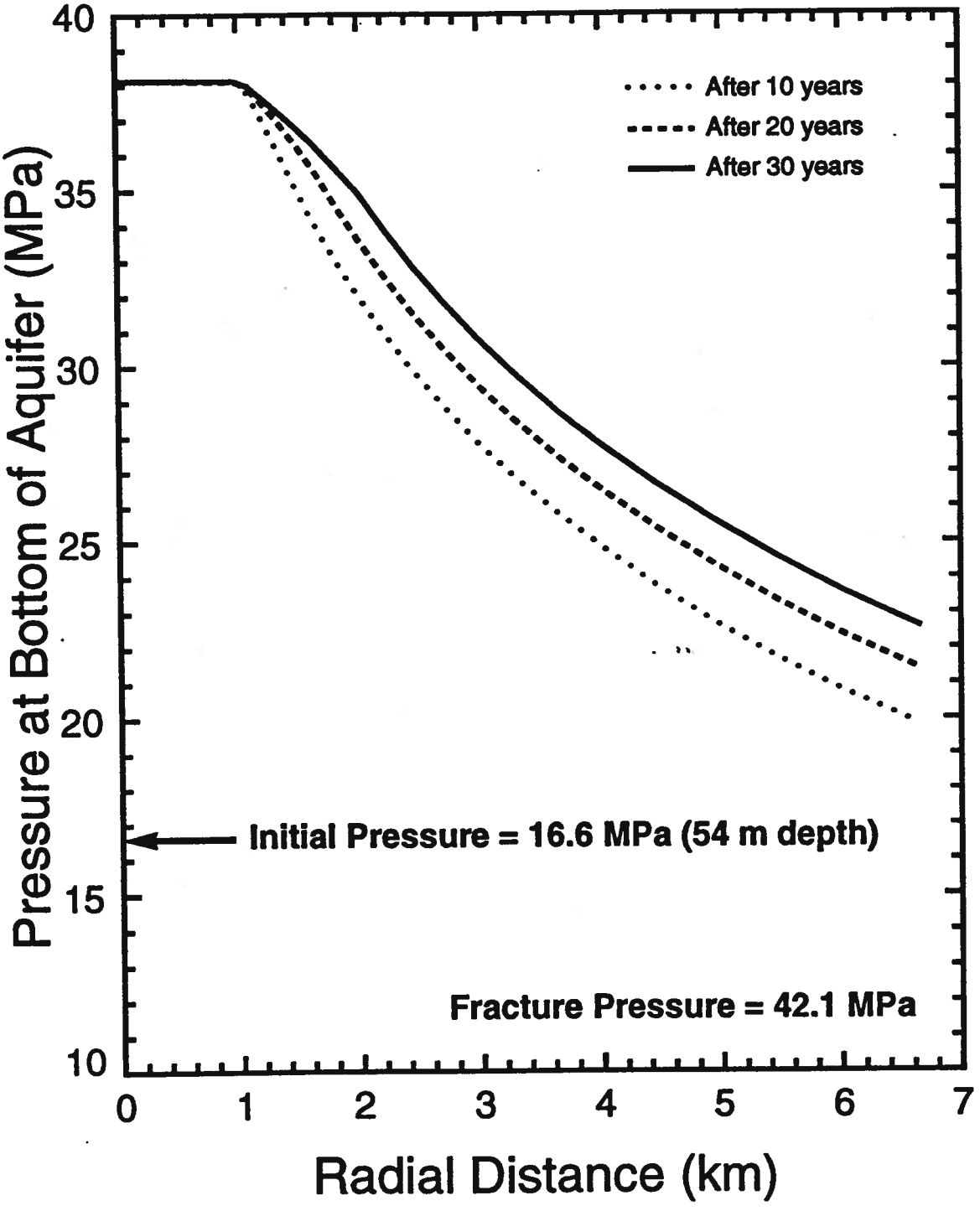

Nisku Carbonate Aquifer

NUMERICAL RUN (CO2_118)

Aquifer Porosity = 0.12 Aquifer Permeability = 400/6.2 md (horizontal)
Injection Pressure = 37.86 MPa

(a) Cumulative CO_2 Injection

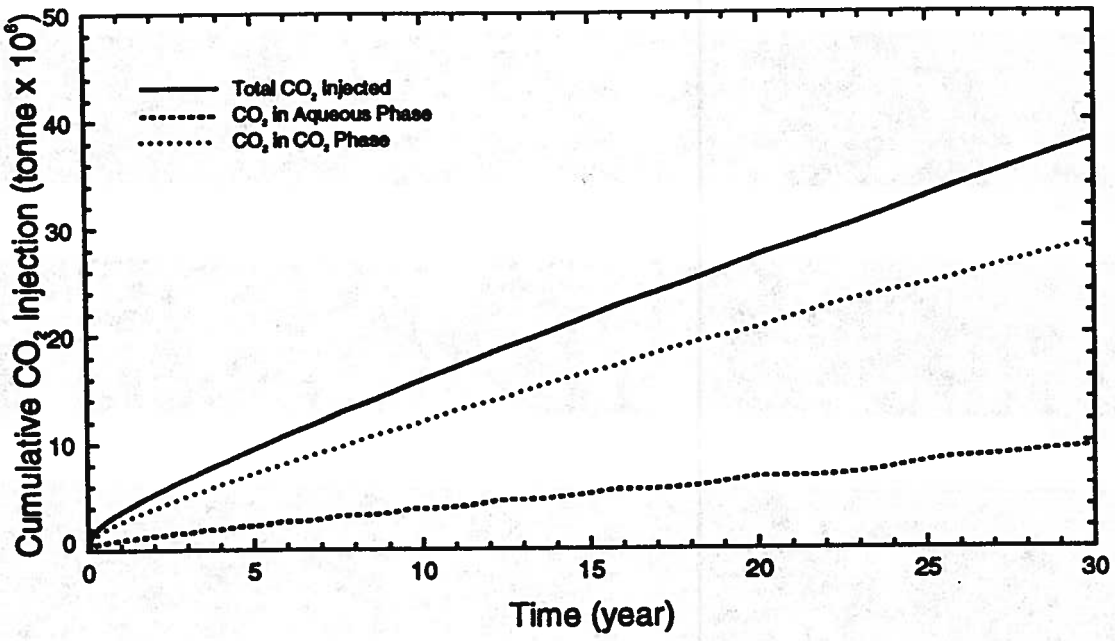

(b) CO_2 Injection Rate

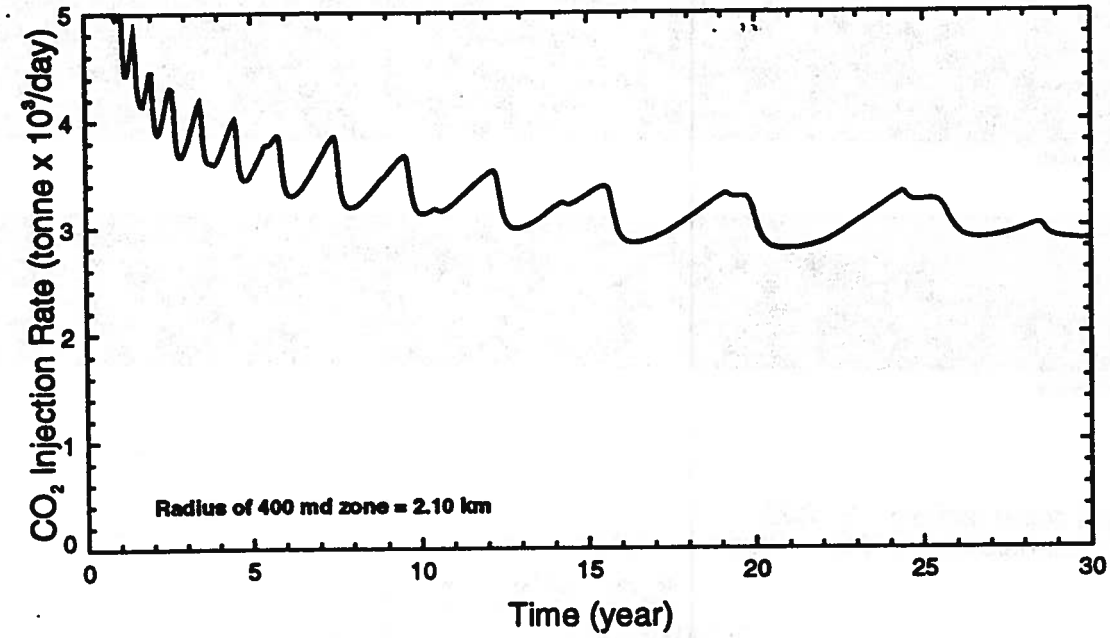

Carbon Dioxide Saturation (Run CO2_118)

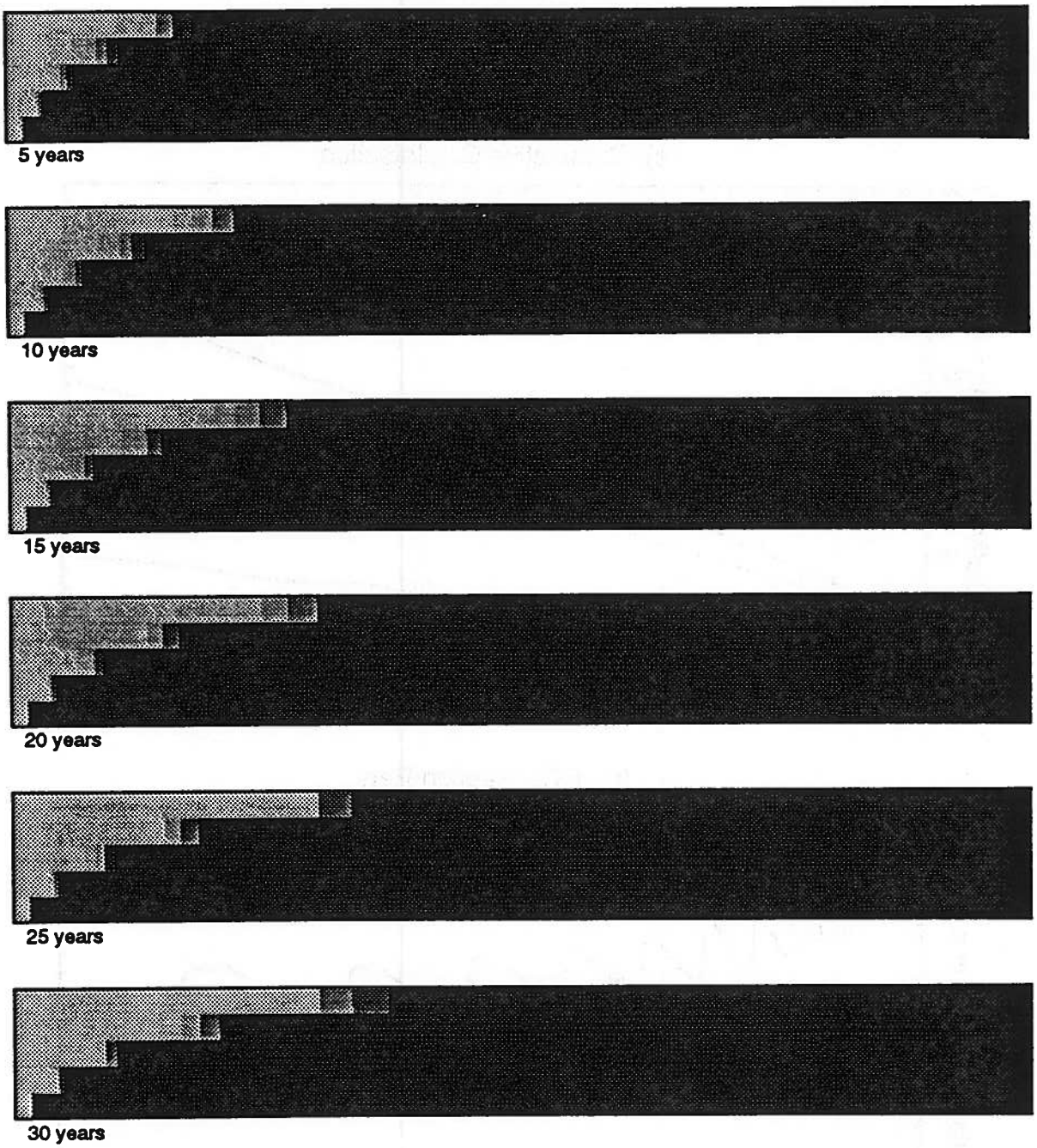

Vertical scale factor = 15.000
Field dimensions: 6999. (horiz.), 60.00 (vert.)

Nisku Carbonate Aquifer

NUMERICAL RUN (CO2_118)

Aquifer Porosity = 0.12 Aquifer Permeability = 400/6.2 md (horizontal)
Injection Pressure = 37.86 MPa Radius of 400 md zone = 2.10 km

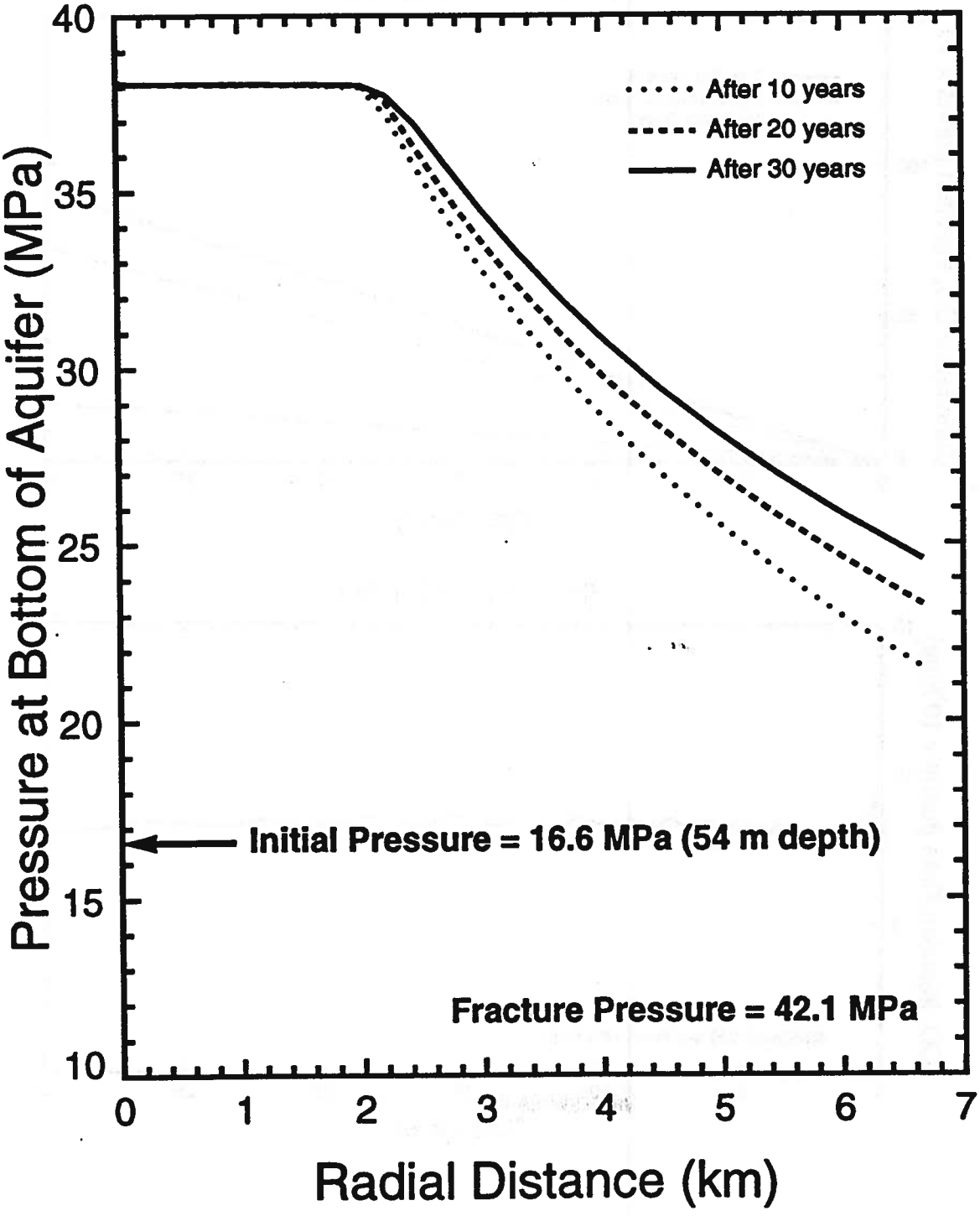

Nisku Carbonate Aquifer

NUMERICAL RUN (CO2_113)

Aquifer Porosity = 0.12 Aquifer Permeability = 100/30 md (horizontal)
Injection Pressure = 37.86 MPa

(a) Cumulative CO_2 Injection

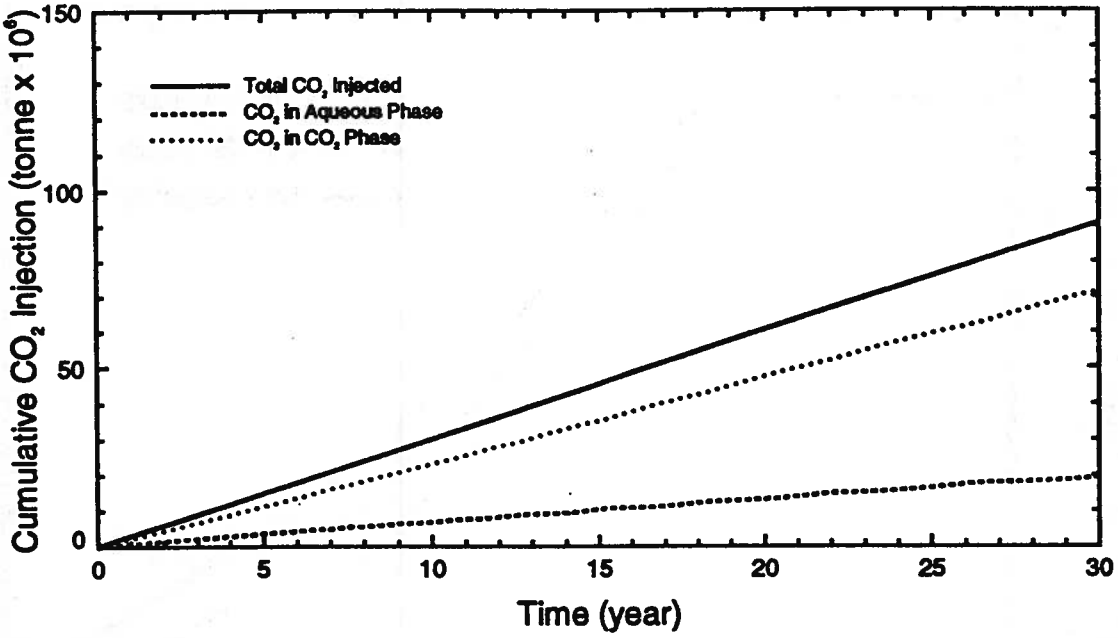

(b) CO_2 Injection Rate

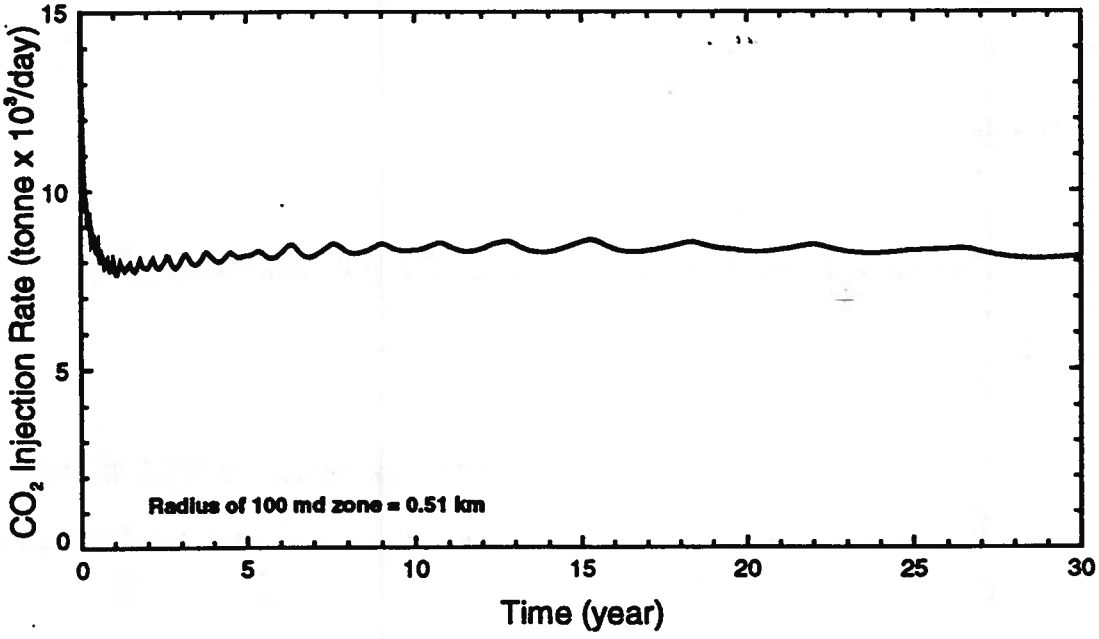

Carbon Dioxide Saturation (Run CO2_113)

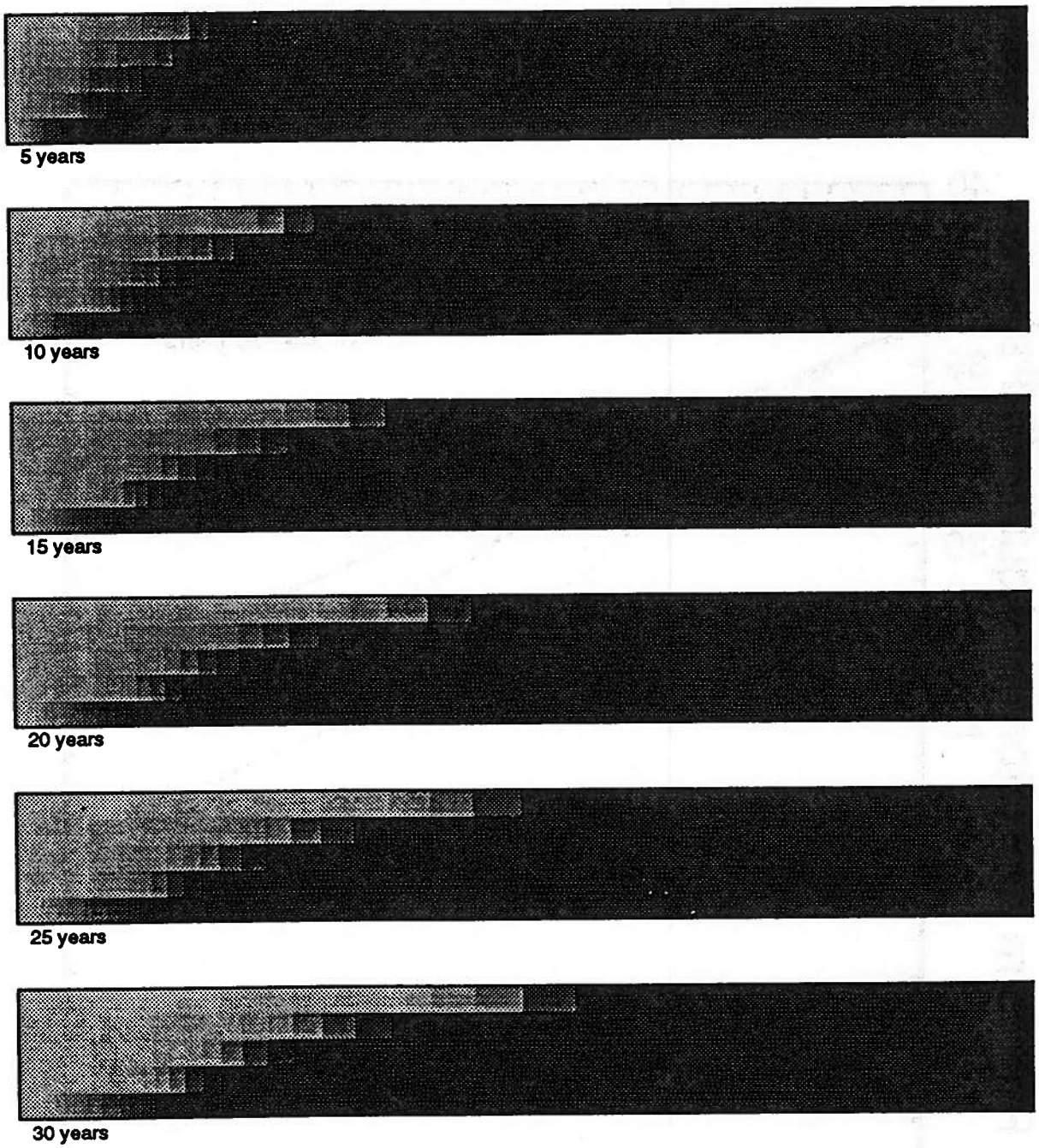

Vertical scale factor = 15.000
Field dimensions: 6999. (horiz.), 60.00 (vert.)

Nisku Carbonate Aquifer

NUMERICAL RUN (CO2_113)

Aquifer Porosity = 0.12 Aquifer Permeability = 100/30 md (horizontal)
Injection Pressure = 37.86 MPa Radius of 100 md zone = 0.51 km

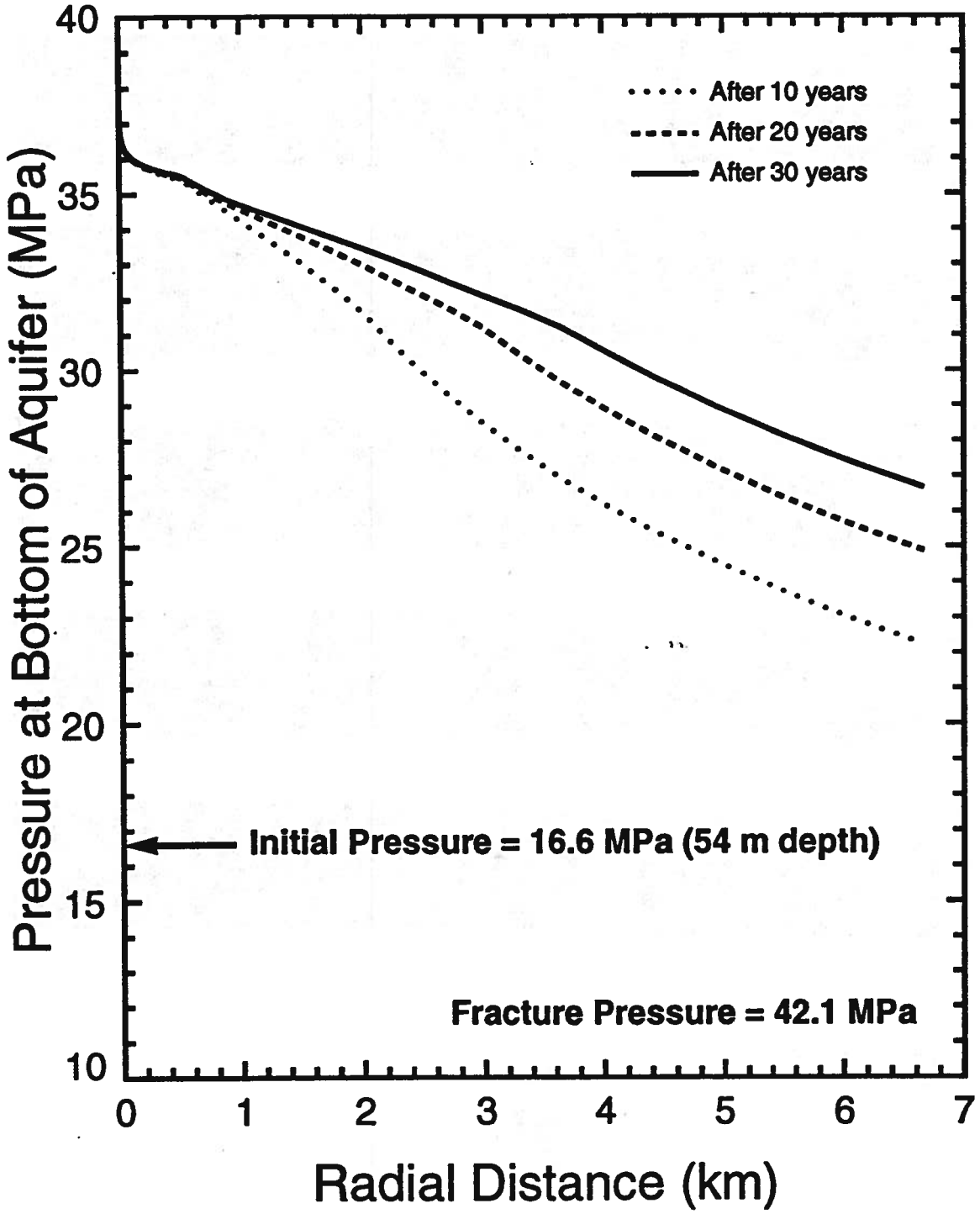

Nisku Carbonate Aquifer

NUMERICAL RUN (CO2_114)

Aquifer Porosity = 0.12 Aquifer Permeability = 100/30 md (horizontal)
Injection Pressure = 37.86 MPa

(a) Cumulative CO_2 Injection

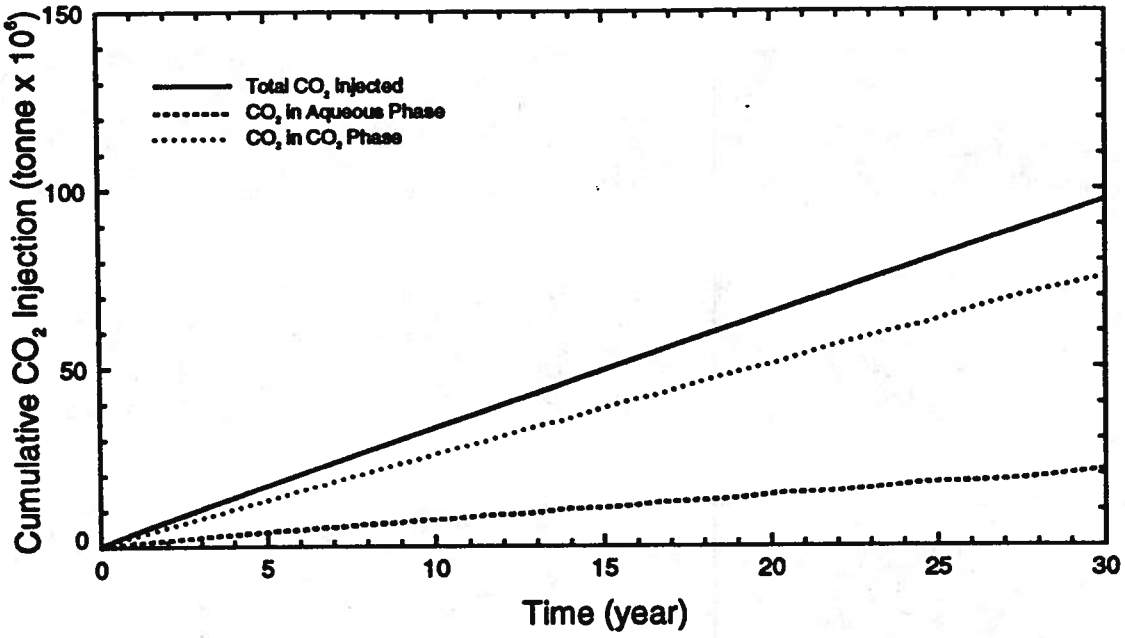

(b) CO_2 Injection Rate

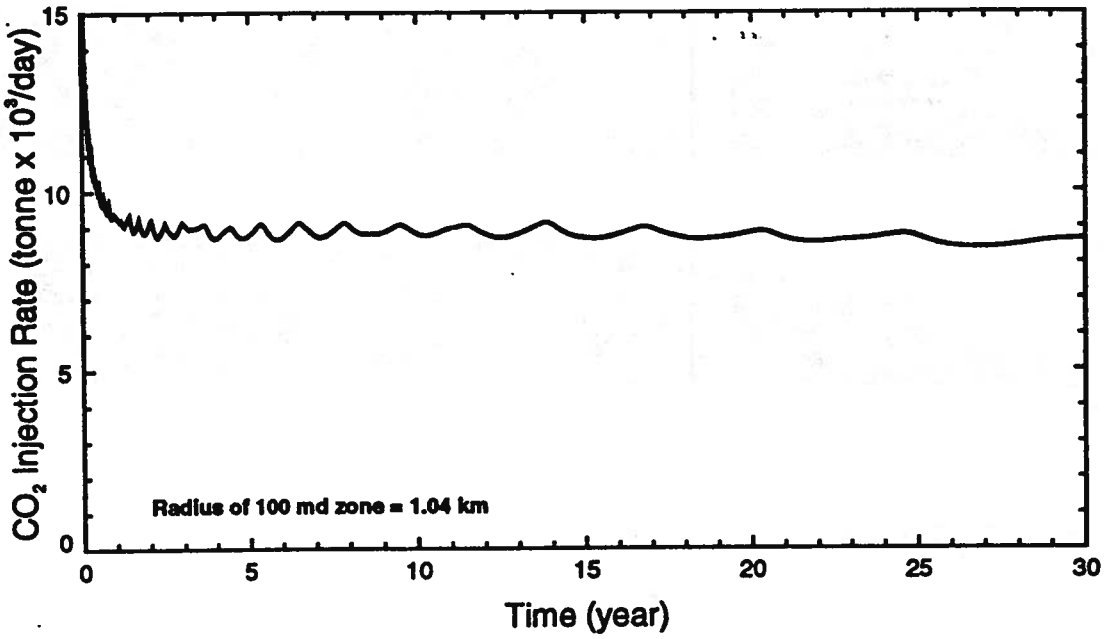

Carbon Dioxide Saturation (Run CO2_114)

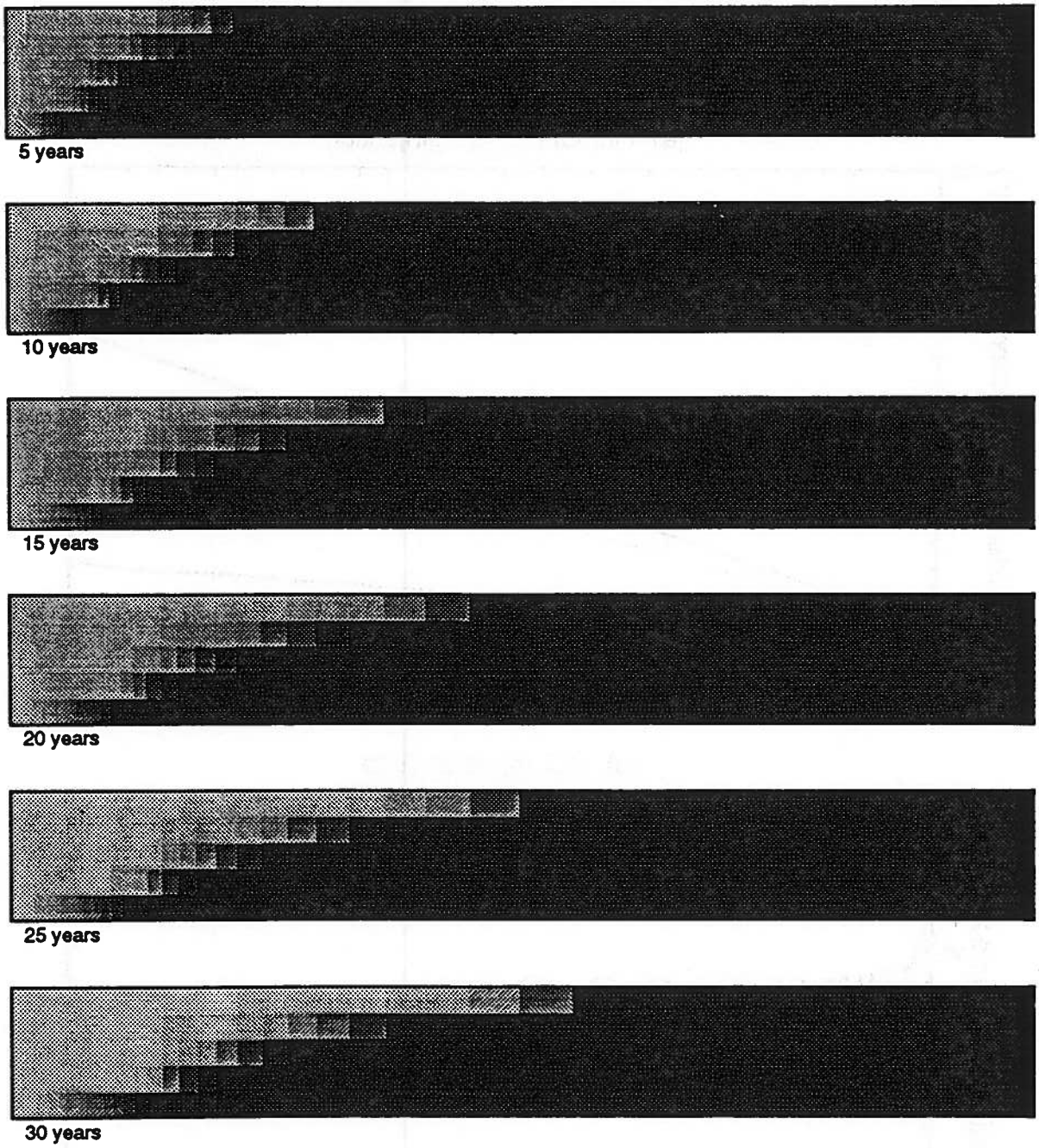

Vertical scale factor = 15.000
Field dimensions: 6999. (horiz.), 60.00 (vert.)

Nisku Carbonate Aquifer

NUMERICAL RUN (CO2_114)

Aquifer Porosity = 0.12 Aquifer Permeability = 100/30 md (horizontal)
Injection Pressure = 37.86 MPa Radius of 100 md zone = 1.04 km

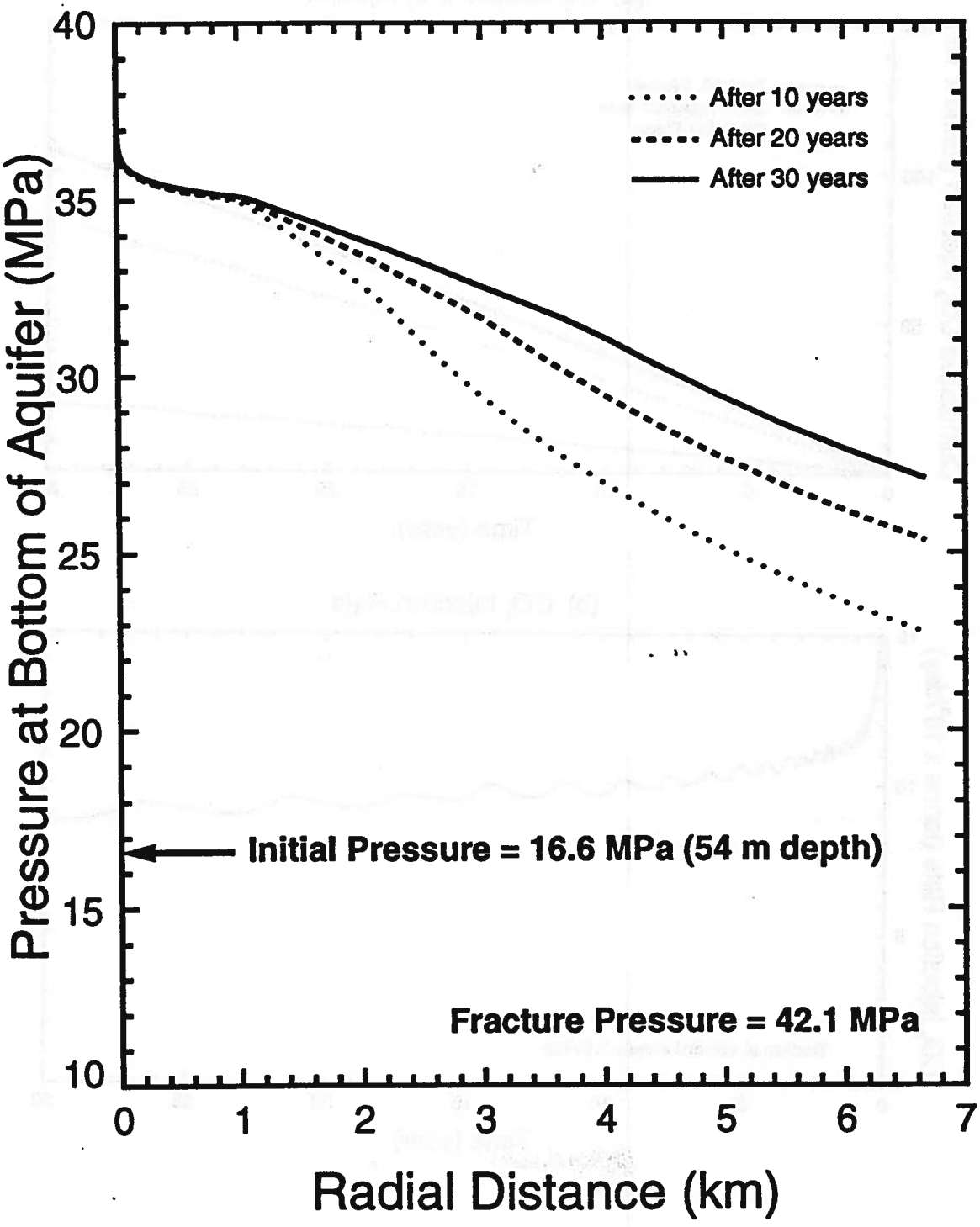

Nisku Carbonate Aquifer

NUMERICAL RUN (CO2_115)

Aquifer Porosity = 0.12 Aquifer Permeability = 100/30 md (horizontal)
Injection Pressure = 37.86 MPa

(a) Cumulative CO_2 Injection

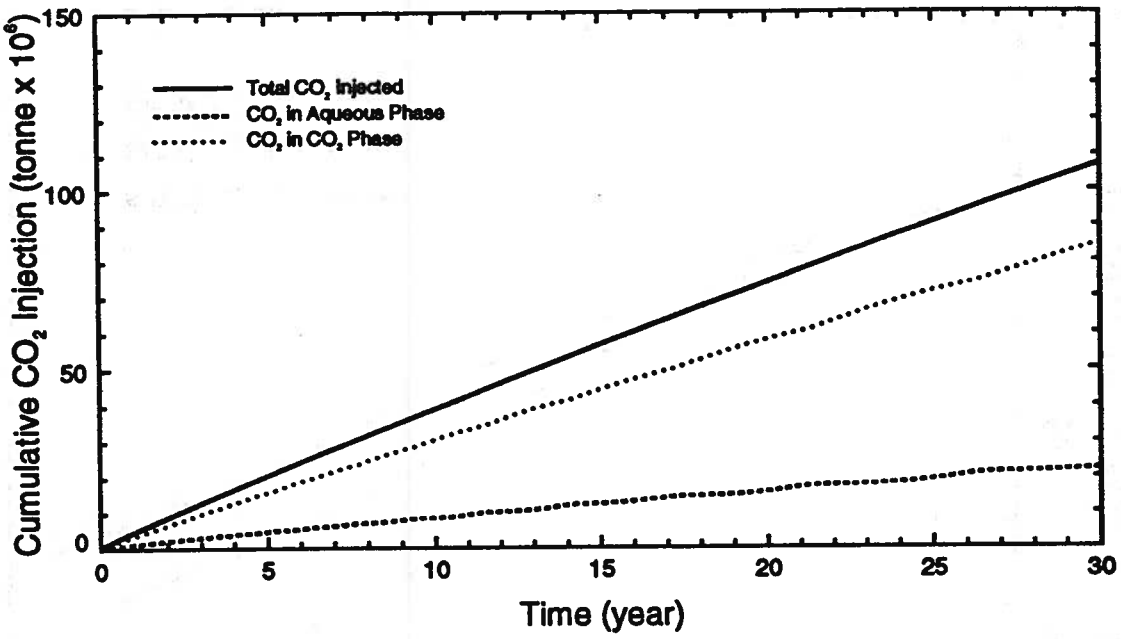

(b) CO_2 Injection Rate

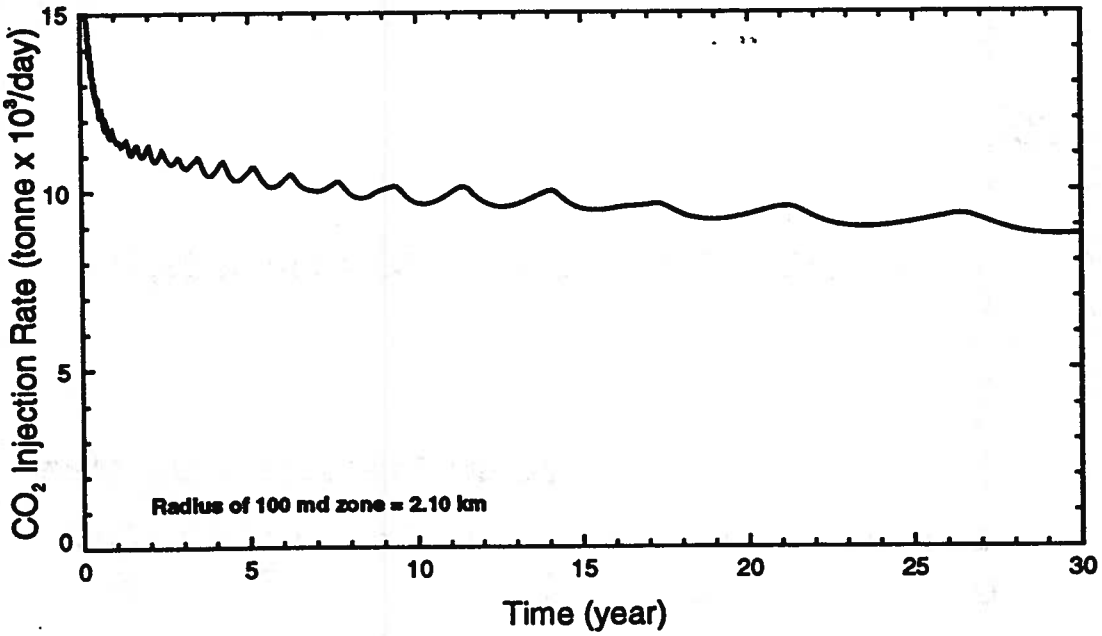

Carbon Dioxide Saturation (Run CO2_115)

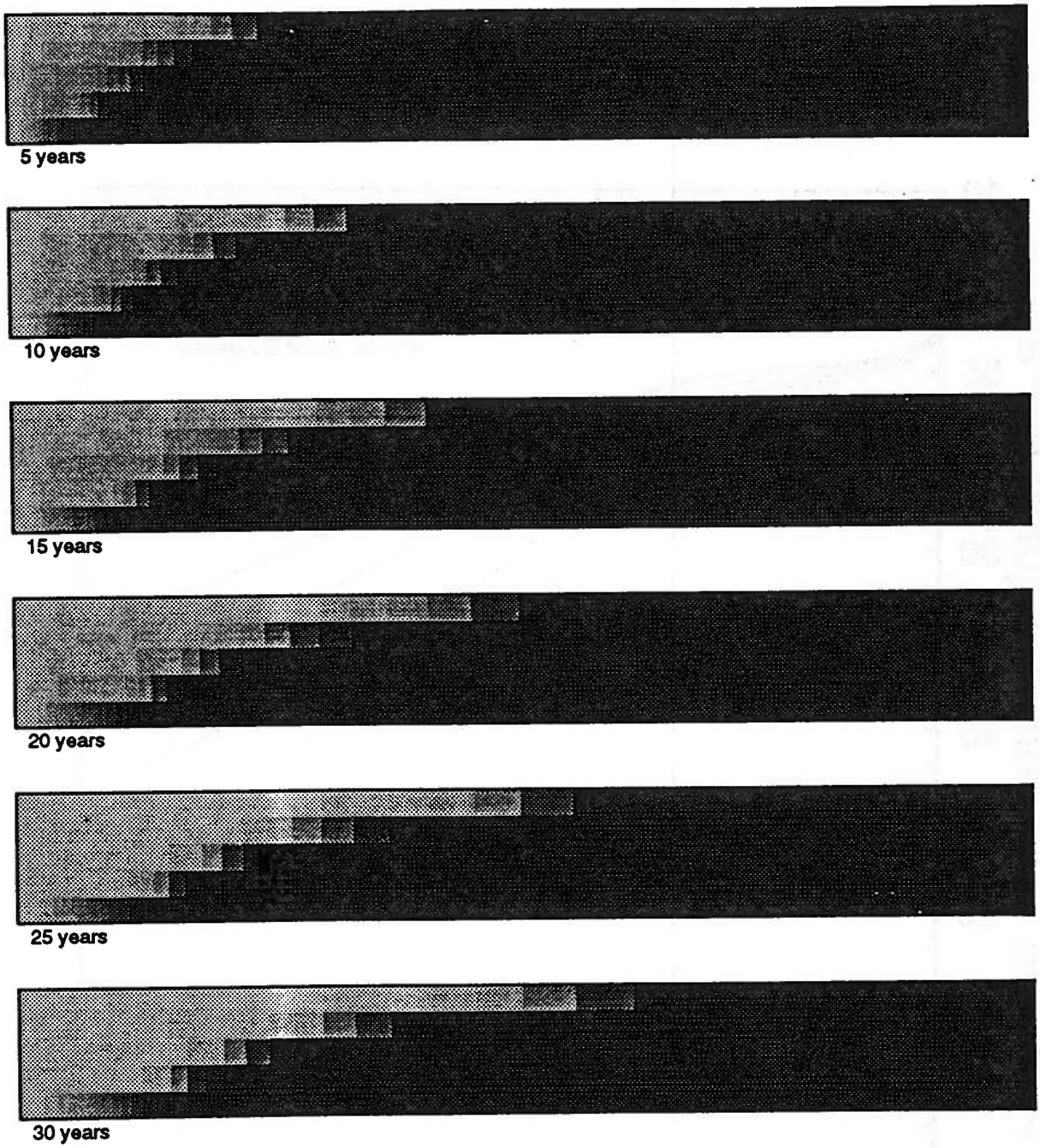

Vertical scale factor = 15.000
Field dimensions: 6999. (horiz.), 60.00 (vert.)

Nisku Carbonate Aquifer

NUMERICAL RUN (CO2_115)

Aquifer Porosity = 0.12 Aquifer Permeability = 100/30 md (horizontal)
Injection Pressure = 37.86 MPa Radius of 100 md zone = 2.10 km

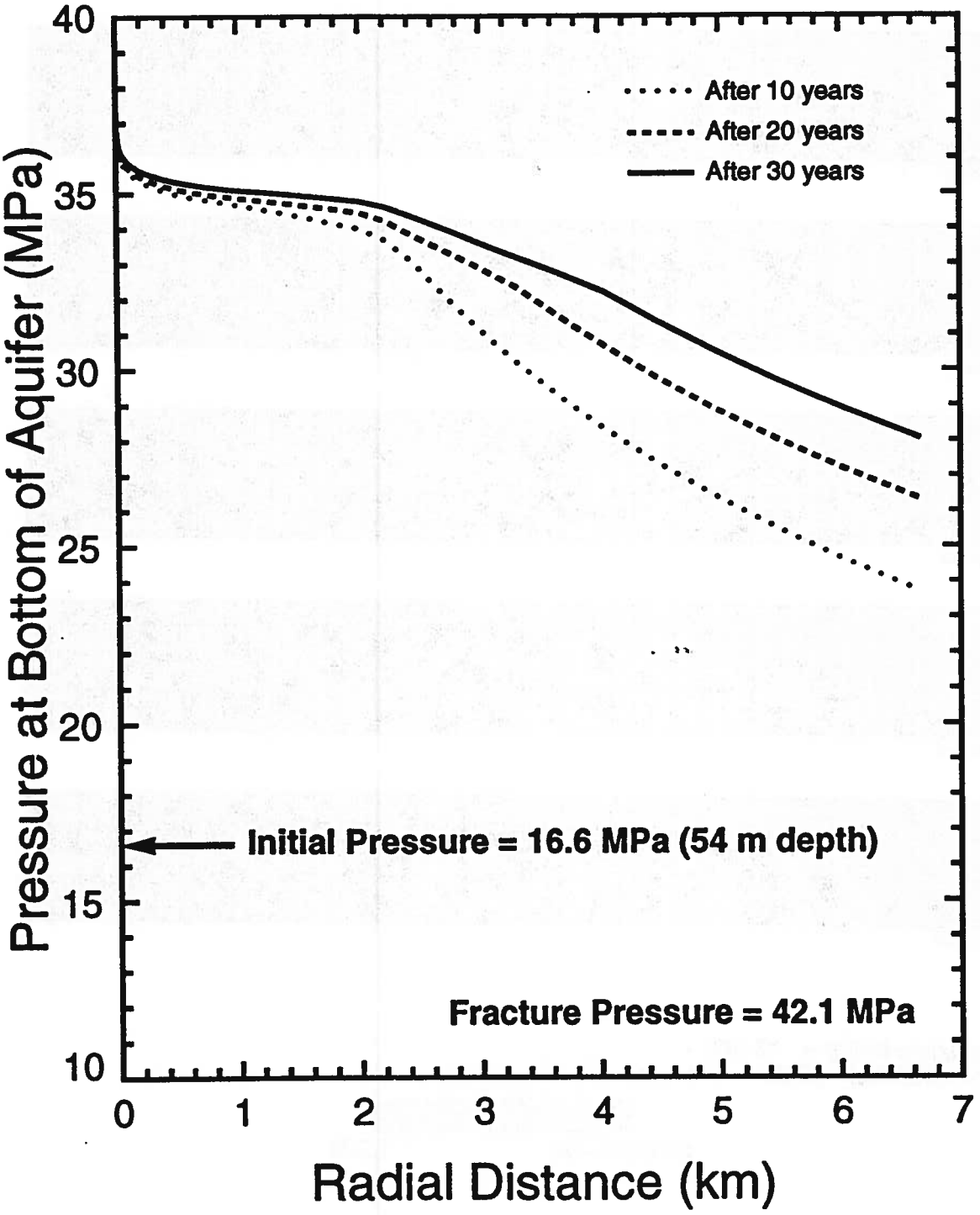

Nisku Carbonate Aquifer

NUMERICAL RUN (CO2_119)

Aquifer Porosity = 0.12 Aquifer Permeability = 400/30 md (horizontal)
Injection Pressure = 37.86 MPa

(a) Cumulative CO_2 Injection

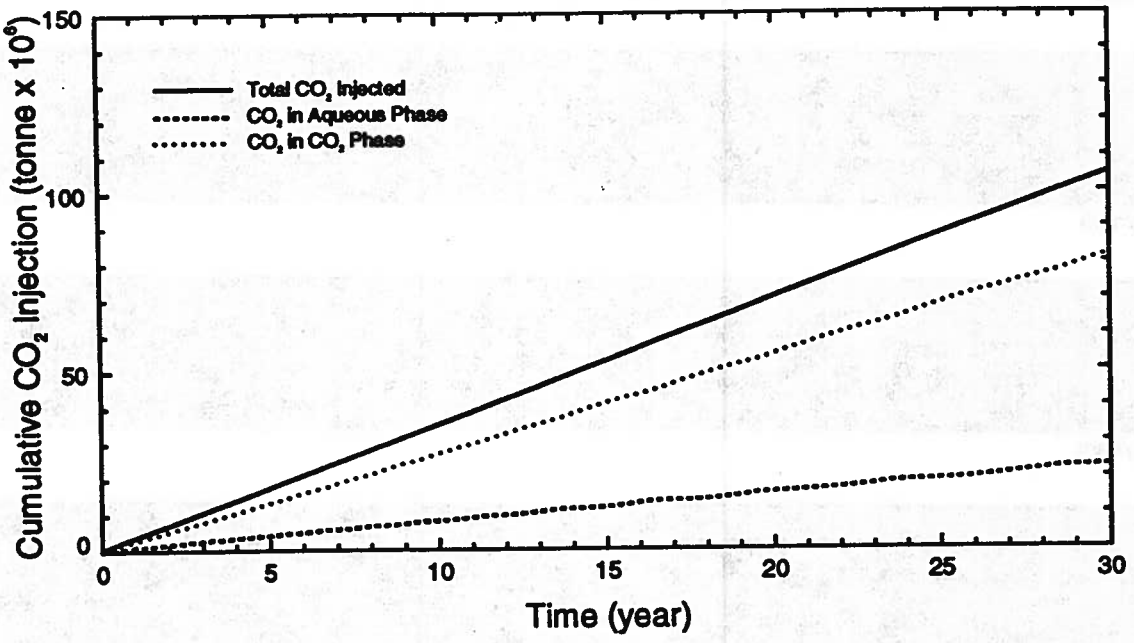

(b) CO_2 Injection Rate

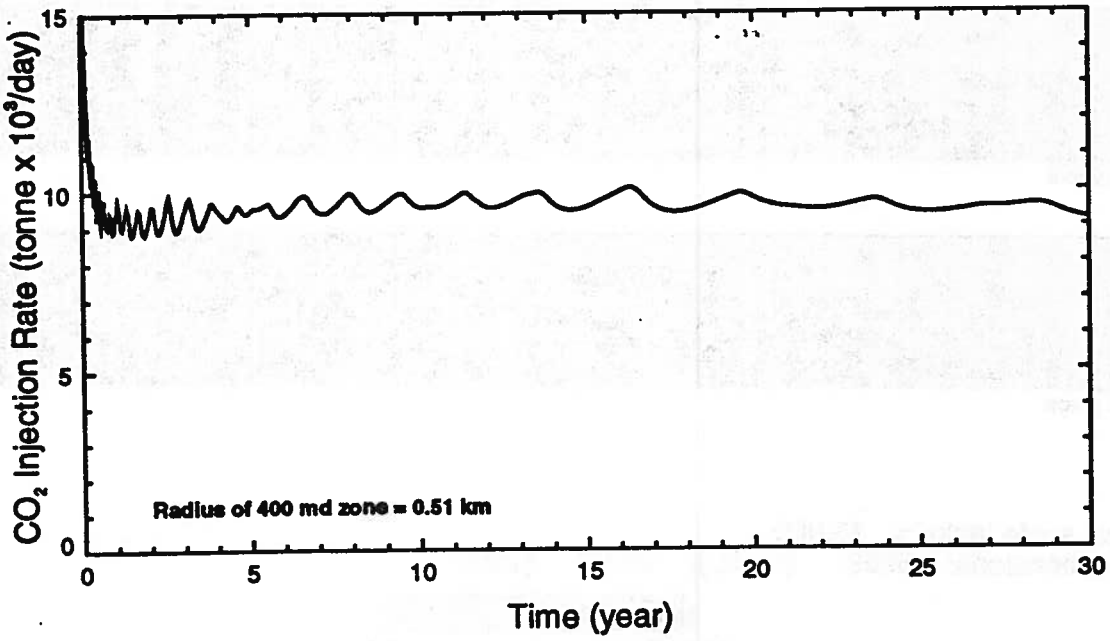

Carbon Dioxide Saturation (Run CO2_119)

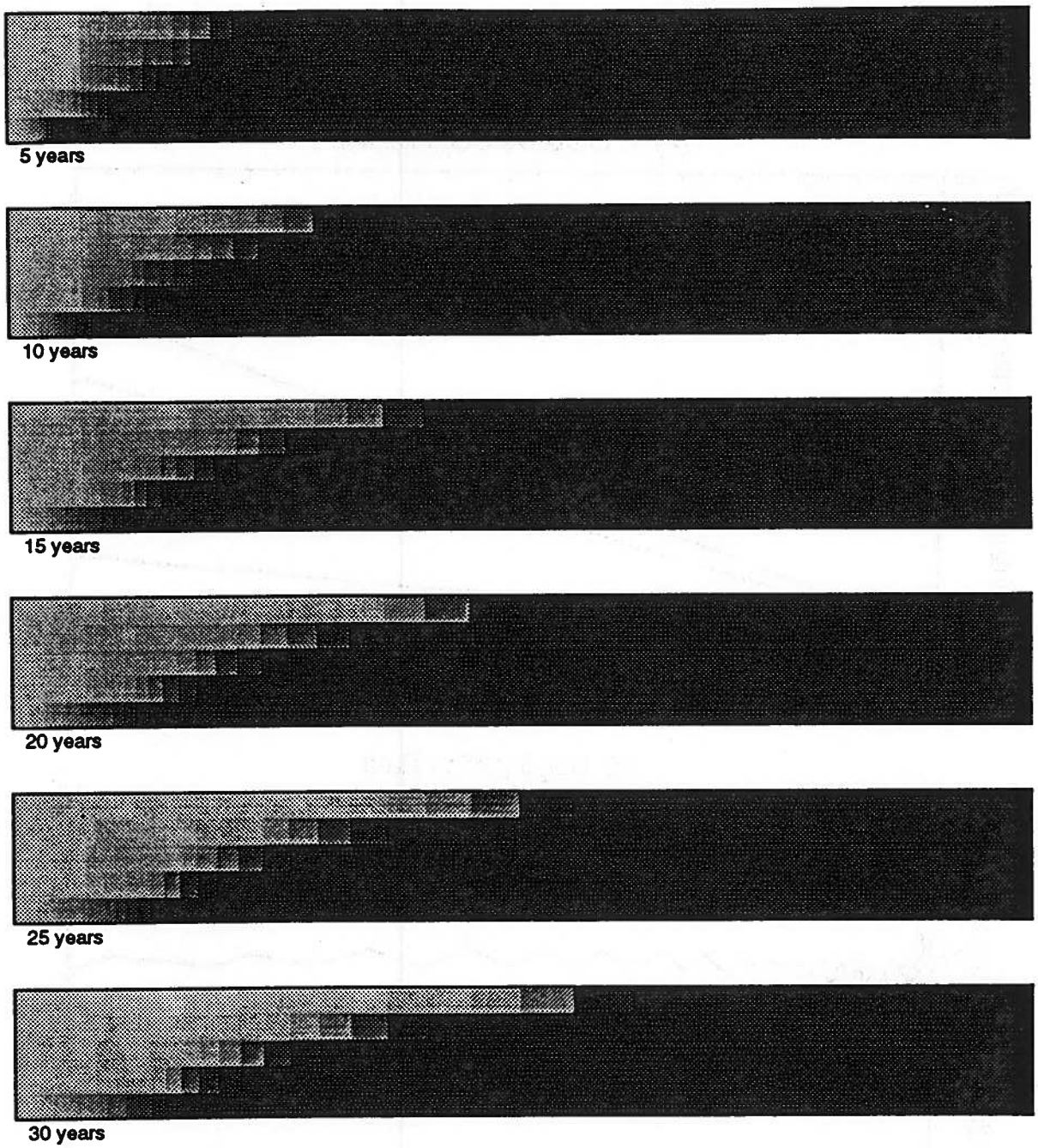

Vertical scale factor = 15.000
Field dimensions: 6999. (horiz.), 60.00 (vert.)

Nisku Carbonate Aquifer

NUMERICAL RUN (CO2_119)

Aquifer Porosity = 0.12 Aquifer Permeability = 400/30 md (horizontal)
Injection Pressure = 37.86 MPa Radius of 400 md zone = 0.51 km

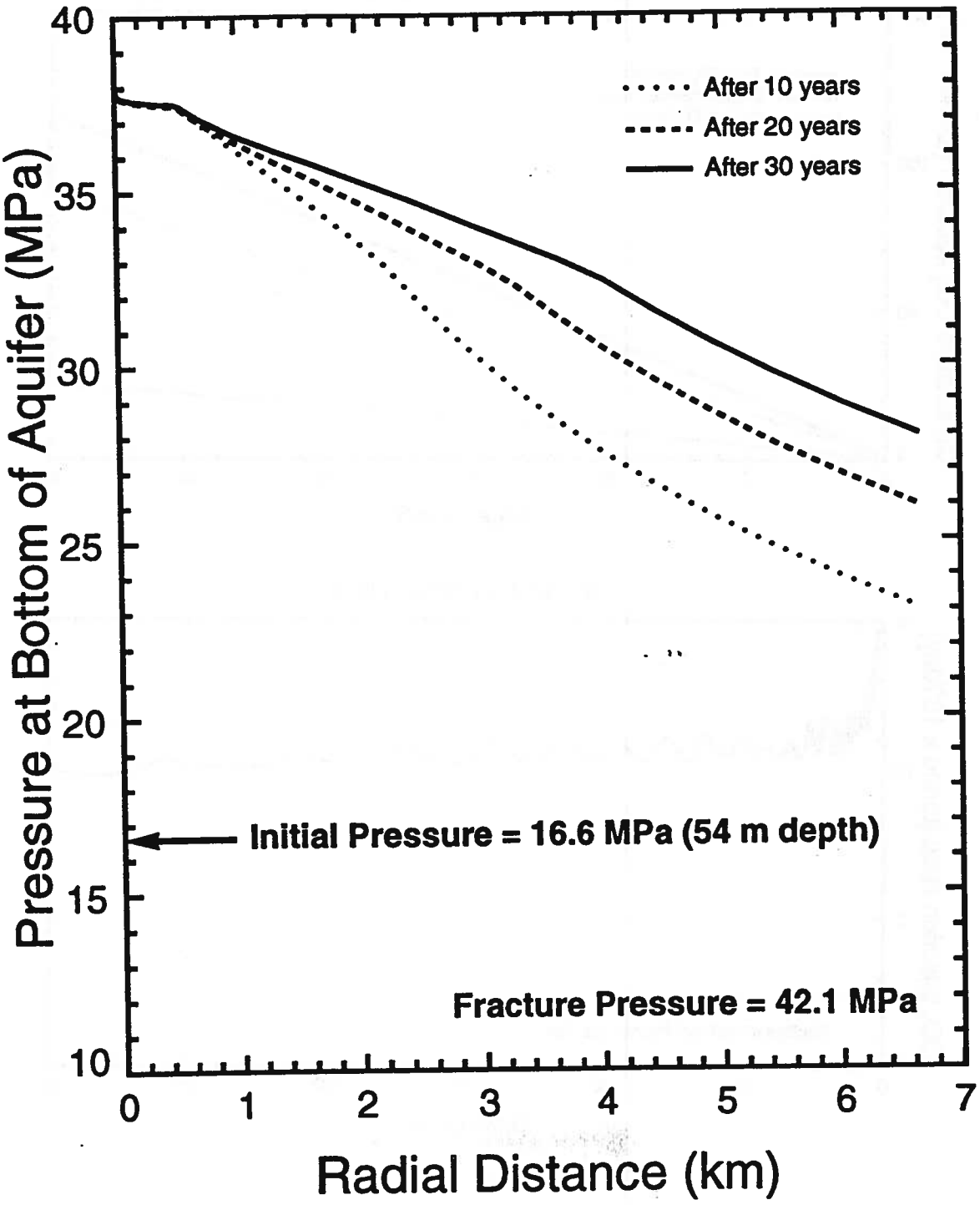

Nisku Carbonate Aquifer

NUMERICAL RUN (CO2_120)

Aquifer Porosity = 0.12 Aquifer Permeability = 400/30 md (horizontal)
Injection Pressure = 37.86 MPa

(a) Cumulative CO_2 Injection

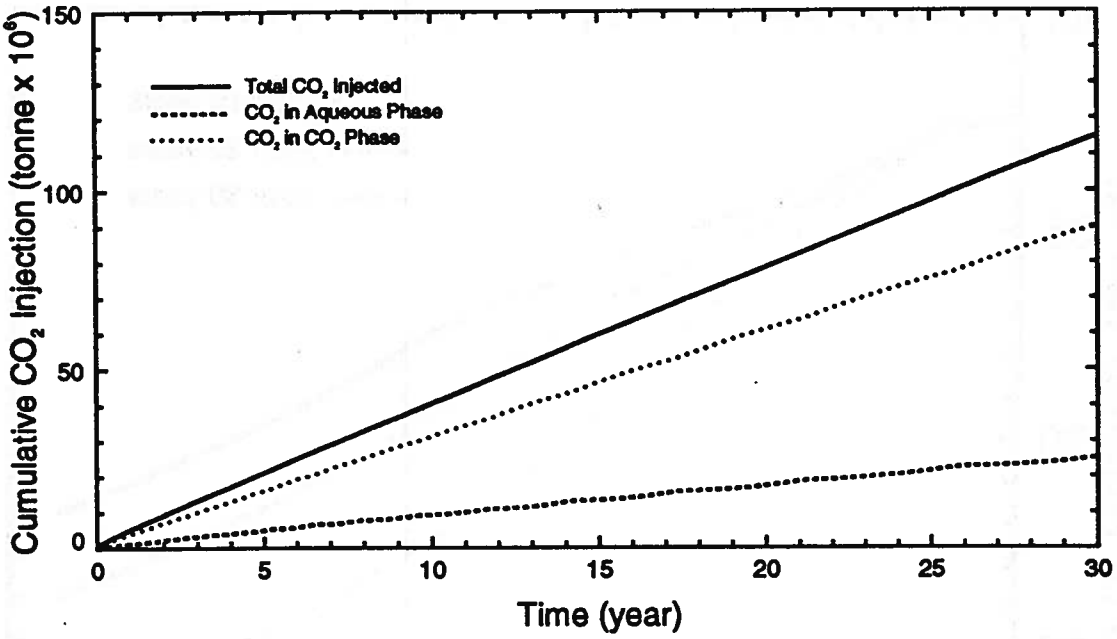

(b) CO_2 Injection Rate

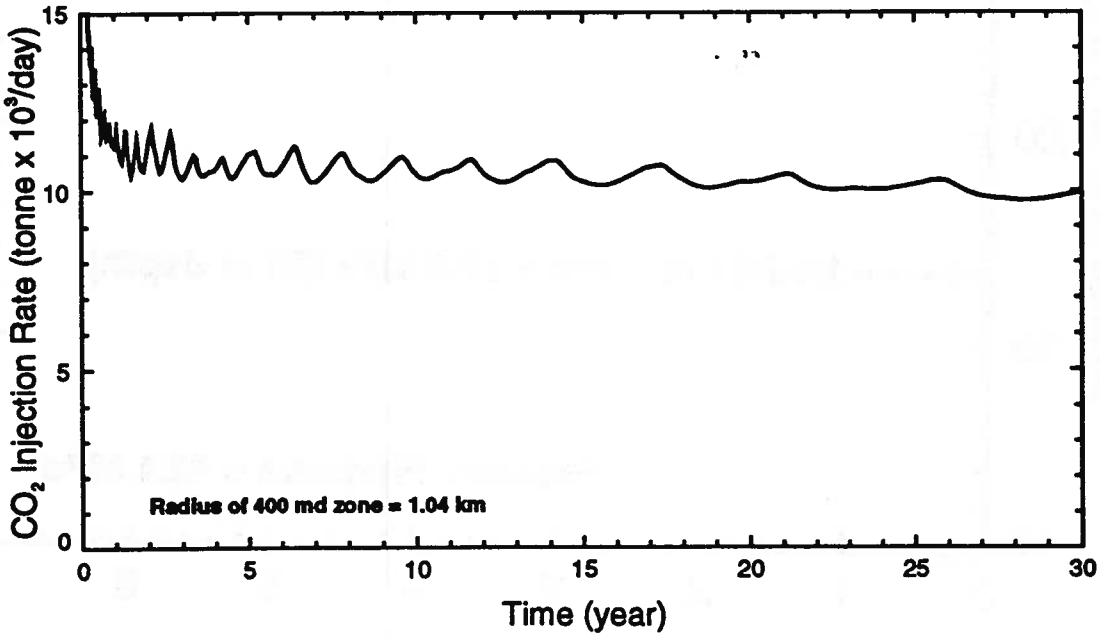

Carbon Dioxide Saturation (Run CO2_120)

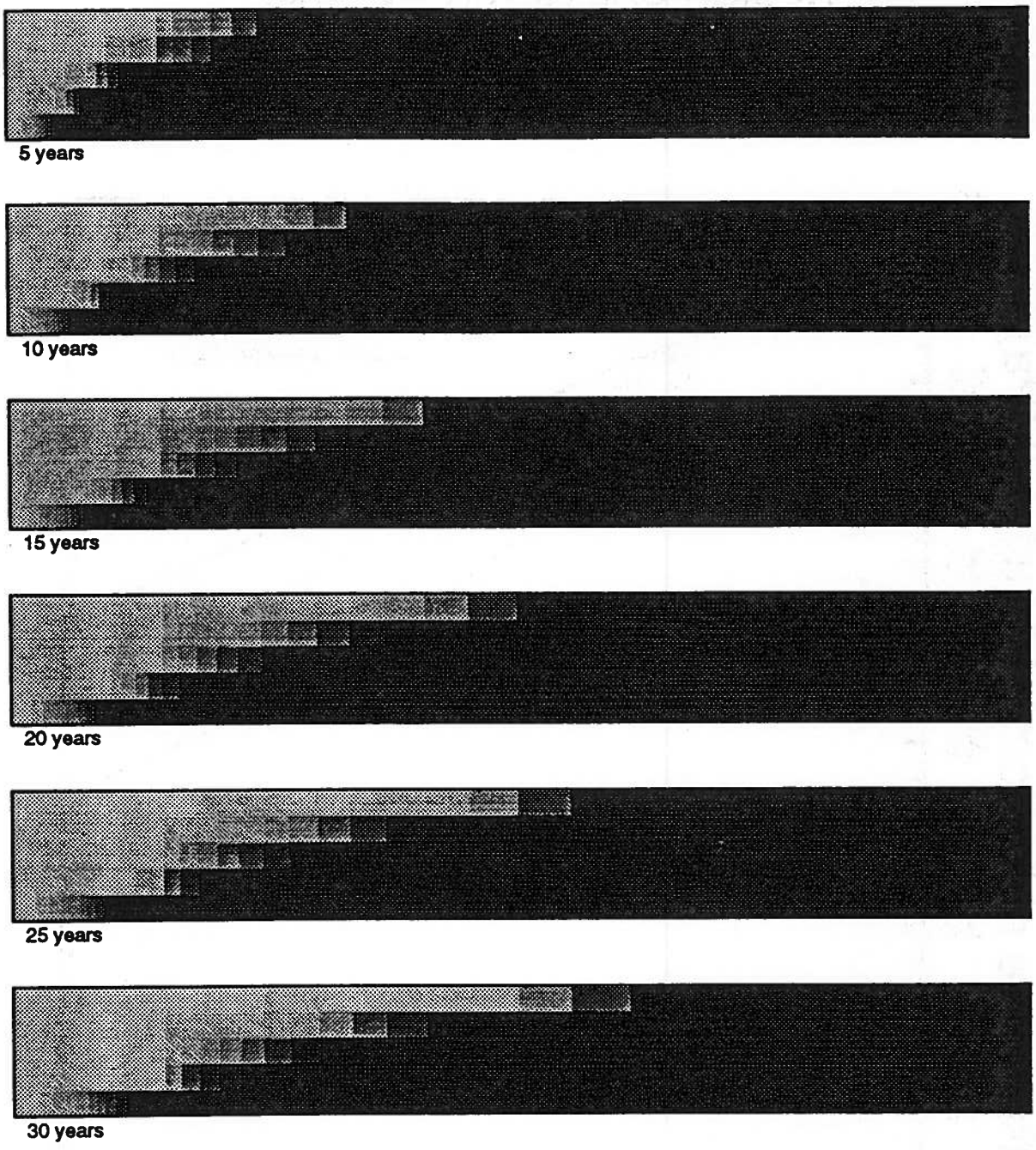

Vertical scale factor = 15.000
Field dimensions: 6999. (horiz.), 60.00 (vert.)

Nisku Carbonate Aquifer

NUMERICAL RUN (CO2_120)

Aquifer Porosity = 0.12 Aquifer Permeability = 400/30 md (horizontal)
Injection Pressure = 37.86 MPa Radius of 400 md zone = 1.04 km

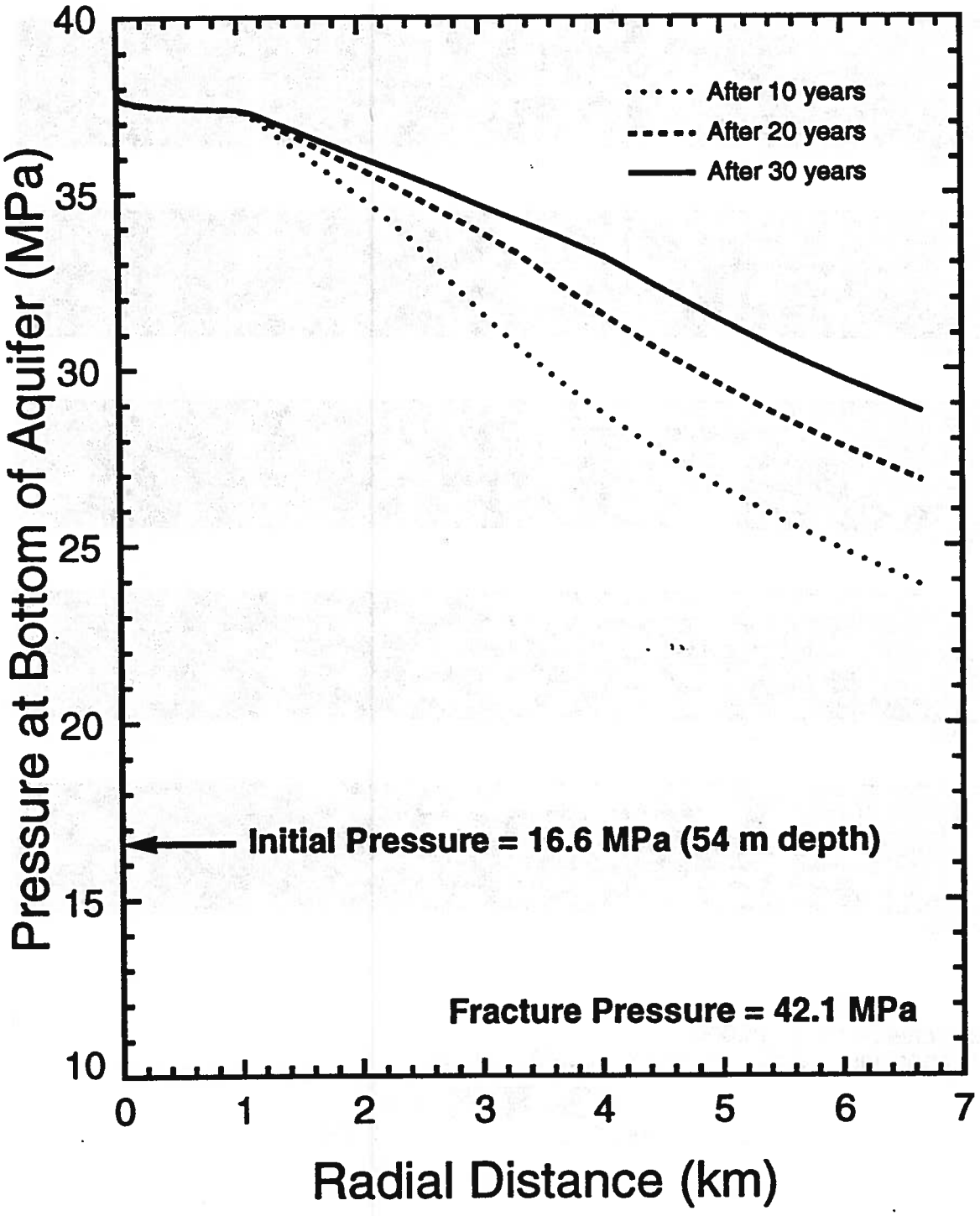

Nisku Carbonate Aquifer

NUMERICAL RUN (CO2_121)

Aquifer Porosity = 0.12 Aquifer Permeability = 400/30 md (horizontal)
Injection Pressure = 37.86 MPa

(a) Cumulative CO_2 Injection

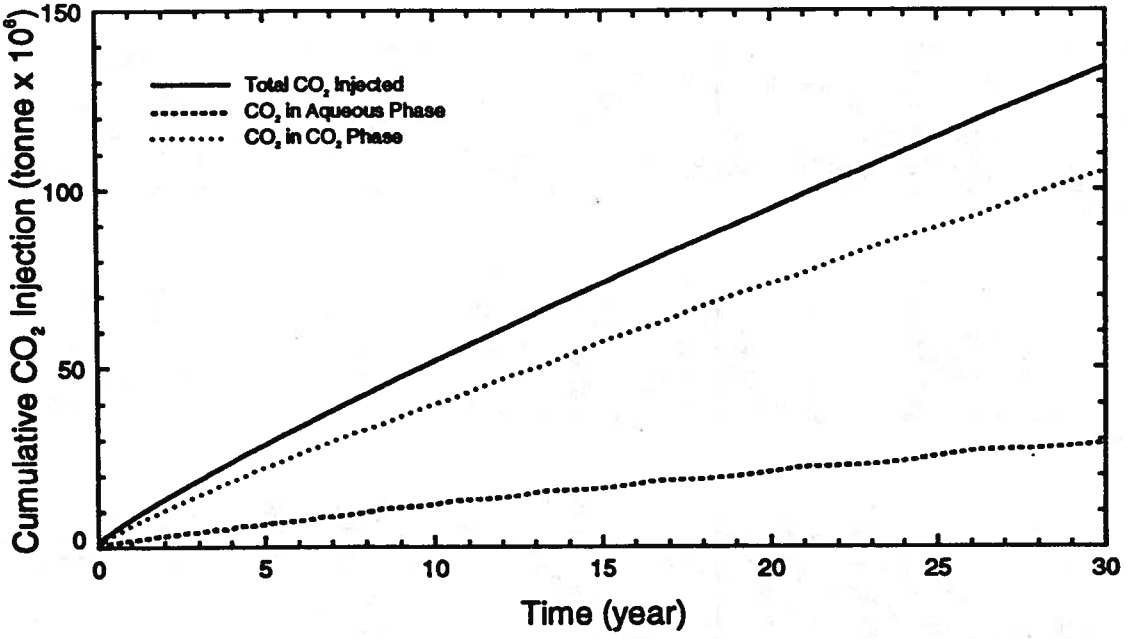

(b) CO_2 Injection Rate

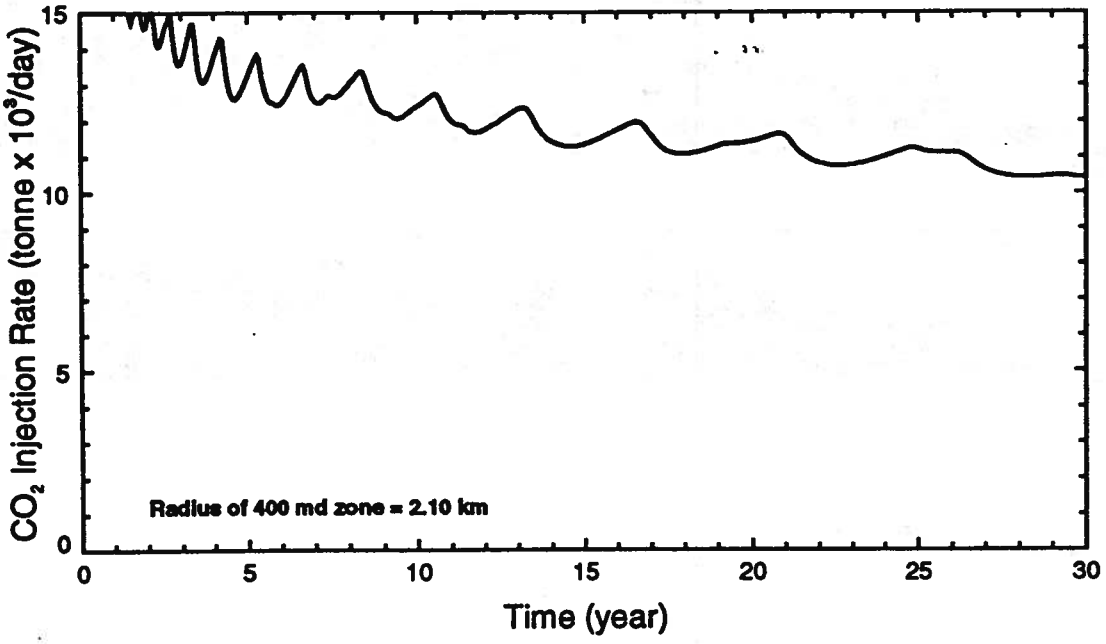

Carbon Dioxide Saturation (Run CO2_121)

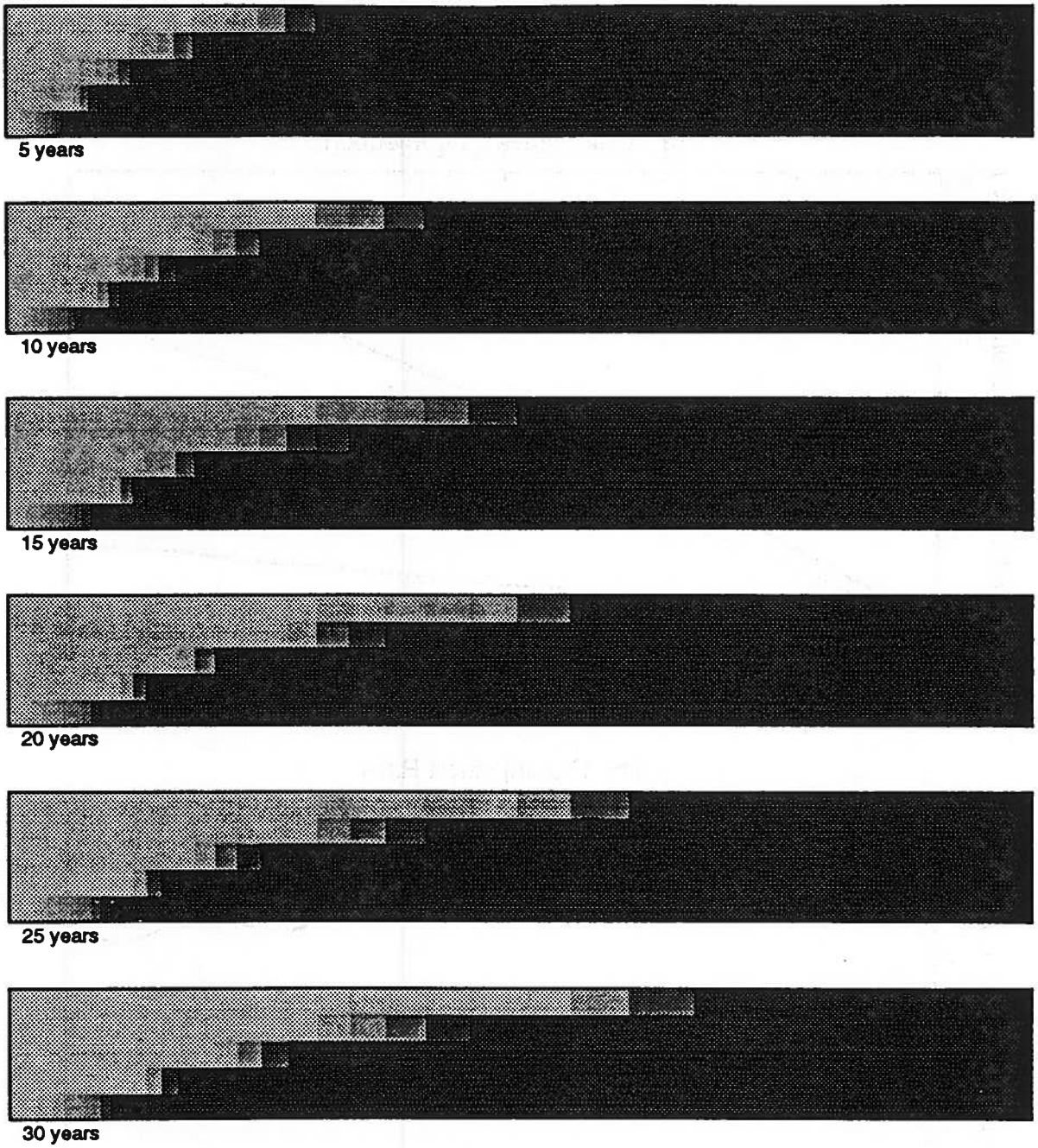

Vertical scale factor = 15.000
Field dimensions: 6999. (horiz.), 60.00 (vert.)

Nisku Carbonate Aquifer

NUMERICAL RUN (CO2_121)

Aquifer Porosity = 0.12 Aquifer Permeability = 400/30 md (horizontal)
Injection Pressure = 37.86 MPa Radius of 400 md zone = 2.10 km